

# **Archive ouverte UNIGE**

https://archive-ouverte.unige.ch

Thèse 2014

**Open Access** 

This version of the publication is provided by the author(s) and made available in accordance with the copyright holder(s).

A kinome-wide RNAi screen to identify genes controlling membrane lipid homeostasis in human cells

------

Gehin, Charlotte

#### How to cite

GEHIN, Charlotte. A kinome-wide RNAi screen to identify genes controlling membrane lipid homeostasis in human cells. Doctoral Thesis, 2014. doi: 10.13097/archive-ouverte/unige:38035

This publication URL: <a href="https://archive-ouverte.unige.ch/unige:38035">https://archive-ouverte.unige.ch/unige:38035</a>

Publication DOI: <u>10.13097/archive-ouverte/unige:38035</u>

© This document is protected by copyright. Please refer to copyright holder(s) for terms of use.

Section de chimie et biochimie Département de biochimie

Professeur H. Riezman

# A Kinome-Wide RNAi Screen to Identify Genes Controlling Membrane Lipid Homeostasis in Human cells

# **THÈSE**

présentée à la Faculté des sciences de l'Université de Genève pour obtenir le grade de Docteur ès sciences, mention biochimie

par

# **Charlotte GEHIN**

de

Hennebont (France)

Thèse Nº4670

GENÈVE Atelier Repromail

2014

# TABLE OF CONTENTS

SUMMARIES	2
1. English summary of the thesis	2
2. Résumé de la thèse en français	4
INTRODUCTION	6
1. Biology of membrane lipids	6
1.1. Lipids are essential components of life	6
1.2. Membrane lipid composition in mammalian cells	8
1.2.1. Glycerophospholipids (GPLs)	11
1.2.2. Sphingolipids (SLs)	17
1.2.3. Sterols	20
1.3. Insights into the canvas of membrane lipid metabolism	22
2. Control of membrane lipid homeostasis	26
2.1. Importance of membrane lipid homeostasis	26
2.2. Overview of mechanisms that control membrane lipid homeostasis	28
2.2.1 Energy sensors and regulatory mechanisms	28
2.2.2 Control of lipid trafficking by the lipid-transfer proteins (LTPs)	33
2.2.3 Control of sphingolipid homeostasis: review	37
3. Aim of the studies	38
MATERIAL AND METHODS	39
1. Experimental procedures	39
2. Statistical analysis of the Kinome-wide RNAi screen	42
RESULTS	44
1. Investigating the genetic control of membrane lipid homeostasis with RNA interfer	ence44
1.1. Choice of siRNA as a tool for genetic perturbation screen in human cells	44
1.2. Mass spectrometry targeted-lipidomics to quantify membrane lipid changes	45

# Table of contents

	1.3. A p	ilot siRNA screen on lipid-related proteins identifies gene-specific lipid changes	46
	1.3.1.	Choice of target genes for the pilot screen	47
	1.3.2.	Efficacy of siRNA-induced gene knockdown	47
	1.3.3.	siRNA gene knockdown is sufficient to detect significant lipid changes	50
	1.3.1.	Cell-population context and gene knockdown effect: example of CERT	56
	1.4. Les	sonss from the pilot screen experiment.	59
2.	Kino	ome-wide RNAi based screen in HeLa MZ cells	62
2	2.1. Exp	perimental conditions	62
2	2.2. Me	mbrane lipid composition of HeLa MZ	62
2	2.3. Dat	a processing	72
4	2.4. Qua	ality controls	77
	2.1.1	Effects of transfection reagent and non-targeting siRNA controls	79
	2.1.2	PLK1 siRNA induces an apoptotic lipid profile	79
	2.1.1	CERT siRNA induces SL, PI and sterol changes	80
4	2.5. Kin	ome-wide RNAi screen results	86
	2.2.4	Observation of lipid behavior.	86
	2.2.5	The puzzle of hit identification	87
	a)	Hit identification using threshold determination	88
	b)	Principal Component analysis (PCA)	91
	c)	Genes with patterns of lipid changes: correlation- vs HIS-based selection	97
	2.2.6	Validation of candidate genes based on literature	109
	2.2.7	Hypothesis-driven analysis of lipid profiles	112
	2.2.8	Ongoing research	115
3.	Scre	ening of Dynamic Amphiphiles as siRNA Delivery System in Mammalian Cells	116
3	3.1. Sun	nmary of the research	116
3	3.2. Arti	icles	117
DI	SCUSS	ION	118
1.	Anal	lysis of candidate genes from the siRNA kinome-wide screen	118
2.	How	to interpret observed modifications of lipid profiles?	122
3.	Less	ons from the screening "experience" and perspectives	126

# Table of contents

APP	ENDIX	127
1.	siRNAs	127
2.	Oligonucleotide sequences of primers	127
3.	Discarded conditions	127
4.	Multiple reaction monitoring assay	127
5.	Data	127
ABE	BREVIATIONS	128
BIB	LIOGRAPHY	129

# **ACKNOWLEDGEMENT**

First of all, I would like to thank the members of my jury, Prof. Fran Platt and Prof. Jean Gruenberg for agreeing to evaluate my work and especially to Fran Platt for accepting to travel for my PhD defense.

Howard, thank you for accepting me in your lab. Thank you for your confidence from the beginning and for supporting me in all the steps of the project. Combined with freedom, your confidence was sometimes a little scary, as it assumed I had also to trust myself. However, it was a very rewarding experience. Thank you also for all the opportunities you gave me to enrich my scientific horizon, including the NCCR, which was a great chance for me. Finally, thank you very much for the lab retreats, for the "raclette" at the chalet and your pasta salad that is really tasty!

These years of PhD would not have been so rewarding without the presence of wise people from the lab: Isabelle for your patience at teaching me how to use the machines, prepare solutions and for your kindness as lab/desk-mate, Ursula for the MRM list and for sharing your experience, Kyohei & Miwa for your calm, kindness and for sharing interesting discussions about "typical" French culture such as cooking shows from M6 or Danse avec les stars;) Thank you especially to my lunchmates with who I could debrief everyday: Gisèle for your Swiss/British spicy humor and for listening to me whatever you had to face personally, Brigitte (merci pour les discussions sur la vie hors du labo et ta positive-attitude), Ludovic for youre supèr Frènche humour, and former lab members Marcy and Tatjana. From the room 368, I also want to thank Auxi (a very precious person) and Thomas for very interesting scientific discussions and your communicative enthusiasm. Good luck to Galih and thank you for your kindness (your name fits well with you). Finally, thank you Aline for your wisdom, your support and all what we lived together these years. I hope I forget nobody...

Oh yes, I forgot someone actually... Alejandro! But Ale, since you are a special hipster (and also a Roux lab member), you deserve a special part in these acknowledgement.

Many thanks also to Fabrice without who, this project wouldn't have been possible. Merci pour ta disponibilité à toute épreuve, d'avoir envoyé mes échantillons à Lausanne et pour les discussions sur tout, à n'importe quelle heure ©

Apart from the lab, I would like to thank my collaborators: the Matile lab and more particularly Prof Stefan Matile who offered me a great project, the occasion to approach the world of Chemistry and to work with very nice people such as Javier, Eun-Kyoung, Oleksander, Duy-Hien, David, Quentin and Sandra. I would like to thank the Pelkmans lab that offered me the siRNA library but also two motivating collaborations with Mathieu Fréchin and Prisca Liberali. I would like to thank Prisca especially for her precious advices in the RNAi project and the energy she transmitted me.

Thank you to XueLi. It's a great pleasure to know you and to share time in meetings together.



Thanks to the NCCR crew: Suzi, Jean-Claude, Caroline and Nolwenn. Beyond your efficiency, it's always very pleasant to speak/joke with you.

Thanks to the Biochemistry department in general and more particularly to people with who I shared special moments such as Aurélie, Sonia, Ana, Sebastien or Natasha from Soldati lab for their humour when I was coming to read microplates. Or people from Jean's lab for their help in my project: Shem for cellprofiler, Cameron, Stefania, Dimitri, MH. Thank you to Reika & Guillaume who were really precious, especially at the beginning of this adventure and to the members from Reika's lab with who I spent hours to discuss in the cell culture room such as Nina or Daniel. Thank you to Myriam amd Christine from the laverie, Jean-Pierre and Olivier for their help. Thank you to Cécile, Marie-Line and Katie for their administrative help.

Many thanks for the evenings (beers,burgers, jazz, parties), discussions and activities (climbing, volley, ice skating, hockey) shared with: Aurélie & Sonia, Ana, Alice, Carole, Chrystelle, Laurent, Manu & Dafne, Sylvain & Christelle, Maria & Dima, Sarah, Sabine, Ludwig, Natasha, Nico & Leo, Valentina, Sandrine, Annika & Thibaud and Guillaume. Thank you to the "Chapusi" that include many people cited before but also Isabelle, Simone, Ricardo and Adriana.

Merci aux amis de Lyon, même s'ils ne sont plus vraiment à Lyon pour ces supers week-ends passés ensemble et pour être toujours là malgré la distance: Marie surtout mais aussi Ronan, Damien, Lionel, Raphaël & Julie, Marc, Pierrick & Chiara, Baudouin. A Guillaume, merci pour ton amitié, tout simplement;)

Merci Francis de m'avoir permis de trouver ma voie. Ce premier stage sous ta supervision a été determinant (je n'oublierai jamais les batailles de glacons non plus ^^).

Merci Pilar pour avoir été mon premier lien à Genève mais surtout pour être devenue une amie. Merci pour votre incroyable énergie, les délicieuses tortillas et le vin le midi.

Merci Maman d'avoir toujours su être à mes côtés pour me donner force et espoir quelles que soient les épreuves. Merci pour les discussions philosophiques, les rêves éveillés et le goût de la nature. Enfin merci pour tous ces puzzles et cahiers d'énigmes que tu me « forçais » à résoudre petite afin de canaliser mon énergie. Tu vois où ça nous mène... Merci Lambert pour l'humour et le piment que tu as su ajouter à cette thèse! Merci a Mamie d'Hennebont et de Cornimont d'avoir cru en moi des les premiers pas. Je pense toujours a vous deux.

Merci Carlos. D'abord pour tout ce que je ne peux pas écrire ici mais que je pense très fort! Et plus particulièrement dans cette aventure, merci d'avoir été là pour me soutenir au quotidien, non seulement moralement mais aussi pour les analyses de pannes du mass spec', les échantillons collectés jusqu'à 2h du matin après le ciné, l'attente 30min +/- 2h sur le parking, ton ordi avec lequel j'ai rédigé, l'envoi express d'échantillons à l'EPFL, les débriefings, les animations scientifiques dans le Valais, et j'en passe ... Dire qu'à la base, tu venais juste me poser une question sur C.elegans au Salon du livre 0:-)



#### **SUMMARIES**

# 1. English summary of the thesis

The control of lipid homeostasis is a fundamental process that allows cells to maintain the unique lipid composition of their membrane compartments and to deal with the energetic fluxes from metabolism. This control is done at several levels and involves lipid sensors, signaling systems, regulators as well as a robust machinery of lipid distribution across membranes. If most of enzymes involved in lipid metabolism are characterized, the question of the genetic control of lipid homeostasis is still outstanding.

In order to find genes that control the homeostasis of membrane lipids, we combined a large-scale RNAi screen with the techniques of targeted lipidomic analysis by mass spectrometry to monitor lipid changes in HeLa cells. For the first time, it was possible to observe the effects of genetic perturbations at the level of hundreds of membrane lipids with different combinations of head groups and fatty acyl chains simultaneously in HeLa cells.

First, I performed a pilot screen with siRNA targeting genes involved in lipid metabolism in order to validate the method. The results showed that siRNA-induced knockdown was sufficient to induce significant lipid changes but it also highlighted the capacity of cells to use compensatory mechanisms to adapt their lipid metabolism in case of direct silencing in lipid metabolic pathways. Moreover, it also showed that lipid changes can differ depending on cell confluence.

Second, a large-scale RNAi screen targeting the human kinome was performed. After validation of the primary screen through the analysis of quality control, 152 kinases were selected as candidate genes involved in the control of membrane lipid homeostasis. Among them, one third was linked to the regulation of central carbon metabolism and energy sensing. The detailed analysis also allowed validation of some hits based on scientific literature.

Finally, in parallel to this project, in the context of the Swiss National Center of Competence in Research (NCCR) Chemical Biology, we also developed and performed a robotically-assisted siRNA transfection assay in HeLa cells stably expressing GPI-eGFP and screened a library of chemicals in order to find compounds able to transfect siRNA in Human cells at least as efficiently than commercially available compounds. The robotic assistance allowed screening six different concentrations of siRNA/amphiphiles complexes from a chemical library comprising more than 200 compounds. These amphiphiles, synthesized in Matile lab (Geneva, Switzerland), resulted from the dynamic and covalent assembly of hydrophobic tails (aldehyde/ketones, thiols) with positively charged heads (hydrazones, oximes or disulfides bridges) (Montenegro et al, 2012). The screen revealed a dozen of active compounds able to carry siRNA into HeLa cells with a knockdown efficiency greater than 50% and little or no toxicity. After confirmation, siRNA transfection with active amphiphiles was optimized in HeLa cells expressing GPI-eGFP in order to reach a knockdown efficiency as good as Lipofectamine TM RNAiMax. A time-course assay revealed that GFP knockdown was faster with dynamic amphiphiles than Lipofectamine TM, suggesting a different manner of crossing cell membranes for siRNA/amphiphiles complexes. siRNA Transfection capacity of active amphiphiles was also performed in challenging cell types, such as Human Primary Skin Fibroblasts (courtesy of Dr Charna Dibner, HUG), with siRNA targeting GAPDH mRNA. The transfection was more efficient with the most active dynamic amphiphiles with Lipofectamine RNAiMax. Then, the characterization siRNA/amphiphiles particles was monitored using Density Light Scattering (DLS). The last step, in collaboration with Pr. Shiroh Futaki (Japan) consisted in determining which cellular mechanisms, such as endocytosis, were involved in the delivery of siRNA by the best amphiphile candidate into HeLa cells.

#### 2. Résumé de la thèse en français

Le contrôle de l'homéostasie lipidique est un processus fondamental qui permet aux cellules à la fois de maintenir une composition lipidique unique dans chacun de ses compartiments membranaires et de gérer les flux énergétiques. Ce contrôle s'effectue à divers niveaux et comprend des capteurs de la composition lipidique membranaire, un système de signalisation et de régulation qui permet à la cellule d'adapter son métabolisme lipidique en fonction des besoins ainsi qu'un robuste système de transport assurant la distribution correcte des lipides dans leurs compartiments cellulaires spécifiques. Si la plupart des enzymes impliquées dans le métabolisme des lipides sont connues, la question du contrôle de l'homéostasie lipidique n'est pas résolue.

Afin de trouver les gènes qui contrôlent l'homéostasie des lipides membranaires, nous avons combiné un crible génétique par ARN interférent (ARNi) aux techniques d'analyse lipidomique ciblée par spectrométrie de masse dans les cellules HeLa. Pour la première fois, il est possible d'observer les effets de perturbations génétiques simultanément au niveau de centaines de lipides membranaires résultant de la combinaison entre différents groupes fonctionnels et chaines d'acides gras.

Dans un premier temps, une expérience pilote de crible génétique a été mise au point pour valider l'utilisation d'ARNi pour étudier la fonction des gènes dans le métabolisme des lipides. Dans ce but, j'ai ciblé des gènes en relation avec le métabolisme des lipides. Les résultats de ce test ont montré que la réduction d'expression des gènes par ARNi était suffisante pour induire des changements lipidiques significatifs. Cependant, ils ont également mis en évidence la capacité des cellules à utiliser des mécanismes compensatoires pour adapter leur métabolisme lipidique en réponse aux déficiences de certaines voies de synthèse. Enfin, ces résultats ont montré que les changements lipidiques pouvaient être différents en fonction de la confluence des cellules au moment de la transfection des ARNi.

Une fois l'expérience pilote validée, un crible ARNi à grande échelle ciblant le kinome humaine a été réalisé. Après filtration des résultats incongrus et validation du set de données par l'analyse des contrôles de la qualité, 152 kinases ont été choisies comme ayant un rôle possible dans le contrôle de l'homéostasie lipidique membranaire. Parmi ces kinases, environ un tiers était

déjà connues pour leur rôle dans le contrôle du métabolisme central du carbone. L'analyse détaillée des gènes candidats a permis de valider certains résultats selon les données de la littérature mais les étapes de confirmation sont toujours en cours.

Enfin, parallèlement à ce projet, dans le cadre du Pôle de recherche national suisse de (PRN) Biologie chimique, nous avons également développé et réalisé une expérience de répression génétique dans les cellules HeLa exprimant de façon stable la protéine GPI -eGFP par une banque de composés chimiques, appelés amphiphiles dynamiques et potentiellement capables de transfecter des ARNi dans des cellules humaines. Une assistance robotisée nous a permis de tester les composés d'une banque comptant plus de 200 amphiphiles et six ratios différents d'assemblage entre les ARNi et amphiphiles. Ces amphiphiles synthétisés dans le laboratoire du Pr. Stefan Matile (Genève, Suisse), résultent de l'assemblage dynamique et covalent entre des chaines carbonées hydrophobes (aldéhyde / cétones, thiols) avec des groupes fonctionnels positivement chargés (hydrazones, oximes ou ponts disulfures). Les résultats du criblage ont identifié une douzaine de composés actifs pouvant transporter les ARNi dans les cellules HeLa avec un rendement de plus de 50 % de répression d'expression des GPI-EGFP et peu ou pas de toxicité. Après confirmation, la transfection des complexes ARNi/ amphiphiles actifs a été optimisée dans les cellules HeLa exprimant GPI -eGFP afin d'atteindre une efficacité de répression au moins aussi bonne que l'agent de transfection commercial Lipofectamine TM RNAiMax. Un test d'activité a également révélé que la répression d'expression de la GFP était plus rapide avec les amphiphiles dynamiques que la Lipofectamine TM, ce qui suggère une autre manière de traverser les membranes cellulaires pour les complexes ARNi/ amphiphiles. L'efficacité de transfection de l'ARNi par les amphiphiles actifs a également été effectuée dans des types cellulaires différents et réputés difficiles à transfecter comme les fibroblastes de peau humaine primaires (remerciements au Dr Charna Dibner, HUG), avec des ARNi ciblant l'ARNm de GAPDH. La transfection était plus efficace avec les amphiphiles dynamiques les plus actifs qu'avec la Lipofectamine RNAiMax. Finalement, la caractérisation des particules ARNi/ amphiphiles a été mesurée par diffusion dynamique de la lumière (DLS). La dernière étape, en collaboration avec le Pr. Shiroh Futaki (Japon) a consisté à déterminer les mécanismes cellulaires impliqués dans le transfert cellulaire des ARNi par les meilleurs candidats amphiphiles dans des cellules HeLa.

# **INTRODUCTION**

# 1. Biology of membrane lipids

# 1.1. Lipids are essential components of life

Lipids are organic molecules essential to life in the same way as amino acids, nucleic acids and sugars. Lipids have always been part of the human diet but their chemical characterization and their link with life has been a long process. Lipid properties such as hydrophobicity and highly calorific matter have been known since the first human populations were making butter or lamps from animal fats and produce vegetable oil. However, the link between lipid chemistry and physiology only started in the 19<sup>th</sup> century with the chemical characterization of cholesterol from gallstones, glycerolipids from fats and some fatty acids by Michel-Eugène Chevreul (1786-1889) (McNamara et al, 2006). Since these first discoveries, with the evolution of extraction and analytical methods, tens of thousands of lipids from many organisms have been characterized but several other organisms remain to be analyzed and techniques are constantly improving (Wenk, 2005). In 2005, the International Classification and Nomenclature Committee have defined lipids on the basis of their hydrophobicity (Fahy et al, 2009). However, this is not the common point to all lipids. Indeed, some of them like phosphoinositides or lipids with large hydrophilic domains such as complex sugars are rather soluble in water-based solvents. Therefore, a consensus definition of lipids could be "fatty acids, their naturally-occurring derivatives (esters or amides), and substances related biosynthetically or functionally to these compounds", as suggested by Christie, the author of the Lipid Library (http://lipidlibrary.aocs.org/)

The main biological function of lipids as structural components of cell membranes was discovered at the turn of the 20th century. First, Charles Overton suggested in 1889 that cell boundaries could be made of lipids since nonpolar and lipid molecules could cross them. Then in 1925, Gortner and Grender calculated the surface area of cell boundaries occupied by lipids using a Langmuir trough and hypothesized that the outer cell membranes were composed of a lipid bilayer, what was confirmed later by electronic microscopy (Adams, 2010). While the fundamental frontier between the inert and life remains an enigmatic question for science, the

lipid bilayer of cell membranes creates a physical border between the cell medium and its outer environment in all living organisms. Cells are the basic units of life and there is no cell without lipid membranes.

How cell membranes appeared during evolution is far from being understood. Instead, the evolution of membrane lipid biosynthetic pathways could be investigated thanks to comparative genomics. The molecular phylogenetic analysis of genes coding for enzymes of lipid biosynthesis pathways in archea, bacteria and eukaryotes, suggest that phospholipids were already synthesized in the most recent common ancestor of the three domains of life. Phospholipids are the major components of cell membranes. Even if the nature of phospholipids differs between archea, bacteria and eukaryotes, all species share homologous enzymes acting in common steps of their phospholipid synthetic pathways. Indeed, while both eukaryotic and bacterial PLs result from the esterification of fatty acyl chains on a glycerol-3-phosphate backbone chains and PLs from archea are made of a glycerol-1-phosphate backbone linked to methyl-branched isoprenoids through ether bonds, genes coding for the synthesis of glycerol backbones, isoprenoids and fatty acids probably come from a common ancestor (Lombard et al, 2012).

Lipids are components of cell membranes but also signaling or energy storage molecules and the precursor of bioactive compounds such as hormones and mediator molecules in immunology. The chemical properties of lipids influence the biophysics of cell membranes as well as their protein composition and the function of these proteins. Stored in droplets, neutral lipids such as triacylglycerols and steryl esters become highly caloric reservoirs of energy. On the contrary, many lipids are synthesized in tiny quantities and their presence is tightly regulated in space and time because of their signaling properties. For instance, the concentration of some sphingolipids can be interpreted as a signal of proliferation or apoptosis for cells, the flip of phosphatidylserine to the outer leaflet of plasma membrane is a sign of apoptosis for neighboring cells (Fadok et al, 1992), the presence of phosphoinositides in specific cell compartments determines the association of proteins with specific organelles (Balla, 2013), protein-lipid associations in the nucleus influence gene expression (Shah et al, 2013), etc. Finally, proteins can be modified with lipids through posttranslational modifications such as acylation (Salaun et al, 2010) or attachment to a glycosylphosphatidylinositol anchor (GPI-anchor) (Kinoshita et al, 2008).

# 1.2. Membrane lipid composition in mammalian cells

In mammalian cells, membrane lipids comprise thousands of molecules that can be classified into three major categories: glycerophospholipids (GPLs), sphingolipids (SLs) and sterols. Each lipid class represents many combinations of molecules with specific subcellular distribution.

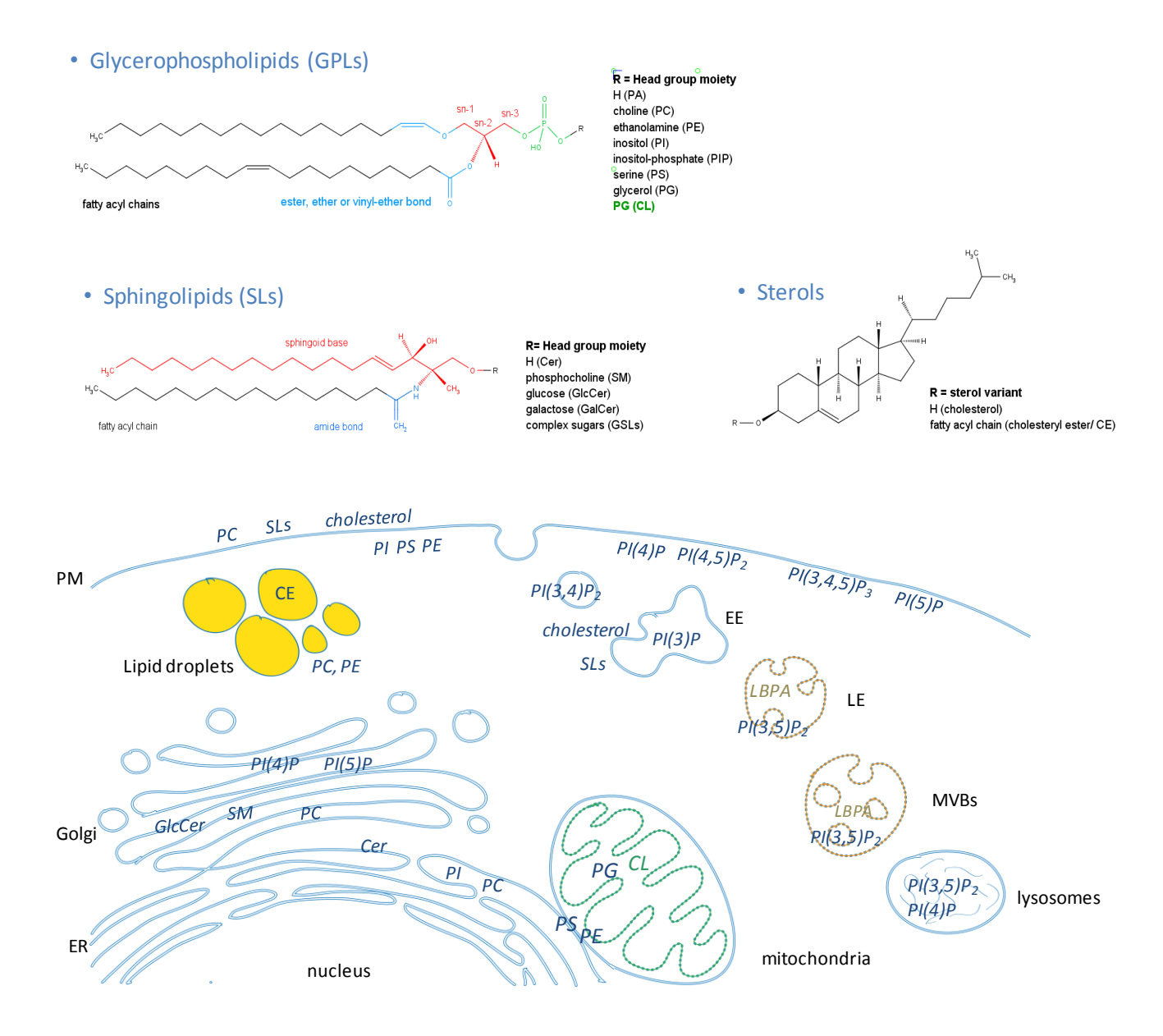


**Figure 1. Structure and localization of major membrane lipids in mammalian cells.** Major membrane lipids (blue) are found in all cell membranes but organelles and specific leaflets are particularly enriched in certain lipid, as indicated on the figure representing subcellular compartments. CE: cholesteryl ester; EE, early endosomes; ER: endoplasmic reticulum; LBPA (brown):lysobiphosphatidic acid; LE: late endosome; MVBs: multivesicular bodies; PM: plasma membranes. Adapted from (Balla, 2013; Loizides-Mangold, 2013; van Meer & de Kroon, 2011).

The lipid composition of membranes differs between organelles as well as between the two layers of the bilayer. These particularities confer specific physical and biochemical properties to the different membranes. Indeed, alone or packed in lipid bilayers, membrane lipids influence the structural and geometrical plasticity of membranes and their capacity to interact with proteins.

Membrane lipids are mostly amphiphilic. Therefore, membrane bilayers are made of a hydrophobic core of fatty acids attached to hydrophilic head groups at the interface with the aqueous phase. These head groups can be anionic (PI, PS, PA, CL) or neutral (PC, PE) and contribute to electrostatic interactions between proteins and the membrane. The ionic composition of the solvent around the bilayer also plays an important role in physical properties of membranes as it influences phase transitions by modifying the size of anionic head groups such as PA and CL at the cell surface. (Dowhan, 2008)

The geometry of individual lipids is influenced by their chemical and structural anatomy. Depending on their head group and their composition in fatty acids, they are either cylindrical or conical. Together, cylinder-shaped lipids have the propensity to form membrane bilayers whereas cone-shaped and inverted cone-shaped lipids such lysophospholipids, PE or DAG are considered as nonbilayer lipids and tend to deform the membrane and increase surface tension. The mixture of bilayer- and nonbilayer-forming lipids affects the asymmetry of membrane bilayers and impacts the movement of proteins, membrane curvature and fusion/fission of vesicles. The fluidity of membranes is greatly influenced by both the shape of lipids and their fatty acyl composition. Lipid bilayers oscillate between ordered ( $L_{\beta}$  or  $L_{\alpha}$ ) and disordered ( $L_{\alpha}$  or  $L_{d}$ ) phases. The presence of unsaturated and branched fatty acids tends to increase membrane fluidity. On the contrary, the insertion of cholesterol reorders the lipid bilayer and controls its lateral organization leading to more specific associations with proteins (Dowhan, 2008). For instance, in the concept of lipid rafts, the association between SLs, cholesterol and specific proteins results in detergentresistant membrane nanodomains that are associated with several biological processes (Lingwood & Simons, 2010) even if they have never been directly observed in vivo due to the lack of good fluorescent lipid markers.

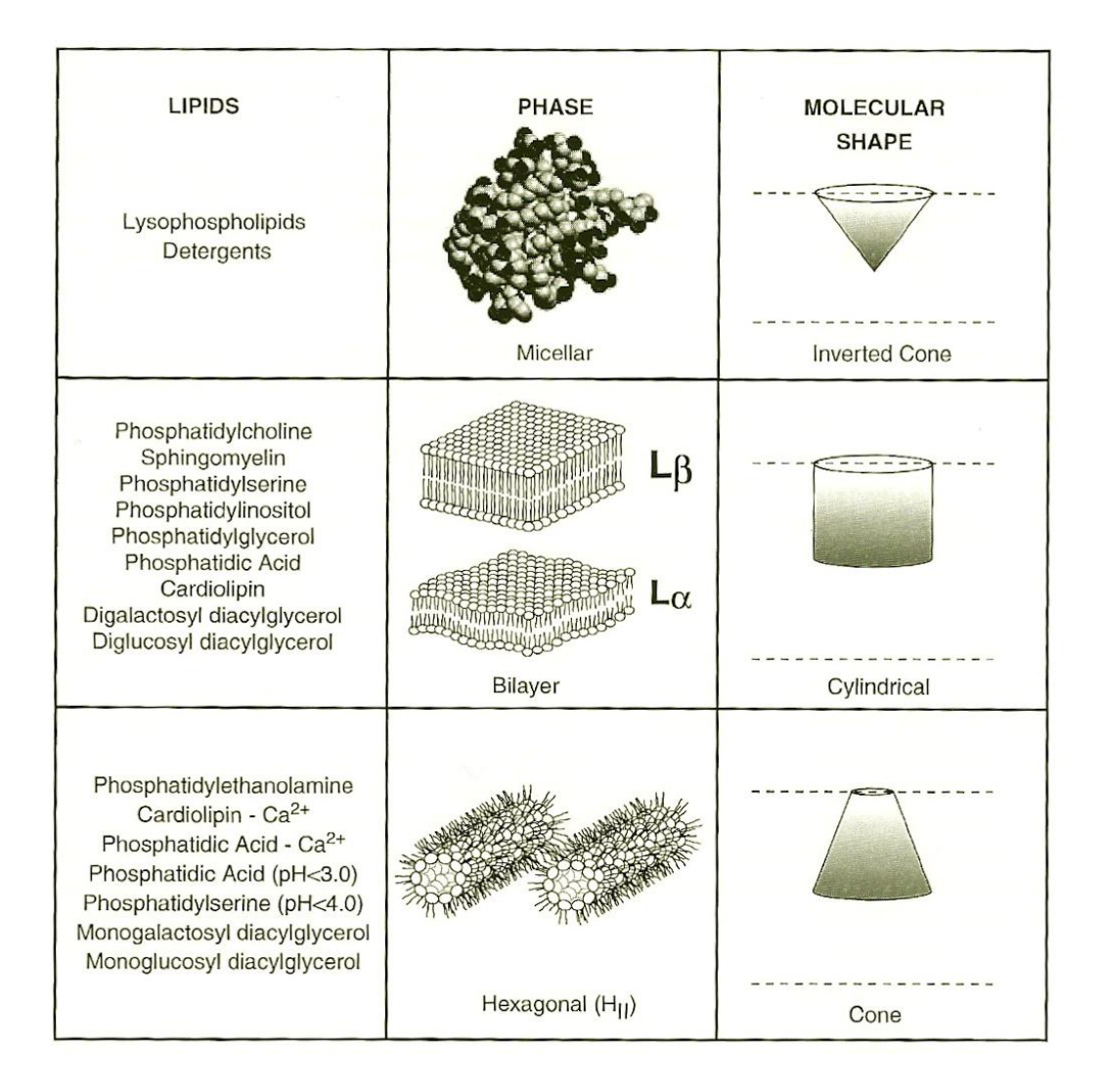


Figure 2. Polymorphic phases and molecular shapes exhibited by lipids. Inverted cone-shaped molecules form micelles. Polar lipids with two long alkyl chains adopt a bilayer or a non-blayer (HII) structure depending on the geometry of the molecule (cylinder- or cone-shaped respectively) and environmental conditions. The  $L\beta$  (ordered gel) and  $L\alpha$  (liquid crystalline) bilayer phases differ in the order within the hydrophobic domain and in mobility of the individual molecules. Reprinted from (Dowhan, 2008)

How does the cell control its membrane lipid composition in order to organize this compartmentalization and maintain the biophysical properties proper to each organelle? Where and how does the cell synthesize membrane lipids and how do they maintain their levels? The goal of the next sections is to answer this question on the basis of our current knowledge.

# 1.2.1. Glycerophospholipids (GPLs)

Glycerophospholipids are the most abundant membrane lipids in mammalian cells. GPLs are glycerol-based phospholipids (PLs), They are amphipathic compounds made of a glycerol-3-phosphate (G3P) backbone, linked to a head group via a phosphodiester bond and to fatty acyl chains through ester, ether or vinyl ether bonds on sn-1 and sn-2 (Hermansson et al, 2011). GPLs are subdivided into different classes according to the nature of their head group (**Fig. 1**). In mammalian cells, major GPLs are phosphatidylcholine (PC) that constitute around 50 mol% of PLs, followed by phosphatidylethanolamine (PE), around 20 mol%, phosphatidylinositol (PI), phosphatidylserine (PS) less than 10 mol% each and phosphatidic acid (PA) and phosphatidylglycerol (PG) in very low amount (van Meer, 2005). PA is the precursor of all GPLs and PG, is an intermediate in the synthesis of cardiolipins (CL), a GPL specific for the inner membrane of mitochondria (IMM).

The synthesis of GPLs starts either in the membrane of the endoplasmic reticulum (ER) or at the outer membrane of mitochondria (OMM). The first step of GPLs synthesis is the formation of PA that results from the successive acylations of G3P on sn-1 by acyl-CoA: glycerol-3-phosphate acyltransferase (GPAT), then on sn-2 by lysophosphatidic acid acyltransferase (LPPAT). GPAT and LPAAT are found both in the ER and mitochondria. From there, PA can be either dephosphorylated into diacylglycerol (DAG), the precursor of PC, PE and PS by PA phosphatase 1 or 2 (PAP1 or 2) or converted into CDP-diacylglycerol (CDP-DG), the precursor of the anionic PI, PG and CL by CDP-diacylglycerol synthase (CDS). CDS exists in different isoforms that localize in the ER to make PI and in mitochondria where PG and CL are synthesized (Hermansson et al, 2011). CDP-DG is converted into PI by phosphatidylinositol synthase (PIS) in the ER (Kim et al, 2011) and PG is made in mitochondria where it is used as substrate in the synthesis of CL by the cardiolipin synthase CLS in the IMM. The structure of CL is unique among GPLs with its four fatty acyl chains and two phosphatidyl moieties linked to glycerol (Houtkooper & Vaz, 2008) (Fig. 3).

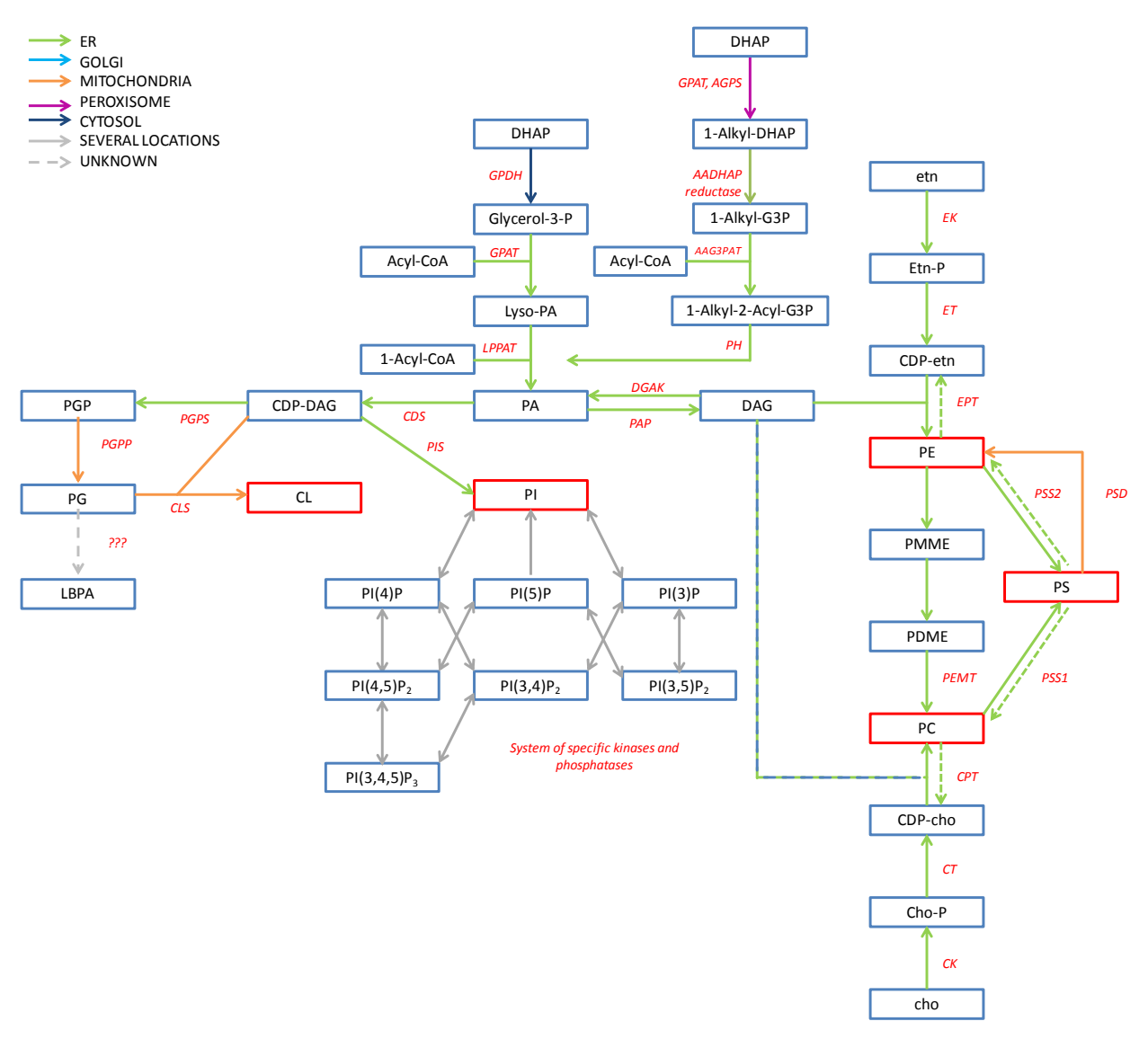


Figure 2. Overview of the glycerophospholipid (GPL) biosynthesis pathway in mammalian cells. The key metabolites (in black), the enzymes catalyzing the respective reactions (in red) and their subcellular localization (arrows) are indicated. Lipids analyzed in this thesis project are surrounded in red. Most of abbreviations are as indicated in the text proper. Supplementary abbreviations are indicated here: DGAK (diacylglycerol kinase), EK (ethanolamine kinase); EPT (ethanolamine phosphotransferase); ET (phosphoethanolamine citidyltransferase); PGPP (phosphatidylglycerol phosphate phosphatese); PGPS (phosphatidylglycerol phosphate synthase). Adapted from various sources cited in the text.

The synthesis of PC and PE starts with the dephosphorylation of PA into DAG at the membrane of the ER by PAP. The PAPs consists in two families: the cytosolic PAP1 or lipins, and the membrane proteins PAP2 or lipid phosphate phosphatase (LPP) that can compensate the activity of lipins in some conditions (Carman & Han, 2006). In mammalian cells, PC is predominantly synthesized through the Kennedy pathway, i.e. *de novo* synthesis in the ER. Choline is first phosphorylated by a choline kinase (CK) into phosphocholine that is then

converted into CDP-choline by a CTP: phosphocholine ctidylyltransferase (CT). This latest reaction is considered as the rate-limiting step of *de novo* PC synthesis in mammalian cells. Finally, the CDP-choline head group is transferred on DAG by CDP-choline: 1, 2-diacylglycerol cholinephosphotransferase (CPT) to make PC. PC can also be synthesized through sequential methylation of PE by phosphatidylethanolamine N-methyltransferase (PEMT) in the ER and in ER mitochondrial-associated membranes (MAMs), to a lower extent. However, this reaction is restricted to hepatocytes in mammals (Hermansson et al, 2011). Contrary to PC, in mammalian cells *de novo* synthesis of PE results from both the Kennedy pathway in the ER and the decarboxylation of PS by phosphatidylserine decarboxylase (PSD) in IMM. However, the importance of each pathway for cell viability depends on the tissue and the pathways cannot compensate for each other. For instance, many cells in culture prefer to make PE by decarboxylation of PS whereas PE made through the Kennedy pathway is indispensable to the function of hepatocytes in mice. Finally, PS is made by base exchange of head groups from PC or PE with L-serine via phosphatidylserine synthase 1 or 2 (PSS1 or 2), respectively in ER-MAM (Hermansson et al, 2011) (Fig. 3).

Other classes of GPLs exist. These compounds can be present in tiny quantities in cells while they play important roles in signaling, structure and metabolism. They can be derived from existing GPLs (phosphoinositides, Lysophospholipids) or result from a different biosynthetic pathway (ether-phospholipids)

# Phosphoinositides (PIPs)

Phosphoinositides are lipid signaling molecules that represent less than 1 mol% of total PLs. They are made from PI by successive phosphorylations and dephosphorylations of the inositol ring by a system of PI- and PIP-kinases and phosphatases (**Fig. 3**). While the PI synthase (PIS) associates with both the ER and specific ER-derived highly mobile organelles, the synthesis of PIPs takes place in various membrane compartments of the cell. However, the distribution of PIPs is characteristic of specific organelles. For instance, the plasma membrane (PM) is enriched in PI(4.5)P2, PI(4)P and PI(3,4,5)P3, early endosomes (EE) are enriched in PI(3)P, late endosomes (LE) in PI(3,5)P2 and the Golgi in PI(4)P (**Fig. 1**). The functions of phosphoinositides cover a wide range of biological processes that were reviewed by Tamas Balla in 2013. To

summarize, "PIPs control organelle biology by regulating vesicular trafficking, but they also modulate lipid distribution and metabolism via their close relationship with lipid transfer proteins. PIPs regulate ion channels, pumps, and transporters and control both endocytic and exocytic processes". (Balla, 2013). Their presence in the nucleus also affects gene expression, DNA repair and the export of mRNA (Monserrate & York, 2010).

#### • Lysophospholipids (lysoPLs)

Lysophospholipids are monoacylated phospholipids where one of the fatty acyl chains is replaced by a hydroxyl group on sn-1 or sn-2 of their glycerol backbone. They are synthesized either by de novo synthesis from glycerol-3-phosphate or by hydrolysis of PLs via the action of phospholipase and acyltransferase. LysoPLs of each PL exist but LysoPCs are the most abundant ones. LysoPLs are important bioactive molecules secreted by cells and found in the plasma of mammals. They are often used as biomarkers of various diseases, such as cancer and inflammation. In cells, they play both structural and signaling roles. With their conical shape, they induce membrane deformation and can modulate the activity or the oligomerization of membrane proteins with which they interact, such as ion channels and G-protein coupled receptors (GPCRs) by modifying their membrane environment (Fig.4) (Grzelczyk & Gendaszewska-Darmach, 2013).

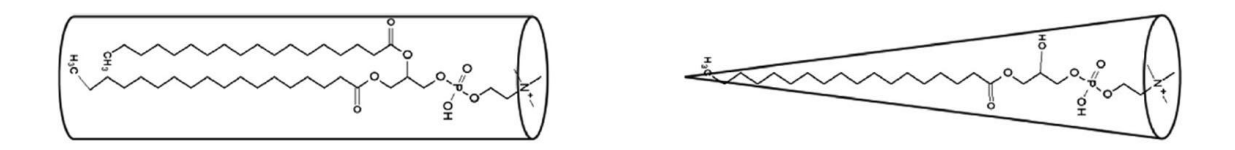


Figure 4. Structures of cylindrical (phosphatidylcholine 18:0) phospholipid (A) and cone shaped (lysophosphatidylcholine 18:0) lysophospholipid (B). Adapted from (Grzelczyk & Gendaszewska-Darmach, 2013)

#### • Ether-phospholipids (Ether-PLs)

In mammalian cells, ether-phospholipids represent an important class of GPLs in which the fatty acyl at the sn-1 position is linked to the glycerol-3-phosphate backbone by an ether bond. Two types of ether bonds are possible: the ether bond itself in platelet activator factors (PAF) and the vinyl-ether bond in plasmalogens (**Fig. 5**).

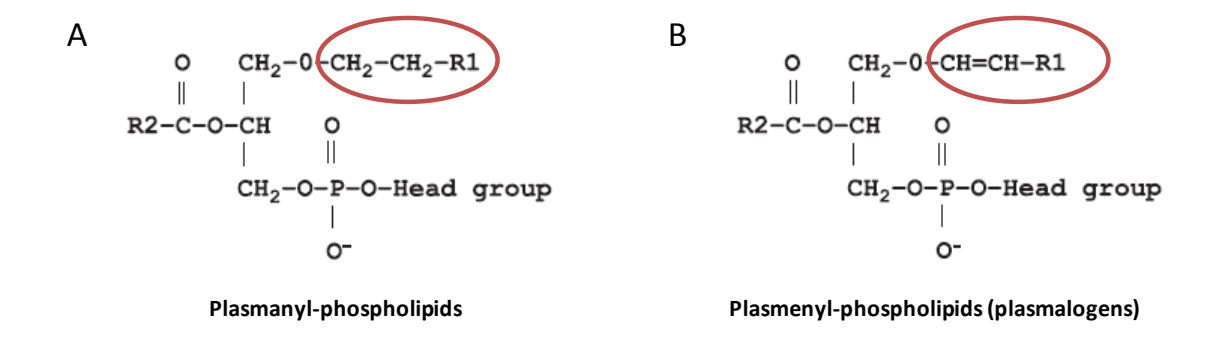


Figure 5. Structure of ether-phospholipids: (A) plasmanyl- and (B) plasmenylphospholipids are characterized by the presence of an ether or a vinyl-ether bond at the sn-1 position of their glycerol backbone, respectively.

The biosynthesis of ether-phospholipids starts in peroxisomes where the precursor glycerol-3-phosphate is first dehydrogenated by a G3P dehydrogenase into dihydroxyacetone phosphate (DHAP). DHAP is then acylated with a long-chain fatty acyl by the glycerone phosphate O-acyltransferase (GNPAT) before that the enzyme alkyl-glycerone phosphate synthase (AGPS) replaces the acyl-chain by a fatty alcohol. Next, 1-alkyl-DHAP is exported from peroxisomes to the ER where it is reduced into 1-alkyl-G3P on which a fatty acyl is esterified by a specific alkyl/acyl-glycerol-3-phosphate acyltransferase (AAG3P-AT). Next steps of the process follow the same pathway than other GPLs (**Fig. 3**) Major plasmalogens are choline and ethanolamine-based (Brites et al, 2004). Plasmalogens are abundant membrane component. For instance, ether-PE represents around 30-50 mol% of total PE in the brain. They play important functions in membrane structure and dynamics as they tend to reduce surface tension and viscosity. They are also a reservoir of polyunsaturated fatty acids (PUFA) and antioxidants thanks to the scavenger property of their vinyl-ether bond (Wallner & Schmitz, 2011).

• Lysobisphosphatidic acid (LBPA)/ Bis(monoglycero)phosphate (BMP)

Lysobiphosphatidic acid is a special type of negatively charged GPL present in low amounts in cells (less than 1%) and concentrated in the inner membrane of late endosomes (≈17mol% of PLs from the LE) and lysosomes. Its structure is unique in the sense that it consists of two monoacyl glycerol backbones linked together by a phosphate group in sn-1 (sn-1'). Both the composition and the position of fatty acyl chains on glycerol determine the conformation of LBPA isomers. *In vivo*, the most abundant ones are acylated with oleic acid in 2, 2' (Goursot et al, 2010) (**Fig. 6**). The biosynthesis pathway of LBPA is still poorly understood and its precursor might be PG. LBPA functions are closely related to its structure. For instance, only the 2,2'-dioleolyl LBPA isomer was shown to be active in the regulation of cholesterol endosomal levels (Matsuo et al, 2004). LBPA can induce membrane invagination and participate to the formation of vesicles in multivesicular bodies (MVBs) and contrary to other GPLs, it is also resistant to hydrolysis by lipases and phospholipases (Gallala & Sandhoff, 2011)

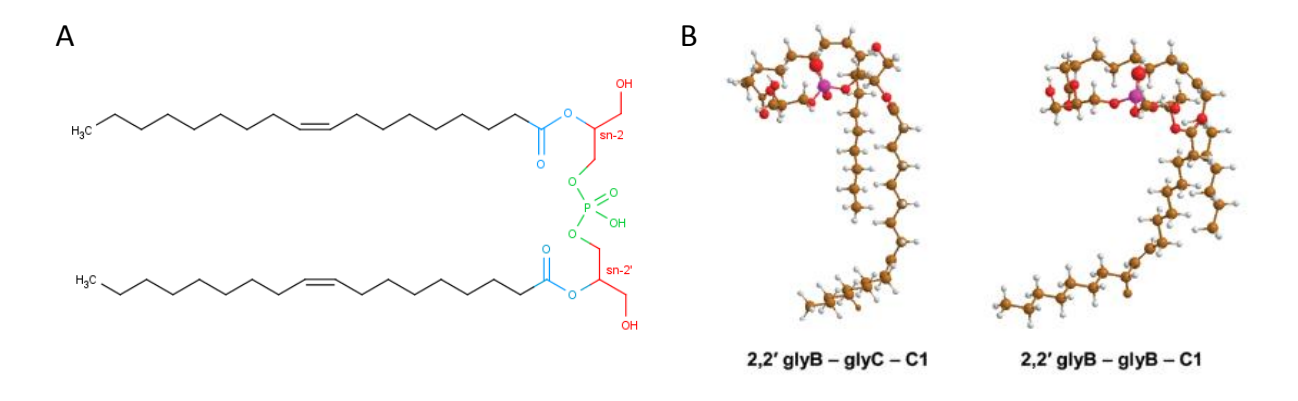


Figure 6. Schematic representation of LBPA with stereospecific numbering (sn) of the glycerol backbone (A) and examples of LBPA conformation based on calculated structures of the most stable 2, 2'LBPA isomers (B). Adapted from (Goursot et al, 2010).

# 1.2.2. Sphingolipids (SLs)

Information about SL synthesis except hydroxylated and dihydrosphingolipids comes from the review co-written with Dr. Maria-Auxiliadora Romero in 2013(Aguilera-Romero et al, 2013) and included further in the introduction. The section about SL synthesis, recycling and breakdown is repeated here in order to keep the logics of the manuscript.

Sphingolipids (SLs) are essential structural components of membranes (Fig. 1) and critical signaling molecules. De novo SL synthesis begins in the endoplasmic reticulum (ER) with the condensation of serine and palmitoyl CoA into 3-ketodihydrosphingosine by serine palmitoyltransferase (SPT) (Fig. 7). This product is reduced to generate sphinganine, the precursor of long-chain bases (LCBs). LCBs vary in chain length, degree of unsaturation and hydroxylation. Combinations of these three parameters define the specific species of LCBs for each organism (Hannich et al, 2011). At the ER, LCBs can be phosphorylated by a kinase or condensed by a ceramide synthase with fatty acyl-CoA, giving dihydroceramides. The number of atoms of the amide-linked fatty acid usually ranges from 14 to 26 and can extend to 36 carbons. The very long chain fatty acids (VLCFA) are produced by specific enzymatic complexes called elongases. In many species the dihydroceramide can be desaturated to form ceramide. The ceramides can then be modified in the ER to produce ceramide phosphoethanolamine or galactosylceramides, or travel to the Golgi through vesicular and non-vesicular transport routes. The mode of transport seems to determine the subsequent fate of the ceramide; conversion to glucosylceramide or sphingomyelin (Hanada et al, 2009). Once in the Golgi, diverse head groups are attached to the C-1 hydroxyl group of the ceramide backbone. The head group donor can be a glycerophospholipid (GPL) or nucleotide sugars to generate either phosphosphingolipids, with simultaneous release of diacylglycerol (DG), or glycosylsphingolipids with release of a nucleotide. The initial sugar of glycosphingolipids, usually glucose, can be extended to more complex glycan structures. Finally, complex SLs travel through the secretory pathway to the plasma membrane, endosomes and lysosomal/vacuole system where their concentration is sensed and regulated. Many declinations of SLs exist. They result from the combination of sphingoid bases with different fatty acid chain length, saturation degrees, hydroxylation, head groups, sugar and phosphate adducts. Here are presented only the ones that were detected by mass spectrometry in this thesis project.

Many reactions of sphingolipid metabolism can be reversed allowing for the rapid interconversion of different metabolic intermediates (Fig. 7). Nonetheless, some steps are irreversible: the initial step catalyzed by SPT and the degradation of long chain base phosphates (LCB-P) by an ER-localized lyase to acyl aldehydes and phosphoethanolamine (EtnP). Deficiencies in both steps have severe consequences in SLmetabolism (Bektas et al, 2010). Apart from these two reactions, there are several possible interconversions between SLs along their metabolic route. For instance, ceramidases regenerate LCBs from ceramides but they can also make ceramides through acylation of LCBs when ceramide synthase activity is compromised (Mao et al, 2000; Okino et al, 2003; Pata et al, 2010). The activity of glycohydrolases or sphingomyelinases produces ceramides from complex SLs that can be recycled again into the sphingolipid pathway (Hannun & Obeid, 2008). As in the anabolic pathway, enzymes responsible for SL turnover have an organelle-specific distribution in cells. In mammals, members of ceramidase and sphingomyelinase families localize in different cell compartments, such as mitochondria, ER, Golgi, lysosome/vacuole and plasma membrane (Hannun & Obeid, 2008). Localization is thought to allow the production of local pools of bioactive SLs, such as ceramides, LCBs and their phospho-derivatives. Several interesting reviews highlight the importance of these degradative pathways in the production of bioactive lipids (Hannun & Obeid, 2008; Kitatani et al, 2008). Sphingolipid turnover, named the salvage route, is also used to feed the sphingolipid synthesis pathway. In mammals, the salvage pathway can be responsible for 10% to 90% of sphingolipid synthesis (Tettamanti et al, 2003). How cells coordinate de novo and salvage pathways to generate the proper amounts of bioactive or structural SLs is an interesting field of research. The complexity of the sphingolipidome might differentiate between these two functions. Growing evidence supports the importance of substrate specificity of enzymes belonging to the degradation pathway in production of bioactive SLs. In mammals, bioactive sphingosine is mainly produced by ceramidase activity (Kitatani et al, 2008). Most of the enzymes of SL metabolism show specific subcellular localization. Therefore, spatial organization of the salvage pathway could be another discriminatory mechanism to differentiate between fates of products and to distinguish between structural and bioactive SLs.

# Dihydrosphingolipids

Dihydrosphingolipids are bioactive compounds. Dihydroceramides (dhCer) are intermediates during *de novo* ceramide synthesis in the ER and can be converted into dihydrosphingomyelin (dhSM) and dihydroglycosylceramides (dhGlcCer) in the Golgi as well as other SLs depending on the cell line (Kok et al, 1997) (**Fig. 7**). Dihydroceramide accumulation due to the ablation or the knockdown of dihydroceramide desaturases that desaturate dihydroceramides into ceramides leads to a global change in the membrane lipid profile (Ruangsiriluk et al, 2012), to autophagy as well as antiapoptotic processes (Siddique et al, 2013) but consequences of dhSLs levels changes depends on the cell type (Fabrias et al, 2012). Finally, it was recently shown that dhCer and dhSM accumulate in the human lens after the age of 65 and impact the biophysical properties of the lens (Deeley et al, 2010).

# Hydroxysphingolipids

In mammalian cells, 2-hydroxysphingolipids are a subset of sphingolipids containing one hydroxylated fatty acid that represent few SLs in most of cell lines and up to 50 mol% of total SLs in skin keratinocytes (Uchida et al, 2007) and in epithelial intestine cells (Dahiya & Brasitus, 1986). 2-hydroxy fatty acids are catalyzed in the ER by fatty acid-2-hydroxylase (FA2H) before condensation with sphinganine by a ceramide synthase during the *de novo* ceramide synthesis (Alderson et al, 2004) (**Fig. 7**). It was shown that all ceramide synthases can utilize 2-hydroxy fatty acids with the same efficiency as the non-hydroxylated ones, both *in vitro* and *in vivo* (Mizutani et al, 2008). The following steps are identical to the synthesis of non-hydroxylated SLs. Hydroxylated SLs play an important role in the differentiation of several cell lines and in the function of the nervous system in which hydroxylated galactosylceramides are essential to the formation of the myelin sheath. Mutations of FA2H in humans and mice cause leukodystrophy and neurodegeneration (Potter et al, 2011). Inside cells, the decrease of hydroxylated SLs associated with FA2H deficiency impacts the organization of cell membranes. For instance, the siRNA knockdown of FA2H is associated with a decrease of glucose and insulin receptors at the plasma membrane of adipocytes (Guo et al, 2010).

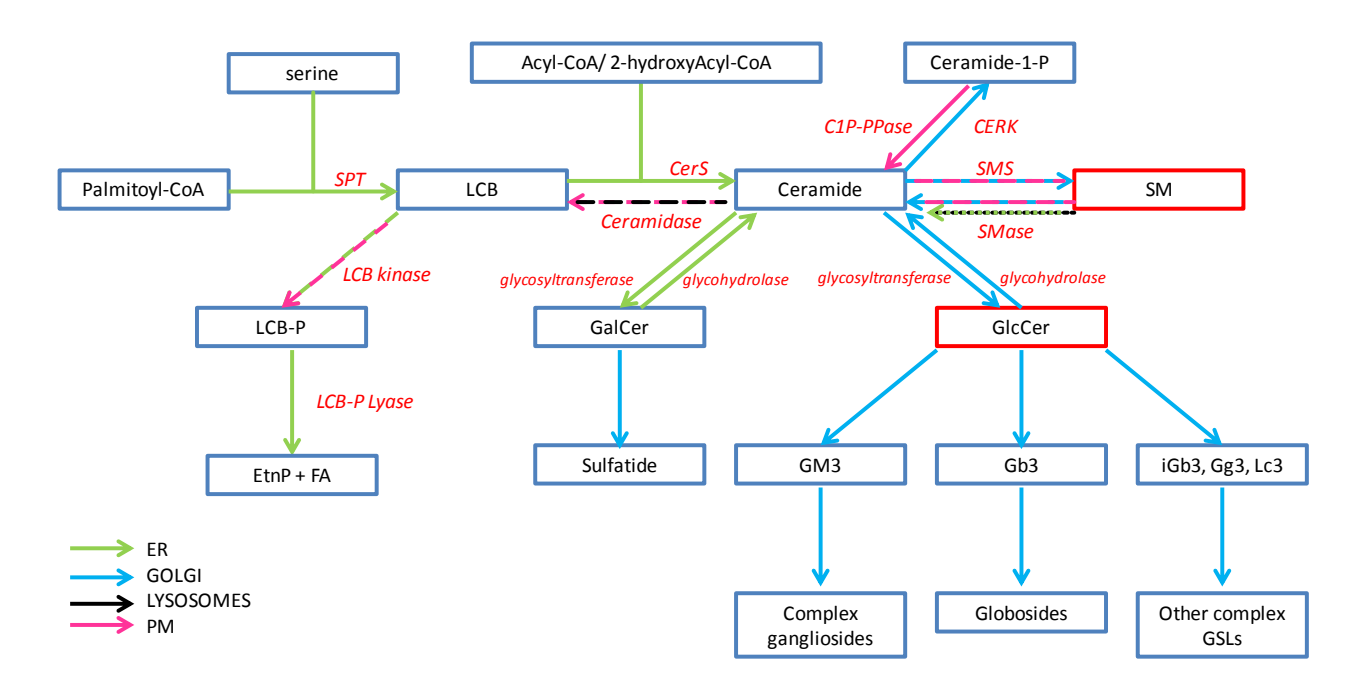
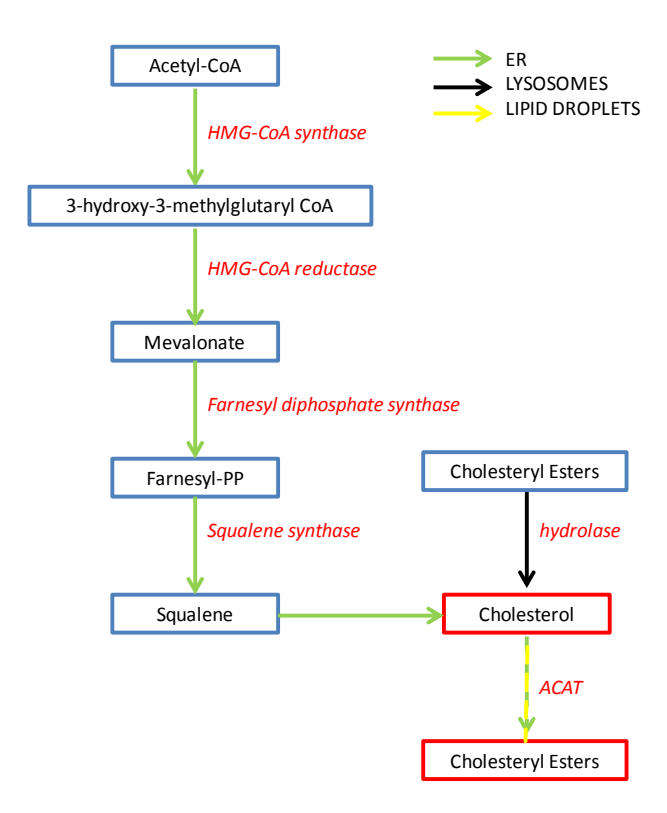


Figure 7. Overview of the sphingolipid (GPL) biosynthesis pathway in mammalian cells. The key metabolites (in black), the enzymes catalyzing the respective reactions (in red) and their subcellular localization (arrows) are indicated. Lipids analyzed in this thesis project are surrounded in red. Most of abbreviations are as indicated in the text proper. Supplementary abbreviations are indicated here: CERK (ceramide kinase); C1P-PPase (ceramide-1-phosphate phosphatase); Gb3 (globotriaosyl); Gg3 (gangliotriaosylceramide); GM3 (ganglioside); iGb3 (Isoglobotrihexosylceramide); Lc3 (lactotriaosylceramides). Infography adapted from the various sources cited in the text.

#### 1.2.3. Sterols

Sterols are a subfamily of steroids, a group of non-hydrolysable lipids that also comprise bile acids and steroid hormones. The structure of sterols is made of a sterane nucleus with four rings and one hydroxylation on carbon 3 (**Fig. 1**). In mammalian cells, the sterols mainly consist of free cholesterol and cholesteryl esters. Cholesterol plays important roles in the fluidity of the plasma membrane as well as the formation of microdomains called "lipid rafts", in interaction with sphingolipids (Simons & Sampaio, 2011). The biosynthesis of cholesterol occurs in the ER with the synthesis of 3-hydroxy-3-methylglutaryl CoA (HMG-CoA) from Acetyl-CoA that is irreversibly reduced into melanovate by the HMG-CoA reductase (HMGCR). Then, mevalonate is converted into 3-isopentenyl pyrophosphate, and six molecules of isopentenyl pyrophosphate are needed to synthesize squalene, the common precursor of all sterols that is also a major component of the skin barrier. Finally squalene is cyclized to form cholesterol (Stryer L., 2012)

(Fig. 8). Cholesterol is often considered as "bad" fat in the collective unconsciousness. This terrible fame comes from the fact that this lipid is associated with atherosclerosis that leads to cardiovascular diseases, the principal cause of death in the world (WHO, 2013). In mammals, cholesterol from diet is absorbed in the intestine and traffics in blood vessels on low-density lipoprotein particles (LDL) that attach to LDL-receptors (LDLR) at the cell surface. Once activated, these receptors are engulfed by cells via clathrin-mediated endocytosis and cholesteryl esters are hydrolyzed in lysosomes before being sent to the ER and the LDLR recycled at the cell surface (Schekman, 2013). From there, free cholesterol is either re-distributed in cell membranes or if in excess, the lipid is re-esterified by acylCoA: cholesterol acyltransferases (ACATs) in the ER and stored in lipid droplets (Brown et al, 1979). The synthesis of LDLR at the cell surface is regulated by the intracellular level of free cholesterol. A deficiency of LDLR leads to hypercholesterolemia and/or atherosclerosis where LDL cannot be internalized by cells, accumulate on the wall of blood vessels and form atheroma plaques (Goldstein & Brown, 1987).



**Figure 8. Overview of the sterol biosynthesis pathway in mammalian cells.** The key metabolites (in black), the enzymes catalyzing the respective reactions (in red) and their subcellular localization (arrows) are indicated. Lipids analyzed in this thesis project are surrounded in red. Most of abbreviations are as indicated in the text proper. Adapted from the various sources cited in the text.

# 1.3. Insights into the canvas of membrane lipid metabolism

In order to understand how cells regulate their lipid levels, it is necessary to consider not only *de novo* lipid biosynthetic pathways but also how these pathways communicate between each other, how they are integrated to the global metabolic network and what the proportion of metabolites coming from food intake is.

Therefore, the purpose of this section is to understand where the metabolites necessary for lipid synthesis come from and how their metabolism may affect lipid levels.

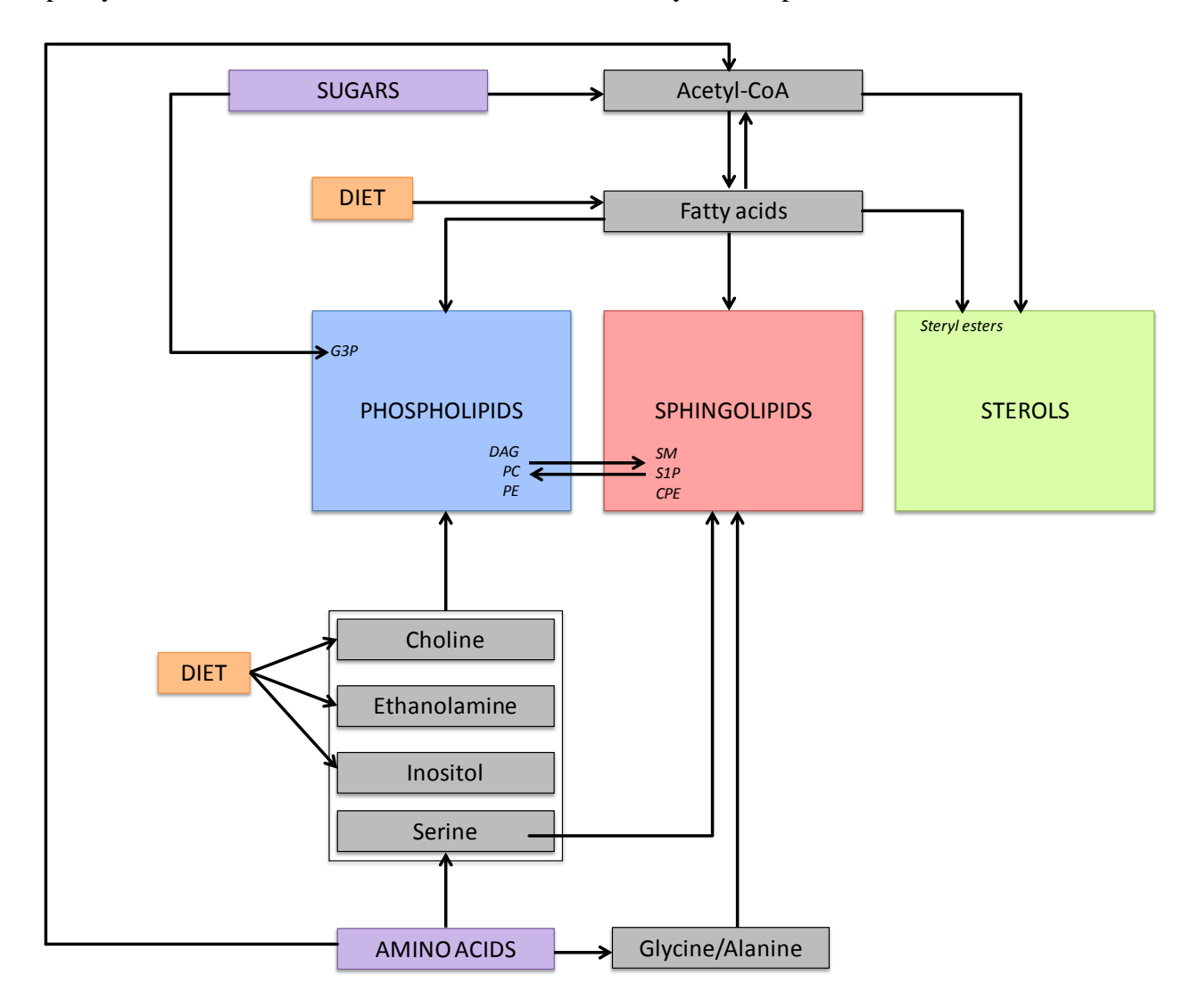


Figure 9. Overview of metabolic crosstalk entering the process of lipid biosynthesis in mammalian cells. Adapted from the various sources cited in the text.

In mammalian cells, most of metabolites needed for lipid synthesis are made by cells themselves but others are only found in diet. This is the case of choline and ethanolamine, the head group components of the most abundant glycerophospholipid species. Cells cannot synthesize them. Therefore, they get them either from food uptake or from the recycling of other lipids. For instance, PC can be produced either from the reuse of phosphocholine resulting from the hydrolysis of SM by sphingomyelinase or from the methylation of PE. In the case of ethanolamine, it can either be released during the decarboxylation of PE into PS or from the degradation of sphingosine-1-phosphate (S1P) by S1P-lyase (Gibellini & Smith, 2010). However, in most cell lines, these represent minor pathways. Myo-inositol that is needed for phosphatidylinositol biosynthesis is derived from glucose-6-phosphate, an intermediate product of glycolysis. However, its synthesis is also limited in animal cells and most of myo-inositol also comes from food, especially fruits (Balla, 2013). On the contrary, serine, the precursor of sphingolipids and the head group component of PS, is an amino acid that can be synthesized by cells and whose the synthesis is highly regulated because of its role in the homeostasis of membrane lipids. Other amino acids can enter in the composition of sphingolipids such as glycine and alanine in order to form alternative sphingoid bases, among which is 1-deoxysphinganine (Zitomer et al, 2009).

Other essential metabolites for lipids are fatty acids, the common component of GPLs, SLs and cholesteryl esters. They are fundamental structural components of membrane bilayers and a major form of energy storage. Fatty acids are synthesized from acetyl-CoA that is carboxylated into malonyl-CoA by the acetyl-CoA carboxylase (ACC) in the cytosol, mainly. Then, acetyl-CoA reacts again with several molecules of malonyl-CoA in a cyclic process in order to produce free fatty acids of different chain length (Wang et al, 2012). Mammalian cells principally synthesize palmitic (C16) and stearic (C18) fatty acids that can be successively elongated and/or desaturated by desaturases and elongase in the cytosol. However, mammalian cells cannot introduce double bonds beyond the  $\Delta 9$  position and need to import fatty acid precursors from plants to synthesize other polyunsaturated fatty acids (PUFA). These essential fatty acids are  $\alpha$ -linolenic and linoleic acids: 18-carbon, polyunsaturated FAs with three and two double bonds respectively that have double bonds at the  $\omega 3$  and  $\omega 6$  positions (Cook, 2008).

Acetyl-CoA doesn't only serve as precursor in the *de novo* synthesis of fatty acids but also of cholesterol and it can be synthesized from different sources in the mitochondrion: beta-oxidation,

oxidative decarboxylation of pyruvate and the catabolism of ketogenic amino acids in a lesser extent (Stryer L., 2012). This makes of acetyl-CoA a hub in the central carbon metabolism. Finally, the common precursor of phospholipid, glycerol-3-phosphate (G3P) also connects lipids to the metabolism of carbohydrates since it results from the reduction of dihydroxyacetone phosphate coming from the breakdown of fructose 1,6-bisphosphate, a intermediate of glycolysis. Alternatively, G3P also results from the phosphorylation of glycerol from the diet by glycerol kinase (Stryer L., 2012).

The connections between lipid, sugar and amino acid biosynthetic pathways are highly coordinated. Depending on their state, cells can shift the metabolic fluxes and promote some pathways to the detriment of others. For instance, proliferating or non-proliferating cells show different metabolic profiles. In proliferating or cancer cells, in order to duplicate their mass before dividing, some enzymes are overexpressed and promote ATP generation through aerobic glycolysis instead of respiration in non-proliferating cells. This process is part of the Warburg effect in cancer cells and it results in more glucose consumption, a lower yield in energy (only 2 ATP per glycolysis compared to 30 ATP during respiration) but more glycolysis intermediates that supplies cells in carbon and nitrogen in order to produce macromolecules to sustain cell division (Ye et al, 2012b). Indeed, the production of DHAP and acetyl-CoA that can be used to synthesize the building blocks of membrane is upregulated. In proliferative cells, many enzymes involved in *de novo* lipid biosynthesis are also activated (**Fig. 10**) (Natter & Kohlwein, 2013). For instance, enzymes needed for de novo PC (Arsenault et al, 2013) and fatty acids synthesis are upregulated. In the case of fatty acids, this leads to higher ratios of saturated and monounsaturated versus polyunsaturated fatty acids since the part of essential fatty acids uptake from nutrients is reduced (Rysman et al, 2010). On the contrary, cells in senescence exhibit almost a contrary metabolic shift with more PC catabolism (Gey & Seeger, 2013) and less synthesis of saturated fatty acids (Ford, 2010).

Before any lipidomics experiment, it is important to know in which metabolic condition we are in order to take in account how they can affect observed lipid changes. Many culture cell lines are derived from cancer. For instance, the HeLa cells are epithelial cells derived from the cervical adenocarcinoma of a patient called Henrietta Lacks, in 1951(Scherer et al, 1953). With time, divisions, selections and maintenance conditions, they diverged from the original cell line and their genome is unstable (Landry et al, 2013). However, these are still proliferating cells and this

is a factor to take in account when interpreting lipid changes notably in their response to stress events. For instance, cancer cells can adapt to hypoxia (Santos & Schulze, 2012). A recent lipidomic analysis of HeLa cells showed that hypoxia caused significant changes in their lipid profile, especially a decrease of PI and the increase of unsaturated fatty acyl chains (Yu et al, 2014).

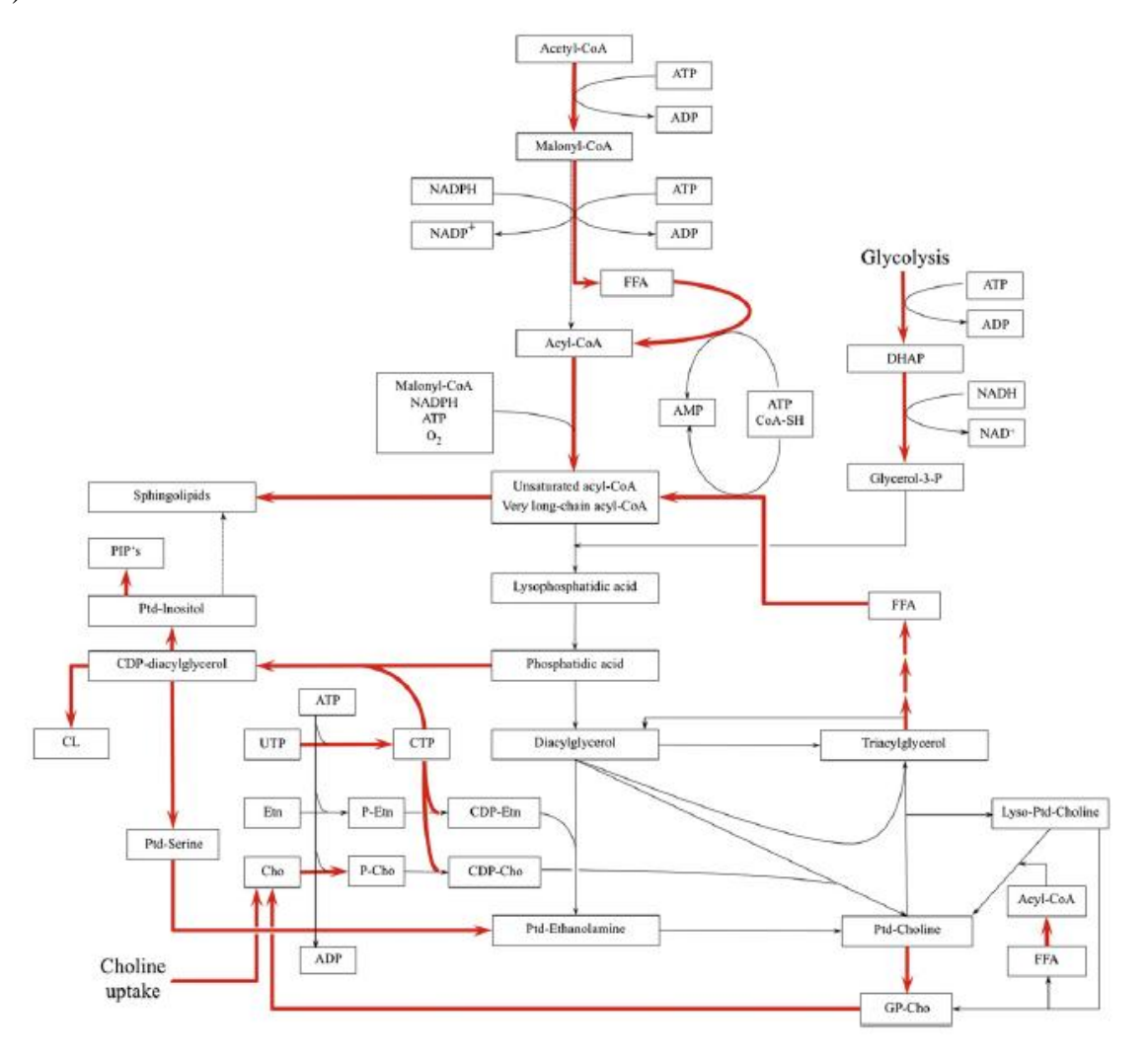


Figure 10. Metabolic pathways for the synthesis of glycerolipids in cancer cells. Due to their increased demand for membrane lipids, most cancers show a lipogenic phenotype. Most prominent are the upregulation of acetyl-CoA carboxylase and fatty acid synthase. Additionally, increased remodeling of phosphatidylcholine is observed in many malignous tissues. Pathways for the synthesis of CTP, the energy donor for phospholipid synthesis, of glycerol-3-phosphate, the FA acceptor in PA synthesis, of unsaturated FA and of phosphocholine are activated in some tumors. The storage formof lipids, triacylglycerol, is also involved in the remodeling ofmembrane lipids in proliferating cells, as suggested by altered regulation of lipases in cancer tissues. Red arrows indicate pathways that were found to play a role in cancer cells. CDP-Cho — CDP-phosphocholine, CDP-Etn — CDP-ethanolamine, Cho — choline, CL — cardiolipin, CTP — cytidine triphosphate, DAG — diacylglycerol, Etn — ethanolamine, FFA — free fatty acids, DHAP — dihydroxyacetone phosphate, G3P — glycerol-3-phosphate, GP-Cho — glycerophosphocholine, PC — phosphatidylcholine, P-Cho — phosphocholine, PE — phosphatidylethanolamine, P-Etn — phosphoethanolamine, PI — phosphatidylinositol, PS — phosphatidylserine, UTP — uridine triphosphate. Reprinted from (Natter & Kohlwein, 2013)

#### 2. Control of membrane lipid homeostasis

#### 2.1. Importance of membrane lipid homeostasis

The metabolism of membrane lipids is controlled at several levels: synthesis, transport, recycling and degradation. While the enzymes involved in the synthesis and breakdown of the most abundant membrane lipids are pretty well characterized, many questions about their regulation remain to be elucidated. Many questions remain also elusive about the regulation of lipid transport and the way cells sense the lipid composition of membranes and adapt their metabolism consequently.

Yet, the control of membrane lipid homeostasis is an essential process that allows cells to maintain both their energetic balance and the structural integrity of the different membranes while keeping a very dynamic trafficking of these membranes. The disruption of membrane lipid homeostasis is associated with several diseases. Some of them are described here with their specific lipid changes and the mechanisms involved when it is known (**Table 1**).

These few examples of diseases are sufficient to show that:

- 1) Many disorders are associated with a lipid phenotype.
- 2) Disorders are not associated with the variation of a single lipid but the combination of several ones and reveal interdependency between metabolic pathways.
- 3) Most of the lipid changes remain uninterpreted, yet.
- 4) There is not yet a complete picture available of the whole modifications of lipids and the hierarchy of events for these diseases.
- 5) Mass spectrometry-based lipidomics coupled to genetic studies greatly improves the knowledge of diseases.

	DISE	DISEASES	MAJOR LIPID MODIFICATIONS	MECHANISMS
		• Obesity		Several genetic deficiencies and diet habits are
2		<ul> <li>Atherosclerosis</li> </ul>	7 Cholesteryl esters, triacylglycerol, fatty acids 1,2,3	involved in the metabolic syndrome.
<u>≥</u>	letabolic syridiolile	• Insulin-resistant Diabetes	7 Lipid oxidation <sup>3</sup>	
		<ul> <li>Steatohepatosis</li> </ul>		
• Ly	<ul> <li>Lysosomal storage diseases</li> </ul>	• Niemann-Pick disease type C	<b>万</b> SM, GSLs, cholesterol in late endosomes⁴	→ NPC1 deficiency Defective lysosomal calcium release
• Pe	<ul> <li>Peroxisomal disorders</li> </ul>		Various disorders linked to deficiencies in etherphospholipid synthesis, peroxisomal beta-oxidation, and alpha-oxidation.	
			ス SM, GM3, LBPA, cholesteryl ester in the prefrontal cortex of AD mice <sup>5</sup>	→ Endolysosomal or autophagy defects?
			カ MUFAs and 凶 PUFAs <sup>6</sup>	→ less PUFA substrates and increase activity of SCD1
		• Alzheimer disease (AD)	→ PAFs, Plasmalogens, PI, PE in brain in late AD <sup>6</sup>	
			≥ SL in Human plasma in late AD 7	
ž 7	<ul> <li>Neurodegenerative diseases</li> </ul>		✓ Sulfatides in early AD 8	
			Several lipid changes in the visual cortex of disease patients <sup>9</sup>	
		<ul> <li>Parkinson disease</li> </ul>	7 Hydroxylated cholesterol <sup>10</sup>	
			N GM111	
		<ul> <li>Huntington disease</li> </ul>	V Cholesterol <sup>12</sup>	→ SREBP deficiency
			Role of bioactive sphingolipids, increase of lipogenesis, lipid biosynthesis <sup>13</sup>	Several mechanisms are involved in cancer
			Changes in phospholipids that can be used as disease marker	pathologies. However, a hallmark of cancer is the Warburg effect that leads to modification in central
•	Cancers		Changes in cardiolipin composition <sup>14</sup>	carbon metabolism that privileges ATP production via aerobic glycolysis
			Upon hypoxia, the lipidomic profile of HeLa cells is modified $^{15}$	Moreover, lipidomic changes depend on cancer types

Table 1. Examples of diseases resulting from the disruption of membrane lipid homeostasis. (Carobbio et al, 2011), 2(Martel et al, 2012), 3(Meikle & Christopher, 2011), <sup>4</sup>(Lloyd-Evans et al, 2008), <sup>5</sup>(Chan et al, 2012), <sup>6</sup>(Bennett et al, 2013), <sup>7</sup>(Han et al, 2011), <sup>8</sup>(Cheng et al, 2013), <sup>9</sup>(Cheng et al, 2011), <sup>10</sup>(Bjorkhem et al, 2013), <sup>11</sup>(Wu et al, 2012), <sup>12</sup>(Valenza et al, 2005), <sup>13</sup>(Santos & Schulze, 2012), <sup>14</sup>(Loizides-Mangold, 2013), <sup>15</sup>(Yu et al, 2014)

# 2.2. Overview of mechanisms that control membrane lipid homeostasis

Lipids are not directly encoded by genes. Therefore, their regulation doesn't rely on their synthesis only, but on the coordinated expression and activity of all the proteins involved in both their metabolism and their transport. How cells decide about the synthesis and the specific distribution of each membrane lipid is an open question. Cells must be able to sense their membrane lipid composition and to adjust both lipid synthesis and distribution depending on their need and of the energy intake. Therefore, the control of membrane lipid homeostasis relies on sensing mechanisms and feedback loops in coordination with the central carbon metabolism. Here, I present an overview of two of these mechanisms in the current state of knowledge as well as the outstanding issues associated with them.

# 2.2.1 Energy sensors and regulatory mechanisms

# • mTOR connects energy sensing to lipid metabolism

The mammalian target of rapamycin also known as mTOR is a serine/threonine kinase that plays a pivotal role in the regulation of cell metabolism. It is part of two multiprotein complexes, named mTORC1 or mTORC2 that phosphorylate different sets of substrates. Both complexes are activated by nutrients and growth factors, are inhibited by stress and regulate cell growth but their composition, their mechanism of regulation, their impact on lipid metabolism and their subcellular localization are different.

The complex mTORC1 is composed of mTOR, raptor and mLST8. It is recruited and activated at the surface of lysosomes but may be also recruited in stress granules by DYRK3 kinase, at the PM by PI(3,5)P2 or in the cytoplasm in order to promote translation initiation. The complete activation of mTORC1 by the effector proteins GTP-bound Rheb and Rag has been recently reviewed by Charles Betz and Michael N. Hall in the Journal of Cell Biology and is summarized on Figure 11. mTORC1 is known to regulate protein synthesis, mitochondrial biogenesis, glycolysis, lipogenesis, lysosome biogenesis and autophagy. In turn, the complex

mTORC2 that comprises mTOR, rictor, SIN1 and mLST8 and that mainly localizes at mitochondria-associated ER membranes (MAMs) (Betz & Hall, 2013) plays a limited role in lipid metabolism in mammals (Laplante & Sabatini, 2009) contrary to yeast where the homolog TORC2 is involved in the regulation of sphingolipids (Aguilera-Romero et al, 2013).

mTORC1 is an energy sensor directly involved in the regulation of lipid homeostasis (**Fig.11**). In the presence of nutrients or signal transduction mediated by growth factors, mTORC1 is activated and induces the expression of genes involved in lipid biosynthesis and lipogenesis through the regulation of transcription factors such as sterol-regulatory element-binding proteins (SREBPs), PPARy and lipins (Laplante & Sabatini, 2009; Laplante & Sabatini, 2013).

- 1) For instance, upon binding of insulin at the cell surface, the activation of the PI3K-Akt signaling pathway leads mTORC1 to induce the positive regulation of SREBPs. SREBPs are transcription factors required for the expression of genes involved in the synthesis of cholesterol, fatty acids, triglycerides and phospholipids. SREBPs are localized in the ER and need to be transported and cleaved in order to translocate into the nucleus. The Akt-mTORC1 pathway induces the cleavage of SREBPs. However, all the effectors of this processing are still unknown (Laplante & Sabatini, 2009; Laplante & Sabatini, 2013). Moreover, the mTORC1 regulation of SREBP occurs through several mechanisms that are not fully understood too. JL Owen and colleagues showed that the processing of SREBP-1 requires the mTORC1 target S6K1 in rat hepatocytes (Owen et al, 2012) but S6K1 was not necessary for this purpose in mouse embryonic fibroblasts (Lewis et al, 2011). In mice, it was also demonstrated that mTORC1 could control the abundance and the localization of nuclear SREBP-1 via the regulation of lipin 1, a phosphatidic phosphatase that is also a transcriptional coactivator (Skelhorne-Gross et al, 2012). mTOR can also phosphorylate lipin 1 to control its localization and its association with phosphatidic acid (PA), which has a direct effect on the synthesis of DAG from PA and a direct impact on glycerophospholipid synthesis (Eaton et al, 2013). Finally, it was recently shown that the kinase MAP4K4 could regulate the adipose lipogenesis by inhibiting the cleavage of SREBP-1 through an AMPK-mTORC1-dependent mechanism (Danai et al, 2013).
- 2) In addition to SREBP-1 and lipin 1, mTORC1 controls fatty acid metabolism through the regulation of PPARγ that activates genes required in the oxidation of fatty acid and triglycerides. However, as for SREBP-1, the regulation of this protein is not fully understood. In the liver,

another peroxisome proliferator-activated receptor called PPAR $\alpha$  regulates ketogenesis and lipid oxidation in response to fasting is regulated by mTORC1 (Laplante & Sabatini, 2009; Laplante & Sabatini, 2013).

3) Finally, mTORC1 indirectly controls lipid homeostasis through the regulation of lysosome biogenesis and autophagy since these processes lead to the degradation of membrane lipids and contribute to regulate the intracellular levels of metabolites (Laplante & Sabatini, 2009; Laplante & Sabatini, 2013).

mTORC1 doesn't only control the metabolism of lipids in response to nutrient uptake or to the binding of growth factors but can also be regulated itself by the level of intracellular lipids (Foster, 2013).

- 1) Phosphatidic acid (PA), which is a central player in glycerophospholipid synthesis binds to mTOR, and is required to ensure the stability of the mTOR complexes (Toschi et al, 2009). Most of the mTOR-associated PAs come from the hydrolysis of phospholipids by phospholipase C (PLC) but could also originate from another pathway such as the de novo synthesis of PA because PLC deficiency doesn't prevent the binding of PA with mTOR (Foster, 2013). For instance, it has recently been demonstrated that mTOR signaling induced by mechanical stimuli in skeletal muscles is regulated by PA synthesized from the phosphorylation of diacylglycerol by diacylglycerol kinase  $\xi$  (DGK $\xi$ ) (You et al, 2014). Moreover, it was suggested that PA could serve as an indicator of phospholipid level in the regulation of lipid metabolism by mTORC1 and 2: first, PA is essential for the activity of mTOR and secondly, it was shown that PA with different fatty acyl chains could differently regulate mTORC1 and 2. Many questions about the regulation of mTOR by PA are outstanding but they raise new possibilities on the control of phospholipid homeostasis.
- 2) A sphingolipid rheostat system regulates mTOR signaling in autophagy. Ceramides and sphingosine-1-phosphate (S1P) are bioactive lipids that tend to promote cell death and survival, respectively. Under amino acid depletion AA(-), acid SMSase is activated and generates ceramide, a suppressor of Akt that leads to the inactivation of mTOR and the induction of autophagy. On the contrary, S1P is a ligand of five G-protein coupled receptors S1P<sub>1</sub>-S1P<sub>5</sub> that

are associated to the activation of various signaling pathway including Akt-mTOR. In AA(-) condition, S1P bound to S1P<sub>3</sub>- counteracts autophagy induction by activating mTOR (Taniguchi et al, 2012; Young et al, 2013).

# AMPK, an essential bioenergetic sensor and its crosstalk with mTOR

The AMP-activated protein kinase (AMPK) is a cellular nutrient and energy sensor that monitors the ratio of AMP/ATP and regulates many metabolic pathways, consequently (**Fig. 11**). The kinase is conserved in all eukaryotes and comprises the catalytic subunit AMPK $\alpha$  and the regulatory subunits AMPK $\beta$  and  $\gamma$ . AMPK  $\gamma$  contains four nucleotide-binding sites also known as CBS motifs and AMPK $\beta$  functions as a hinge that links the three subunits together. Each subunit exists in 2-3 isoforms in mammals. To be active, the AMPK $\alpha$  subunit needs to be phosphorylated. The major upstream kinases phosphorylating Thr 172 of AMPK $\alpha$  is a complex composed of LKB1 (STK11), STRAD and MO25. The binding of AMP or ADP on AMPK promotes its activation either by inducing the phosphorylation of Thr 172 or by preventing its dephosphorylation (Hardie et al, 2012). In some cells, such as HeLa cells that don't express LKB1, AMPK $\alpha$  can still be phosphorylated at Thr 172 by CAMKK $\beta$ , a Ca2+/calmodulin-dependent protein kinases (CAMKKs). This phosphorylation is triggered by a rise in cytosolic Ca<sup>2+</sup>. Whatever the upstream kinase, the phosphorylation of AMPK is independent of the levels of AMP (Fogarty et al, 2010). Alternatively, the TRAIL-induced transforming growth factor-beta-activating kinase 1 (TAK-1) can also phosphorylate AMPK $\alpha$  (Herrero-Martin et al, 2009).

AMPK can be activated by metabolic stress and hormones. The metabolic stress induces the increase of the ratio of AMP or ADP/ATP either by inhibiting the catabolic generation of ATP or by accelerating its consumption. In response to these signals, AMPK switches on the catabolic processes that produce ATP and restricts anabolic pathways that consume this ATP through the phosphorylation of many substrates. Among them, some are directly linked to lipid metabolism such as acetyl-CoA carboxylase 1 and 2 (ACC1 and 2) in fatty acid synthesis, 3-hydroxy-3-methylglutaryl-CoA reductase (HMGCR) that acts on cholesterol biosynthesis, SREBP-1c that controls the expression of lipogenesis enzymes, and enzymes that regulate the synthesis of triglycerides or the uptake of fatty acids (Hardie et al, 2012). To maintain energy homeostasis,

AMPK can also act on the regulation of mTOR (Fig. 11). Indeed, AMPK inhibits the activity of mTORC1 through the phosphorylation of its components such as raptor or the regulatory tuberous sclerosis complex 1/2 (TSC1-TSC2) that prevents the assembly of mTORC1. By inhibiting mTOR, which negatively regulates autophagy, AMPK promotes it (Inoki et al, 2012).

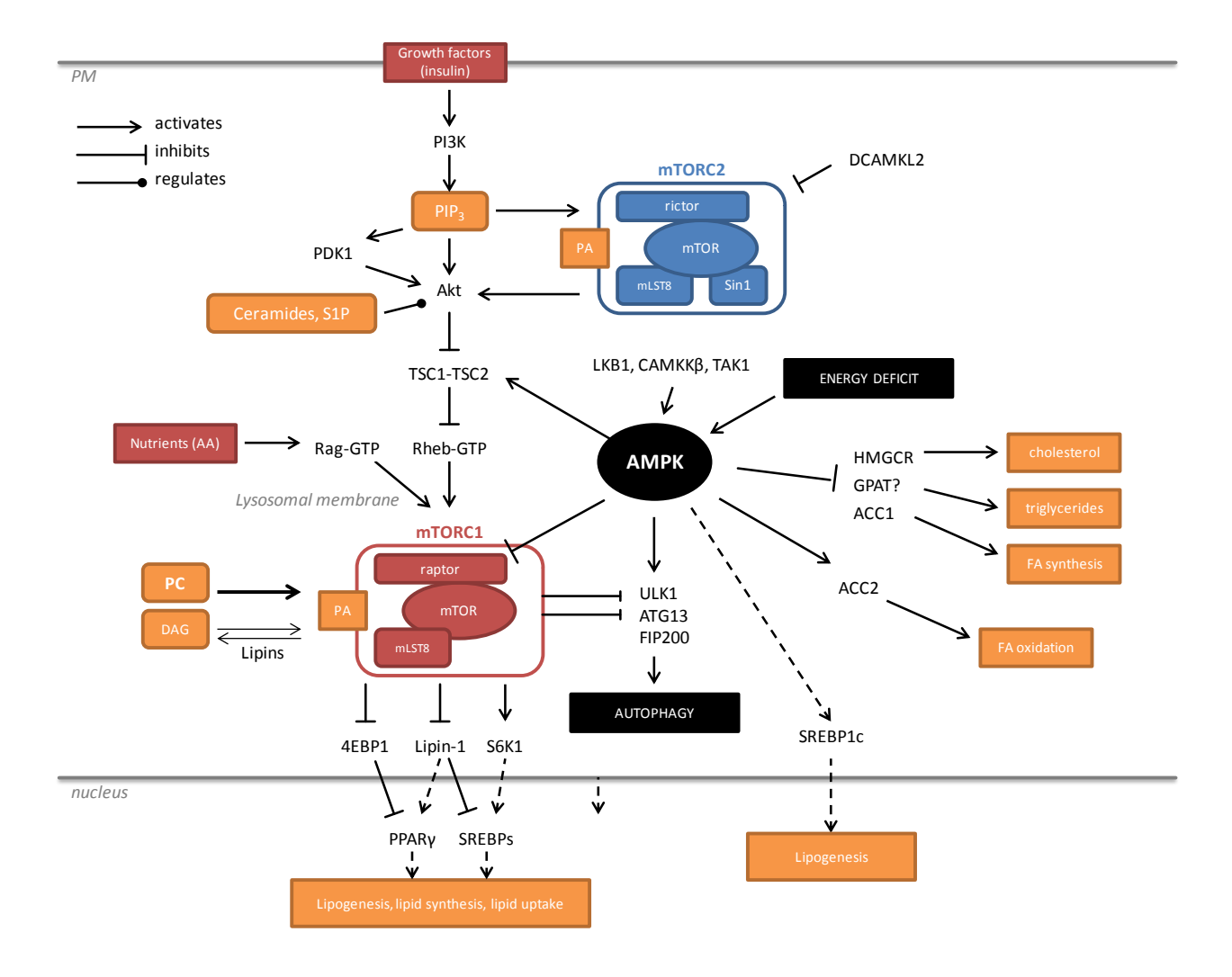


**Figure 11.** Crosstalks between AMPK and mTOR in the control of energy and lipid homeostasis in mammals. The activation of mTORC1 in response to growth factors induces many anabolic processes that favor cell growth and proliferation including *de novo* lipid synthesis by activating several transcription factors and by preventing autophagy. In turn, AMPK also regulates lipid homeostais but in response to metabolic stress by blocking ATP-consuming pathways, while activating the catabolic ones. Adapted from the various sources cited in the text.

# 2.2.2 Control of lipid trafficking by the lipid-transfer proteins (LTPs)

The control of lipid homeostasis doesn't only involve lipid sensors and regulators but also a robust system of distribution to ensure the correct localization of lipids in space and time, the unique composition of organelles as well as the regulation of many signaling pathways.

Along the secretory pathway, from the ER where lipid synthesis starts to the PM, the lipid composition of membranes changes and becomes very asymmetric. Lipids move between organelles by vesicular or non-vesicular mechanisms such as the spontaneous desorption and more likely the active transport by transfer proteins. Between the two leaflets of organelles, the asymmetry depends on the side where lipids are synthesized, their spontaneous flip-flop and the action of flippases and translocases. Many but not all lipid transfer proteins have already been described and the mechanisms that control their function gives rise to growing interest. Interestingly, they already reveal the interdependency between signaling pathways and lipid metabolism, as well as between lipids themselves. Here, I propose to describe one of these mechanisms as well as the questions they raise in the control of membrane lipid homeostasis.

Typically, lipid-transfer proteins (LTPs) are soluble factors with hydrophobic lipid-binding pockets covered by a lid that transport lipids in aqueous phase. LTPs are subdivided in different families according to their similarities and the lipids they transport. They are: oxysterol-related proteins (ORPs), SEC14, PI-transfer proteins (PITPs), steroidogenic acute regulatory protein-related lipid transfer (START) domain family proteins (STARDs), glycolipid transfer proteins (GLTPs) and SCP-2 (unspecified LTPs). LTPs can be specific for one or more lipids. For instance, the START protein CERT is specific for ceramides whereas SCP-2 can transfer phospholipids, glycolipids and sterols. The functions and lipid affinities of each LTPs have already been described in very interesting reviews (D'Angelo et al, 2008; Drin, 2014; Lev, 2010). The membrane association, lipid absorption and the flux direction of lipid transport by LTPs mostly depend on the membrane composition. Lipids are transported from concentrated donor places toward less concentrated acceptor membranes. However, lipid-protein specificity and lipid concentration are not the only parameters that control the transfer of lipids. Indeed, most of LTPs don't only comprise a lipid-binding domain but also other domains that condition their association with lipids according to the membrane environment.

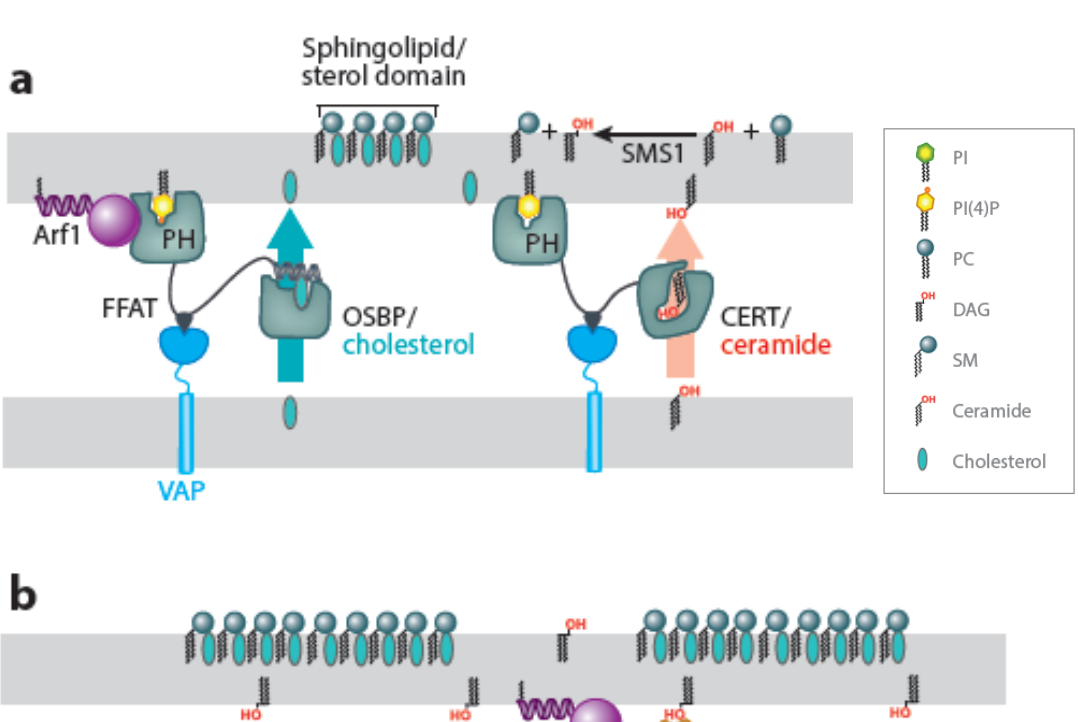
This is the case of CERT. The mechanism regulating the specific transfer of ceramides from ER to Golgi by CERT illustrates the link between membrane lipid homeostasis and the regulation of lipid transfer proteins. CERT is 68kDa cytoplasmic protein that comprises a N-terminal pleckstrin homology domain (PH) that is recognized by the phosphoinositide PI(4)P enriched at the Golgi membrane, a START domain that catalyzes the inter-membrane transfer of ceramide, a short peptide motif named two phenylalanines in an acidic tract (FFAT) that can bind to the ER-membrane resident VAMP-associated protein (VAP) and a serine-repeated motif (SRM) that can be phosphorylated to repress both the functions of PH and START domains. The presence of the START domain alone is not sufficient to ensure the ER-to-Golgi ceramide transport *in vivo*. The activity of CERT is regulated by its other domains and is coordinated to sterol homeostasis through the activity of the oxysterol binding protein (OSBP), another LTP very similar to CERT that can be either cytosolic or bound to VAP at the surface of the ER by a FFAT domain, too (Hanada et al, 2007).

CERT exists in two conformations: inactive when phosphorylated on its SRM domain by the protein kinase D (PKD) or by casein kinase gamma 2 (CKI $\gamma$ 2) (Tomishige et al, 2009) and active upon dephosphorylation by the protein phosphatase 2C $\xi$  (PP2C $\xi$ ).

PKD has a dual role in the regulation of CERT. The transfer of ceramides from ER-to-Golgi by CERT induces the synthesis of SM and the release of DAG at the Golgi membrane. DAG is a cone-shaped lipid and a second messenger that induces membrane curvature and the recruitment of PKD that phosphorylates CERT and represses its localization to the Golgi (Fugmann et al, 2007). Another substrate of PKD is PI4KIIIβ. Upon phosphorylation PI4KIIIβ induces the synthesis of PI(4)P in the Golgi which in turn promotes the recruitment of PI4P-binding proteins at the Golgi membrane (Nhek et al, 2010). With its PH domain, CERT is a PI(4)P binding protein but it's not the only LTP in this case: the VAP-bound OSBP, too. As CERT, OSBP is recruited to the Golgi by PI(4)P and its Golgi-localization is also repressed PKD-mediated phosphorylation (Nhek et al, 2010). Moreover, SM and cholesterol are co-regulated. Upon excess of free cholesterol in cells or in the presence of 25-hydroxycholesterol, OSBP translocates to the Golgi where it specifically stimulates the translocation of CERT (Perry & Ridgway, 2006). This coordinated translocation of CERT to the Golgi seems associated with the specific recruitment of rPI4KIIα, a PI(4)P kinase, around OSBP at the Golgi membrane (Banerji et al, 2010). Since the structural association between SM and cholesterol at the PM is essential to ensure many

biological processes and the biophysical properties of the PM, Guillaume Drin suggests that OSBP could bridge the ER with the Golgi membrane in membrane contact sites (MCSs) to facilitate the recruitment of CERT and regulate both SM and cholesterol in a concerted way to favor the formation of SM/cholesterol domains at the PM (Fig 12) (Drin, 2014). However, some questions remain to be solved such as the precise mechanism of association between CERT and the Golgi. Indeed, It was demonstrated that the PH domain of CERT is required for its activity (Hanada et al, 2003) but nuclear magnetic resonance (NMR) studies show that the affinity of CERT PH domain for PI(4)P is weak compared to PH domains of other proteins, probably because of a conformational flexibility in the ligand-binding pocket (Prashek et al, 2013). The presence of a basic groove near the PI(4)P recognition site in the PH domain is required for CERT activity and might stabilize this recognition (Sugiki et al, 2012). However, the precise mechanism by which CERT binds to the Golgi remains elusive and doesn't exclude the intervention of still unknown effectors at the Golgi membrane.

Other mechanisms seem to regulate CERT. For instance, in response to pro-apoptotic stress, the disassembly of the Golgi coupled to the caspase-mediated cleavage of CERT leads to the decrease of ceramide trafficking (Chandran & Machamer, 2012). A recent article from F.G. Tafesse and colleagues also suggests that CERT could be the first line of defense against apoptosis by preventing the routing of ER-resident ceramides to mitochondria (Tafesse et al, 2014). On the other side, the interaction between CERT and VAP seems also to be affected by the phosphorylation of a serine adjacent to the FFAT motif. The phosphorylation of S315 in the SRM motif also down-regulates the activity of CERT (Chandran & Machamer, 2012; Kumagai et al, 2014). Finally, little is known about the transcriptional regulation of this protein essential in sphingolipid metabolism whereas its expression greatly influences the resistance of cancer cells to chemotherapeutic drugs (Swanton et al, 2007).



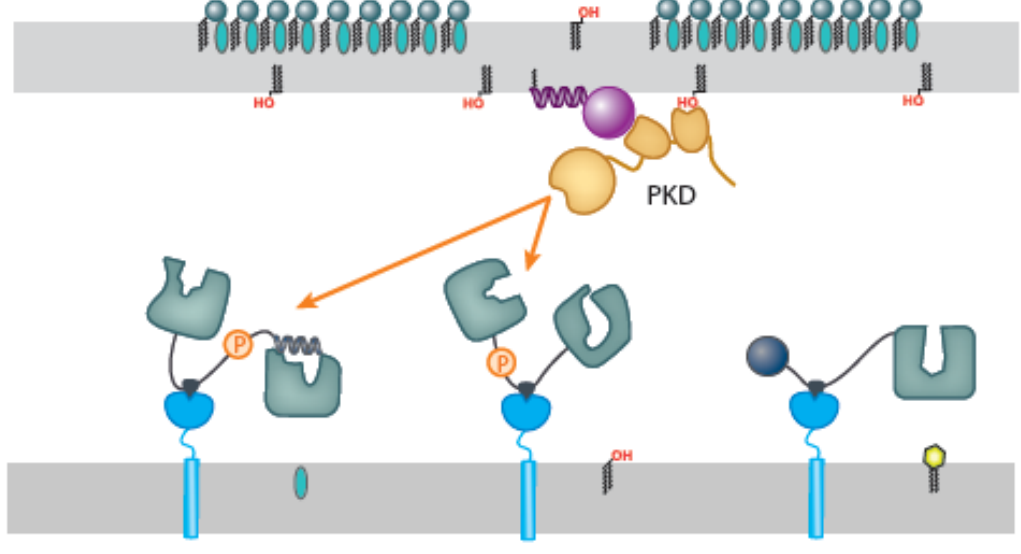


Figure 12. Mechasnism of CERT-mediated transfer or ceramide from ER-to-Golgi in mammals.. (a) Oxysterol-binding protein (OSBP) interacts via its PH domain with PI(4)P and Arf1–GTP and through its FFAT motif with ER-resident VAP receptors. As such, OSBP could bridge the ER and the trans-Golgi membrane and facilitate the recruitment of ceramide transfer protein (CERT) by PI(4)P and VAP receptors. CERT delivers ceramide into the trans-Golgi, thereby promoting sphingomyelin (SM) synthesis. (b) The completion of sterol transport; the consumption of PI(4)P; and the diacylglycerol (DAG)- and Arf1-dependent recruitment of protein kinase D (PKD), which negatively regulates via phosphorylation the Golgi localization of OSBP and CERT, trigger the disassembly of the membrane contact site (MCS) and stop lipid trafficking. Abbreviations: PC, phosphatidycholine; PI, phosphatidylinositol; VAP, VAMP-associated protein. Reprinted from (Drin, 2014).

# 2.2.3 Control of sphingolipid homeostasis: review

This review was co-written with Dr. Maria-Auxiliadora Aguilera Romero and published in 2013 in BBA – Molecular and Cellular Biology of Lipids. It proposes an overview of the mechanisms that control sphingolipid homeostasis in eukaryotes and the issues they raise.

Aguilera-Romero A, Gehin C, Riezman H (2013) Sphingolipid homeostasis in the web of metabolic routes. *Biochimica et biophysica acta* 1841(5):647-56. doi: 10.1016/j.bbalip.2013.10.014

## 3. Aim of the studies

The control of lipid homeostasis is a fundamental process that allows cells to maintain the unique lipid composition of their membrane compartments and to deal with the energetic fluxes from metabolism. This control is done at several levels and involves lipid sensors, signaling systems, regulators as well as a robust machinery of lipid distribution across membranes. If most enzymes involved in lipid metabolism are now characterized, the question of the genetic control of lipid homeostasis is still outstanding.

In order to find genes that control the homeostasis of membrane lipids, we combined a large-scale RNAi screen with the techniques of targeted lipidomic analysis by mass spectrometry to monitor lipid changes in HeLa cells. After validation of the method through a pilot screen with siRNA targeting genes with a connection to lipid metabolism, a large-scale RNAi screen targeting the human kinome was performed. For the first time, it was possible to observe the effects of genetic perturbations on the level of hundreds of membrane lipids with different combinations of head groups and fatty acyl chains simultaneously in HeLa cells. This thesis particularly deals with the development of the method as well as the results from the primary screen.

In parallel to this project, in the context of the Swiss National Center of Competence in Research (NCCR) Chemical Biology, we also developed and performed a robotically-assisted screen of a novel class of chemicals in order to find compounds able to transfect siRNA into human cells with some advantages over as commercially available compounds.

#### MATERIAL AND METHODS

## 1. Experimental procedures

#### siRNA screen

Cell culture and siRNA transfection. HeLa MZ (Marino Zerial, MPI-Dresden) cells were maintained in DMEM, high glucose, GlutaMAX<sup>TM</sup>, supplement pyruvate (Life technologies) with 10% FCS without antibiotics. The same batch of FCS was used all along the kinome-wide siRNA screen. All cells were grown at 37°C and 5% CO2. 72pmol siRNA was delivered by forward transfection. HeLa cells were transiently transfected with siRNA in 6cm dishes using Lipofectamine RNAiMAX (Invitrogen) according to the manufacturer's instructions.

Pilot, primary and confirmation screens. The sequences of all custom siRNA libraries used for this study are listed in Appendix (127). The pilot screen was run using a custom library of siRNAs from Qiagen, in three independent experiments performed on separate days. For the pilot screen, each gene was targeted by two different siRNAs in individual wells. The kinome-wide primary screen was run using the MISSION® siRNA Human Kinase Library (Sigma-Aldrich) consisting of 719 pools of three different siRNA oligos targeting the same gene transcript. The screen also comprised controls: siControl, a negative control consisting in a non-targeting sequence of siRNA sharing homology with the human genome (AllStars Negative Control siRNA from Qiagen) and the CERT ON-TARGETplus Smartpool siRNAs from Dharmacon (positive control). The screen was run in duplicate in independent experiments on separate days. For the confirmation screen, unpooled Silencer® Select siRNAs for 59 of the top hits were purchased as a custom library from Ambion (Life Technologies), with each gene transcript being targeted by three different siRNAs in individual wells. These siRNAs were forward transfected individually into HeLa MZ cells and their lipid composition was assessed by mass spectrometry.

RNA extraction and quantitative reverse transcriptase PCR (qRT-PCR). HeLa MZ in 6cm dishes were forward transfected as described in the previous paragraph. 72h later, one tenth of cells were extracted with the RNeasy kit (Qiagen), reverse transcribed with Superscript II

(Invitrogen), and analyzed in triplicate by qRT-PCR using a single color real-time PCR detection system and specific DNA primers (Microsynth) designed with NCBI Primer-BLAST. The results were normalized to TATA box-binding protein (TBP) expression. The sequences of all oligonucleotides used for this study are listed in Appendix (127).

# **Lipid extraction protocols**

Chemicals and lipid standards. DLPC 12:0/12:0 (850335), PE 17:0/14:1 (PE31:1, LM-1104), PI 17:0/14:1 (PI31:1, LM-1504), PS 17:0/14:1 (PS31:1, LM-1304), C17:0 ceramide (860517), C12:0 SM (860583) and Glucosyl C8:0 Cer (860540) were used as internal lipid standards and were purchased from Avanti Polar Lipids Inc. (Alabaster, AL). Ergosterol was used as sterol standard and was purchased from Fluka (Buchs, Switzerland).

Methyl tert-butyl ether (MTBE) was from Fluka (Buchs). Methyl amine (33% in absolute ethanol) was from Sigma Aldrich (Steinheim, Germany). HPLC-grade chloroform was purchased from Acros (Geel, Belgium), LC-MS grade methanol and LC-MS grade ammonium acetate were from Fluka. LC-MS grade water was purchased from Biosolve (Valkenswaard, The Netherlands).

Lipid analysis. Lipid extracts were prepared using the MTBE protocol (Matyash et al, 2008). Briefly, after 72h of siRNA transfection, HeLa MZ cells from 6cm dishes were harvested and resuspended in 100 μl H<sub>2</sub>O. The suspension was transferred into a 2 ml Eppendorf tube. 360 μl methanol and a mix of internal standards were added (400 pmol DLPC, 1000 pmol PE31:1, 1000 pmol PI31:1, 3300 pmol PS31:1, 2500 pmol C12SM, 500 pmol C17Cer and 100 pmol C8GC). Samples were vortexed and 1.2 ml of MTBE was added. Samples were placed for 10 min on a multitube vortexer at 4°C (Lab-tek International, Christchurch, New Zealand) followed by an incubation for 1 hr at room temperature (RT) on a shaker. Phase separation was induced by addition of 200 μl MS-grade water. After 10 min of incubation at RT samples were centrifuged at 1000 g for 10 min. The upper (organic) phase was transferred into a 13 mm glass tube with a Teflon-lined cap and the lower phase was reextracted with 400 μl artificial upper phase (MTBE / methanol / H2O 10:3:1.5). In total 1500 μl of organic phase was recovered from each sample, split into three parts and dried in a CentriVap Vacuum Concentrator (Labconco, MO, USA). One

part was treated by alkaline hydrolysis to enrich for sphingolipids and the other two aliquots were used for glycerophospholipid/phosphorus assay and sterol analysis, respectively.

Alkaline hydrolysis was used to deacylate glycerophospholipids according to the method by Clarke (Clarke & Dawson, 1981). Briefly, 1 ml freshly prepared monomethylamine reagent (methylamine/ $H_2O/n$ -butanol/methanol at 5:3:1:4 (vol/vol)) was added to the dried lipid extract and then incubated at 53°C for 1 hr in a water bath. Lipids were cooled to RT and then dried. For desalting, the dried lipid extract was resuspended in 300  $\mu$ l water-saturated n-butanol and then extracted with 150  $\mu$ l  $H_2O$ . The organic phase was collected, and the aqueous phase was reextracted twice with 300  $\mu$ l water-saturated n-butanol. The organic phases were pooled and dried in a CentriVap Vacuum Concentrator.

# Sterols analysis by Gas-liquid mass spectrometry (GC/MS)

One third of total lipid extract was resuspended in  $500\mu$ L of MS-grade chloroform/methanol (1:1) solution and injected into a VARIAN CP-3800 gas chromatograph equipped with a Factor Four Capillary Column VF-5ms 15m x 0.32 mm i.d. DF =100. Identification and quantification of sterol species were performed using a VARIAN 320MS as described in (Guan et al, 2010)

## Phospholipids and sphingolipids analysis by electrospray ionization mass spectrometry (ESI-MS)

Identification and quantification of phospholipid and sphingolipid molecular species were performed using multiple reaction monitoring with a TSQ Vantage Triple Stage Quadrupole Mass Spectrometer (Thermo Scientific) equipped with a robotic nanoflow ion source, Nanomate HD (Advion Biosciences, Ithaca, NY). Each individual ion dissociation pathway was optimized with regard to collision energy. Lipid concentrations were calculated relative to the relevant internal standards as described in (Epstein et al, 2012) and then normalized to the total phosphorus content of each total lipid extract to adjust for difference in cell size, membrane content, and extraction efficiency.

# **Determination of total phosphorus content.**

The dried total lipid extract was resuspended in 250  $\mu$ l chloroform/methanol (1:1) and 50  $\mu$ l were placed into a 13 mm disposable pyrex tube. The solvent was completely evaporated and 0, 2, 5, 10, 20  $\mu$ l of a 3 mM KH2PO4 standard solution were placed into separate pyrex tubes. To each tube 20  $\mu$ l of water and 140  $\mu$ l of 70% perchloric acid were added. Samples were heated at 180°C for 1 hr in a hood. Tubes were then removed from the block and kept at RT for 5 min. Then 800  $\mu$ l of freshly prepared H<sub>2</sub>O / 1.25% NH<sub>4</sub>Molybdate (100 mg / 8 ml H<sub>2</sub>O) / 10% ascorbic acid (100 mg / 6 ml H<sub>2</sub>O) in the ratio of 5:2:1 were added. Tubes were heated at 100°C for 5 min with a marble on each tube to prevent evaporation. Tubes were cooled at RT for 5 min. 100  $\mu$ l of each sample was then transferred into a 96-well microplate and the absorbance at 820 nm was measured (Rouser et al, 1970).

# **Determination of Glycosphingolipid species**

Sphingolipids were extracted using the MTBE/methylamine protocol. Samples were resolved on HPTLC silica gel 60  $F_{254}$  (Merck). To distinguish GalCer and GlcCer the HPTLC plates were impregnated with borate as described previously (Gupta et al, 2010). After dipping the plates into a 1% aqueous sodium tetraborate solution, the HPTLC plates were activated at  $120^{\circ}$ C for 30 min. Sphingolipids were resolved with the solvent system of chloroform/methanol/water (100:30:4). Glycosylated sphingolipids were visualized by putting the whole plate quickly in a sulfuric acid/Orcinol solution (0.1% Orcinol, 5%  $H_2SO_4$ ) and heating the plate at  $110^{\circ}$ C for 3min.

# 2. Statistical analysis of the Kinome-wide RNAi screen

Data formatting and normalization. In all screening experiments, lipid quantities were first  $\log_2$  transformed. Then, sample-based normalization was performed using the z-score according to the following formula:  $Z = (x_i - \bar{x})/\sigma_x$ , where  $x_i$  is the lipid level of the gene i,  $\bar{x}$  is average of lipid levels of all samples from the same series, and  $\sigma_x$  is the standard deviation of lipid quantities of all samples from the same series (Birmingham et al, 2009).

Filter on toxic conditions and technical issues. Images of cells 72h post siRNA transfection were analyzed with the open-source image analysis software CellProfiler (Carpenter et al, 2006). Samples with less than 80% of occupied area covered by objects (=cells) were considered as representative of samples with too few cells for objective interpretation of results. siRNA conditions resulting in few cells, cytotoxicity, incomplete lipid profiles due to mass spectrometry technical issues and unpaired correlation between biological replicates were discarded from the global analysis. Discarded conditions are listed in the appendix (127)

Selection of primary hits. Two different statistical methods were used for hit selection. First, threshold determination was performed for each phenotypic score using the ranking method. Specifically, this corresponds to cutoff phenotypic scores of |z| >= k, where k is a preset constant that represents the mean of the dataset  $\pm kSD$ , where SD is the standard deviation. Genes with one or more phenotypic scores above the cutoff values were selected as hits. (Zhang, 2011a).

In addition, functional genetic interaction was predicted for genes with directed hierarchical relationships between pairwise variables using the hierarchical interaction score (HIS) method as described (Snijder et al, 2013). For each gene, a HIS was calculated and predicted gene interactions were visualized with the open source software <a href="http://www.his2graph.net/">http://www.his2graph.net/</a> and Cytoscape (Shannon et al, 2003). Genes with top-scoring hierarchical interactions were selected as hits.

*Graphical representation.* Graphical representations and statistical analysis of RNAi datasets were performed using Excel and Partek Genomics Suite 6.6.

Omics and reference datasets. Gene-enrichment annotation of hit kinases was performed using the websites DAVID (Huang da et al, 2009), STRING (Jensen et al, 2009) and WEBGESTALT (Wang et al, 2013), as well as datasets published in literature or unpublished from other lab projects (yeast data from Aline Santos) and collaborators (endocytome data Prisca Liberali, Pelkmans lab, Zurich). Published levels of gene expression in HeLa cells were retrieved from the web database Genevestigator. Yeast homologs were retrieved using Ensembl Biomart <a href="http://www.ensembl.org/biomart/martview/d1111d7a07f83994b3c68c2d2a08db73">http://www.ensembl.org/biomart/martview/d1111d7a07f83994b3c68c2d2a08db73</a>.

#### **RESULTS**

# 1. Investigating the genetic control of membrane lipid homeostasis with RNA interference

#### 1.1. Choice of siRNA as a tool for genetic perturbation screen in human cells.

In order to assess the function of kinases in membrane lipid homeostasis, a genetic perturbation screen based on RNA interference (RNAi) was performed in HeLa cell lines because their genes can be efficiently silenced with short interference RNA (siRNA) (Elbashir et al, 2001).

RNAi is a post-transcriptional regulatory mechanism that consists in transiently silencing the expression of a target gene through the repression or the cleavage of its mRNA by the RNA-induced silencing complex (RISC). RISC is made of proteins and a short ssRNA sequence complementary to the target mRNA that results from the unwinding of an endogenous (microRNAs) or an exogenous (siRNA) dsRNA by the Ago2 protein (Hammond et al, 2001). Fire and Mello who first observed that the introduction of exogenous dsRNA in *C.elegans* could induce RNAi (Fire et al, 1998) opened the way to siRNA-induced gene knockdown screens in higher eucaryotes. Current techniques lead to transient or long-term RNAi using siRNAs or short-hairpin RNA (shRNA), respectively. For this project, I chose siRNAs in order to stay in conditions comparable to other genetic screens performed by collaborating groups from SystemsX.ch, the Swiss Research Initiative in Systems Biology, such as the teams of Lucas Pelkmans (Zurich) and Jean Gruenberg (Geneva). Moreover, I obtained the siRNA library from the Pelkmans lab.

In mammalian cells, loss-of-function genetic screens are largely based on RNAi induced gene knockdown. Contrary to yeast, knockout gene libraries are not available. At least, it was not the case when this project started in 2009. Since, libraries of mutant mammalian cell lines have been created thanks to recent nuclease-based genome editing technologies (Shalem et al, 2014). Moreover, contrary to gene knockout experiments, siRNA-induced gene silencing offers the advantage to assess the function of essential genes, since it transiently decreases their mRNA levels without completely suppressing them from the genome.

# 1.2. Mass spectrometry targeted-lipidomics to quantify membrane lipid changes.

In order to quantify membrane lipid changes induced by siRNA gene knockdown in mammalian cells, a targeted-lipidomics approach developed in our group by Dr. Ursula Loizides-Mangold and Isabelle Riezman (Guan et al, 2010) (Loizides-Mangold et al, 2012). First, the detection of most abundant PLs and SLs species present in different mammalian cell lines was performed by shotgun lipidomics using the LTQ-Orbitrap mass spectrometer. Then, lipid species were identified using the lipid mass references described in literature and online ressources such as LIPID MAPS structure Databases (Sud et al, 2007) and KEGG (Kanehisa et al, 2014; Wixon & Kell, 2000). However, current databases of chemicals are incomplete. Thus, several lipid species with different combinations of head groups, acyl chains and additional chemical groups, such as hydroxylations or phosphate, were found manually by Dr. Ursula Loizides-Mangold.

Next, a multiple reaction monitoring assay was developed to selectively quantify PLs and SLs species described previously using a triple stage quadrupole mass spectrometer coupled to an electron spray ionization source (Fig. 1.). The masses of parent and fragment ions used for this study are listed in the appendix (p127). This list allowed to detect and quantify more than 800 molecules if present in the sample. However, the mass of several sphingolipids was overlapping because of dehydration and others were not detected in all samples. Thus, this list was reduced for analysis (see p127). In order to quantify lipids, internal lipid standards representative of each different lipid classes were added to cells before lipid extraction allowing the semi-absolute quantification of lipid molecules thanks to pre-established standard curves. Absolute quantification was not possible for PLs and SLs because it supposes the presence of specific internal standards for each lipid species. For the analysis of SLs, a mild alkaline hydrolysis step was added to the lipid extraction process in order to reduce ion suppression during MS analysis caused by GPLs. Finally, cholesterol and sterol esters were quantified separately by GC-MS using the ergosterol internal standard (Fig. 1).

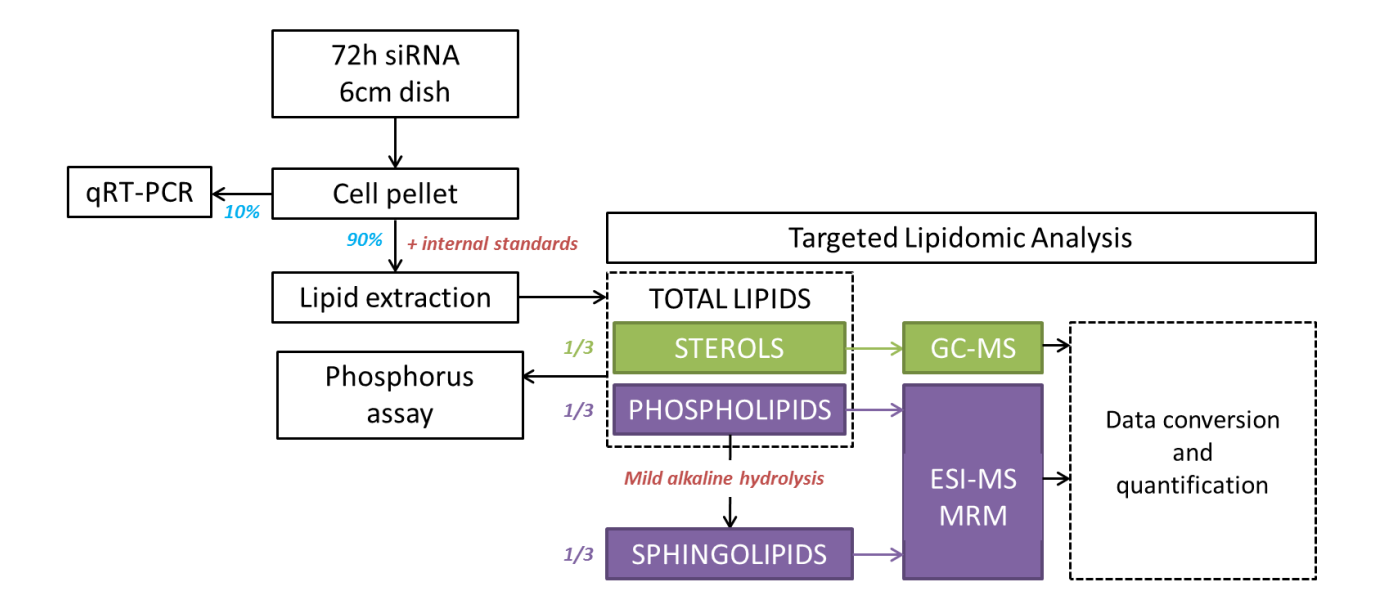


**Figure 1. General Overview of the screening procedure.** 72h after siRNA transfection, Human cells were harvested and their lipid extracted to be analyzed either by GC- or ESI-MS depending on the lipid species. A fraction of the cell pellet was reserved for validation of the gene knockdown by qRT-PCR. A fraction of the lipid extract before base treatment (methylamine) was used for the determination of total phosphorus.

## 1.3. A pilot siRNA screen on lipid-related proteins identifies gene-specific lipid changes

When this project started in 2009, studies combining genetics and quantitative lipid analysis by mass spectrometry were emerging. In 2009, Guan XL and colleagues had just described functional interactions between SLs and sterol metabolism with this approach. By determining the lipid profile of yeast mutants in sterol metabolism using mass spectrometry, they observed yeast cells specifically adjust their SLs composition according to the presence of different sterol structures in their membrane (Guan et al, 2009). With this study, they demonstrated the validity of the method for yeast. However, for higher eucaryotes such as human cell lines, where genetic perturbation screens are generally based on RNAi, no such study had been published yet. In 2008, Grimard V. and colleagues reported lipidomic observations from a kinome-wide siRNA screen performed in HeLa cells. However, they used thin-layer chromatography (TLC) to monitor lipid changes instead of mass spectrometry (Grimard et al, 2008). TLC is a method of lipid analysis much less sensitive than mass spectrometry and they could not distinguish lipid species inside each lipid class, leading to a loss of information important for the comprehension of membrane

lipid homeostasis, such as acyl chain distribution, phosphorylation or the unsaturation degree of SLs and GPLs. Later, in 2011, Ursula Loizides-Mangold reported that siRNA knockdown of genes coding for enzymes from the GPI-anchored protein synthesis pathway and their corresponding mutant cell lines share similar lipid profiles (Loizides-Mangold et al, 2012). Meanwhile, I was performing a pilot screen on lipid-related proteins to assess the validity of the RNAi approach to identify gene specific lipid changes in HeLa cells. Several studies have combined siRNA-induced gene knockdown with lipid studies. However, no one combined a genetic screen to the lipidomics approach.

# 1.3.1. Choice of target genes for the pilot screen

In order to assess the ability of siRNAs to induce significant and reproducible membrane lipid changes, I chose a set of target genes coding for proteins acting in lipid homeostasis (**Table 1**) and for which the knockout or gene silencing experiments affecting the membrane lipid composition of mammalian cells had been previously described. I privileged the ones known to be expressed in my cell system, the HeLa cell line, based on the web database Genevestigator (Hruz et al, 2011). The expression of target genes in the HeLa cell line from the lab was then confirmed using qRT-PCR (**Fig. 2**). Planning to further screen the kinome, I also privileged gene targets among kinases.

#### 1.3.2. Efficacy of siRNA-induced gene knockdown

In order to study the roles of selected target genes (**Table 1**) in regulating membrane lipid levels in HeLa cells and assess the off-target effects, each target gene was knocked down independently using two different siRNAs. Each experiment was repeated two to three times independently. 72h post siRNA transfection, the efficacy of siRNA-induced gene knockdown on the transcript levels of each target gene was monitored using qRT-PCR. Ten percent of the cell pellet used for quantitative lipid analysis was reserved for this purpose in a spare tube before lipid extraction (**Fig. 1**.). Oligonucleotide primers were designed using the open-source software NCBI Primer-Blast (Ye et al, 2012a). The sequences of all oligonucleotides used for this experiment are listed in the appendix (p29). mRNA levels were measured using Real-Time PCR and normalized to TBP mRNA (**Fig. 2**.). Most siRNA experiments induced more than 70% of gene knockdown compared to non-transfected HeLa cells. Only the silencing of CERS2 and CERS3 genes could not be quantified due to a loss of samples.

# Results

Target gene	Encoded protein and functions in lipid metabolism					
CHKA choline kinase alpha	<ul> <li>CK-alpha (Choline kinase alpha)</li> <li>Catalyzes the first step in PC biosynthesis and contributes to PE biosynthesis.         Phosphorylates Cho and EthN.     </li> <li>CHKA siRNA in breast cancer cells and decreases PC level (Glunde et al, 2005)</li> <li>CHKA siRNA in HeLa cells decreases PCho and slightly decreases the pool of PC (Yalcin et al, 2010)</li> <li>Homozygous mutant mice (Chka(-/-)) are embryonic lethal (Wu &amp; Vance, 2010)</li> <li>Heterozygous mutant mice (Chka(+/-)) are viable and show no reduction in PC (Wu et al, 2008)</li> </ul>					
CHKB choline kinase beta	<ul> <li>CKB (Choline/Ethanolamine kinase)</li> <li>Catalyzes the first step in PE biosynthesis. Phosphorylates ethanolamine, and can also act on choline (in vitro). May not significantly contribute to in vivo PC biosynthesis</li> <li>Overexpression of CHKB in HEK293 and MDCK increases PE levels</li> <li>Homozygous mutant mice (Chkb(-/-)) survive to adulthood but show muscular dystrophy and impairment on PC biosynthesis.(Wu &amp; Vance, 2010)</li> </ul>					
ETNK1 ethanolamine kinase 1	<ul> <li>EK1 (Ethanolamine kinase 1)</li> <li>Highly specific for EthN phosphorylation. May be a rate-controlling step in PE biosynthesis</li> <li>Overexpression of a mammalian ETNK1 accelerates the CDP-ethanolamine pathway (Lykidis et al, 2001)</li> </ul>	9.89				
FA2H fatty acid 2- hydroxylase	<ul> <li>FA2H/FAAH</li> <li>Required for alpha-hydroxylation of free FA and the formation of alpha-hydroxylated SLs</li> <li>Decreased FA2H activity changes the SM profile in fibroblasts (Dan et al, 2011)</li> </ul>	8.75				
HMGCR 3-hydroxy-3- methylglutaryl- CoA	<ul> <li>HMG-CoA reductase (3-hydroxy-3-methylglutaryl-coenzyme A reductase)</li> <li>Rate-limiting enzyme for cholesterol synthesis. Normally in mammalian cells this enzyme is suppressed by cholesterol derived from the internalization and degradation of low density lipoprotein (LDL) via the LDL receptor.</li> <li>HMGCR siRNA leads to a significant increase in binding and internalization of LDL particles in vitro in mouse and human cells (Hibbitt et al, 2012)</li> </ul>	12.98				
CERS1-5 Ceramide synthase 1-5	<ul> <li>CerS1-5 (Ceramide synthase 1-5)</li> <li>ceramide synthase (CerS) enzymes catalyze the formation of (dihydro) ceramide</li> <li>Overexpression, knockout and knockdown experiments show that individual CerS isoforms produce ceramides with characteristic acyl-chain distributions (Mullen et al, 2012)</li> </ul>	1 (9.71); 2 (15.23); 3 (8.06); 4 (9.73); 5 (13.30)				
LDLR low-density lipoprotein receptor	<ul> <li>LDL receptor (Low-density lipoprotein receptor)</li> <li>Binds LDL, the major cholesterol-carrying lipoprotein of plasma, and transports it into cells by endocytosis</li> </ul>	13.48				
NPC1 Niemann-Pick disease, type C1	<ul> <li>NPC1(Niemann-Pick C1 protein)</li> <li>Intracellular cholesterol transporter which acts in concert with NPC2 and plays an important role in the egress of cholesterol from the endosomal/lysosomal compartment</li> <li>NPC1 siRNA in HeLa cells leads to cholesterol accumulation in late endosomes (Ganley &amp; Pfeffer, 2006)</li> <li>NPC1 and NPC2 deficient cells are characterized by an increased storage of lipids (Lloyd-Evans &amp; Platt, 2010)</li> </ul>	13.25				
NPC2 Niemann-Pick disease, type C2	<ul> <li>NPC2 (Niemann-Pick C1 protein)</li> <li>Intracellular cholesterol transporter which acts in concert with NPC1 and plays an important role in the egress of cholesterol from the endosomal/lysosomal compartment</li> <li>NPC1 and NPC2 deficient cells are characterized by an increased storage of lipids (Lloyd-Evans &amp; Platt, 2010)</li> </ul>	15.20				
PISD phosphatidylserine decarboxylase	<ul> <li>PISD (Phosphatidylserine decarboxylase proenzyme)</li> <li>catalyze the formation of PE by decarboxylation of PS</li> <li>Homozygous mutant mice (pisd(-/-))are embryonic lethal (Steenbergen et al, 2005)</li> <li>Heterozygous mutant mice (pisd(+/-)) are viable and show no lipid change (Steenbergen et al, 2005)</li> </ul>	12.22				

Target gene	Encoded protein and functions in lipid metabolism					
PRKAA1 protein kinase, AMP-activated, alpha 1 catalytic subunit	<ul> <li>AMPK subunit alpha-1(5'-AMP-activated protein kinase catalytic subunit alpha-1)</li> <li>Catalytic subunit of AMP-activated protein kinase (AMPK), an energy sensor protein kinase that plays a key role in regulating cellular energy metabolism. (Faubert et al, 2013)</li> </ul>	11.60				
PRKAA2 protein kinase, AMP-activated, alpha 2 catalytic subunit	<ul> <li>AMPK subunit alpha-1(5'-AMP-activated protein kinase catalytic subunit alpha-2)</li> <li>Catalytic subunit of AMP-activated protein kinase (AMPK), an energy sensor protein kinase that plays a key role in regulating cellular energy metabolism. (Faubert et al, 2013)</li> </ul>	11.36				
SPHK1 Sphingosine kinase 1	<ul> <li>SPK1</li> <li>Catalyzes the phosphorylation of sphingosine to form sphingosine 1-phosphate</li> <li>SPHK1 siRNA in MCF-2 breast cancer cells increases ceramides (Taha et al, 2006)</li> <li>SPHK1 siRNA in HEK293 cells increases de novo synthesis of ceramides (Maceyka et al, 2005)</li> </ul>	13.79				
SPHK2 Sphingosine kinase 2	<ul> <li>SPK2</li> <li>Catalyzes the phosphorylation of sphingosine to form sphingosine 1-phosphate</li> <li>SPHK2 siRNA in HEK293 cells decreases de novo synthesis of ceramides (Maceyka et al, 2005)</li> </ul>	11.39				
collagen, type IV, alpha 3 (Goodpasture antigen) binding protein	<ul> <li>hCERT (Ceramide transfer protein)/ StARD11 (START domain-containing protein 11)</li> <li>Shelters Cer inside its START domain and mediates the intracellular trafficking of ceramides in a non-vesicular manner from ER to Golgi.</li> <li>CERT mutant CHO cells are defective in SM synthesis (Hanada et al, 2009)</li> <li>Homozygous CERT mutant mice are embryonic lethal with a decrease of SM (Hanada et al, 2009)</li> </ul>	12.63				

**Table 1. Pilot siRNA screen of gene-related lipids.** Name(s), function(s) and theoretical level of expression in HeLa cells of candidate genes based on the web databases Uniprot and Genevestigator (median signal intensity on Human Genome 47k array expressed in Log2 scale). Expression level: low (<10), medium (10-12) and high (>12).

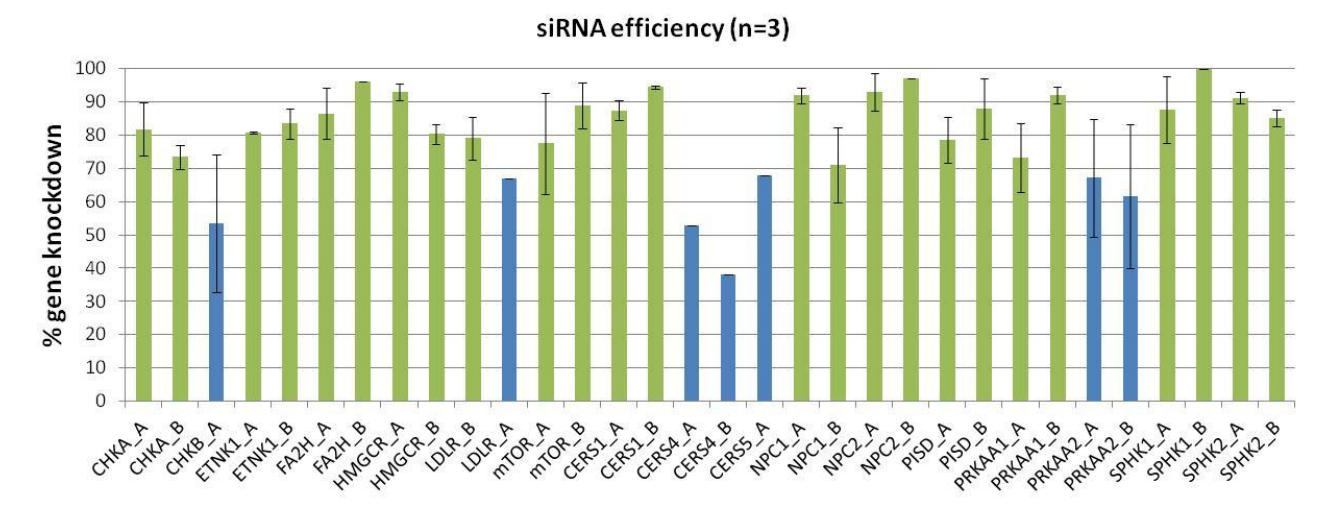


**Figure 2. Gene downregulation by targeted siRNA.** HeLa cells were transfected with 14.4nM siRNA against target genes for 72 h. Cells were harvested, and RNA was extracted for q-PCR analysis of expression of genes. q-PCR data are normalized to TBP mRNA expression, and data are means ± standard errors of the mean (SEM) for three independent experiments. Green bars represent siRNA-induced knockdown >70% compared to non-transfected HeLa cells.

# 1.3.3. siRNA gene knockdown is sufficient to detect significant lipid changes

In order to determine the effects of gene knockdown on the steady-state lipid levels in HeLa cells, I analyzed their lipid composition using mass spectrometry. Following siRNA treatment, lipids were extracted and analyzed using ESI/MS. Then, lipid quantities were normalized to the amount of total phosphorus in order to adjust for difference in cell size, membrane content, and extraction efficiency. Then, data were compiled into heat map showing log2-fold change of each lipid species in siRNA-treated cells over siControl-treated cells (**Fig. 3A and Fig. 4**). To screen for significant changes in lipids, I used unpaired, two-tailed Student's t-tests to compare each siRNA to siControl (**Fig. 3B and Fig. 5**). The whole dataset of the pilot screen is available in the appendix (p127)

Most of siRNAs induced slight changes in membrane lipid composition (**Fig 3B and 5**) but these changes were reproducible for the two different siRNAs targeting the same gene (A and B), in most of lipid classes: more for sphingolipids than phospholipids (**Table 2**, **Fig. 3A and 4**). Except for the siRNA-induced knockdown of *PISD* and *CHKA* that decreased PC and ether PC, respectively (**Fig. 3A and 4**.), the siRNA-induced knockdown of genes involved in PLs homeostasis (*CHKA*, *CHKB*, *ETNK1* and *PISD*) didn't have significant effect on the total pool of

PC, PE, PI and PS. No significant and reproducible effect on SLs and sterols were observed, either.

Among the genes involved in the synthesis, trafficking and regulation of cholesterol levels (*HMGCR*, *LDLR*, *NPC1*, *NPC2*, *PRKAA1* and *PRKAA2*), only *PRKAA1* silencing showed a significant and reproducible increase of cholesterol and a decrease of PI (**Fig. 3B**.). Finally, siHMGCR led to a decrease of GlcCer (**Fig. 3B**.)

target genes	SM	Cer	GlcCer	PC	PE	PI	PS	all lipids
CHKA	0.6	0.5	0.5	0.8	0.3	0.4	0.3	0.5
CHKB	0.6	0.7	0.6	0.7	0.4	0.3	0.9	0.5
ETNK1	0.5	0.7	0.6	0.7	-0.1	0.6	0.9	0.7
FA2H	0.6	0.4	0.5	0.1	-0.1	0.1	0.1	0.4
HMGCR	0.8	0.7	0.2	0.3	0.5	0.7	0.8	0.6
CERS1	0.4	0.6	0.7	0.3	0.1	0.6	0.7	0.4
CERS2	0.9	0.8	0.5	0.1	0.6	0.6	0.9	0.7
CERS3	0.8	0.7	0.7	0.6	0.7	0.6	0.8	0.7
CERS4	0.8	0.8	0.5	0.0	0.4	0.1	0.0	0.3
CERS5	1.0	0.8	0.8	0.4	0.3	0.5	0.7	0.6
LDLR	0.8	0.7	0.7	0.4	0.2	0.1	-0.1	0.3
NPC1	0.5	0.6	0.5	-0.1	-0.2	-0.2	0.7	0.2
NPC2	0.6	0.8	0.5	0.9	0.1	0.4	0.9	0.6
PISD	0.6	0.4	0.6	0.3	0.5	0.5	0.6	0.4
PRKAA1	0.2	0.8	0.3	0.1	0.0	0.5	0.7	0.4
PRKAA2	0.3	0.9	0.3	0.5	0.5	0.3	0.7	0.5
SPHK1	0.7	0.8	0.3	0.5	0.3	0.2	0.8	0.7
SPHK2	0.5	0.5	0.6	0.5	0.5	0.2	-0.6	0.4

Table 2. Correlation between lipid profiles obtained with two different siRNAs per gene. Similarities of lipid changes between gene knockdown experiments performed with two different siRNAs (A or B) targeting the same gene were evaluated by calculating correlation coefficient Pearson between the two series of log2 fold change. For each target gene, lipid profiles were considered reproducible (green boxes) between the two experiments with different siRNAs for Pearson correlation coef. ≥0.5. Negative coefficient represent opposite lipid profiles (red boxes).

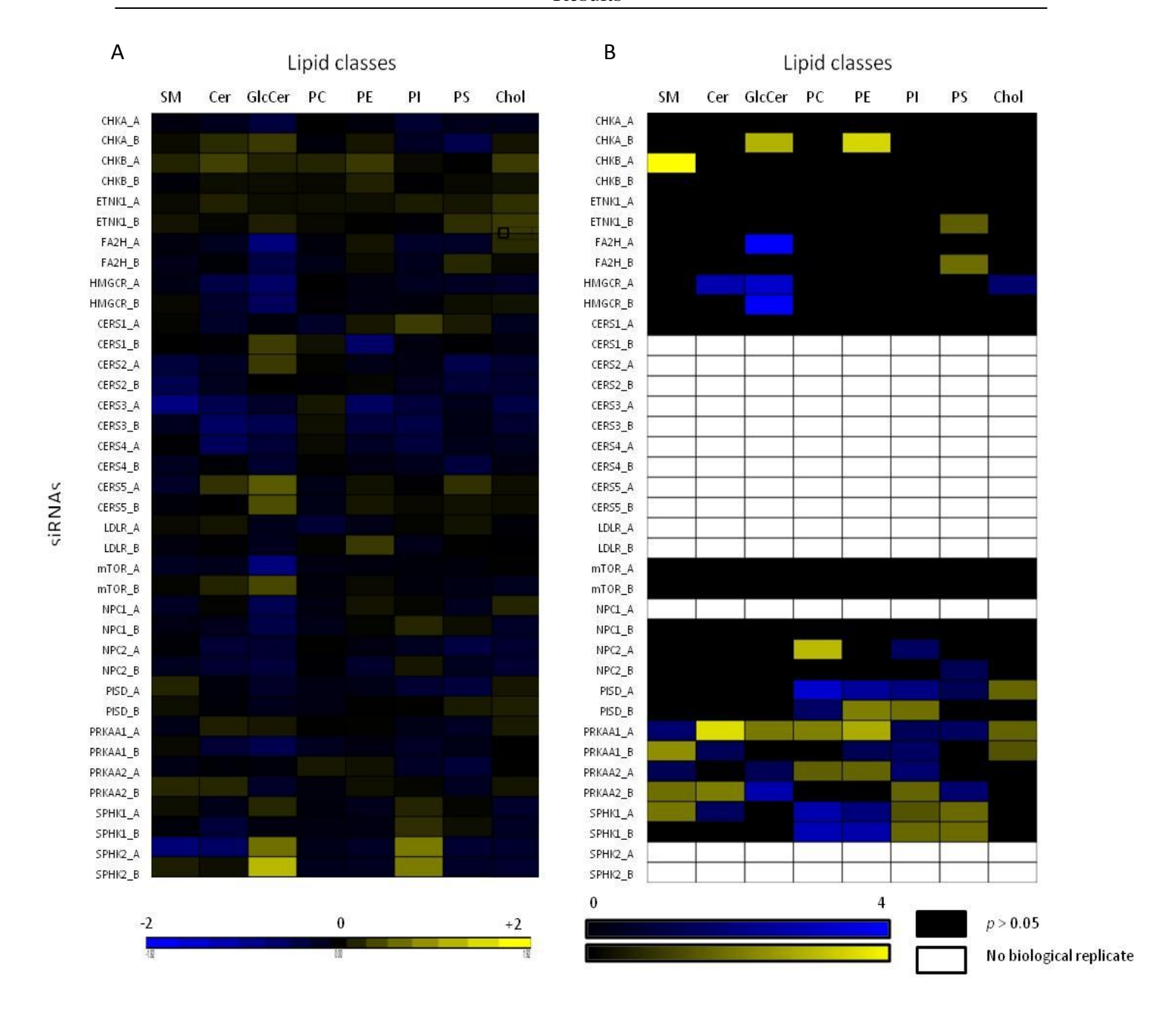
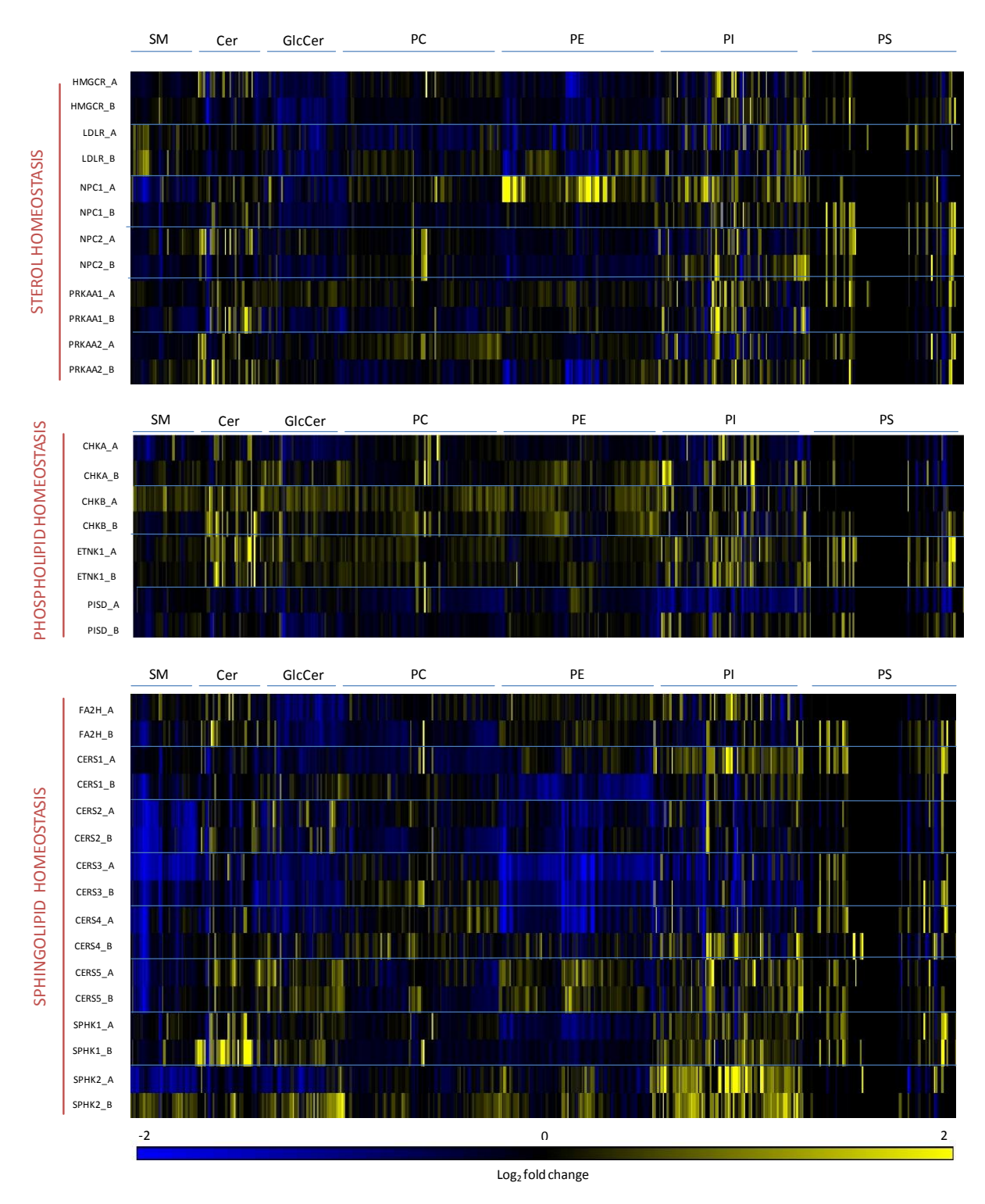
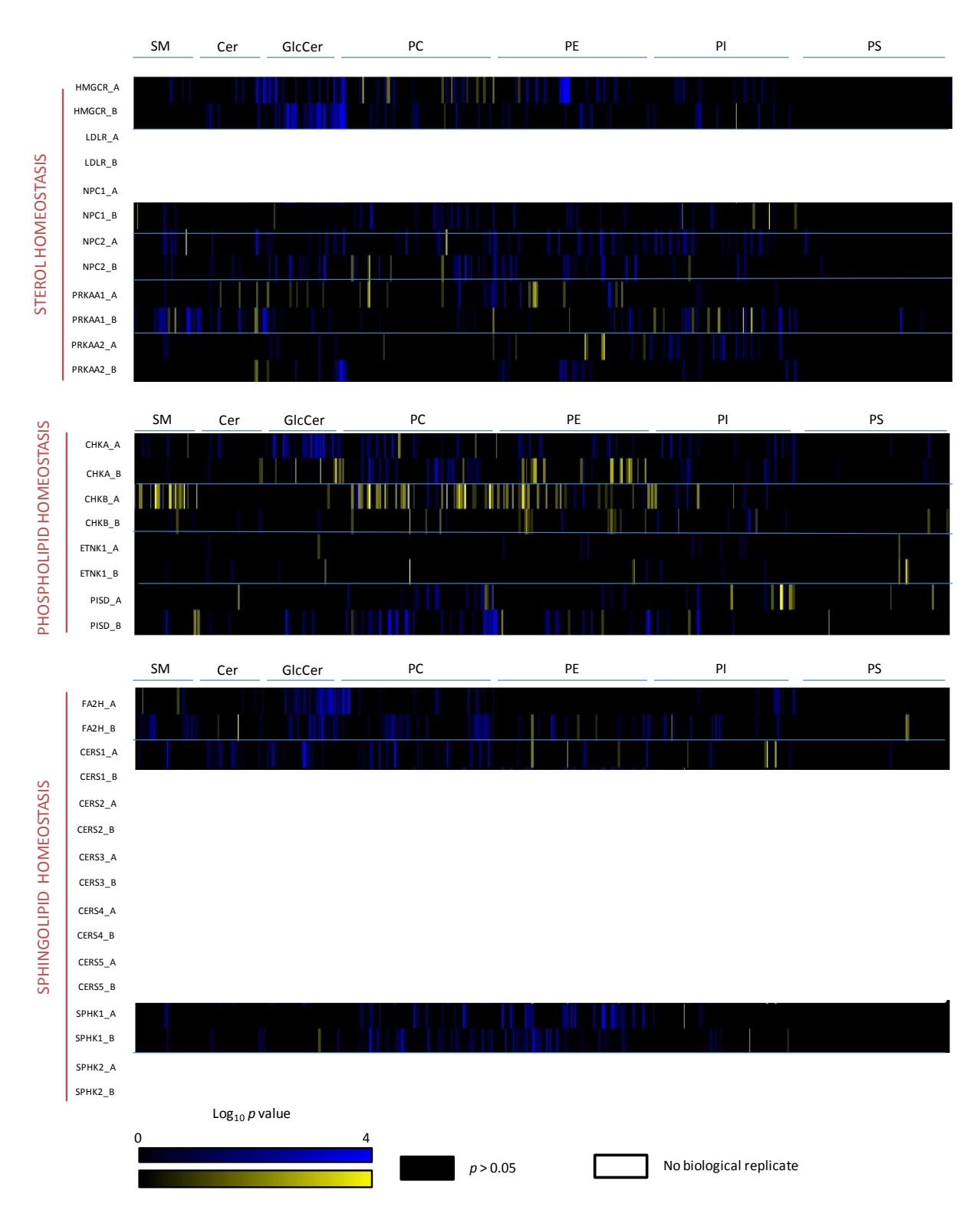


Figure 3. A pilot siRNA screen on lipid-related proteins induce changes in multiple lipid species. HeLa cells were transfected with 14nM siRNA targeted against genes involved in the regulation of lipid homeostasis and lipid masses were determined by ESI/MS. A) Lipid levels were normalized to the amount of total lipid phosphate. Lipid changes are displayed as a heat map of the log2 of the mean fold change versus siControl (negative control siRNA). Blue and yellow boxes indicate a decrease and an increase of lipid level, respectively. B) Heatmap of statistically significant changes in lipids following siRNA knockdown. Lipid level changes are displayed as a heatmap of the log10 of the p value calculated from Student's t test of siRNA vs. siControl. Yellow boxes indicate a significant increase and blue boxes indicate a significant decrease. Black indicates no significant change. Data represent three to five independent experiments SM: sphingomyelin; Cer: ceramides; GlcCer: glycosylceramide; PC: phosphatidylcholine; PE: phosphatidylethanolamine; PI: phosphatidylinositol PS: phosphatidylserine and chol: cholesterol.



**Figure 4.** A pilot siRNA screen on lipid-related proteins induces changes in multiple lipid species. HeLa cells were transfected with 14nM siRNA targeted against genes involved in the regulation of PLs, SLs and sterol homeostasis lipid masses were determined by ESI/MS. Lipid levels were normalized to the amount of total lipid phosphate. Lipid changes are displayed as a heat map of the log2 of the mean fold change versus siControl. Blue and yellow boxes indicate a decrease and an increase of lipid, respectively. Data represent one to three independent experiments.



**Figure 5. Heatmap of statistically significant changes in lipids following siRNA knockdown**. Lipid level changes are displayed as a heatmap of the -log10 of the p value calcuted from Student's t test of siRNA vs. siControl. Yellow boxes indicate a significant increase and blue boxes indicate a significant decrease. Black indicates no significant change and white boxes indicate no biological replicate. Data represent one to three independent experiments

The siRNA-induced knockdown of genes involved in SL homeostasis showed the strongest phenotypes. The knockdown of siFA2H induced a strong decrease of hydroxylated SM and GlcCer (**Fig 5.**) and the silencing of sphingosine kinases tended to increase PI and GlcCer (**Fig. 3.** and **4.**). The siRNA against SPHK1 also induced a decrease of S1P compared to the mean amount of S1P of the whole dataset (data not shown) but since this bioactive sphingolipid species was not detectable in most of samples, this change cannot be considered as statistically significant. Even if the siRNA experiments were performed only once for ceramide synthases the effects *CERS1-5* gene silencing on SLs were reproducible for the two different siRNAs, A and B (**Fig 5.** and **Table 2.**). Moreover, the individual silencing of these five ceramide synthases induced a chain-length specific phenotype in SLs (**Fig. 6.**). As shown by Mullen, T.D. and coworkers with MCF-7 cells (Mullen et al, 2011), the knockdown of CERS2 and CERS5 led to a specific increase of C14-18 and C18-26 sphingolipids, respectively. Moreover, in most of HeLa cells treated with siRNAs against ceramide synthases, SM levels were not much affected, except for siCERS2 that also induced a decrease of C18 to C26 sphingomyelin. Finally, GlcCer was particularly increased in cells treated with siCERS5 (**Fig. 6.**).

In summary, this pilot screen showed that siRNA-mediated knockdown of lipid-related genes could induce reproducible changes in the lipid composition of HeLa cells, often in agreement with previous published studies. Moreover, our lipidomics approach allowed the observation of multiple changes in different lipid classes simultaneously.

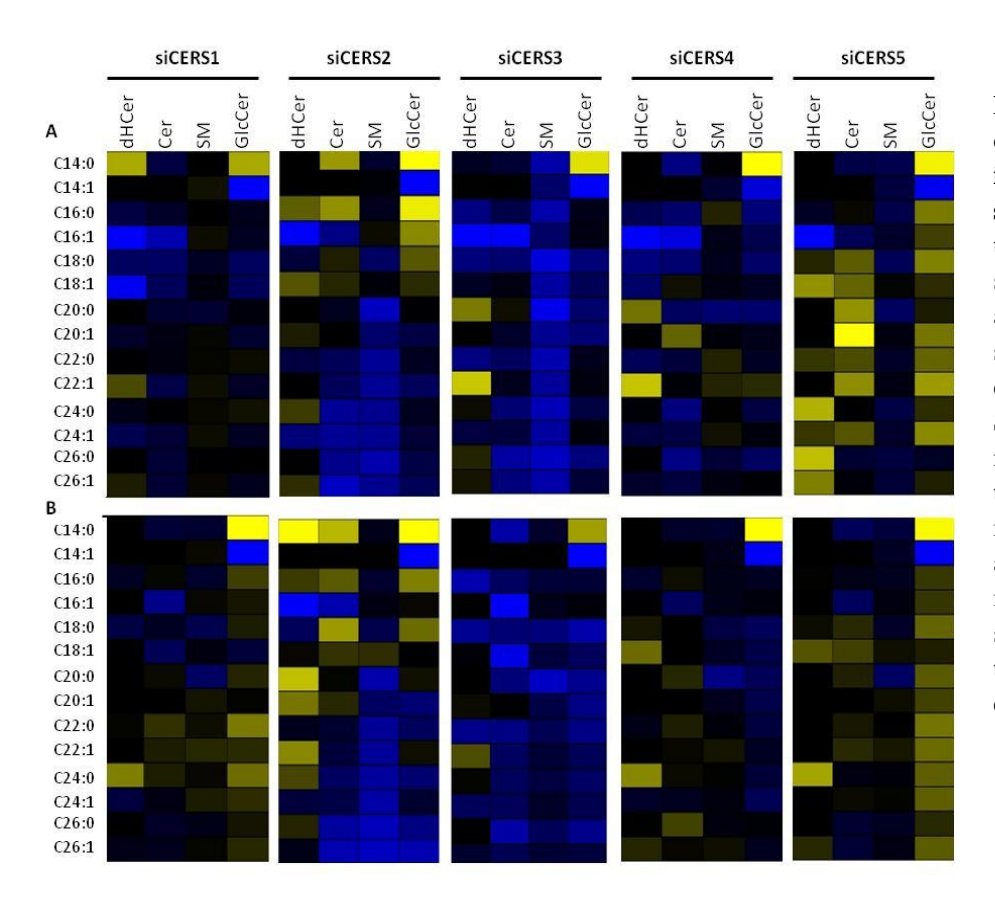


Figure 6. SiRNA knockdown of CERS1-5 induces changes multiple sphingolipid species. HeLa cells were transfected with two different siRNA (A and B) targeted against CERS1-5, sphingolipid masses were determined by ESI/MS. Sphingolipid levels were normalized to the amount of total phosphorus. Sphingolipid mass changes are displayed as a heat map of the log2 of the mean fold change versus siControl. Data represent one three independent experiments.

#### 1.3.1. Cell-population context and gene knockdown effect: example of CERT

In this pilot screen experiment, the siRNA-induced knockdown of *COL3A4BP was also tested*. *COL3A4BP* (standing for collagen, type IV, alpha 3-binding protein) is a gene with multiple mRNA splicing variants: GPBP, CERT<sub>L</sub> and CERT/GPBPΔ26. GPBP and CERT<sub>L</sub>, as well as GPBPΔ26 and CERT are identical but encode for different proteins. In 2003, Hanada K. and coworkers identified CERT as the factor impaired in LY-A cells, a mammalian mutant cell line defective in SM synthesis. CERT (standing for ceramide transfer protein) is responsible for the *in vivo* non-vesicular trafficking of ceramides between the ER and Golgi for conversion to SM (Hanada et al, 2003). In 2009, Wang X. and colleagues demonstrated that mice deficient in CERT were embryonic lethal and showed a ~60% decrease in SM, accompanied with an increase of ceramides (Wang et al, 2009). In parallel, it was shown that the downregulation of CERT by siRNA in C6 glioma cells significantly affects the levels of SM, too (Giussani et al, 2008). As

previously reported, the siRNA-induced knockdown of CERT performed in the lab with HeLa cells also led to a significant decrease of SM. This decrease was coupled to significant increase of GlcCer and sterol esters. However, by comparing data in the lab with Dr. Ursula Loizides-Mangold, different results were observed concerning the increase of sterol esters. The only difference between our two experiments was cell confluence at the time of siRNA transfection. Can cell confluence impact on the effects of CERT knockdown on membrane lipid composition? The influence of cell-density in response to siRNA-induced knockdown has already been studied in image-based RNAi screen. For instance, it was shown that siRNA transfection of adherent mammalian cells induced different responses in cell islets edges compared to cells at the middle of the islets (Snijder et al, 2012). Moreover, cell density is also known to influence the lipid composition of cells. In 1997, Cansell M. and colleagues analyzed the lipid composition of human endothelial cells in exponential growth phase and at confluence. Cells growth-arrested by contact inhibition at confluence accumulate more cholesterol than cells in division and their fatty acid distribution in PLs is different as well, while total amounts of PLs and FA are not changed (Cansell et al, 1997).

In order to assess the importance of confluence on the effects of CERT knockdown, I seeded 2.10<sup>5</sup> cells per 6cm dish and transfected them with siRNA against *COL3A4BP* after 24h (sparse cells), 48h (50% confluence) or 72h (dense) of cell culture, respectively (**Fig 8.** and **Fig. 9.**). Following siRNA treatment, membrane lipid levels were analyzed using ESI/MS and normalized to the amount of total phosphorus. I measured the efficacy of siRNA-induced knockdown on CERT mRNA specifically by qRT-PCR (**Fig. 8B** and **Fig. 9B**). Ten percent of the cell pellet used for quantitative lipid analysis was reserved for this purpose in a spare tube before lipid extraction. In order to determine if the effect was cell type or CERT-specific, I performed the experiment in two Human cell lines: HeLa and HeLa MZ from Marino Zerial (MPI-CBG, Dresden). Despite having the same origin, the two cell lines differ in the fatty acid composition in their SLs. The major SM in HeLa MZ cells is SM42:2 instead of SM34:1 in HeLa (**Fig. 7A**). Moreover, their profile of glycosphingolipids is also different: GlcCer are detectable by TLC in both cell lines while GalCer seems present in HeLa, only (**Fig. 7B**).

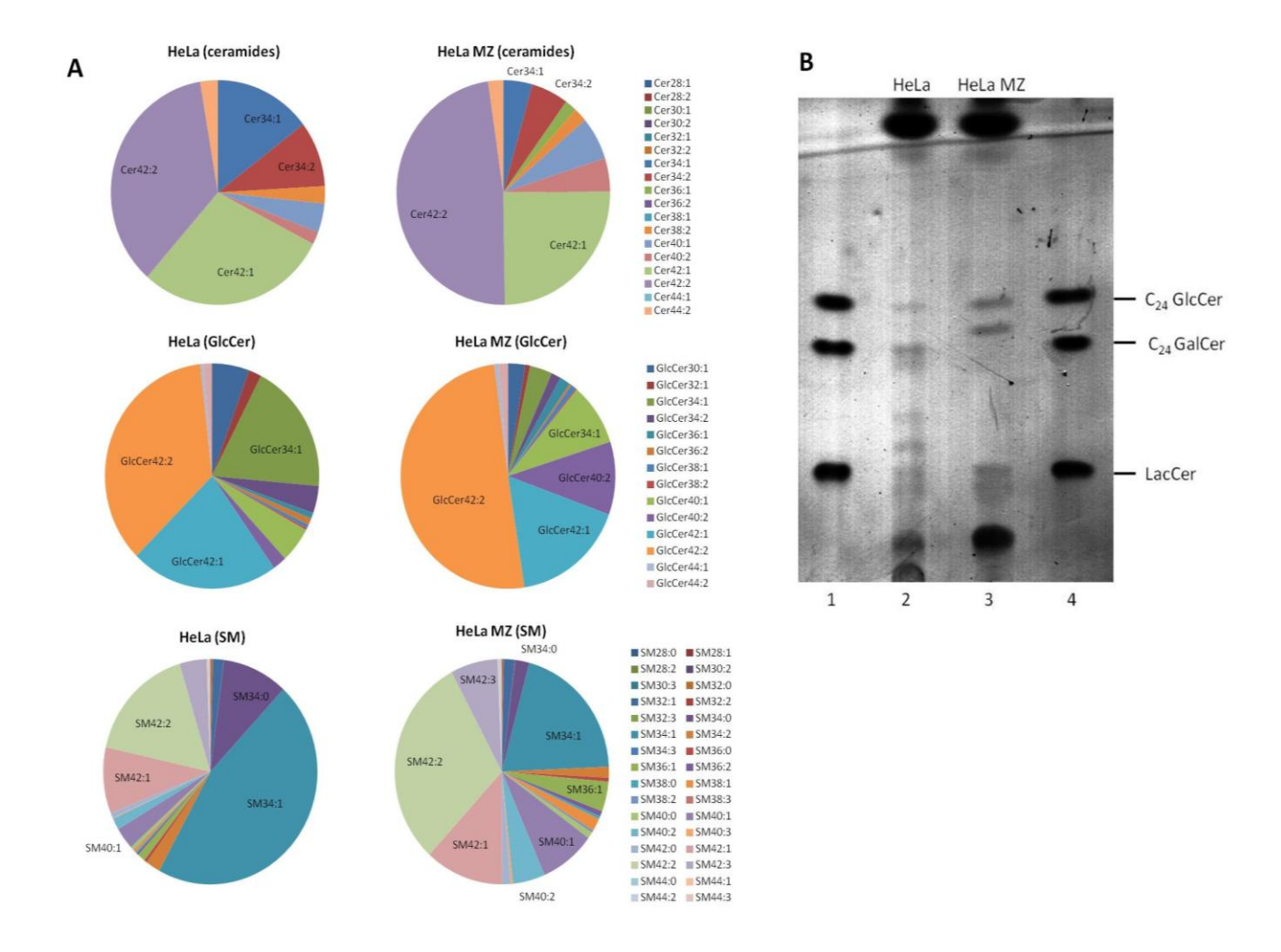


Figure 7. Sphingolipid composition of HeLa and HeLa MZ cell lines. A. Distribution of fatty acyl chains of sphingolipids in HeLa and HeLa MZ cell lines. B. Determination of glycosphingolipid species in HeLa and HeLa MZ. 50μL of sphingolipid extracts from HeLa (column 2) and HeLa MZ (column 3) were analyzed by TLC. To distinguish GalCer and GlcCer the HPTLC plates were impregnated with borate. Glycosylated lipids were visualized with Orcinol and determined by comparison with standards (columns 1 and 4).

Whatever the cell line and the confluence, the downregulation of CERT induced specific changes in sphingolipids and sterol esters while the amounts of phospholipids and cholesterol remained unchanged. In average, the quantity of SM was reduced by 20-60% in CERT-silenced cells, while the levels of Cer and GlcCer tended to increase and the amount of steryl esters was sometimes doubled compared to siControl (**Fig 8.** and **Fig. 9.**) However, these changes differed specifically depending on the cell line and their density at the time of siRNA transfection. Maximal changes occurred for cells transfected at 50% confluence (after 48h culture), whatever the cell line. While the gene silencing of CERT was higher than 70% in every condition

compared to non-transfected cells, the effects of the siRNA-induced knockdown of CERT in dense cells (after 72h of cell culture) were less important for SM and steryl esters than in 50% confluent cells (48h), whatever the cell line, contrary to Cer and GlcCer, which continued to accumulate in dense cells (72h) in HeLa MZ. After 72h of cell culture, the gene silencing of CERT in HeLa MZ (**Fig. 8B**) induced around 80% increase of both Cer and GlcCer, against 40-50% increase when cells were transfected after 48h culture (**Fig. 8A and C**). This result was opposite in HeLa where Cer and GlcCer quantities also decrease when cells are transfected with CERT siRNA after 72h of cell culture (**Fig. 9A and C**).

This experiment shows that cell confluence is an important factor to control when observing lipid changes after siRNA transfection of adherent cells. Ideally, as in imaging experiments, it is important to distinguish the results according to cell proliferation phases (Snijder et al, 2012) and avoid false negative hits. In lipidomics experiments, this discrimination is not possible but we could perform every siRNA experiment at multiple cell confluences, or at least take care to work with the same initial cell number to ensure certain reproducibility between biological replicates.

# 1.4. Lessons from the pilot screen experiment.

This pilot screen confirms some data from literature and unexpected results that could be interpreted with further analysis. The knockdown of target genes directly involved in the synthesis of lipids such as choline, ethanolamine kinases or HMGCR, didn't affect specifically the lipids they synthesize. This confirms the necessity of large-scale screen studies in lipidomics in order to find regulators of membrane lipid homeostasis. Moreover, the silencing of CERT highlights the probability to find false negative hits depending on the cell confluence at the time of cell transfection. Data obtained with two different siRNAs per gene also show that off-target effects can strongly influence the lipid profile and that hits retrieved from large-scale RNAi screen need to be confirmed with different siRNAs per gene. Finally, this "small" dataset highlights the complexity of analyzing hundreds of phenotypic readouts, here lipid quantities, obtained with three different machines and the necessity to use adapted bioinformatics tools

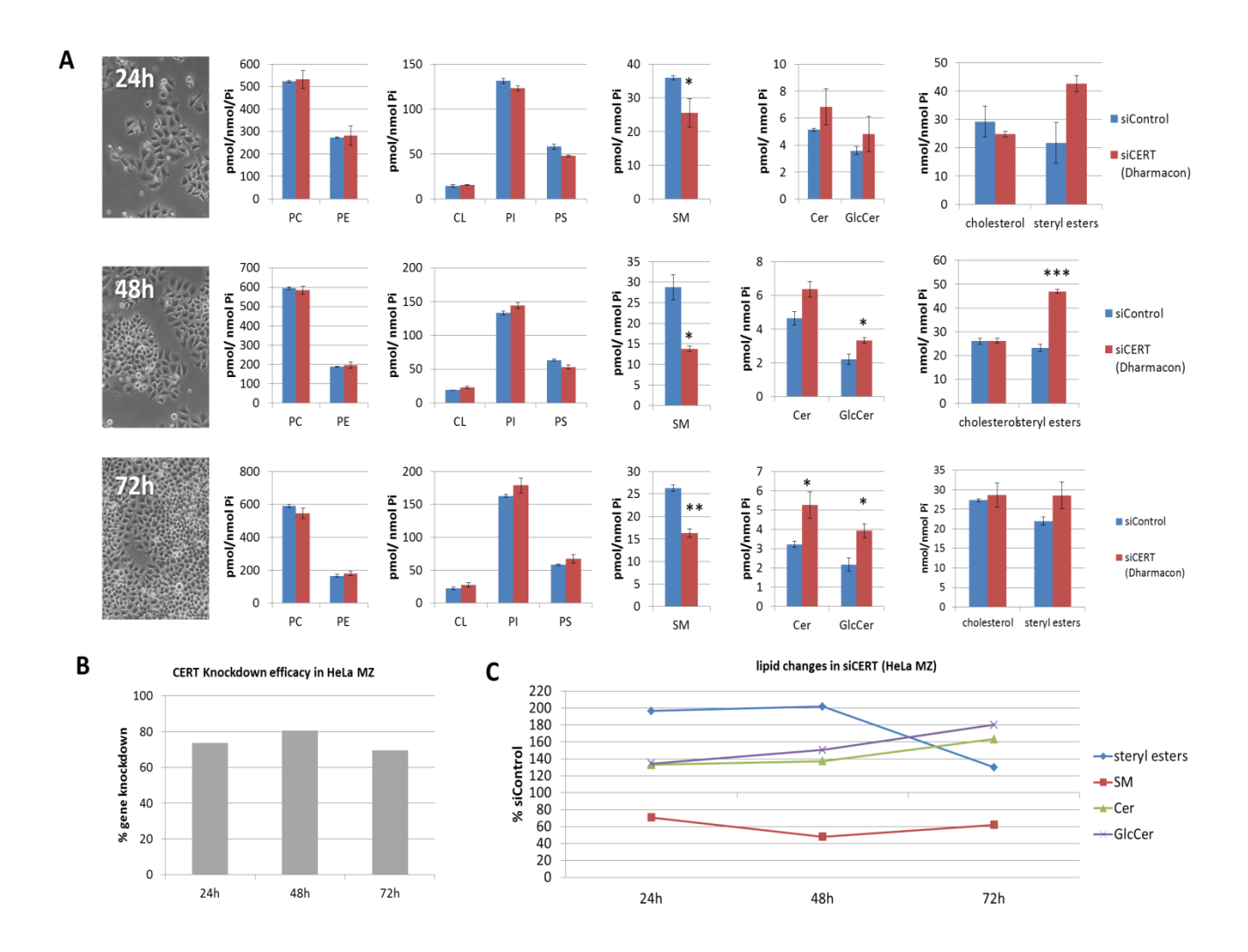


Figure 8. Knockdown of CERT in HeLa MZ cells at different confluences induces gradual changes both in SL and steryl esters. A. HeLa MZ cells were seeded at 2.  $10^5$  cells per 6cm dish and transfected with 14.4 nM of siRNA targeted against *COL3A4BP* at different cell confluence (after 24h, 48h or 72h of cell culture) and lipid masses were determined by ESI/MS and GC/MS (sterols). Lipid levels were normalized to the amount of total lipid phosphate and compared to siControl. **B.** CERT mRNA downregulation. 72h after siRNA transfection, cells were harvested, and RNA was extracted for q-PCR analysis of gene expression. q-PCR data are normalized to TBP mRNA expression and compared to non-transfected HeLa cells. **C.** Percentage of lipids in cells transfected with siRNA against *COL3A4BP* at different confluences and compared to siControl. Data and data are means  $\pm$  standard errors of the mean (SEM) and .represent three independent experiments. \*, P < 0.05; \*\*\*, P < 0.01; \*\*\*\*, P < 0.005 versus siControl.

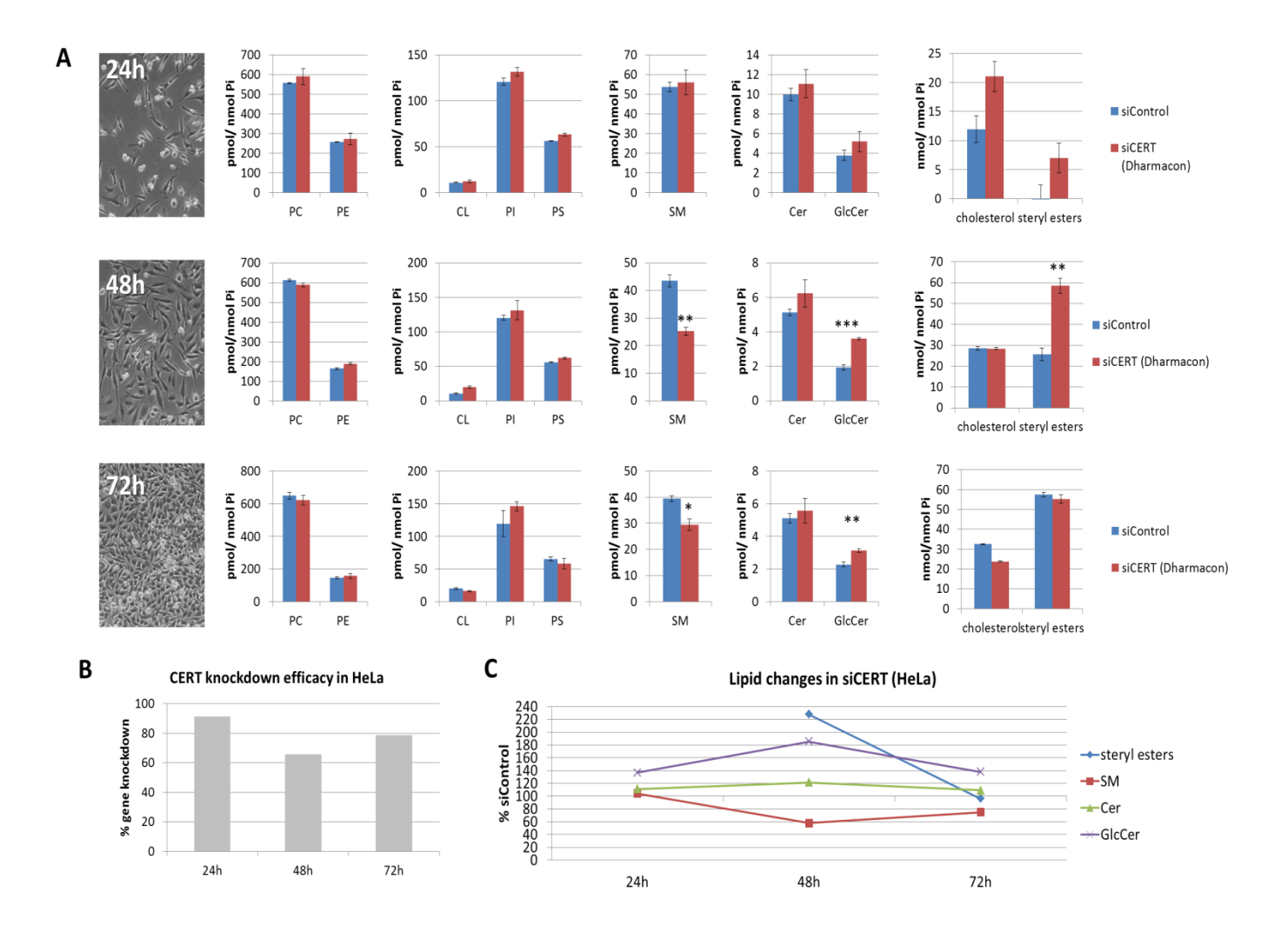


Figure 9. Knockdown of CERT in HeLa cells at different confluences induces gradual changes both in SL and steryl esters. A. HeLa cells were seeded at 2.  $10^5$  cells per 6cm dish and transfected with 14.4 nM of siRNA targeted against *COL3A4BP* at different cell confluence (after 24h, 48h or 72h of cell culture) and lipid masses were determined by ESI/MS and GC/MS (sterols). Lipid levels were normalized to the amount of total lipid phosphate and compared to siControl. B. CERT mRNA downregulation. 72h after siRNA transfection, cells were harvested, and RNA was extracted for q-PCR analysis of gene expression. q-PCR data are normalized to TBP mRNA expression and compared to non-transfected HeLa cells. C. Percentage of lipids in cells transfected with siRNA against *COL3A4BP* at different confluences and compared to siControl. Data are means  $\pm$  standard errors of the mean (SEM) and .represent three independent experiments. \*, P < 0.05; \*\*\*, P < 0.01; \*\*\*\*, P < 0.005 versus siControl.

#### 2. Kinome-wide RNAi based screen in HeLa MZ cells

# 2.1. Experimental conditions

Regulators of membrane lipid homeostasis in mammalian cells are still far from being fully identified. Good candidates could come from the kinase family that comprises more than 500 genes (Manning et al, 2002) which regulate several cell mechanisms, including lipid-related genes. In order to explore the function of kinases in membrane lipid homeostasis, a kinome-wide siRNA screen was performed in human cells. After development of the technique at the scale of a pilot screen targeting about 20 genes, the siRNA-induced knockdown of 715 kinase transcripts, including protein, lipid and sugar kinases was processed, in duplicate. This primary screen was run using pools of three siRNAs per gene from MISSION® siRNA Human Kinase Library (Sigma-Aldrich) in order to decrease the probability of off-target effects (Jackson & Linsley, 2010). HeLa MZ from Marino Zerial (MPI Dresden) were used in order to be in the experimental conditions similar to other RNAi screens performed in the groups of Lucas Pelkmans (Zurich) and Jean Gruenberg (Geneva) and enable the comparison of our datasets. Finally, the whole screen was run using complete cell medium with fetal calf serum coming from the same batch series.

As for the pilot screen, after 72h siRNA transfection, cells were harvested, lipids extracted and analyzed by ESI/MS (PLs and SLs) and GC/MS (sterols) (**Fig. 1.**). Changes in lipid profiles and hits determination were then estimated using statistical tools.

## 2.2. Membrane lipid composition of HeLa MZ

First, the lipid profile of untreated HeLa MZ samples from the screen was characterized. In the absence of treatment, cells were cultivated in the same conditions than cells treated with siRNA or transfection reagents alone, i.e. the same medium, number of cells at day 0 and harvested after four days of culture. For each membrane lipid class, the major lipids as well as the distributions of fatty acyl chains of different length or degrees of saturation, the proportions of

hydroxylated sphingolipids, ether phospholipids and the profile of lysophospholipids are described (**Fig. 10-17**).

# • Sphingolipids:

Whatever the SL class, hydroxysphingolipids (SL-OH) represent around 20 mol% of total SL. The distribution of fatty acyl chains differ between SL classes as well as between SL and their dihydro or hydroxylated form inside each SL class. In sphingomyelin (SM) and ceramides (Cer), the major species are SM/Cer 42:2 and SM/Cer 34:1 whereas the second major SM/Cer-OH is 40:1. SM-OH are also more unsaturated suggesting that the activity of ceramide synthases involved in SL and SL-OH synthesis are different in HeLa MZ. On the contrary, the distribution of fatty acyl chains is identical between GlcCer and GlcCer-OH. Major GlcCer species are 42:2 and 40:1. In Cer and GlcCer, the fatty acyl distribution of dihydro-forms are completely different with enrichment in shorter chains, especially C16 dihydroceramides.

# Phospholipids:

Quantified phospholipids (PL) include LysoPLs and ether species (etherPL). EtherPLs represent between 4 and 19 mol% of total PLs. LysoPLs, less than 1 mol%. Whatever the category, PLs comprise between 0 and 6 double bonds but the major species are the most saturated ones and ether lipids are also more saturated. This is particularly true for phosphatidylserine (PS) where most of PS have one unsaturation whereas etherPS are saturated. The distribution of fatty acyl chain length differs between PL and ether PL, except for phosphatidylcholine (PC) and ether PC. The major PCs are PC34:1, PC32:1 and PC36, which corresponds to the pattern of LysoPCs that results from the hydrolysis of PC by phospholipases and for which the major species comprise either C16:0 or C18:1fatty acyl chains on sn-1 of glycerol-3-phosphate. This correspondence is also found in other PLs. Indeed, the major PE species are PE36:2, PE36:1, PE34:1 and PE34:2 and LysoPE18:1, 18:0 and 16:0. The major PI species are PI36:1, PI36:2, PI34:1 or the polyunsaturated PI38:4, and the major LysoPI are LysoPI18:0 and 18:1. Finally, major PS species are PE36:1 and 34:1 and LysoPS18:0, 18:1 and 16:0.

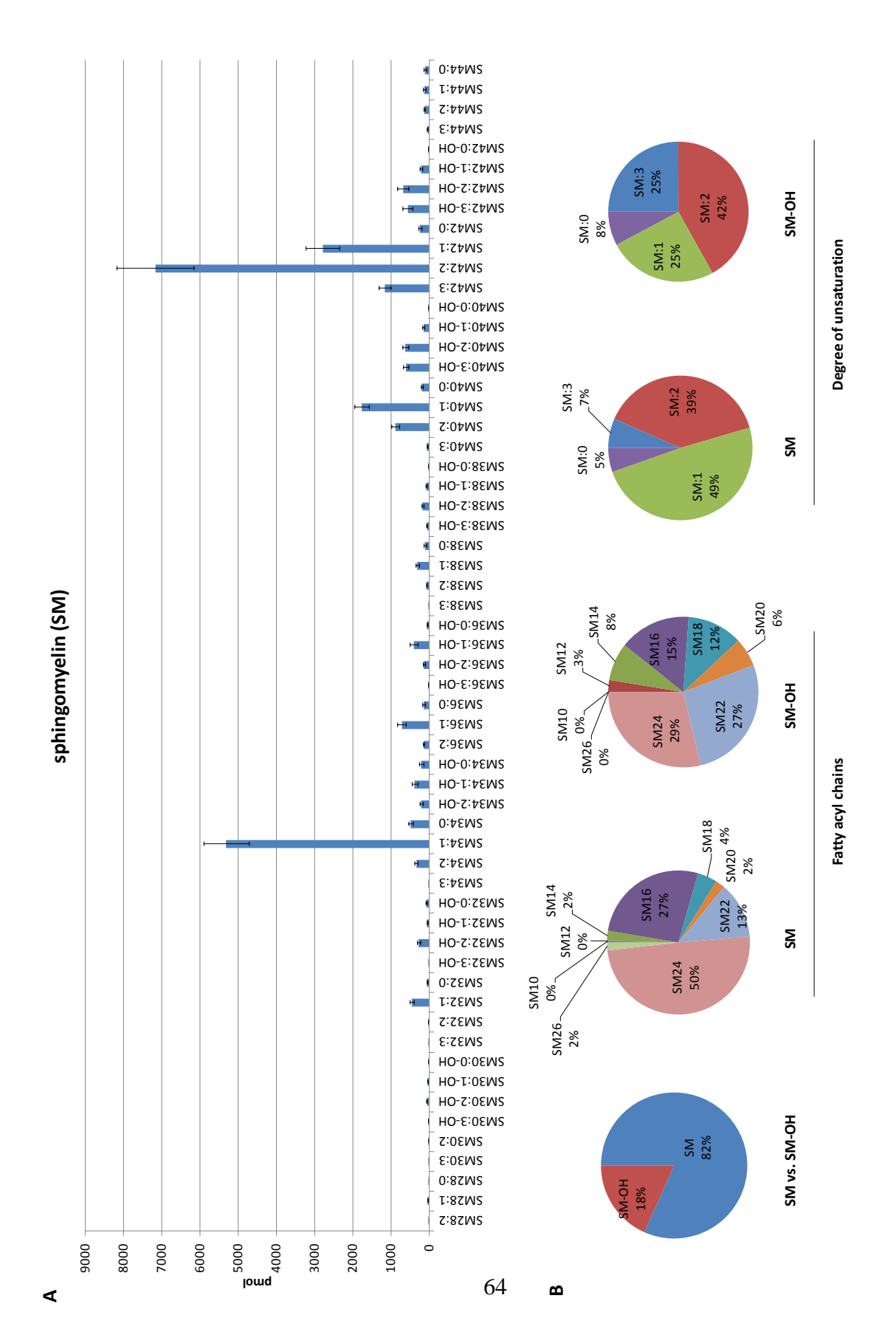


Figure 10. Distribution of sphingomyelin (SM) species in HeLa MZ. A. Average quantity of individual SM species ± SEM (n=15). B. hydroxylated SM vs SM and distribution of fatty acid chain length and unsaturation degrees in SM and hydroxylated

SM.

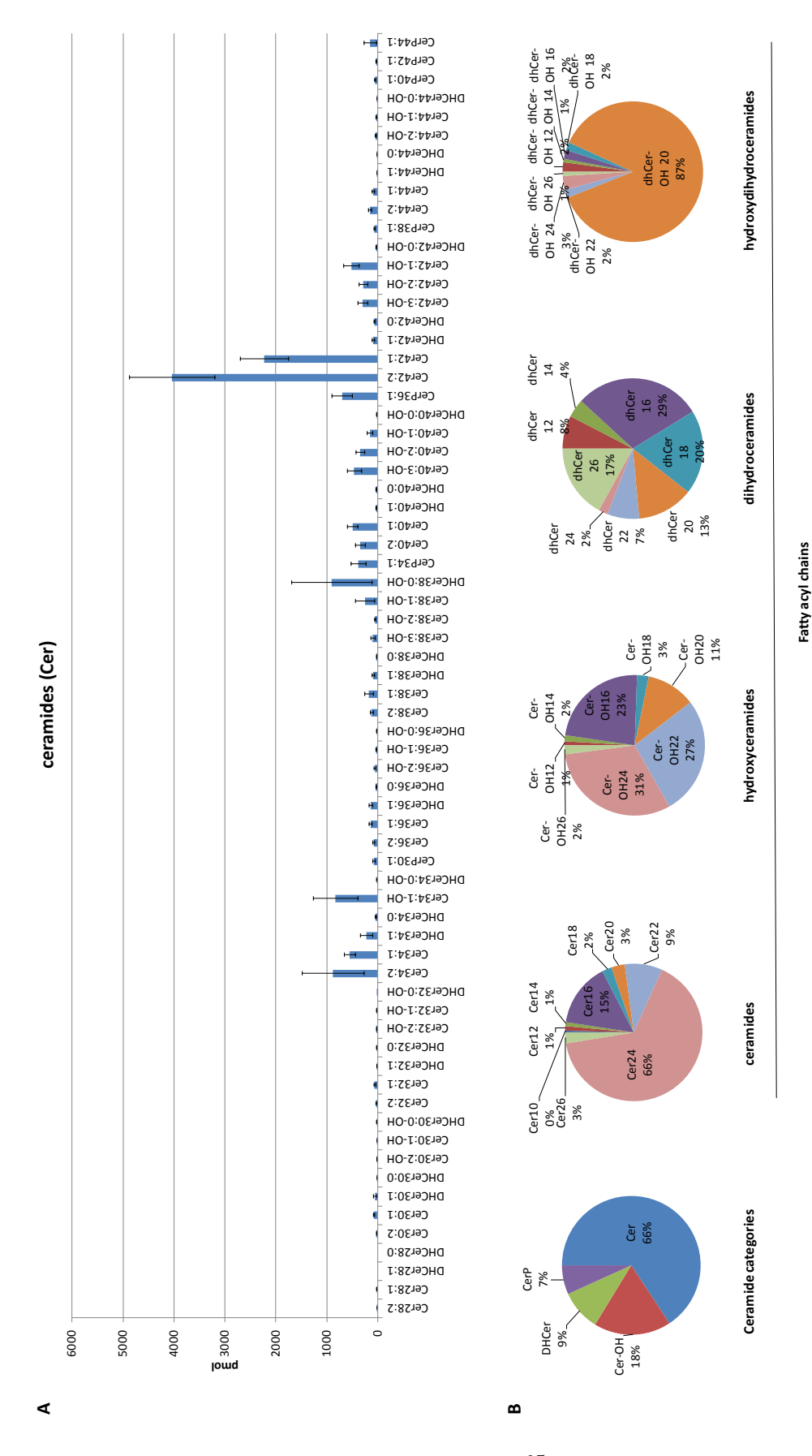


Figure 11. Distribution of ceramides (Cer) species in HeLa MZ. A. Average quantity of individual Cer species  $\pm$  SEM (n=15). B. Proportion of dihydroceramides, hydroxylated -Cer vand Cer plus distribution of fatty acid chain length and unsaturation degrees in Cer and hydroxylated Cer.

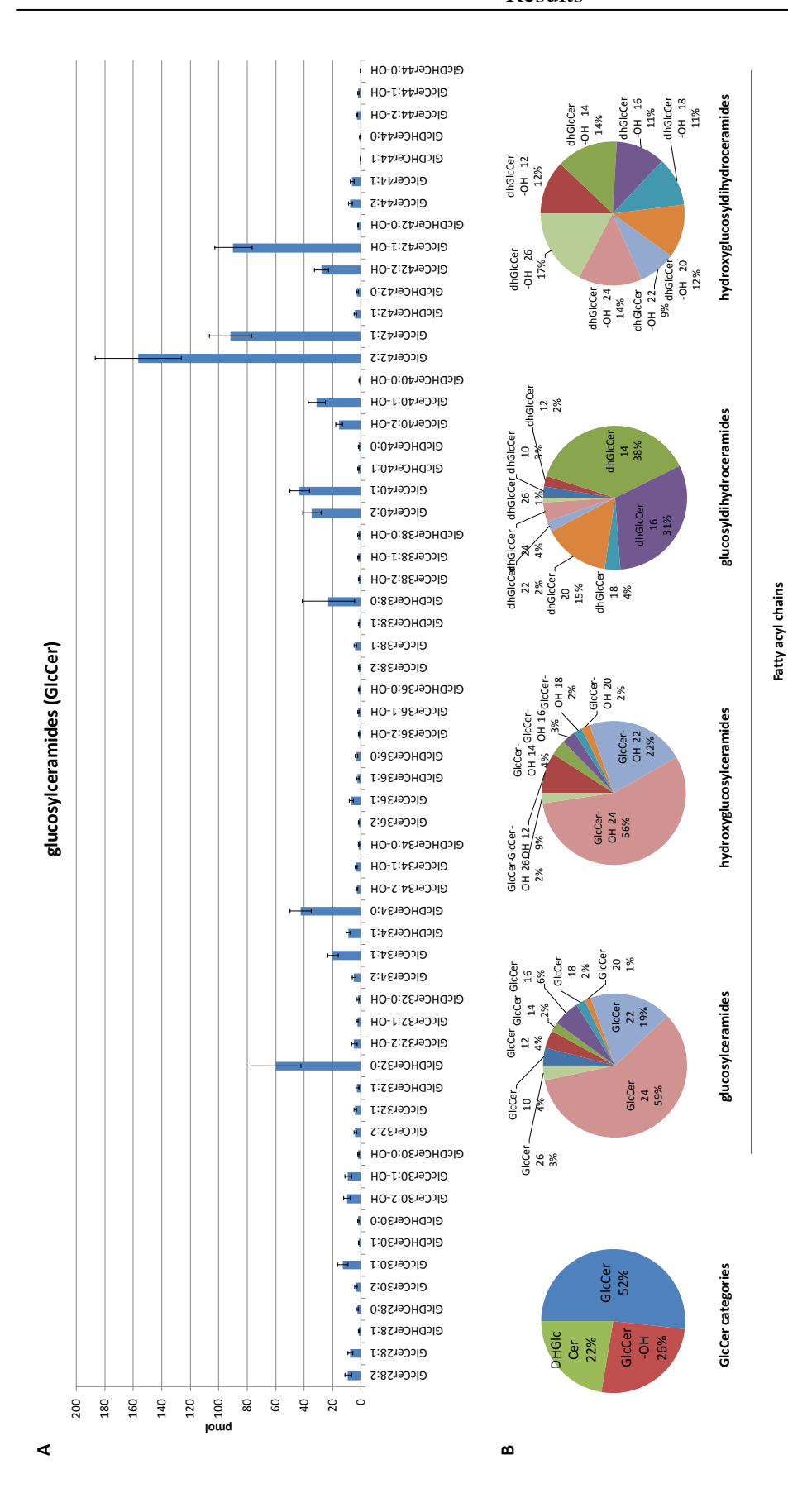


Figure 12. Distribution of glucosylceramides (GlcCer) species in HeLa MZ. A. Average quantity of individual GlcCer species ± SEM (n=15). B. Proportion of dihydroceramides, hydroxylated -GlcCer vand GlcCer plus distribution of fatty acid chain length and unsaturation degrees in GlcCer and hydroxylated GlcCer.

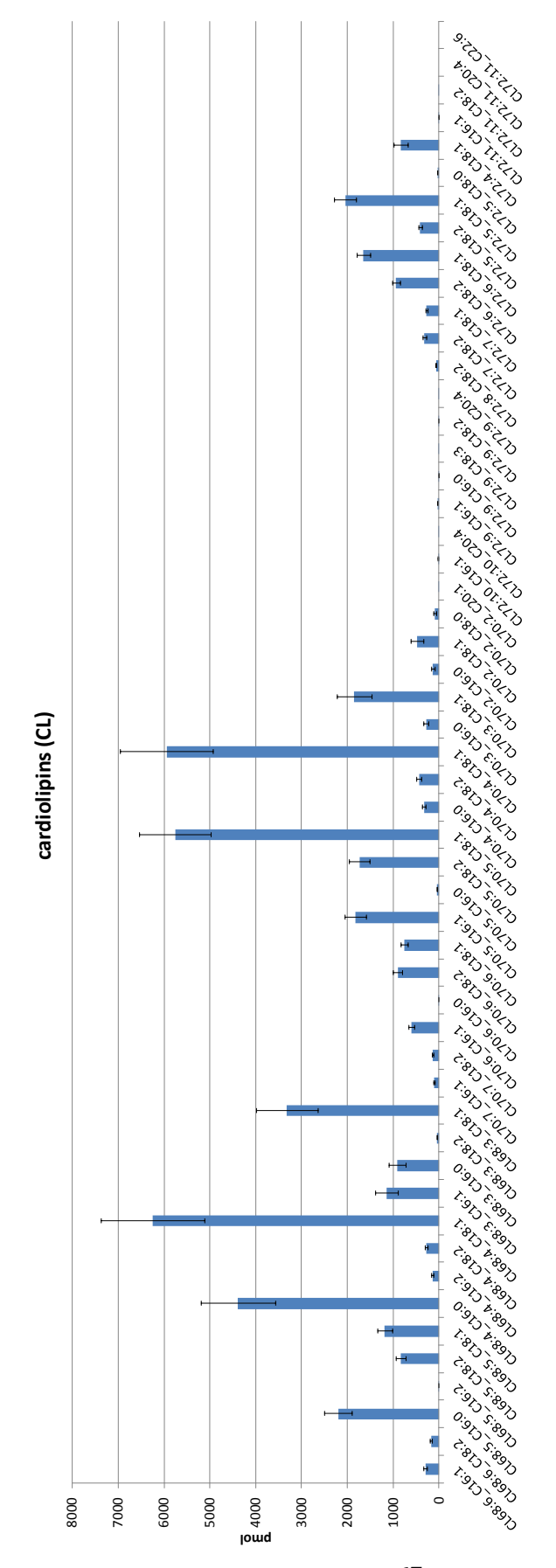
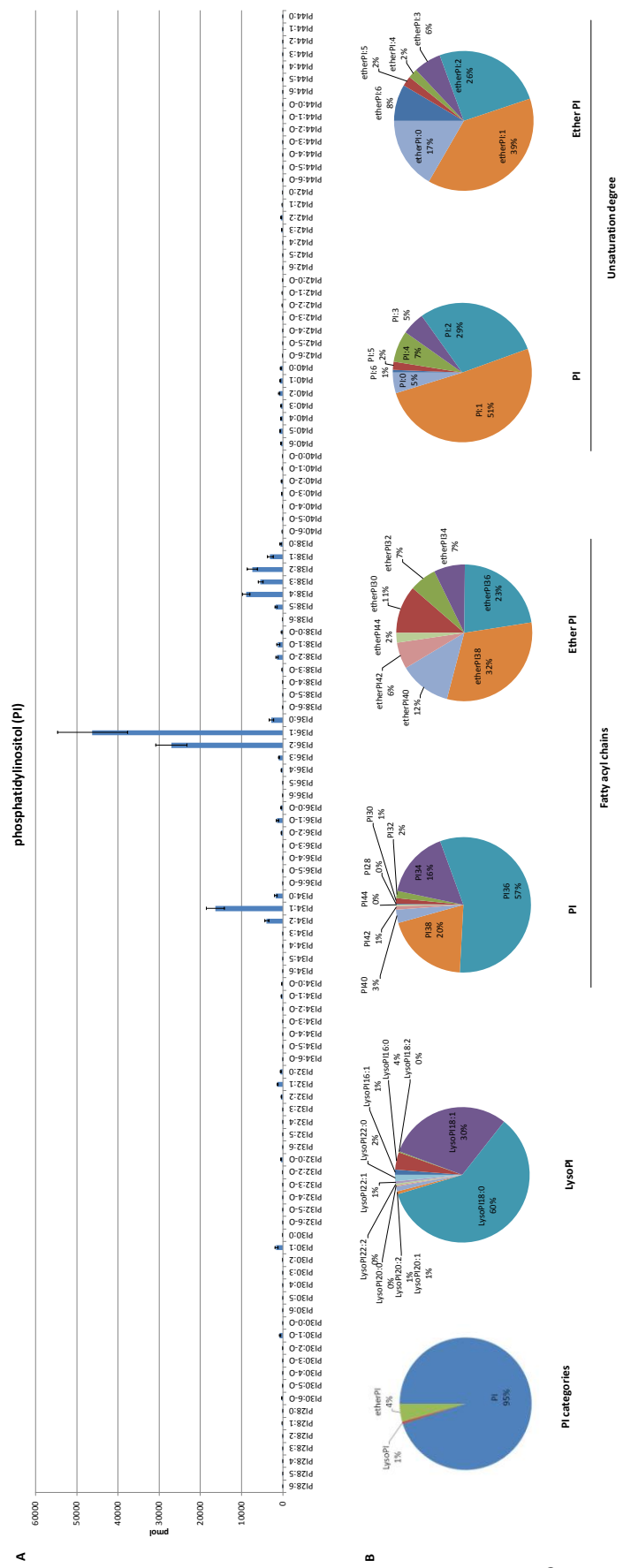
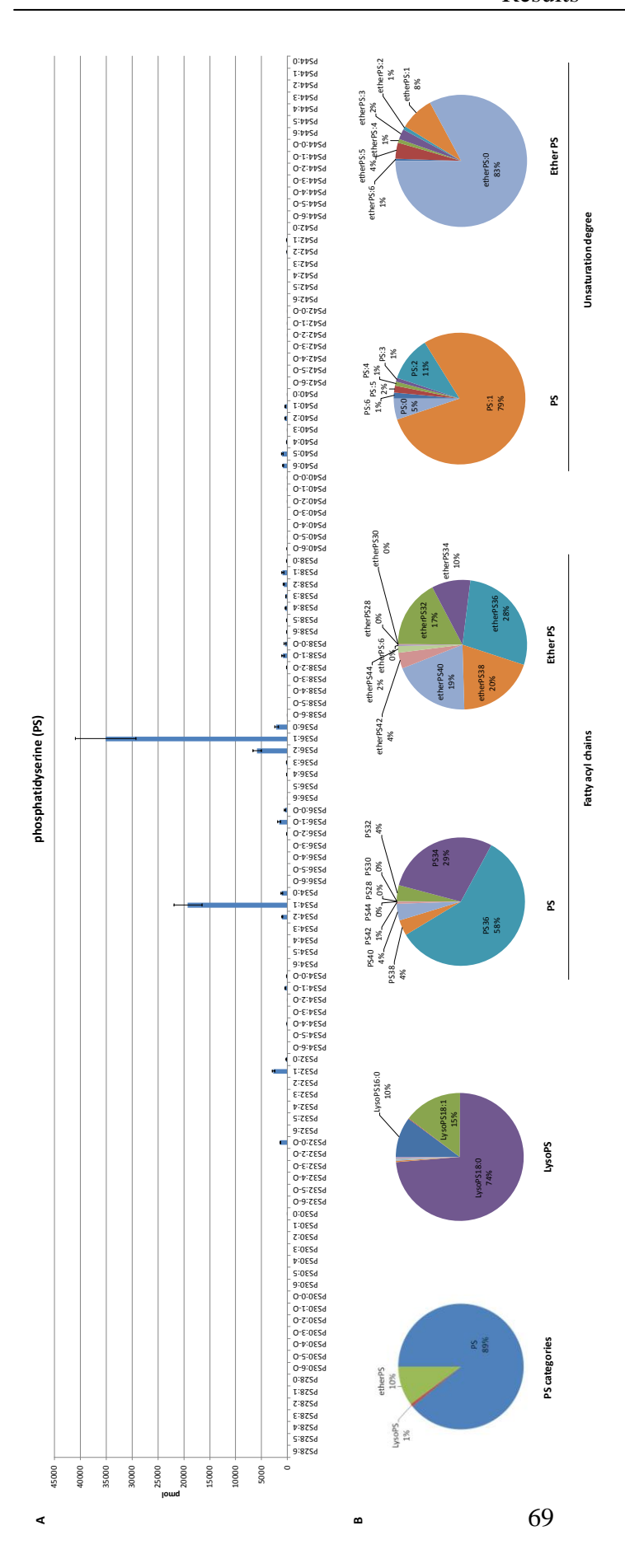


Figure 13. Distribution of cardiolipins (CL) species in HeLa MZ. Average quantity of individual CL species ± SEM (n=15)



(n=15) B. Proportion of Lyso-,PI, ether-PI and PI plus distribution of fatty acid chain length and unsaturation degrees in PI and Figure 14. Distribution of phosphatidylinositol (PI) species in HeLa MZ. A. Average quantity of individual PI species ± SEM ether-PI.



(n=15). B. Proportion of Lyso-, PS, ether-PS and PS plus distribution of fatty acid chain length and unsaturation degrees in PS and Figure 15. Distribution of phosphatidylserine (PS) species in HeLa MZ. A. Average quantity of individual PS species ± SEM ether-PS.

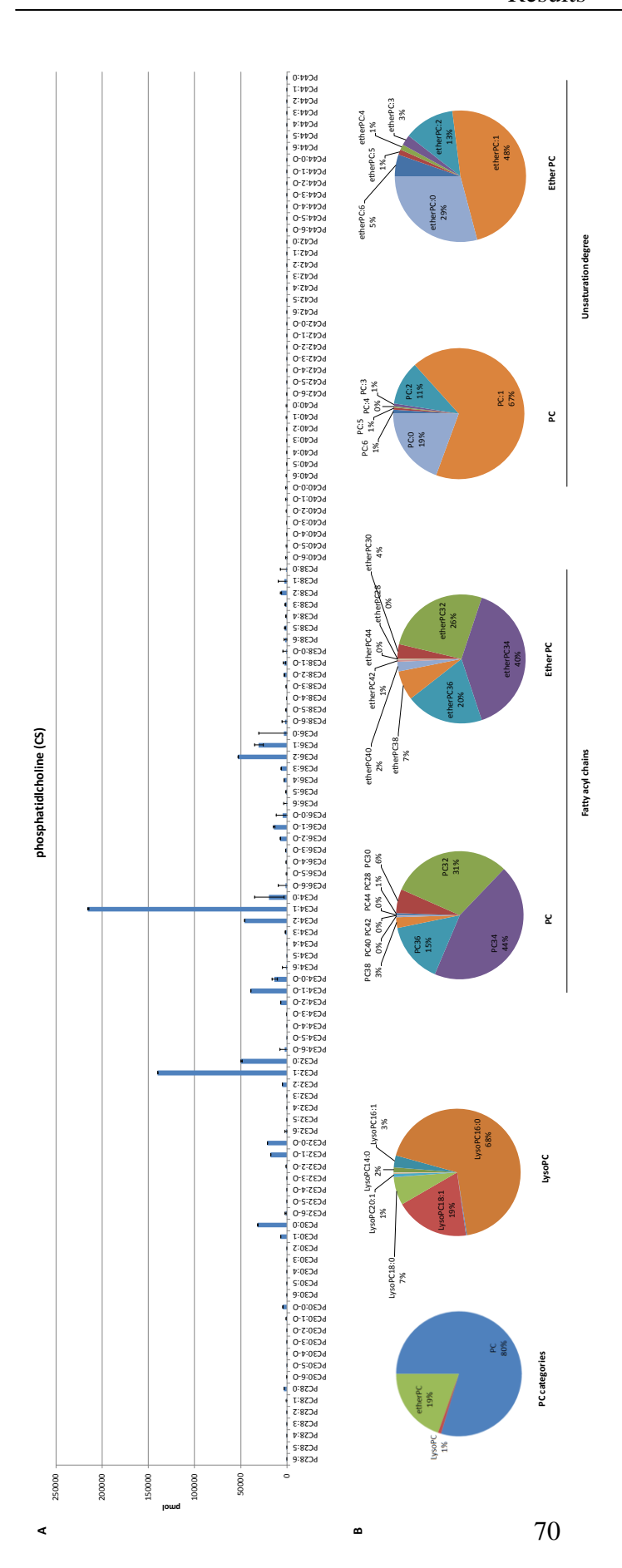


Figure 16. Distribution of phosphatidylcholine (PC) species in HeLa MZ. A. Average quantity of individual PC species ± SEM (n=15)B. Proportion of Lyso-,PC, ether-PC and PC plus distribution of fatty acid chain length and unsaturation degrees in PC and ether-PC.

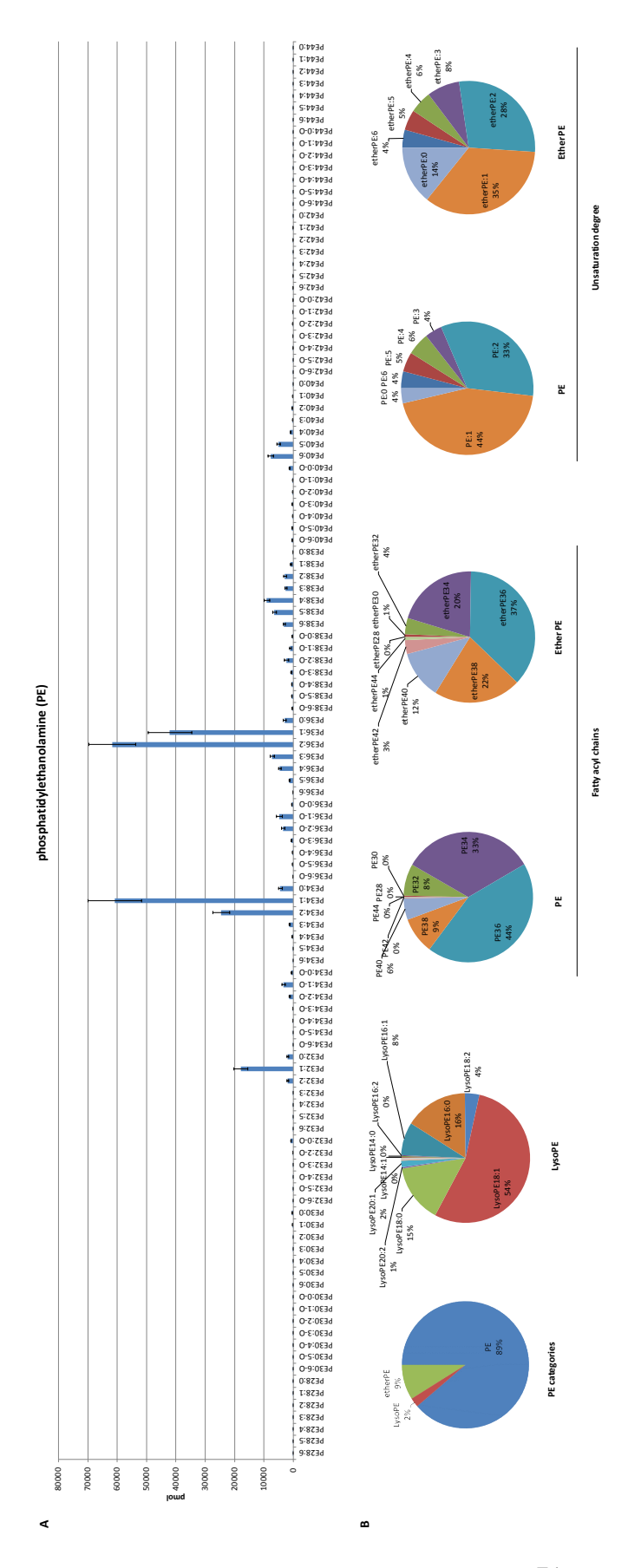
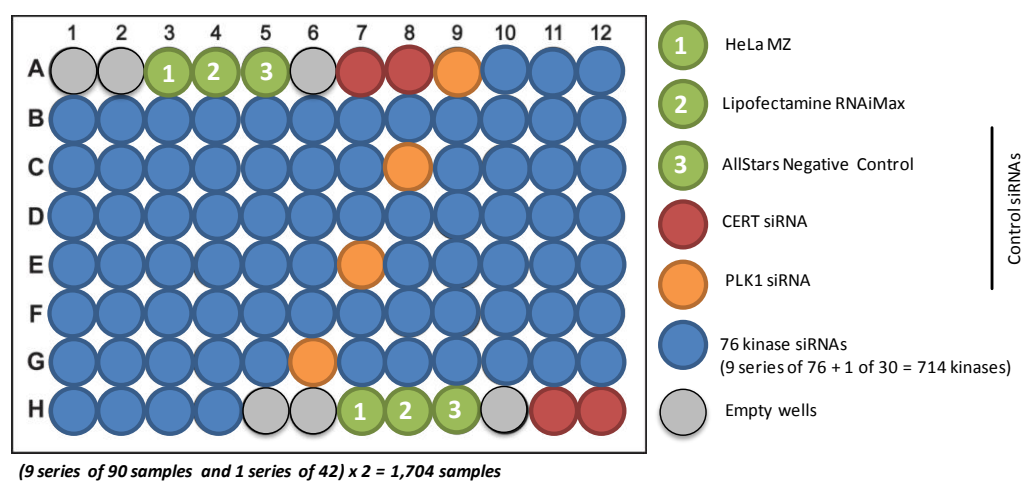


Figure 17. Distribution of phosphatidylethanolamine (PE) species in HeLa MZ. A. Average quantity of individual PE species ± SEM (n=15). B. Proportion of Lyso-, PE, ether-PE and PE plus distribution of fatty acid chain length and unsaturation degrees in PE and ether-PE.

## 2.3. Data processing

In order to optimize the running time of samples by mass spectrometry, which was the most time-consuming part of the experiment, cells were transfected and lipids analyzed by series of 90 conditions since the robotic nanoflow ion source (Nanomate) could infuse up to 96 lipid extracts per MS run. All series were repeated in two independent experiments (**Fig. 18**)

#### A. Plate layout of sample series



#### B. Sample analysis

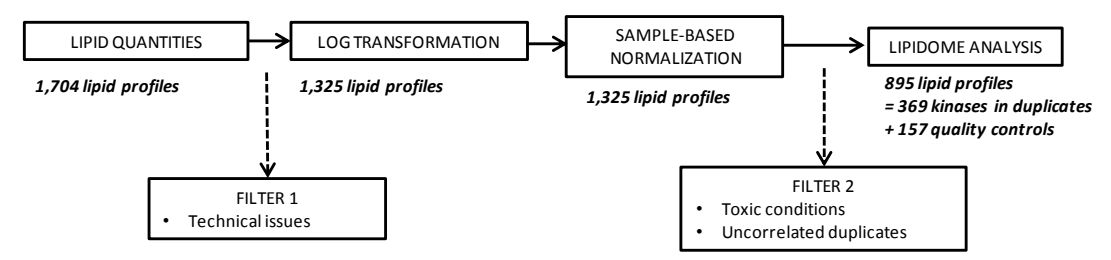


**Figure 18. General overview of the analysis procedure. 1.** Cell transfection, lipid extraction and analysis by mass spectrometry were performed by series of 90 samples in order to optimize the performance of mass spectrometry using the robotic nanoflow ion source (Nanomate). **2.** Lipidomic analysis of the screen was performed after discarding unreliable samples, log transformation and sample-based normalization of data (=lipid quantities) with z-score

First, siRNAs with incomplete lipid profiles due to technical issues were filtered from the dataset analysis. Next, in order to adjust for difference in cell size, membrane content, and extraction efficiency, the quantity of each lipid species was normalized to the sum of PLs (PC, PE, PI, PS, CL) in every sample. For practical reasons, the phosphorus assay of the 1,702 total

lipid extracts was not performed but the total content of PLs in lipid extracts should be proportional to phosphorus levels measured (Rouser et al, 1970).

Then, phospholipid-corrected lipid quantities were log<sub>2</sub>-transformed. As shown in Figure 11, lipid quantities from the kinome-wide screen rather follow a Poisson than a normal distribution. Log-transformation of raw data makes the distribution more symmetric and approximately normal in most lipid categories (**Fig. 19**). This transformation is usually necessary in siRNA screen experiments to formally conduct statistical analysis for quality control and hit selection (Zhang, 2011b).

Finally, log<sub>2</sub>-transformed data were normalized in order to correct systematic errors from the data and allow comparison of data from different experimental series (**Fig. 19**). Many normalization methods exist in RNA interference screens. They can be control or sample-based. Control-based normalizations require a statistically significant number of controls. However, only two Allstars negative controls were used per experimental series in this screen and as reported in the following sections, all negative controls (Allstars, Lipofectamine RNAiMax and untreated HeLa MZ) showed lower levels of SLs compared to the mean of all samples. Therefore, a sampled-based normalization was more suitable in order to analyze this primary RNAi screen (Birmingham et al, 2009). Among possible techniques: the z-score, strictly standardized mean difference (SSMD), B score and their respective robust version (z-score\*, SSMD\*, B score\*). Knowing that at least three replicates per siRNA are necessary to observe statistically significant SSMD (Zhang, 2011a) and that B scores is made for datasets with within-plate systematic effects, log<sub>2</sub>-transformed data were normalized per plate with the z-score (**Fig. 19 and 20**).

Z-score was calculated using the following formula:  $Z=(x_i-\bar{x})/\sigma_x$ , where  $x_i$  is the lipid quantity of the gene i,  $\bar{x}$  is the average of lipid quantities of all samples, and  $\sigma_x$  is the standard deviation of lipid quantities of all samples. Z-score is a measure of standard deviation. According to its sign, positive or negative, it represents data above or below the mean of all samples, respectively. The z-score was calculated either for every lipid quantity or for the sum of lipid quantities per lipid class or per chemical feature inside lipid class (chain-length, unsaturation degree, functional groups such as hydroxylation, ether, phosphate, etc.). Z-score data are normally distributed and sample-based normalization per experimental series prevented the batch effect (**Fig. 20**).

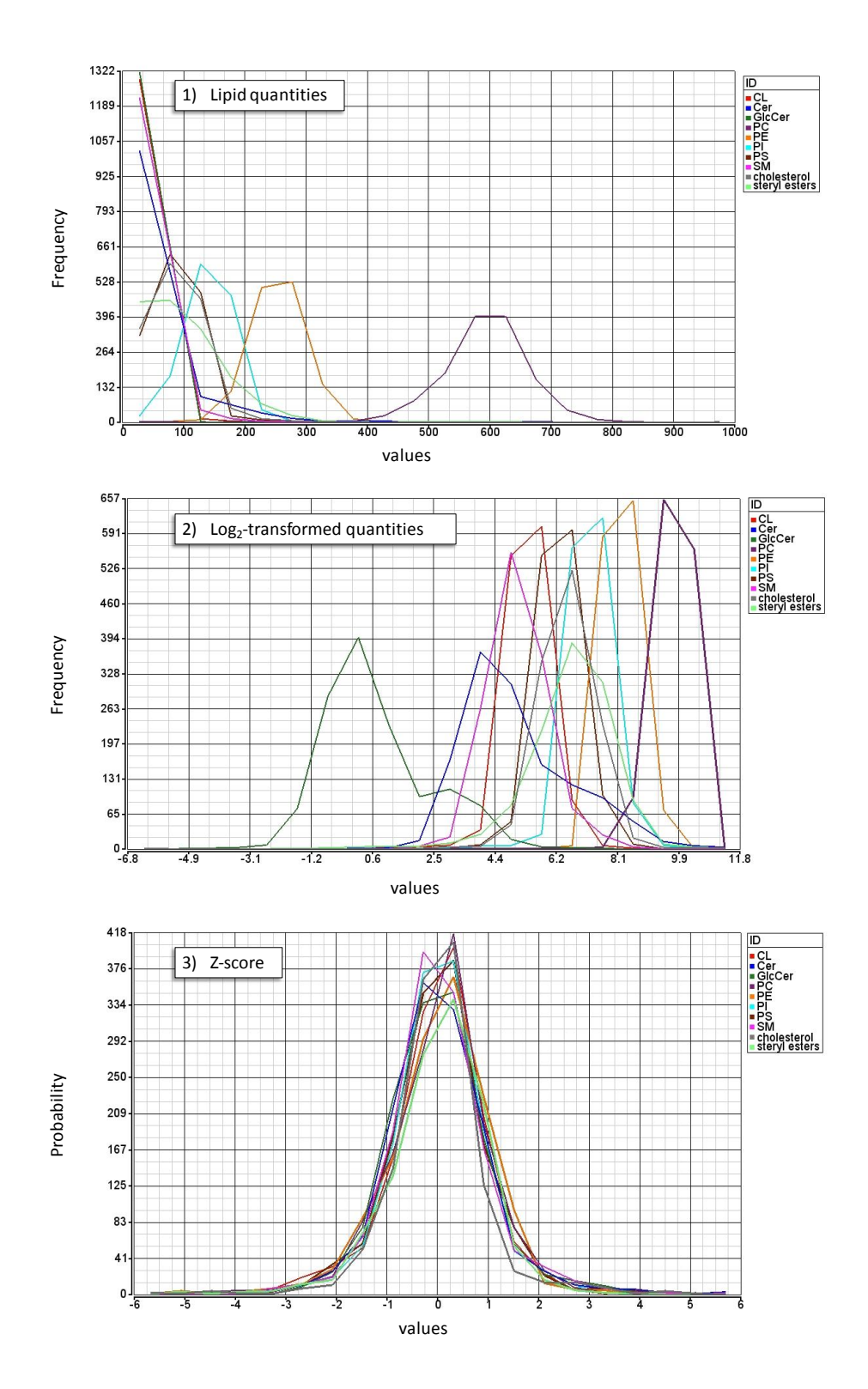


**Figure 19. Kinome-wide siRNA screen data transformation and normalization.** After filtering of conditions with incomplete lipid profiles, lipid quantities of 1,325 conditions were **1**) normalized to the sum of PLs, **2**) log<sub>2</sub>-transformed and **3**) sample-based normalized by calculating their z-score. The resulting dataset is normal and can be statistically analyzed for hit selection.

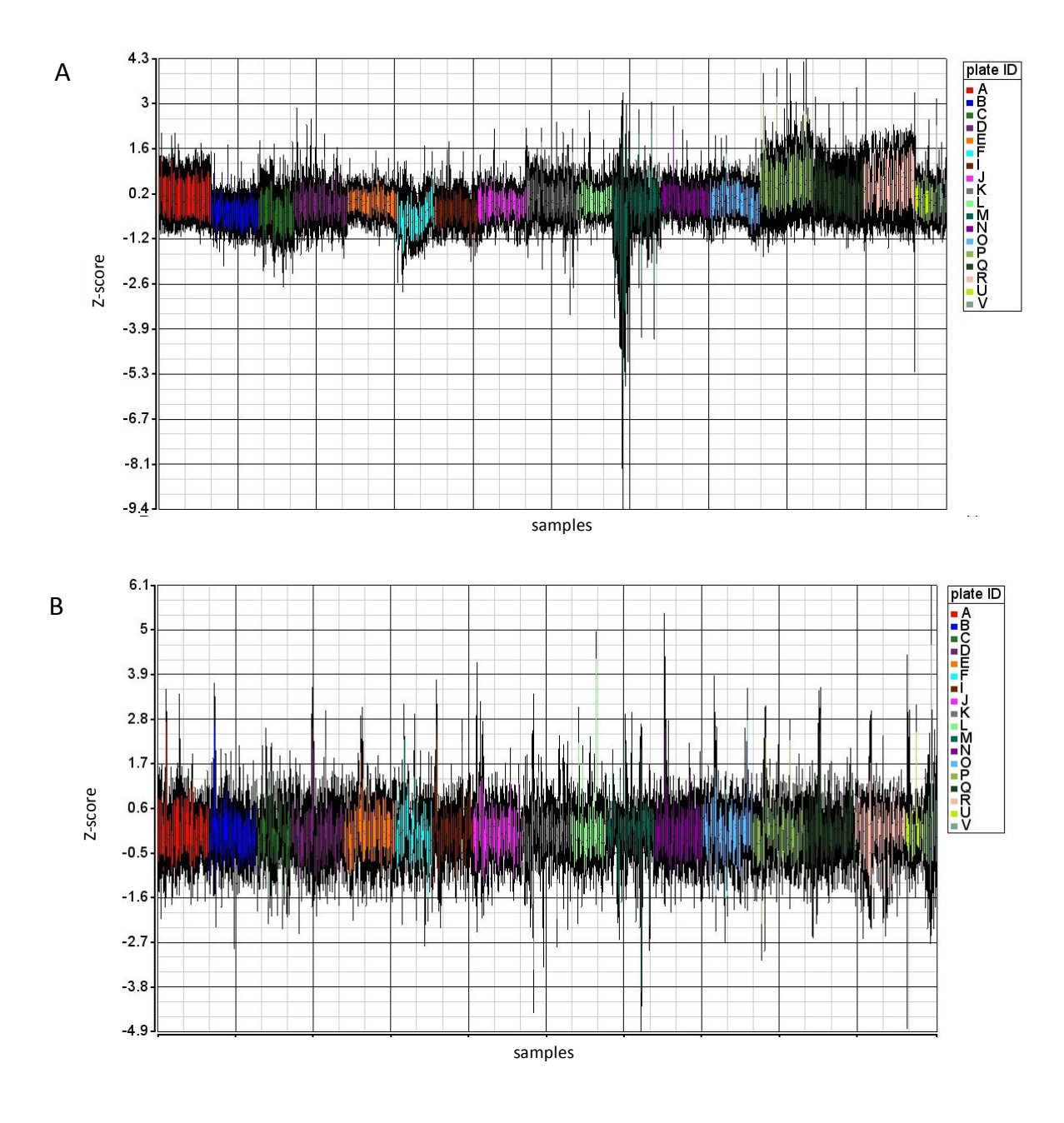


**Figure 20. Distribution of z-score values for all lipids (Y axis) per sample (X axis).** A.sample-based normalization over the whole screen (1,325 samples) or **B.** per experimental series. Colors represent samples from the same experimental series, also named "plate ID" in the legend.

In order to avoid analyzing siRNA conditions associated with apoptosis or cell necrosis due to siRNA-induced toxicity, genes with a significant effect on cell numbers were discarded from the z-score log<sub>2</sub> transformed dataset. This toxicity is due to several factors, including cell confluence at the time of transfection (Snijder et al, 2012), the decrease of an essential targeted protein, such as Polo-Like kinase 1 (PLK1) (Liu & Erikson, 2003), or the off-target effect (Jackson & Linsley, 2010). Cytotoxicity leads to a reduced number of cells, which results in turn in a characteristic lipid profile showing a decrease of quantities for all lipids. In order to automatically discriminate samples with few cells from the others, images of cells 72h post siRNA transfection were analyzed with the open-source image analysis software CellProfiler (Carpenter et al, 2006) and samples where the pictures of cells showed less than 70% of surface area occupied were discarded from the final analysis (Fig. 21).

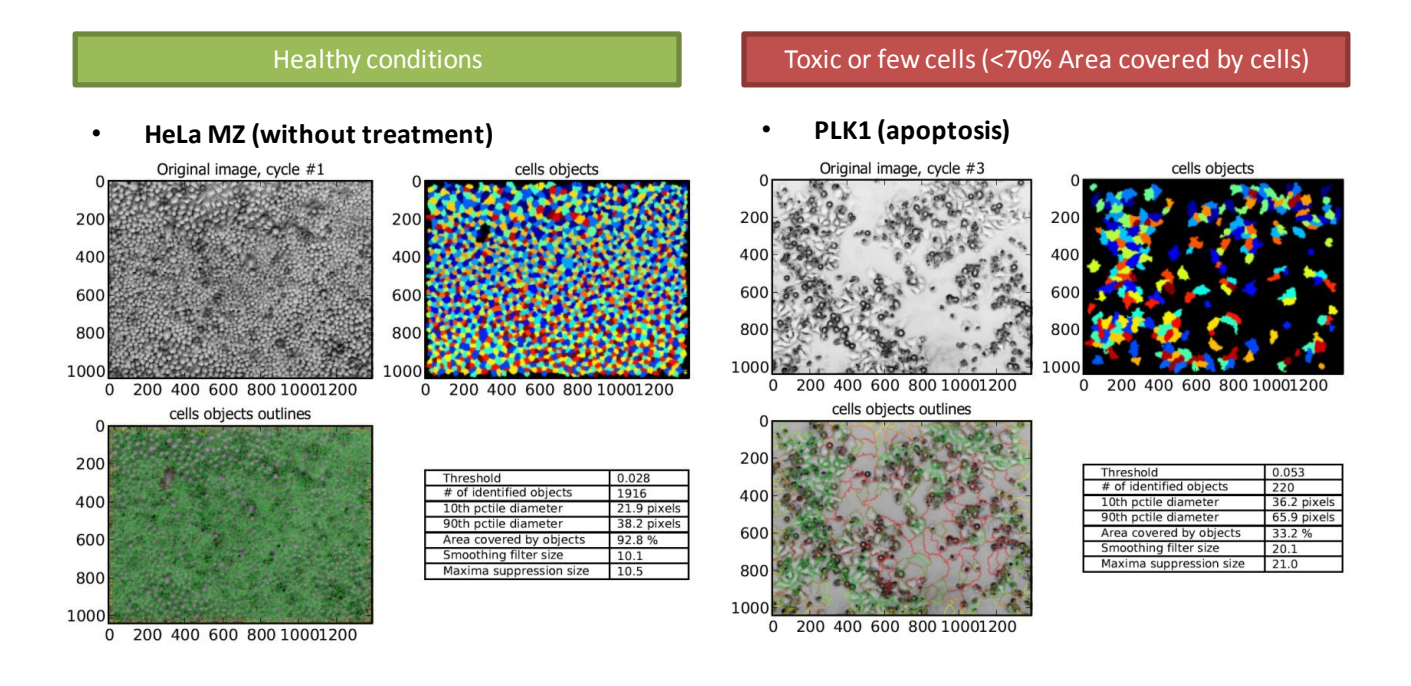


**Figure 21. Image analysis pipeline using the open-source software CellProfiler.** Samples with less than 70% of occupied area covered by objects (=cells) were considered as representative of samples with too few cells for objective interpretation of results. Their lipid profiles correlated with their cell phenotype and were discarded from the analysis.

In addition, siRNA conditions with only one biological replicate or for which, two biological replicates showed opposite lipid changes (Pearson correlation null or <0 between the z-score log<sub>2</sub> transformed profiles of two biological replicates) were discarded from the dataset, as well.

The raw dataset, calculations and discarded conditions with their justification are listed in the appendix (127).

## 2.4. Quality controls

In order to assess the quality of the screening experiment, several control conditions were added in each series of samples: either non-treated cells (HeLa MZ), cells treated with the transfection reagent alone (Lipofectamine RNAiMAx) or transfected with 14.4nM of non-targeting siRNA (siControl), or of siRNA against PLK1 and CERT (**Fig. 18**). Then, lipid levels in each sample were quantified using mass spectrometry, normalized to the total sum of PLs, log2-transformed and sample-based normalized with z-score, as described previously.

In order to validate the pertinence of the normalization, the level of lipids in control conditions was compared between all steps of the normalization process (**Fig. 24-20**). First, lipid quantities were normalized to the sum of PLs in every sample. A priori, it is not correct to sum the quantity of every individual lipid species because mass spectrometry method doesn't allow the absolute quantification of every lipid. However, when comparing the average sum of PLs to the average number of cells estimated from microscopy pictures using the open-source software CellProfiler, it appears that these two measurements are well correlated since the Pearson correlation coefficient is higher than 0.5 in most of experimental series (**Fig. 22A**). Moreover, the sum of PLs is strongly correlated to the sum of all lipids and PC in the whole screening dataset. The sum of PLs is also correlated to SL and sterols but to a lower extent (**Fig. 22B-E**). The correlation coefficient between PLs and SLs depends on the experimental series.

The comparison of average sums of total lipids before and after normalization to the sum of PLs shows that this normalization is able to correct the general variation of lipid levels in quality controls (**Fig. 23**).

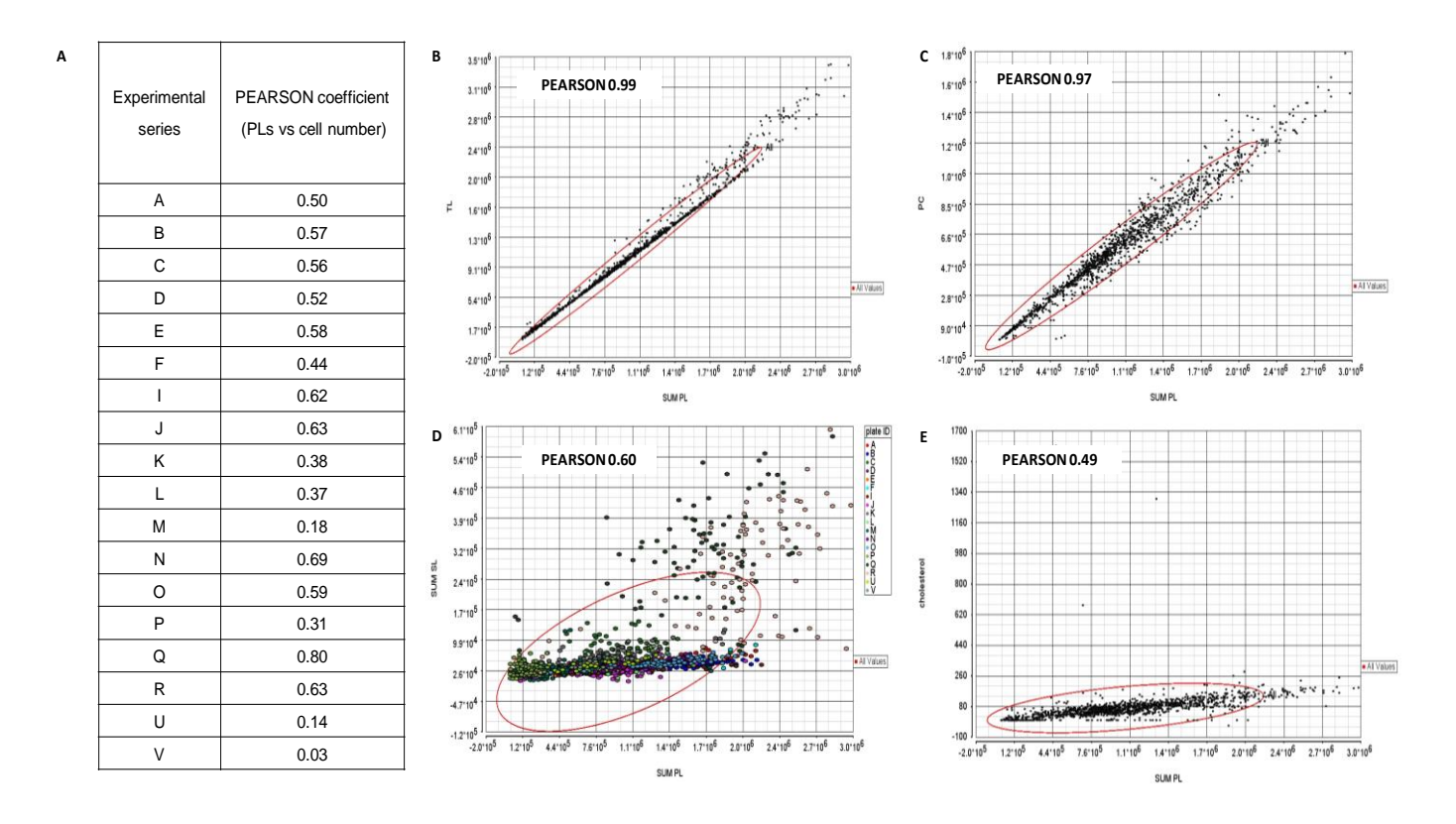


**Figure 22.** Correlation between lipid quantities and cell number. **A.** The Pearson correlation coefficient between the sum of PLs for each sample and its corresponding cell number estimated with CellProfiler (Carpenter et al, 2006) was calculated for every experimental series The Pearson correlation between the sum of PLs and the sum of all **B.** lipids, **C.** PC, **D.** SLs and **E.** cholesterol was calculated for the 1,325 samples before filtering.

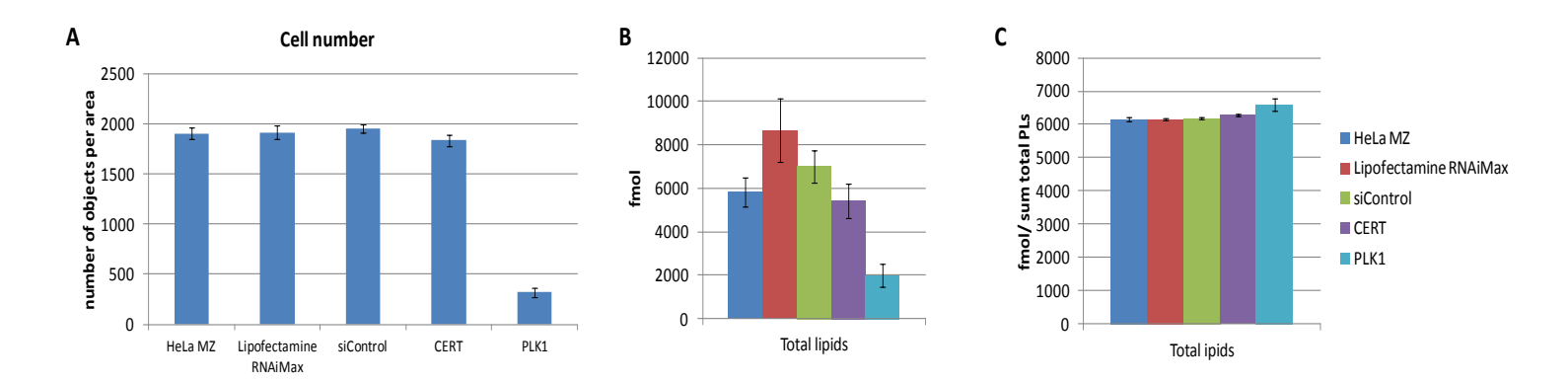


Figure 23. Correlation between lipid quantity and cell number in quality controls and normalization. HeLa MZ cells were seeded at  $4.10^5$  cells per 6cm dish and either treated with the transfection reagent alone (Lipofectamine RNAiMAx) or transfected with 14.4nM of non-targeting siRNA (siControl), siRNA against *PLK1* or *CERT*. Average lipid levels are expressed in fmol. **A.** Average number of objects (=cells) per area calculated from microscopy pictures with CellProfiler **B.** Average sum of all lipid quantities per siRNA condition before and **C.** after normalization to the sum of total PLs. Data are means  $\pm$  standard errors of the mean (SEM) and represent between 20 and 80 independent experiments. \*, P < 0.05; \*\*, P < 0.01; \*\*\*, P < 0.005 versus siControl.

## 2.1.1 Effects of transfection reagent and non-targeting siRNA controls

The transfection reagent used for the kinome-wide screen experiment was Lipofectamine<sup>TM</sup> RNAiMax from Life Technology. As most of siRNA transfection reagents, this is a proprietary liposome-based formulation made of cationic lipids that could eventually interfere with the lipid composition of treated cells. In order to assess the effects of this liposome-based transfection reagent on the lipid profile of HeLa MZ, the lipid composition of HeLa MZ was compared to the one from HeLa MZ treated with Lipofectamine RNAiMax, at the same concentration as for siRNA transfection. In addition, these conditions were compared to the lipid profiles of HeLa MZ transfected with a non-targeting siRNA, the AllStars siRNA negative control from Qiagen (siControl). Each series of samples from the kinome-wide RNAi screen comprised two replicates of each of these three negative controls (Fig. 10.). As expected, none of these negative controls had significant effects on the lipid profile of HeLa MZ (Fig. 24-28). However, it is worth noting that after sample-based normalization in z-score, these three negative controls show significantly less ceramides and glucosylceramides compared to the mean of all siRNA conditions from the screen. Moreover, Cer and GlcCer levels in non-treated HeLa MZ are significantly lower compared to siControl, suggesting that siRNA transfection in HeLa MZ naturally induces an increase of these sphingolipids that could be the expression of a cellular stress (Fig. 25D, 27C) and 28C).

### 2.1.2 PLK1 siRNA induces an apoptotic lipid profile

If negative controls chosen for this screen are classical in large-scale RNAi screens, positive controls were more difficult to find. Indeed, none is used routinely in the recent field of lipidomics. A good positive control should induce a specific effect for every phenotypic readout in order to allow statistically significant hit selection. In our case, it means finding either a target gene whose the silencing or drug inhibition induces a significant change in different lipid classes simultaneously or several target genes which has combined effects on all lipid classes. Since the kinome-wide RNAi screen was performed with the purpose to find such a target genes, no positive control could be used in the screen. Moreover, for practical and economic reasons, the efficacy of gene knockdown could not be controlled for all siRNA experiments from the screen

by qRT-PCR. However, in order to control the efficacy of the siRNA transfection reagents and conditions throughout the screen, siRNAs against PLK1 and CERT were used as additional quality controls. The silencing of PLK1 is a control of transfection, classically used in large-scale RNAi screening experiments that induces apoptosis. Five siRNA transfections against PLK1 were randomly performed in each series of samples. As expected, most of them induced cell death, meaning a sharp reduction in the number of cells (Fig. 23A) correlated with a global decrease of lipids (Fig. 23B). Lipids play an important role in apoptosis through their function in the cascade of signaling events and in membrane remodeling. Moreover, the lipid composition of apoptotic membranes is modified: ceramides are up-regulated and contribute to signaling events in mitochondria, PS molecules are exposed at the outer leaflet of plasma membrane, many of PLs are peroxidized under the oxidative stress that accompanies apoptosis and the level of CLs, the major mitochondrial lipids decrease leading to the release of cytochrome c with which it interacts (Crimi & Esposti, 2011; McMillin & Dowhan, 2002). In *PLK1* silenced-cells, beyond the general reduction of lipids, significant changes in the ratio between the levels of lipid classes could indeed be observed: SL increased, sterol esters and CL decreased while PLs and sterols remained unchanged relative to other lipid classes and compared to siControl (Fig. 24-25). In addition, the fatty acid distribution of sphingolipids was also modified, with a more important increase of shorter chains in general, and of C16 ceramides in particular (Fig. 26-28). All together, these modifications show that siRNA-induced knockdown of PLK1 specifically induced a programmed cell death, as expected. These effects were observed all along the screen, showing there was no problem of transfection conditions. Moreover, as the silencing of ceramide synthases in the pilot screen, the *PLK1* siRNA quality control emphasizes the importance of not only analyzing the levels of lipid classes but also the distribution of fatty acids inside lipid classes in order to well characterize phenomena.

## 2.1.1 CERT siRNA induces SL, PI and sterol changes

Two transfections of siRNA targeting CERT were performed per series, as an additional quality control of the kinome-wide screening experiment. As previously described in the pilot screen, the siRNA knockdown of CERT induced a significant decrease of SM, coupled to an

increase of sterol esters and C22-24 ceramides compared to siControl. Moreover, compared to the pilot screen experiment, an additional increase of PI was observed. (**Fig. 24-28**).

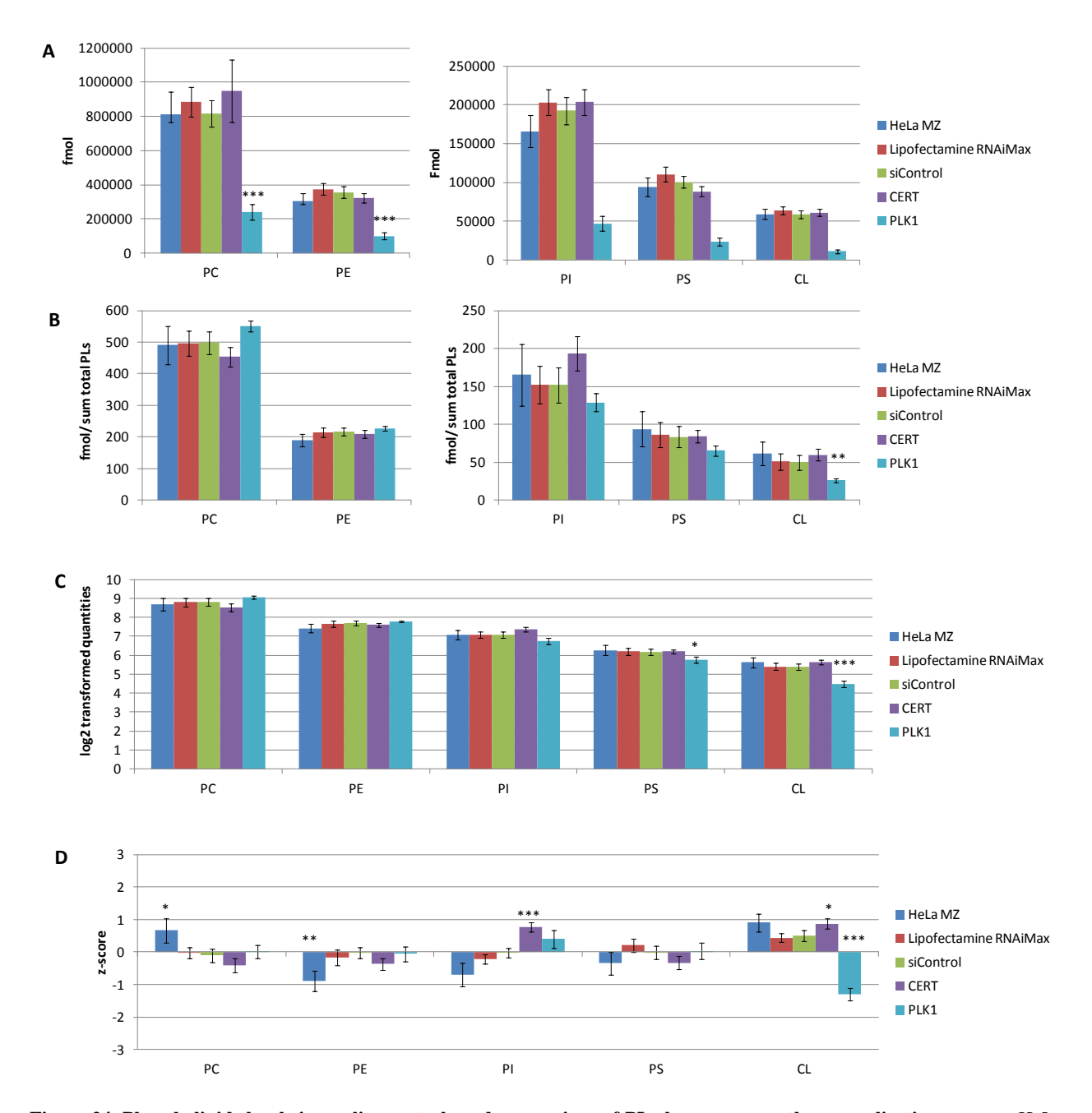


Figure 24. Phospholipids levels in quality controls and comparison of PL changes across the normalization process. HeLa MZ cells were seeded at 4.  $10^5$  cells per 6cm dish and either treated with the transfection reagent alone (Lipofectamine RNAiMAx) or transfected with 14.4nM of non-targeting siRNA (siControl), siRNA against *PLK1* or *CERT*. HeLa MZ represent non-transfected cells. Lipid masses were determined by ESI/MS. Average sum of lipid species per lipid class: **A)** before normalization, expressed in fmol, **B)** after normalization to the sum of total PLs per sample, **C)** after log2 transformation and **D)** sample-based normalization with z-score. Significant changes in lipids were tested with unpaired, two-tailed Student's t-tests to compare each siRNA to siControl \*, P < 0.1; \*\*, P < 0.05; \*\*\*, P < 0.01. Data are means  $\pm$  standard errors of the mean (SEM) and represent between 20 and 80 independent experiments.

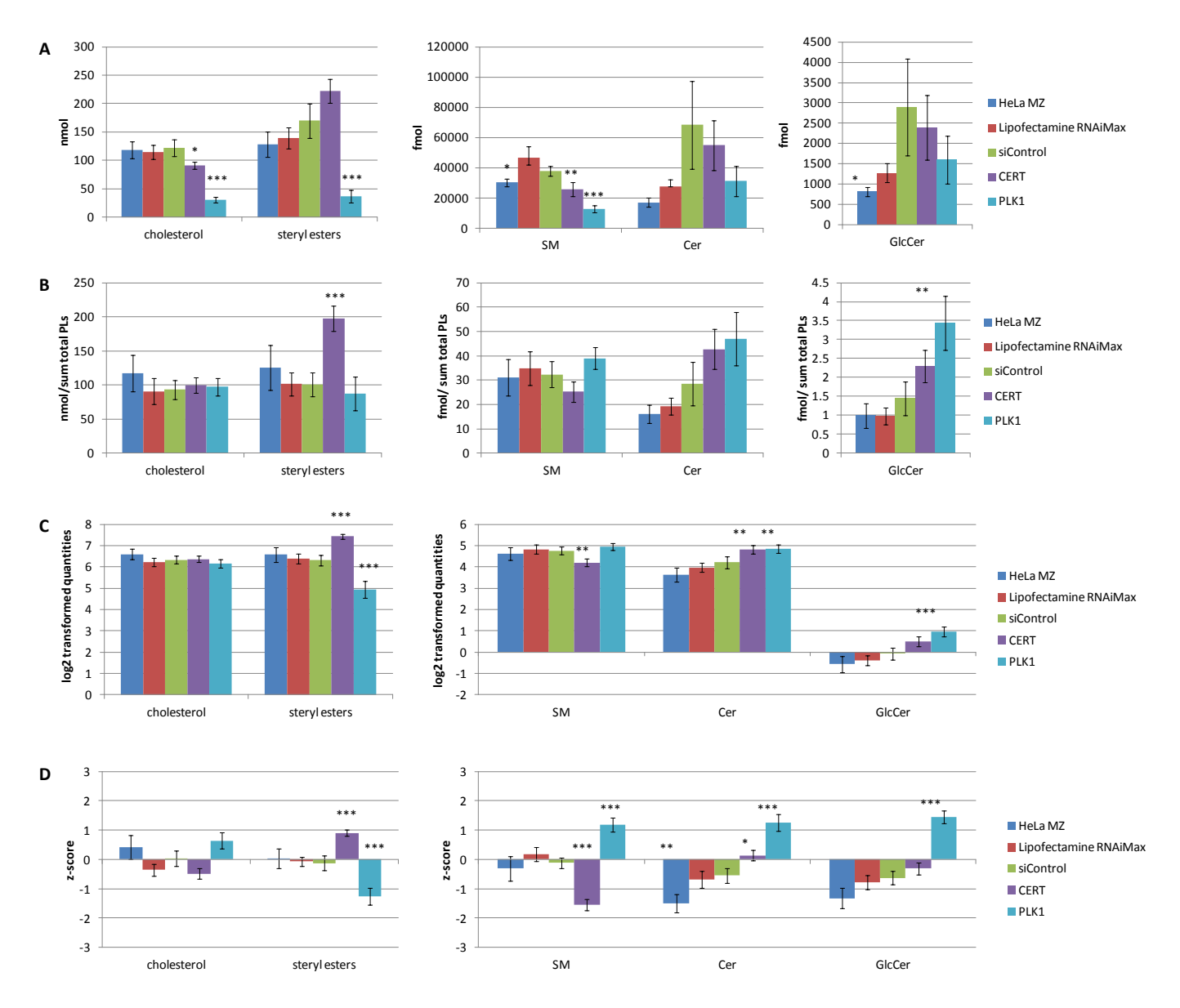
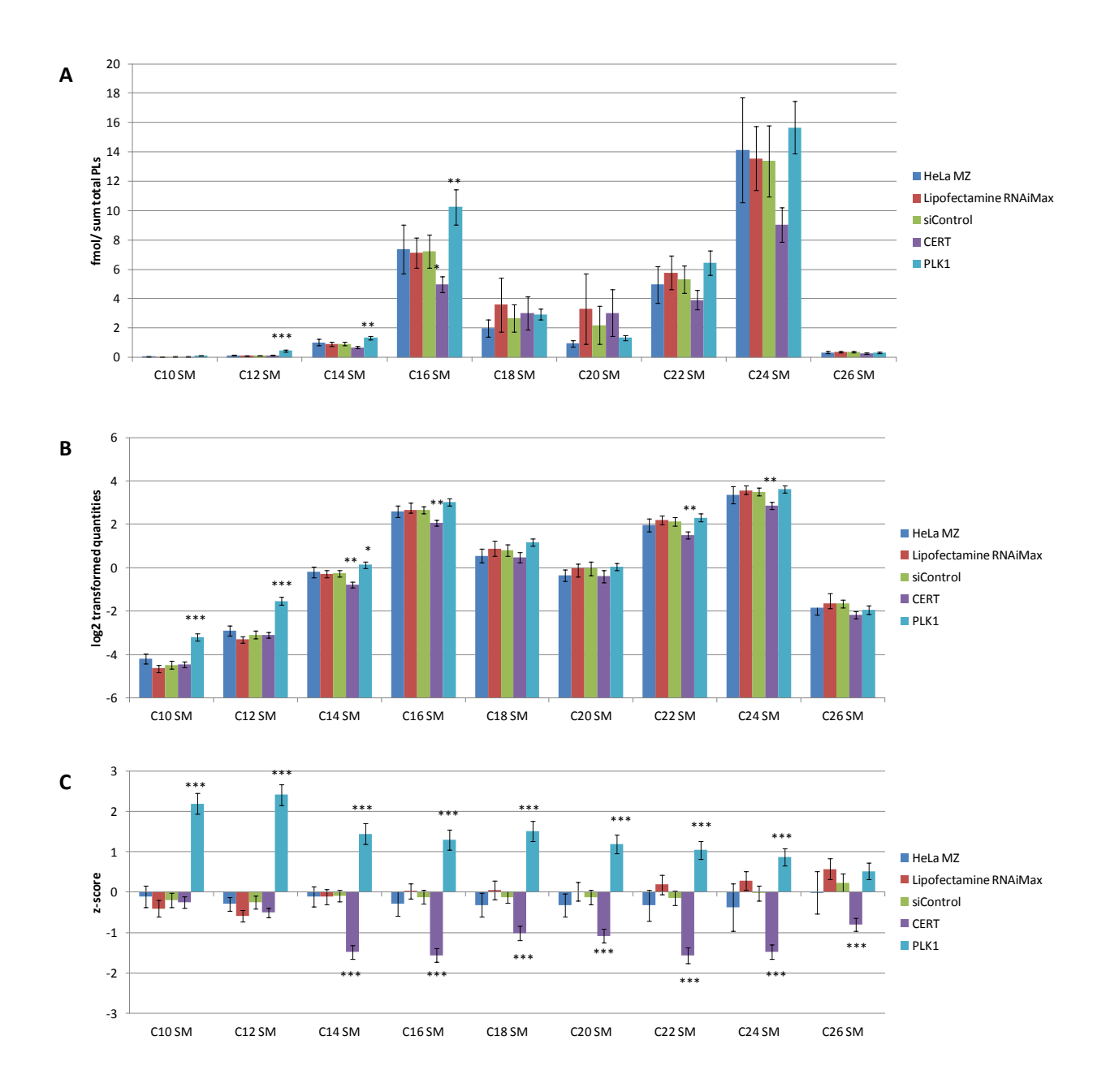
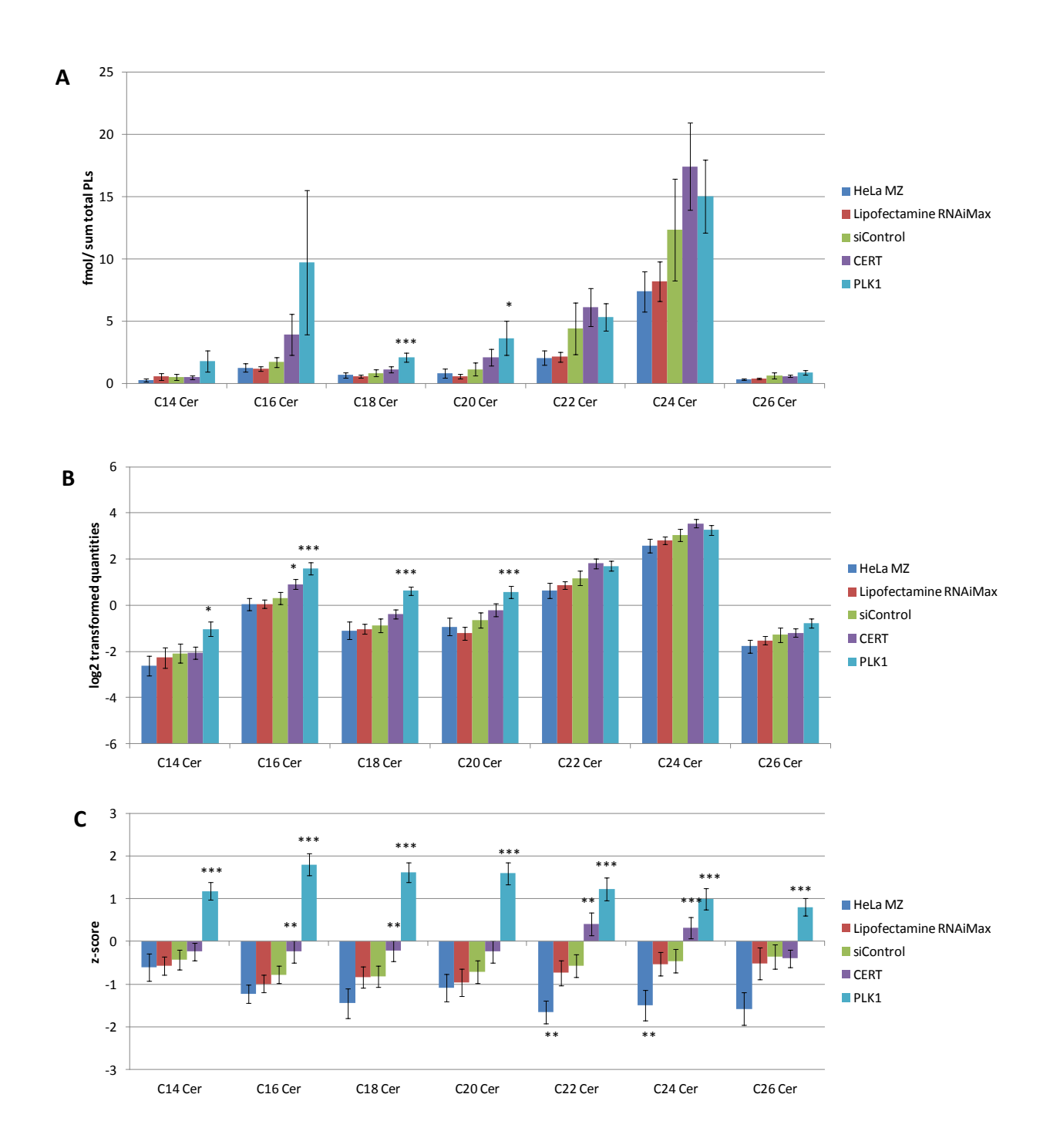


Figure 25. Sterols and sphingolipid levels in quality controls and comparison of lipid changes across the normalization process. HeLa MZ cells were seeded at 4.  $10^5$  cells per 6cm dish and either treated with the transfection reagent alone (Lipofectamine RNAiMAx) or transfected with 14.4nM of non-targeting siRNA (siControl), siRNA against *PLK1* or *CERT*. HeLa MZ represent non-transfected cells. Lipid masses were determined by ESI/MS and GC/MS (sterols). Average sum of lipid species per lipid class: **A**) before normalization, expressed in fmol, **B**) after normalization to the sum of total PLs per sample, **C**) after log2 transformation and **D**) sample-based normalization with z-score. Significant changes in lipids were tested with unpaired, two-tailed Student's t-tests to compare each siRNA to siControl \*, P < 0.1; \*\*\*, P < 0.05; \*\*\*\*, P < 0.01. Data are means  $\pm$  standard errors of the mean (SEM) and represent between 20 and 80 independent experiments.



**Figure 26.** Chain length distribution of SM in quality controls and comparison of lipid changes across the normalization process. HeLa MZ cells were seeded at 4. 10<sup>5</sup> cells per 6cm dish and either treated with the transfection reagent alone (Lipofectamine RNAiMAx) or transfected with 14.4nM of non-targeting siRNA (siControl), siRNA against *PLK1* or *CERT*. HeLa MZ represent non-transfected cells. Lipid masses were determined by ESI/MS and GC/MS (sterols). Average sum of lipid species per lipid class: **A**) before normalization, expressed in fmol, **B**) after normalization to the sum of total PLs per sample, **C**) after log2 transformation and **D**) sample-based normalization with z-score. Significant changes in lipids were tested with unpaired, two-tailed Student's t-tests to compare each siRNA to siControl \*, P<0.1; \*\*\*, P<0.05; \*\*\*\*, P<0.01. Data are means ± standard errors of the mean (SEM) and represent between 20 and 80 independent experiments.

.



**Figure 27.** Chain length distribution of Cer in quality controls and comparison of lipid changes across the normalization process. HeLa MZ cells were seeded at 4. 10<sup>5</sup> cells per 6cm dish and either treated with the transfection reagent alone (Lipofectamine RNAiMAx) or transfected with 14.4nM of non-targeting siRNA (siControl), siRNA against *PLK1* or *CERT*. HeLa MZ represent non-transfected cells. Lipid masses were determined by ESI/MS and GC/MS (sterols). Average sum of lipid species per lipid class: **A)** before normalization, expressed in fmol, **B)** after normalization to the sum of total PLs per sample, **C)** after log2 transformation and **D)** sample-based normalization with z-score. Significant changes in lipids were tested with unpaired, two-tailed Student's t-tests to compare each siRNA to siControl \*, P<0.1; \*\*\*, P<0.05; \*\*\*\*, P<0.01. Data are means ± standard errors of the mean (SEM) and represent between 20 and 80 independent experiments.

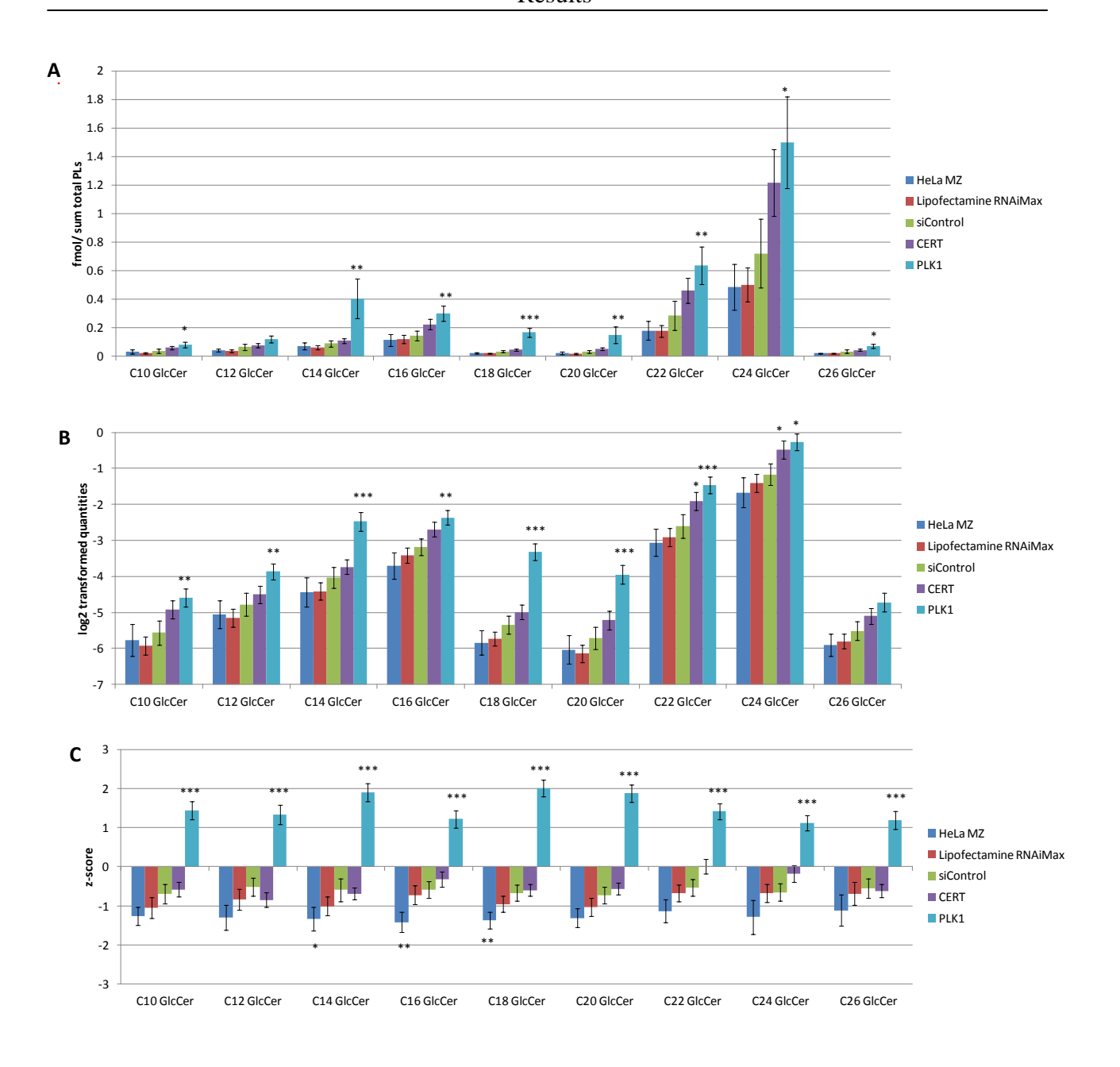
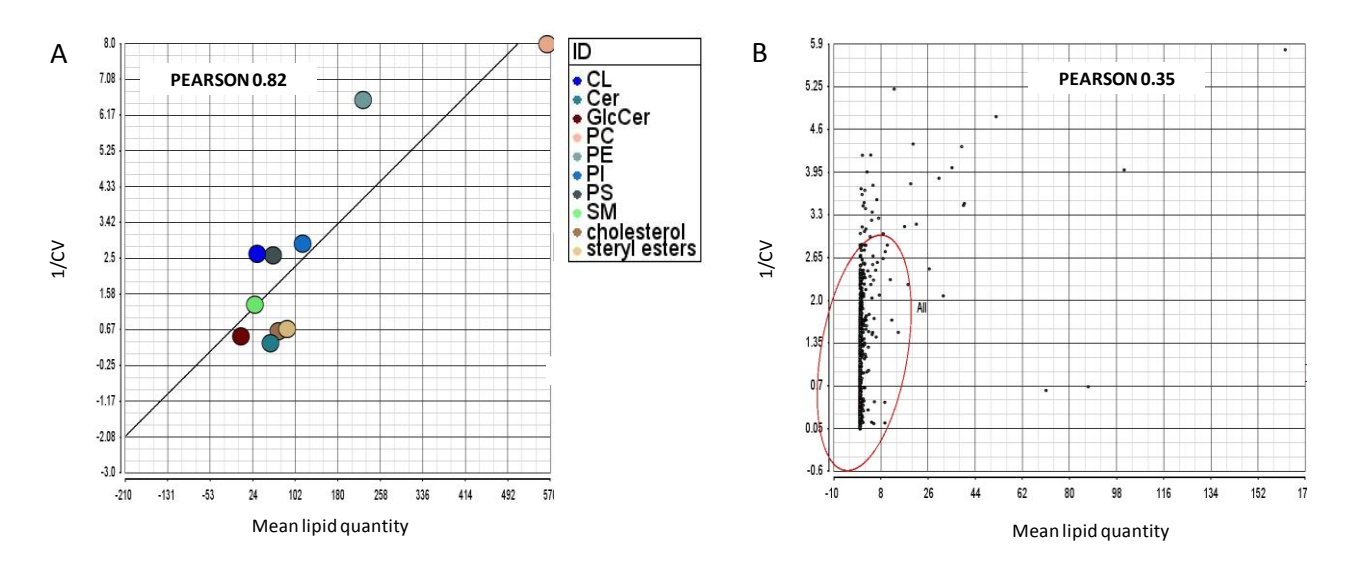


Figure 28. Chain length distribution of GlcCer in quality controls and comparison of lipid changes across the normalization process. HeLa MZ cells were seeded at 4. 10<sup>5</sup> cells per 6cm dish and either treated with the transfection reagent alone (Lipofectamine RNAiMAx) or transfected with 14.4nM of non-targeting siRNA (siControl), siRNA against *PLK1* or *CERT*. HeLa MZ represent non-transfected cells. Lipid masses were determined by ESI/MS and GC/MS (sterols). Average sum of lipid species per lipid class: **A)** before normalization, expressed in fmol, **B)** after normalization to the sum of total PLs per sample, **C)** after log2 transformation and **D)** sample-based normalization with z-score. Significant changes in lipids were tested with unpaired, two-tailed Student's t-tests to compare each siRNA to siControl \*, P<0.1; \*\*\*, P<0.05; \*\*\*\*, P<0.01. Data are means ± standard errors of the mean (SEM) and represent between 20 and 80 independent experiments.

### 2.5. Kinome-wide RNAi screen results

# 2.2.4 Observation of lipid behavior.



**Figure 29. Correlation between lipid quantities and their variability.** Scatter plot representing mean lipid quantities versus the inverse of the coefficient of variation (1/CV) for each **A.** lipid class or **B.** individual lipid species quantified by mass spectrometry over 1,472 samples.

More than 800 lipid molecules were quantified by mass spectrometry for each siRNA conditions. In order to be able to determine significant lipid changes during the process of hit selection, the variability of the different lipid categories was investigated. First, it is noteworthy that the coefficient of variation (CV) of lipid levels is inversely proportional to their abundance, in a general manner. PLs, the most abundant lipids in mammalian cells have a lower CV than SLs and sterols. Moreover, the CV of PLs is <1, which corresponds to low variance distribution, contrary to SL and sterols (Fig. 29A). The correlation between CV and lipid quantities is strong (Pearson correlation coef >0.8) when considering the sum of lipids of each class that is mostly influenced by the quantity of major lipid species (Fig. 29A). However, when plotting every individual lipid versus its corresponding 1/CV value, such correlation is less obvious (Fig. 29B). Indeed, most of molecules quantified by mass spectrometry are very low abundant lipids and their variability may not only depend on their abundance but also on their function in cells, degradation, recycling processes, food intake or on the efficacy of lipid extraction. Knowing this,

all individual lipid species were kept in the screen analysis because whatever the variability of considered lipids, I assumed that it didn't prevent to observe significant changes However, in order to overcome difficulties of hit selection and biases in hierarchical clustering due to the weight of variability of individual lipid species, lipids quantities were summed according to their categories: lipid class, chemical characteristics (i.e. hydroxylation, ether, etc.), chain length or unsaturation degree.

## 2.2.5 The puzzle of hit identification

After normalization and filtering of the dataset, the lipid profiles of 368 kinase siRNA-induced knockdowns were compared for hit identification. Every lipid change was expressed as the mean of z-score log2-transformed lipid quantities of two biological replicates. The whole dataset is available in the Appendix (50). Several methods for hit selection exist in large-scale RNAi screening experiments. They depend on the format of the screen: its scale, the number of replicates, the presence and the strength of controls, the normality of the dataset, the variability of phenotypic readouts and more importantly: the objective of the analysis. (Birmingham et al, 2009). The purpose of this kinome-wide RNAi screen was multiple: exploratory and hypothesis-driven. While the hypothesis-driven analyzes often complement previous studies to confirm or infirm hypotheses concerning specific genes, the exploratory analysis of the screen is based on statistical tools able to recognize sets of genes with potentially interesting lipid profiles and doesn't require upstream hypotheses. The combination of both approaches is necessary to retrieve a maximum of benefits from the screening analysis. This chapter is mainly devoted to the exploratory approach and to the comparison of different statistical tools for hit identification with their interests and limitations.

# a) Hit identification using threshold determination

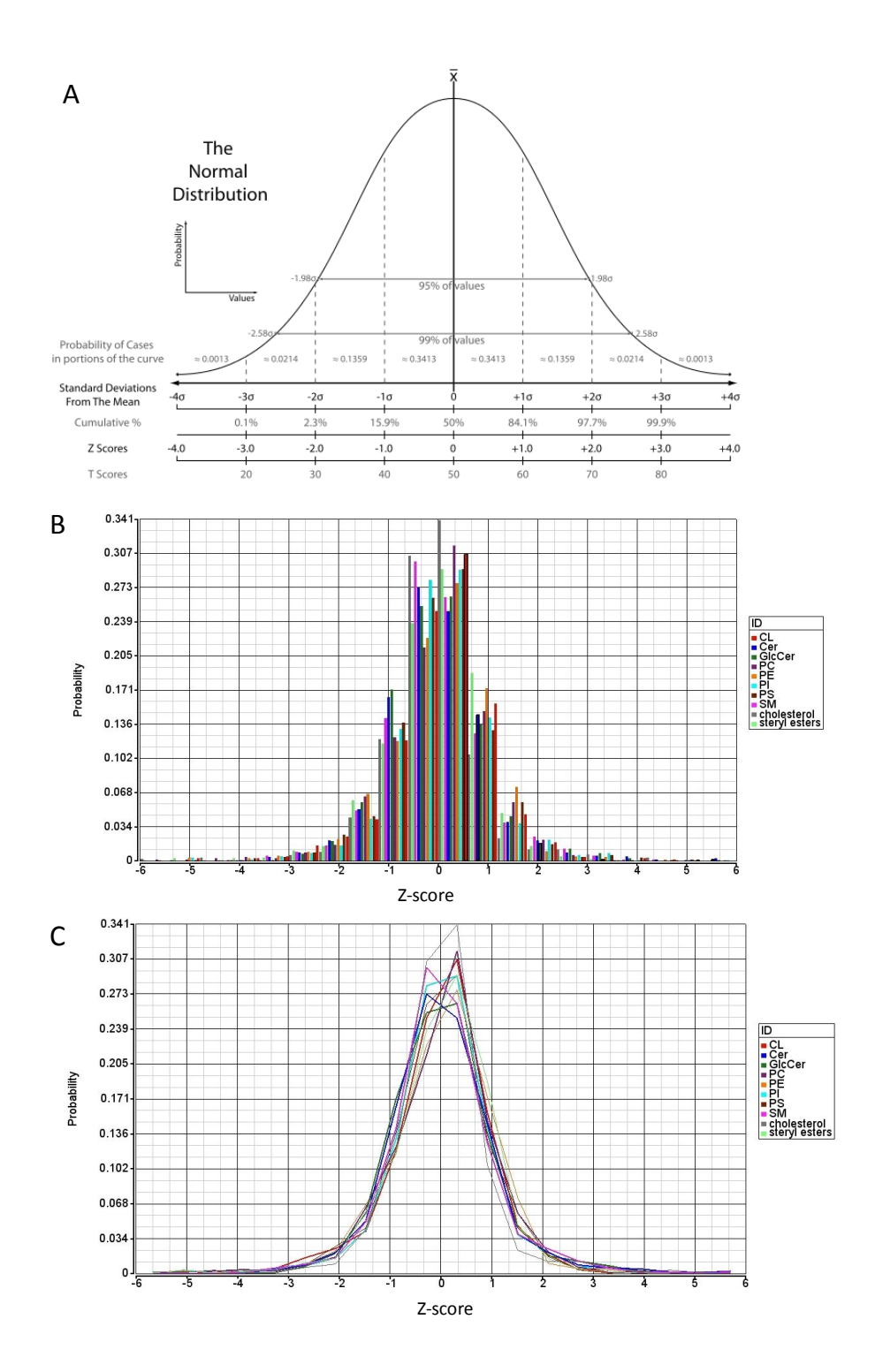


**Figure 30. Normal distribution and probability equivalence. A.** In a normal distribution, the distance from the mean is equivalent to different probabilities. **B and C.** Z-score distribution per lipid category over 1,325 samples with corresponding probabilities (Y axis). A and B are histograms of the same dataset represented in two different views (bars or lines)

In order to identify hits in every individual lipid categories, threshold determination was performed for each phenotypic score using the ranking method. This classical method of hit identification consists in considering: "Mean + or - k standard deviation (SD)" where k is a preset constant, which correlates the interval between the mean and  $\pm k$  SD to the probability for selected hits to be significant. In z-score data sets, the value of z is equivalent to  $\pm k$  SD. In a normal distribution, data are usually considered as significant for  $mean \pm k$  SD with k>= 2 or 3 (**Fig. 30A**). However, in my conditions, whatever the lipid category,  $\approx$ 90% of samples had a z-score |z| < 1. I could choose a more stringent cutoff value. However, knowing that I'm interested in several lipids at the same time, I preferred selecting more candidates to compare in order to increase the probability to find genes with the same pattern of lipid changes and sharing maybe the same function in lipid homeostasis. Thus, genes with phenotypic scores above the cutoff values |z| >= 1 were selected as hits (Birmingham et al, 2009). With this method, genes significantly affecting each individual lipid category, chain length and unsaturation degree could be identified.

The list of hit genes per lipid category could be studied independently. However, as shown in Table 3, most of hits affect different lipid classes, simultaneously. Among them, several are part of MAPK, AMPK and PI3K-MTOR signaling pathways, which are known to be key regulators in the energy balance in cells.

In order to better understand how these genes affect lipid homeostasis, it is necessary to group them according to their combinations of lipid changes. Different tools exist with their advantages and limitations. No method is bad. They simply present the results in different ways and all can help to build hypotheses. In the following sections, some of them are described.

PC		PE		PI		PS		CL	
-	+	-	+	-	+	-	+	2	+
CDK8	ACVR2B	ACVR2B	CDK8	ACVRL1	AATK	ACVRL1	ACVR1C	ACVR1B	ABCC1
DCK	AKT3	ALDH18A1	CLK4	ADCK2	CAMK1D	ADCK1	ADRBK1	ALS2CR2	BRAF
DYRK4	ALDH18A1	FGFR2	CSK	CABC1	GUCY2C	AKT2	FLT3	CHEK1	ERBB4
ERBB4	CHEK1	GCK	DCAMKL2	CAMK1G	INSR	ALDH18A1	FLT4	CHUK	FLJ25006
FASTK	DCAMKL2	GRK5	DYRK4	CHEK1	MAP2K6	CABC1	MAP2K1	EPHA6	HK3
MAP2K1	DGKI	GRK6	FLT3	CHUK	MPP1	CHEK1	MAP2K6	GRK7	INSR
MAP3K10	DLG4	HCK	LRRK2	DCAMKL2	PIP5K1C	CLK4	MAP3K1	HIPK3	LIMK1
MAP3K12	GRK5	KALRN	MAP2K1	DLG4	PKLR	CSK	MAP3K10	KALRN	LMTK3
MLKL	GRK6	KSR2	MAP3K12	ERBB3	PRKAR1A	DLG4	MAP4K4	LOC91461	MAP3K1
MPP1	GRK7	LIMK2	MAP3K15	GRK7	PRKCH	EPHA3	MAPK10	PGK1	MAP4K2
МҮОЗВ	KALRN	MASTL	MAP4K4	HIPK3	PRKDC	ERBB3	MATK	PIP5K3	MATK
PDK4	LCK	MPP2	МАРК6	LCK	RBKS	KALRN	NME6	PRPF4B	MET
PIP5K1C	LIMK2	PDK3	MAPK7	MAGI2	RFK	LCK	NTRK1	PTK7	MVK
PIP5K2B	MAGI2	PGK1	МАРК9	MAP2K1	RP6-213H19.1	MARVELD3	PIK3CD	RAF1	NEK9
PKLR	MPP2	PIK3CG	MLKL	MAP3K15	RPS6KC1	MPP2	PIP5K1C	RAPGEF3	NRBP2
PRKAA1	PDK3	PIM1	MYO3B	MARVELD3	SKP1A	NEK5	PRKAG1	RPS6KA4	PBK
PRKAR1A	PGK1	PRKAR1A	PBK	MATK	SRPK1	PDGFRA	PRKAR1A	SPHK2	PCK2
PRKG1	PIM1	PRKCA	PHKG2	NTRK3	TXNDC3	PDK3	PRPS2	SRMS	PFKFB3
PRPS2	PRPF4B	PRPF4B	PIP5K2B	PGK1	ULK1	PGK1	RALB		PIP5K1C
PTK6	SPHK2	RPS6KC1	PKM2	PIM1		PI4K2B	RPS6KC1		PIP5K2B
RPS6KC1	SRC	SPHK2	PRKG1	PRPF4B		PIK4CA	SKP1A		PRKAA1
SGK	SRMS	SRC	PRPS2	RPS6KA4		PRPF4B	SRPK1		RIPK2
SKP1A	TJP1	TJP1	РТК6	TNK1		PTK2	TAOK2		ROCK1
SRPK1	TNK1	TJP2	ROCK2	TYRO3		PXK	TJP3		SGK
STK17B	TRIM28	TNK1	RPS6KL1	YES1		RPS6KA4	VRK2		SRPK1
STK24	ULK1	TRIM28	SNF1LK			SRC			TJP1
TJP3	WNK1	ULK1	STK16			SRPK2			TJP3
UHMK1	WNK3	WNK1	STK17B			STK31			UHMK1
	YES1	WNK3	STK24			TJP2			YSK4
			UHMK1			TRIM33			
						ULK1			

Table 3. Major hits per lipid class. For each lipid class, list of genes with phenotypic scores above the cutoff values |z| >= 1 were selected as hits. Genes inducing an increase or a decrease of lipid levels are grouped in columns (+) or (-), respectively. Genes in blue induce a change in only one lipid category. Genes that induce a change in several lipid categories are in black.

SM		Cer		GlcCer		cholesterol		steryl esters	
-	+	-	+	-	+	-	+	-	+
ALS2CR2	CDC14B	ADCK1	CDC14B	ACVR1C	ANKK1	ABL2	CAMKK1	ACVR1B	ADCK1
BCR	CDK8	ALS2CR2	FLT4	ACVR2B	BRD3	CLK4 CSK	CDC14B CHEK2	ACVRL1 ADCK2	BRAF DCAMKL
CAMK1D	FLT4	ATR	FRAP1	ADCK1	FASTK	DCAMKL2	CLK3	ADRBK1	EPHA3
DCAMKL1	FRAP1	AURKC	MAP3K10	ATR	FLT4	ERN2	DCK	BRSK2	ERBB4
GRK6	GALK1	BCR	MAST1	AURKC		HERC2	DYRK4	CASK	FLJ40852
					GALK1	КНК	FLT4	CDC14B	FLT4
KALRN	GUCY2C	C9orf96	PRKAR1A	BCR	MAP3K1	KIAA0999	KALRN	CHUK	FN3K
LYN	MAP3K10	CAMK1D	PRKD3	CABC1	MAPK12	MAK	MARVELD3	CLK3	FRAP1
PBK	MAST1	CDK2	PRPS2	CSNK1A1L	PIK4CA	MAP3K11	PRKAR1A	CLK4	KDR
PRPF4B	PRKAR1A	DCAMKL1	SNF1LK2	DCAMKL2	PRKAR1A	MAPK12	PRKD3	CSK	MAP2K5
PTK6	PRKD3	EVI5L	TJP3	EPHA7	PTK7	MAPK8	TJP2 TJP3	DGKA DLG4	MAP4K2 MPP1
PXK	PRPS2	GRK6	TTBK2	EVI5L	SRPK1	MPP1	TSSK6	ERBB3	MYLK2
WNK3	SNF1LK2	KALRN		MAP3K15	STK32C	PGK1	WNK1	FGFR2	NEK2
	TJP3	LYN		MAP3K4	TP53RK	PI4K2B		ITPKA	PBK
	TTBK2	MAPK7		MARK1	ULK1	PIK3CG		LRRK2	PFKM
		MPP2		MARK4		PRPS1		NME4	PINK1
		PBK		MLKL		RAB38		PANK3	PRKAR1A
		PDK3		PFKFB1		RAF1		PFKFB3	РТК6
		PIK3C2G		PI4K2B		RIPK4 SCYL3		PFKL PIK3CG	RFK RPS6KL1
						TAF1L		PIM1	TGFBR1
		PRPF4B		PIK3C2B		TSSK2		PKM2	TJP3
		PTK6		PIK3C2G		UHMK1		PKN1	WNK3
		PXK		PRKACG		ULK1		PRPF4B	
		SRPK2		PRKCA				RIPK4	
		STK31		PRKG2				RPS6KA4	
		WNK3		PRPF4B				SGK	
				PSKH1				SNF1LK2	
				PXK				TAF1L TJP2	
				RAPGEF3				TNK1	
				RPS6KA4				TRIM33	
				STK31				TSSK1	
				TEK				TSSK2	
				200				TSSK6	
				TRIM24				ULK3	
				TRIM33				WNK1	

### b) Principal Component analysis (PCA)

Then, to determine whether certain genes induced specific combinations of lipid changes, a Principal Component Analysis (PCA) of the dataset was performed. PCA is a linear transformation that converts n original variables, here lipid categories, into 2 or 3 dimensions, allowing to visualize more clearly how the variables are correlated. PCAs were performed using Partek Genomics Suite. All variables are represented in bi-plots by vectors (Fig. 31 and 32), and the direction and length of the vector indicate how much each variable contributes to the two principal components in the plot. Here, 2-dimensions representations were chosen because the first two principal coordinates explained enough of the variance in my data (between 42 and 90% depending on the variables, cf. Fig. 30-32). For instance, in Fig. 30A, the first principal component, on the horizontal axis, has positive coefficients for the different variables (PI, PS, cholesterol, steryl esters, CL and sphingolipids). That is why the eight vectors are directed into the right half of the plot. The largest coefficient in the first principal component is cholesterol. The second principal component, on the vertical axis, has positive coefficients for the variables cholesterol, steryl esters, PI, PS, CL, PE and negative coefficients for PC and sphingolipids. This indicates that the second component distinguishes these two clusters of variables that tend to have opposite variations. These 2-D bi-plots also include a point for each of the 368 genes, with coordinates indicating the score of each observation for the two principal components in the plot. For example, points near the left edge of this plot have the lowest scores for the first principal component. The points are scaled with respect to the maximum score value and maximum coefficient length, so only their relative locations can be determined from the plot.

The analysis of the 2-D bi-plots representing PCAs with different combinations of lipid classes that allows to select genes that vary the most according to individual or combinations of lipid categories. I performed a PCA for major lipid classes but also for chain length and unsaturations inside each lipid class in order to find genes that showed changes specific of chain length, for instance. We can observe that whatever the bi-plot, most of genes cluster in a cloud in the middle of variables and represent genes with few changes of lipid levels.

The first PCA, on major lipid classes (**Fig. 30**) shows the general tendency of lipid changes in the screen. Some clusters of lipid changes can be observed. In general, sphingolipids tend to change together. Idem for PI, PS and cholesterol. On the contrary, PC and PE tend to show

opposite directions. As a proof of concept, Fig. 30A was performed with the normalized 1,325 samples before filtering on toxic conditions and includes both duplicates per gene, including the controls. As observed previously, negative controls C100N, C100M and C100S standing for HeLa MZ, Lipofectamine RNAiMax and siControl, respectively, all cluster in the middle of the plot because of their lack of effect. On the contrary, samples treated with siRNA against CERT are a bit eccentric with more positive coefficient on the Y axis toward steryl esters and samples treated with siPLK1 (Control) are completely dispersed from the centre with a phenotype in sphingolipids.

Then, the same PCA was performed with the final dataset grouping averaged z-scores of duplicates showing correlated lipid profiles and no toxicity. From this PCA, some genes with extreme changes for some lipids could be selected. PRKA1R1A for instance, that codes for a genes involved in the control of autophagy, is localized at the upper right edge, in the opposite direction of PC and PE. When coming back to the z-score values, it corresponds to an increase of all lipids except PC and PE. The other PCAs were performed in order to dissect lipid changes observed inside each lipid categories and select genes with specific changes. I could describe the hits observed for each PCA but the hit analysis is still ongoing and involves projects in collaboration with other groups. Instead, I will rather describe how lipids change inside each lipid class according to the composition in fatty acyl chains (Fig. 31 and 32). Indeed, each lipid class comprises itself hundreds of lipids that differ in their fatty acyl composition. In mammalian cells, fatty acyl chains of membrane lipids usually range from 12 to 26 carbons and comprise between 0 to 6 double bonds (Cook, 2008). The combinations of fatty acyl chains differ between SLs and PLs. For instance, shorter and more polyunsaturated FAs are found in PLs. Moreover, while for PLs several combinations of FA are possible and not distinguishable using the TSQ mass spectrometer, SLs are made of a fixed 18 carbons-long sphingoid base acylated with a FA ranging from 14 to 26 carbons depending on the specific ceramide synthases (Aguilera-Romero et al, 2013). FA present in membrane lipids come either from de novo synthesis, diet, such as essential FAs or from the combination of both through sequential pathways of fatty acid desaturation and chain elongation (Cook, 2008). Moreover, as described in the introduction, fatty acyl chains can be hydroxylated in sphingolipids, bound the glycerol backbone through ether linkage in phospholipids, or lipids can also comprise only one hydrophobic chain, as in lysophospholipids and dihydroceramides.

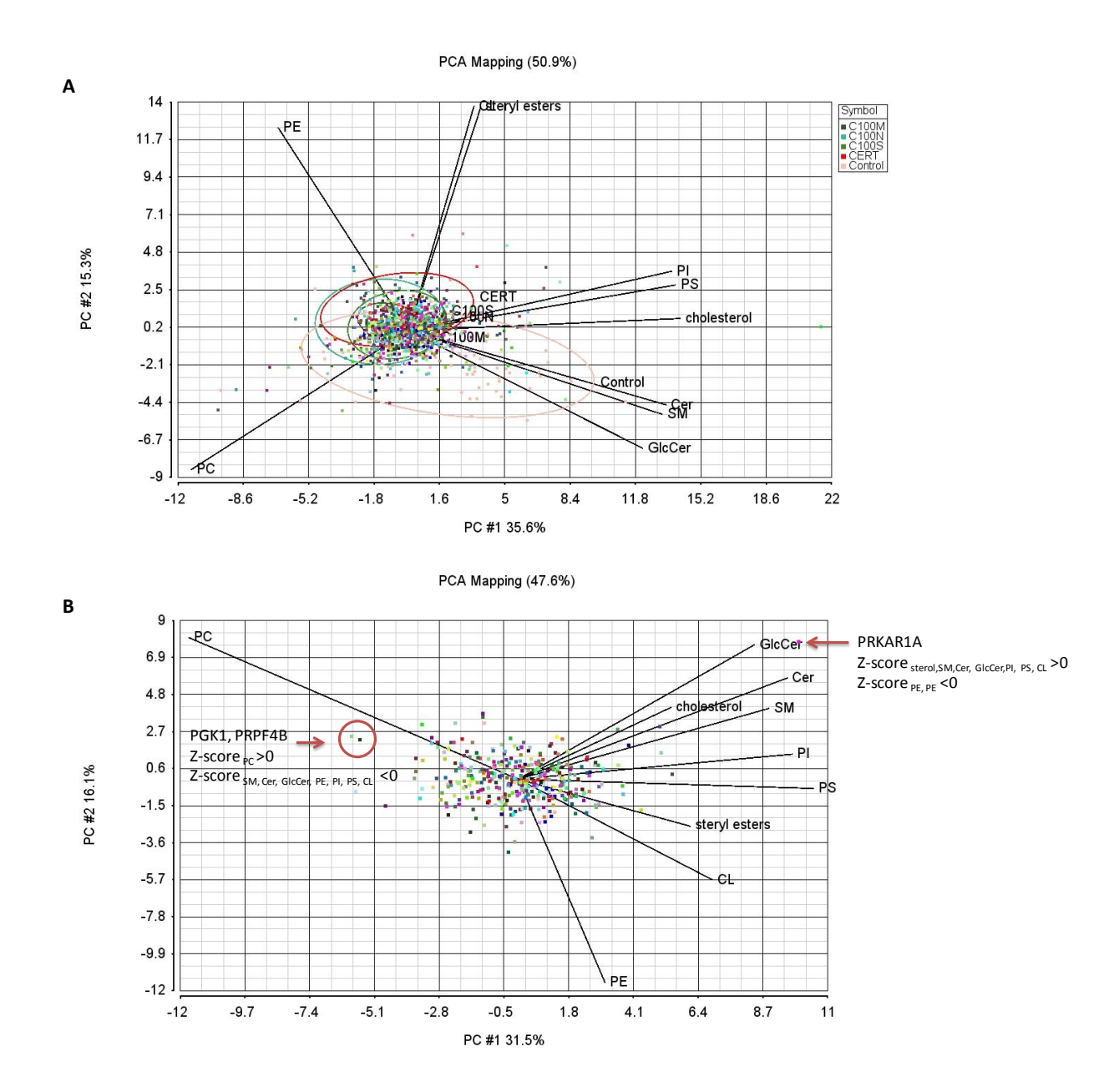


**Figure 30. Principal Component Analysis (PCA) of lipid classes.** The z-score data from the kinome-wide RNAi screen were analyzed by PCA using Partek Genomics Suite **A.** before (1,325 samples) and **B.** after filtering and averaging the two duplicates (368 genes). % (percentage of PCA mapping expressed in the title of each graph) of the variation in samples was revealed in the first two components. The first principal component named PC#1 is represented by the X axis and the second principal component by the Y axis (PC#2). Lipid categories appeared to be a source of variation and are indicated by the different vectors.

First, for phospholipids (**Fig. 31**), it is noteworthy that genes show different changes between the different classes of PLs but that globally vectors representing variables Lyso- and ether species point in the same direction as their diacylester counterparts. When comparing changes in unsaturation degree, we can notice that whatever the PL category, variations in very unsaturated PLs (>2 unsaturations) differ from variations observed for saturated or monounsaturated lipids. Finally, whatever the PL category, variations according to fatty acyl chain lengths can generally be clustered in two groups: short chains versus long chains, even if the precise composition of these two groups differs between PL categories.

Concerning sphingolipids (**Fig. 32**), variations depend more on the lipid class (SM, Cer or GlcCer) than the unsaturation degree of the fatty acyl chain, its number or its nature (SL, hydroxySL or dihydro-). However, when comparing variations depending on the fatty acyl chain, it is noteworthy that depending on the SL class, variations affect differently different cluster of fatty acyl chains. For instance, in SM, variations observed for C14 and C16 differ from longer chains and from C10-C12. For ceramides, four groups can be distinguished: group 1 with C16, group2 with C22-24, group 3 with C18, C20 and C26 and group 4 with C10-14. Knowing that ceramide synthases are specific from fatty acyl chain length, it is possible from this PCA to select genes that affect specifically these different groups and maybe find regulators of ceramide synthesis. Finally, in glucosylceramides there is only a division in variations between the major GlcCer (C22, C24, C16) and the others.

In conclusion, from this analysis with PCA, we learn that major changes observed in lipid profiles can be first attributed to general changes between lipid classes and inside each lipid class mainly from the unsaturation degree in phospholipids and from the fatty acyl chain length in sphingolipids.

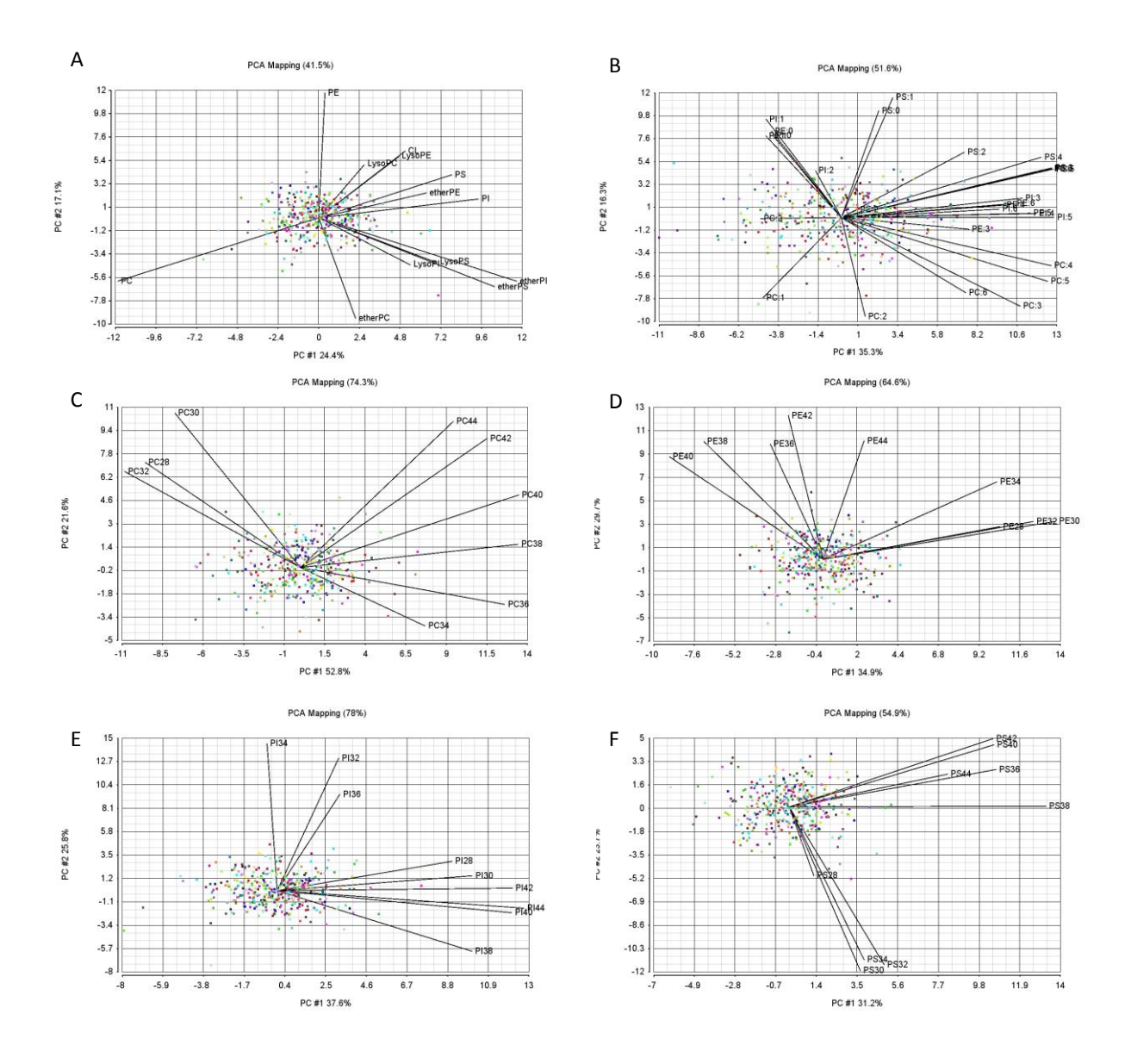


**Figure 31. Principal Component Analysis (PCA) of lipid classes.** The z-score data from the kinome-wide RNAi screen were analyzed by PCA using Partek Genomics Suite after filtering and averaging the two duplicates (368 genes). % (percentage of PCA mapping expressed in the title of each graph) of the variation in samples was revealed in the first two components. The first principal component, named PC#1, is represented by the X axis and the second principal component by the Y axis (PC#2). Lipid categories appeared to be a source of variation and are indicated by the different vectors. Changes according to **A.** main PL classes. **B.** degree of unsaturations in PLs and chain length in **C.** PC, **D.** PE, **E.** PI and **F.** PS

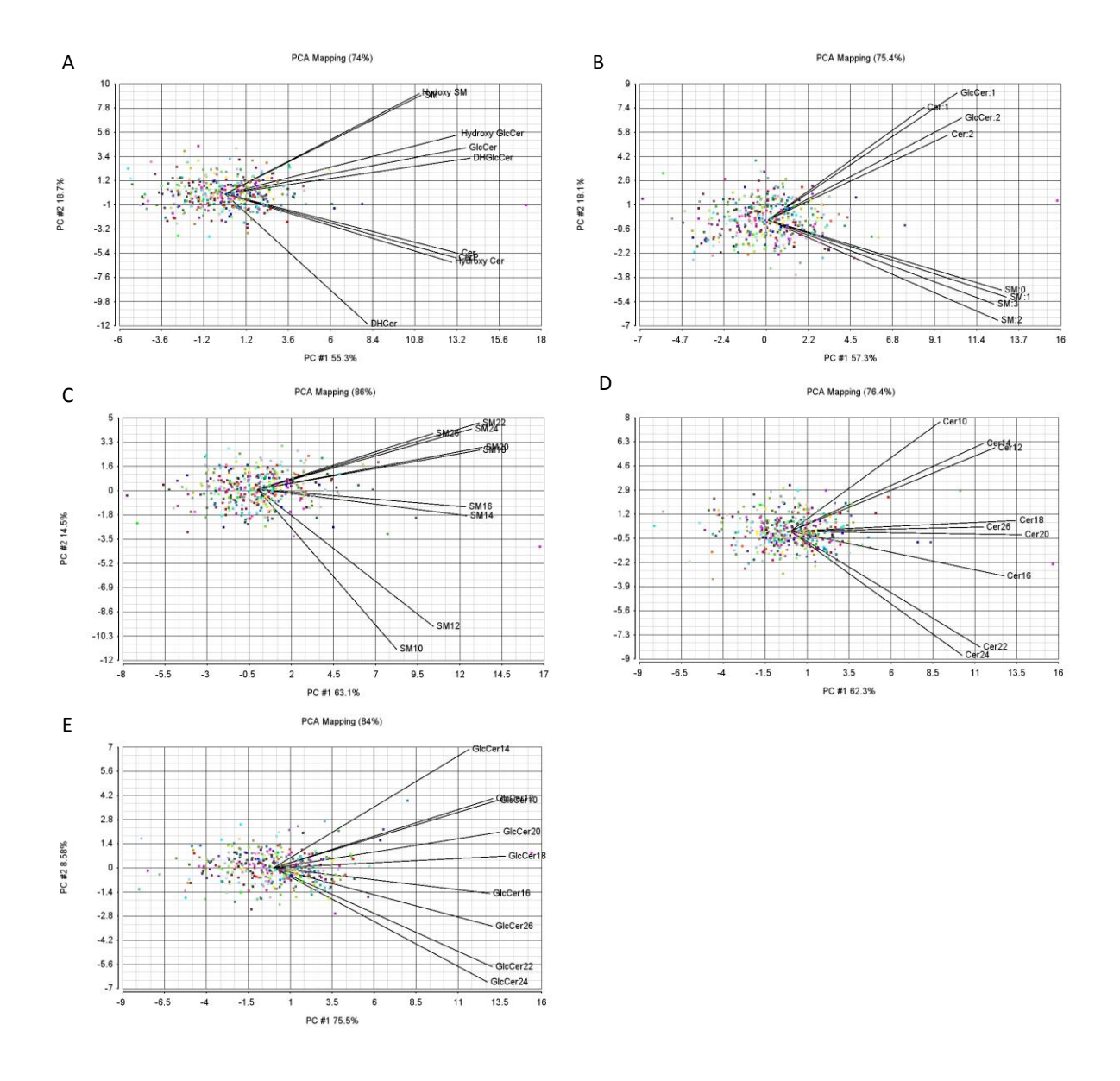


**Figure 31. Principal Component Analysis (PCA) of lipid classes.** The z-score data from the kinome-wide RNAi screen were analyzed by PCA using Partek Genomics Suite after filtering and averaging the two duplicates (368 genes). % (percentage of PCA mapping expressed in the title of each graph) of the variation in samples was revealed in the first two components. The first principal component, named PC#1, is represented by the X axis and the second principal component by the Y axis (PC#2). Lipid categories appeared to be a source of variation and are indicated by the different vectors. Changes according to **A.** main SL classes. **B.** degree of unsaturations in SLs and chain length in **C.** SM, **D.** Cer, **E.** GlcCer.

## c) Genes with patterns of lipid changes: correlation- vs HIS-based selection

In parallel to hit selection per individual lipid categories or per specific combinations of lipid changes, techniques based on correlation were used in order to identify groups of genes with similar patterns of lipid changes. First, a similarity matrix was performed in order to identify genes whose the change was correlating for most of lipids, whatever the strength of these changes. Lipid changes, expressed as the mean z-score of two biological replicates, of 368 kinases were compared over 778 lipids; the correlation between genes was calculated using Pearson and ranges between -1 (blue) and 1 (yellow) in the similarity matrix (**Fig. 33**). Among the 368 input kinases, 35 show a particularly correlated phenotype. (**Fig. 33A, red box**). The heat map representation of lipid changes for selected kinases shows that they are not 100% correlating over the whole lipidome and that subsets of genes are even more correlated (i.e. TRIM24 ad TRIM33) (**Fig. 33B**)

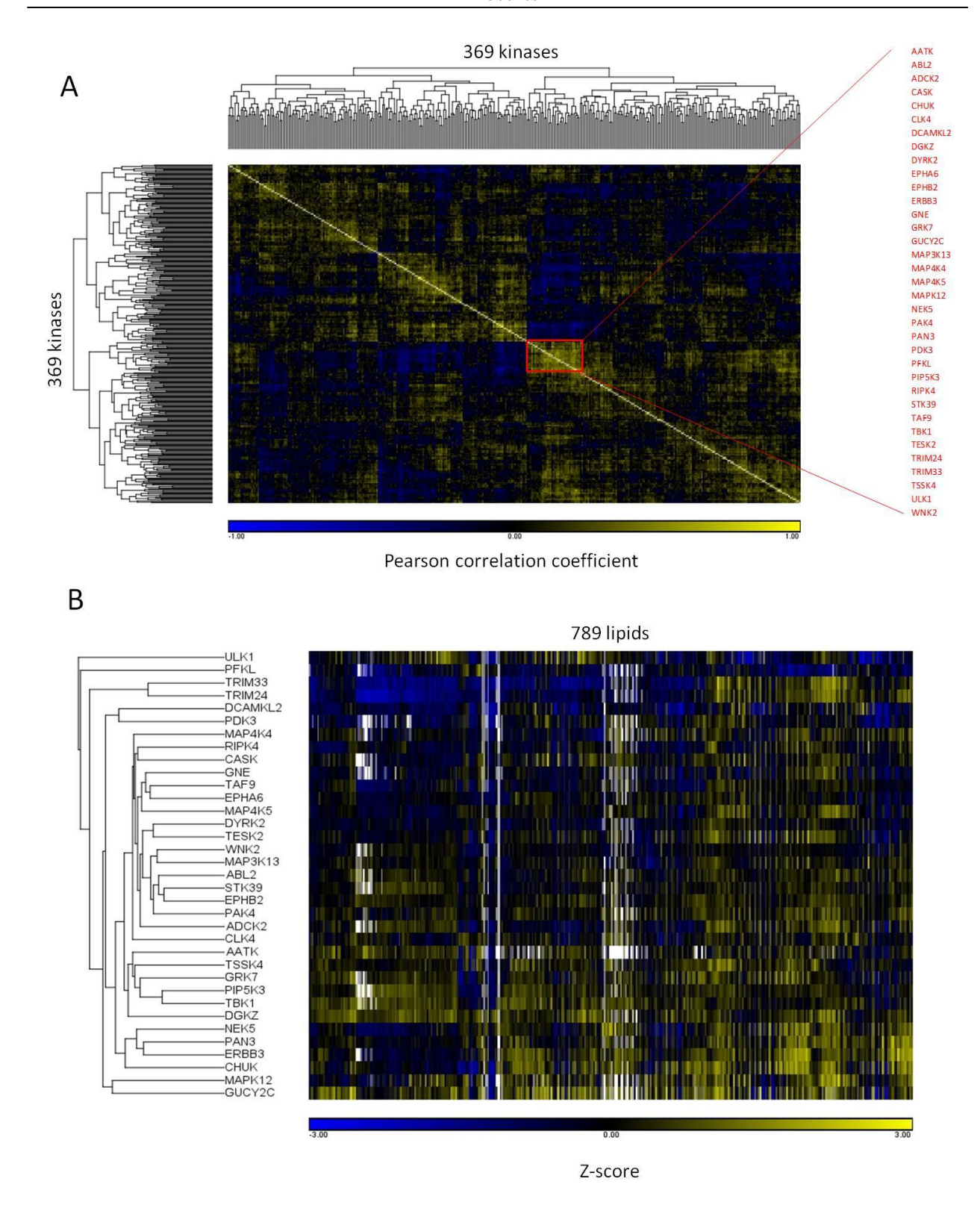


**Figure 33. Similarity matrix and heat map representation of lipid changes for selected kinases with correlated lipid profiles. A.** Similarity matrix of 368 kinases. The color scale represents the Pearson correlation between the lipidomic profiles (z-score) of 368 kinases. Negative and positive correlations are represented in blue and yellow, respectively. **B.** The profile of lipid changes for selected kinases with correlating lipid profiles from the similarity matrix was represented by a heat map. Decrease or increase of lipid levels is represented in blue or yellow, respectively.

Other sets of genes with correlated or anti-correlated profiles of lipid changes can be found with this method but this is a slow process and it doesn't inform directly about which lipid levels are affected nor the strength of these changes.

A more intuitive technique to find genes with lipid patterns is hierarchical clustering. As the similarity matrix, hierarchical clustering is based on correlation. This is an iterative process that finds and joins the pairs of genes with the most similar profiles of phenotypic changes. Pairs of genes are considered as similar if their profiles of phenotypic changes are correlated. The hierarchical clustering represented as heat maps allows to visualize simultaneously genes with correlated lipid profiles and the strength of this correlation that is proportional to the length of the dendrogram root, the direction of phenotypic changes per variable (increase and decrease are expressed color-coded) and their strength (intensity of the color is proportional to the value of the z-score). However, as shown in Figure 34, the hierarchical clustering of lipids changes from the 368 kinases over either the 778 individual lipid species or the major lipid classes is represented as a heat map is not easily interpretable (Fig. 34). Indeed, correlation is found only for pairs of genes with similar patterns over the whole phenotypic profile. As represented for genes A, B and F in Figure 28. On the contrary, genes with strong similarities for only a part of the phenotypic readouts, such as genes C and E (Fig. 35.) are not correlating with gene A. Thus A, C and E are not considered as linked together while we can imagine that different genes have the same function in the regulation of some observed phenomena but not all of them. Therefore, depending on the screen, correlation-based statistical methods can produce a lot of false negative hits and being hardly interpretable.

In order to overcome this limitation, Berend Snijder and Prisca Liberali from the group of Lucas Pelkmans (ETH Zurich, Switzerland) conceived a novel tool of statistical analysis of genetic perturbation screens named hierarchical interaction score (HIS). The HIS was originally conceived in order to find functionally interacting genes across RNAi screens with different readouts. A HIS is calculated for every pair of genes and top-scoring gene interactions are attributed to genes that present similar strong changes either for a subset or all the phenotypic readouts (**Fig. 35.**). While correlation considers all the dataset and shows non-directional links between genes that have the same pattern in all condition even if the strength of phenotypic

changes is very different, HIS considers nested effects. Two genes are linked when they have the same phenotypes in subset of lipids. Moreover, genes with a good correlation have a good HIS. Whatever the context, it allows to find hit genes and to prioritize their relationships

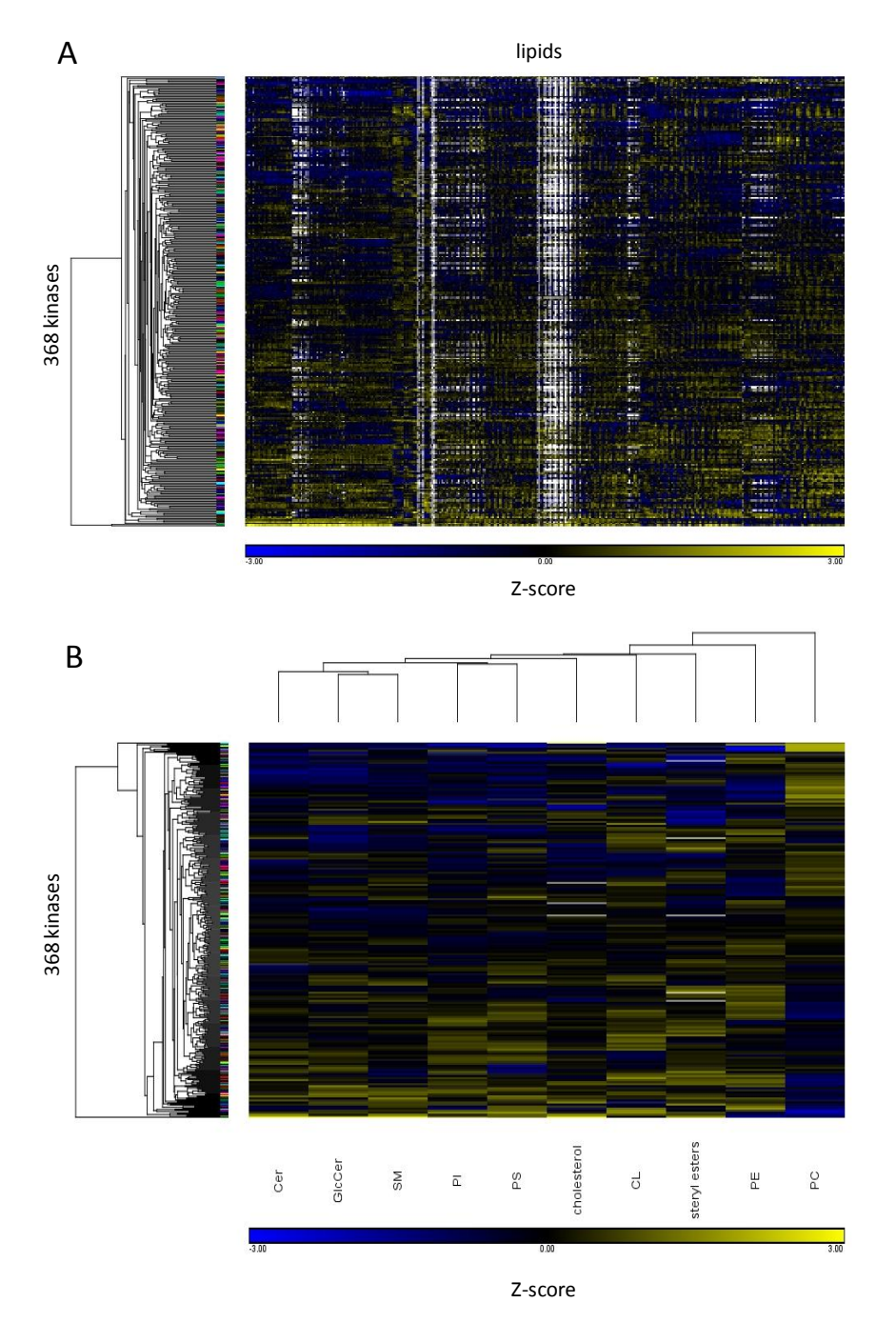


Figure 34. Heat map of lipid changes resulting from the kinome-wide siRNA knockdown in HeLa MZ cells. A. Individual lipid and B. lipid class level changes are displayed as a heat map of the z-score log<sub>2</sub>-transformed lipid quantities. Yellow boxes indicate an increase and blue boxes a decrease of lipid levels. Black boxes represent no change and white boxes indicate missing values. Data represent the mean of two independent experiments.

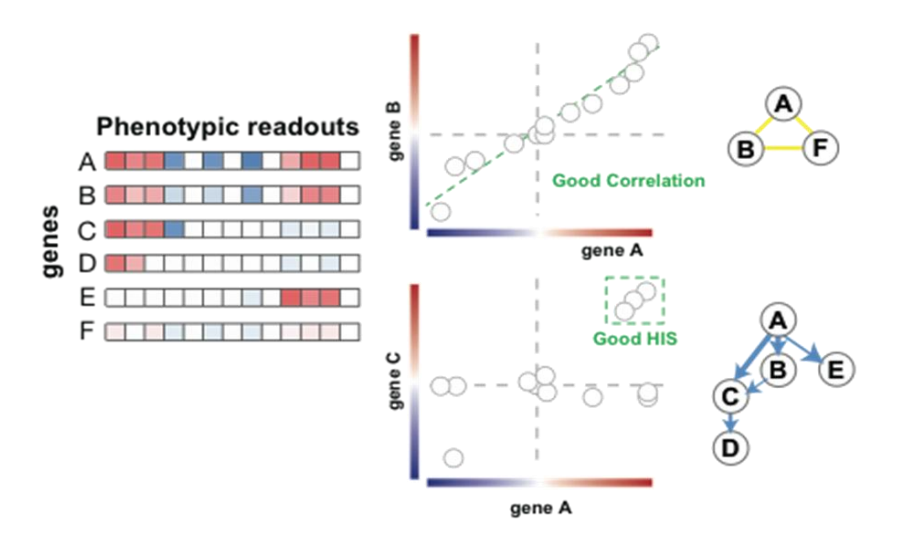


Figure 35. Comparison between correlation- and HIS-based clustering of genes with several phenotypic readouts. (from Prisca Liberali)

Therefore, in order to find genes probably linked in the regulation of all or a subset of the 10 analyzed lipid classes (PC, PE, PI, PS, CL, SM, Cer, GlcCer, cholesterol and steryl esters), the hierarchical interaction scores (HIS) of 368 kinases genes was calculated and the genes with top-scoring hierarchical interactions were selected as hits. Over 368 candidate kinases, the 1,000 strongest interactions were visualized using the open source software <a href="http://www.his2graph.net/">http://www.his2graph.net/</a> (Fig. 36).

Gene interactions are graphically represented as a network of genes that cluster into sub networks of different colors corresponding to specific patterns of lipid changes. Individual examination of lipid profiles from selected hits expressed as heat maps of z-score per lipid class confirmed that the genes induce specific patterns of lipid changes. Moreover, most of genes retrieved from the HIS analysis correspond to hit genes identified after threshold determination in individual lipid classes (**Table 3**) meaning that HIS analysis is able to select the strongest phenotypes and to sort them hierarchically. Now, their phenotype is more readable. Moreover, the HIS is also able to find less strong phenotypes and associate them to the analysis since as indicated with red arrows on Figure 37, the network also comprise additional hits that were not identified with the threshold method since their z-score was below the cutoff value. The letters (A-G) associated with individual heat maps correspond to the sub networks observed on the HIS

graphical representation (**Fig. 36 and 37**.). Thanks to normalization with total PLs, no gene with a significant decrease or increase in all lipids that could be due to a modification of the cell number was selected as hits. Instead, some sub networks reveal clusters of genes showing similar patterns.

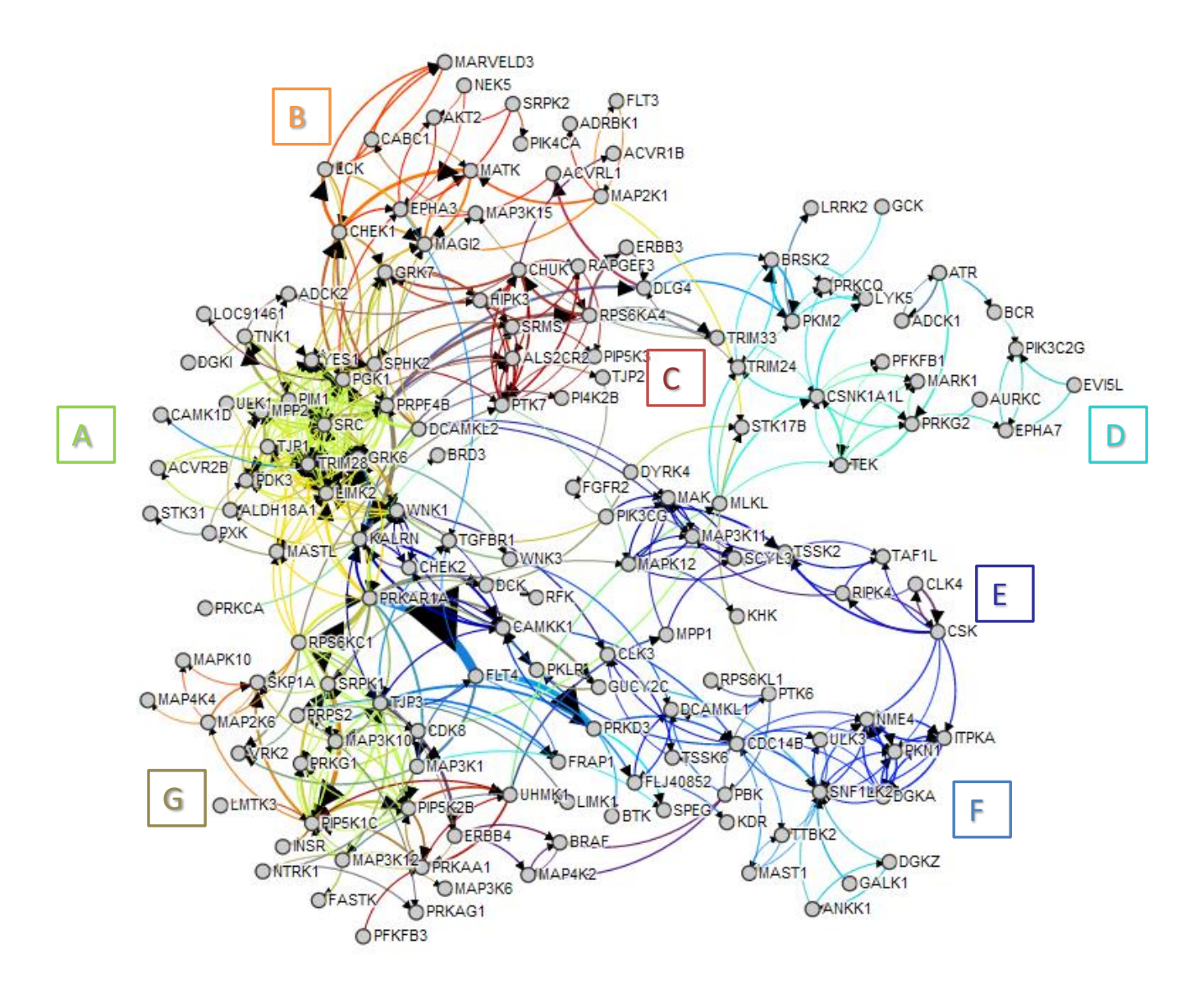
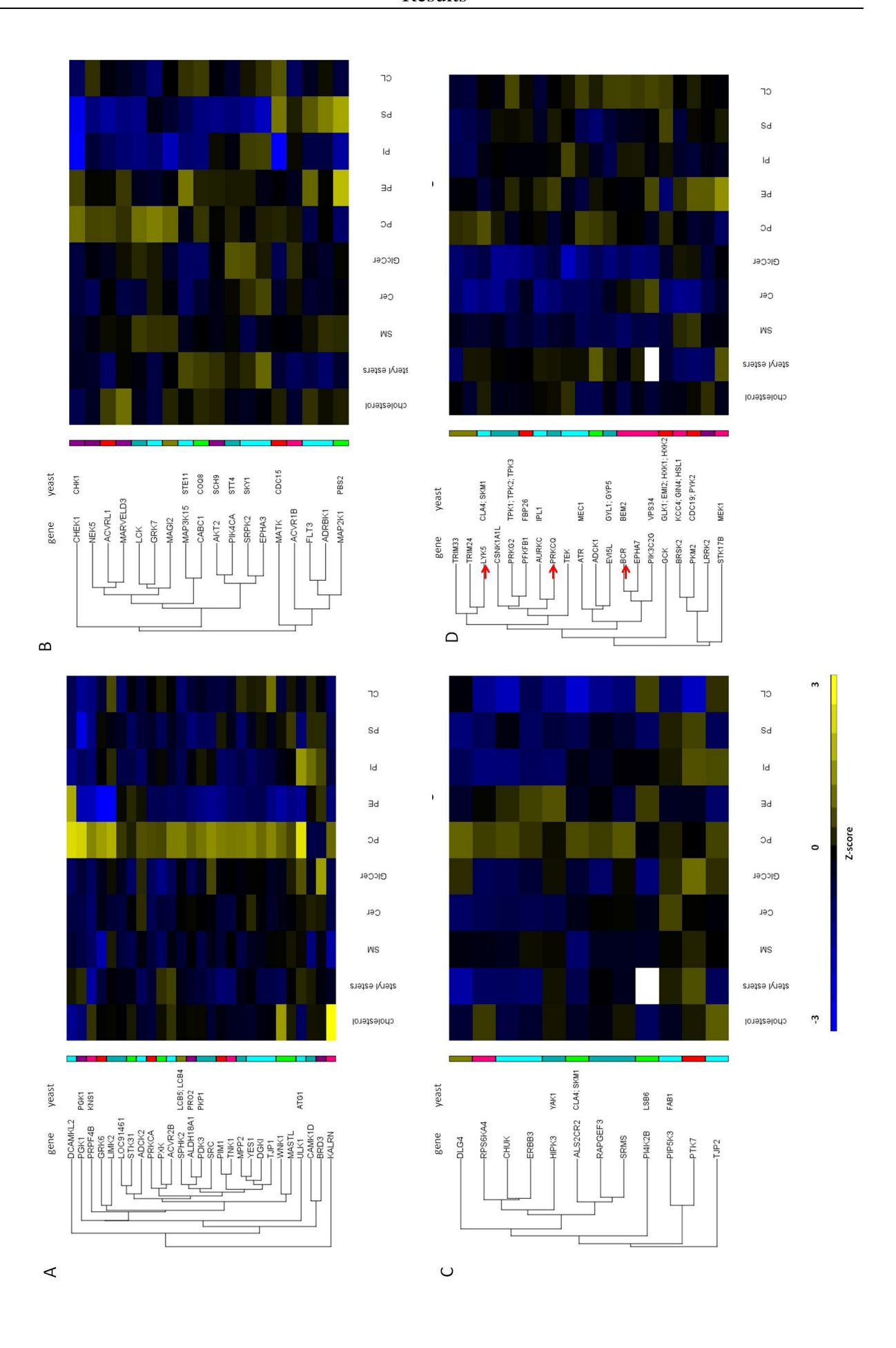
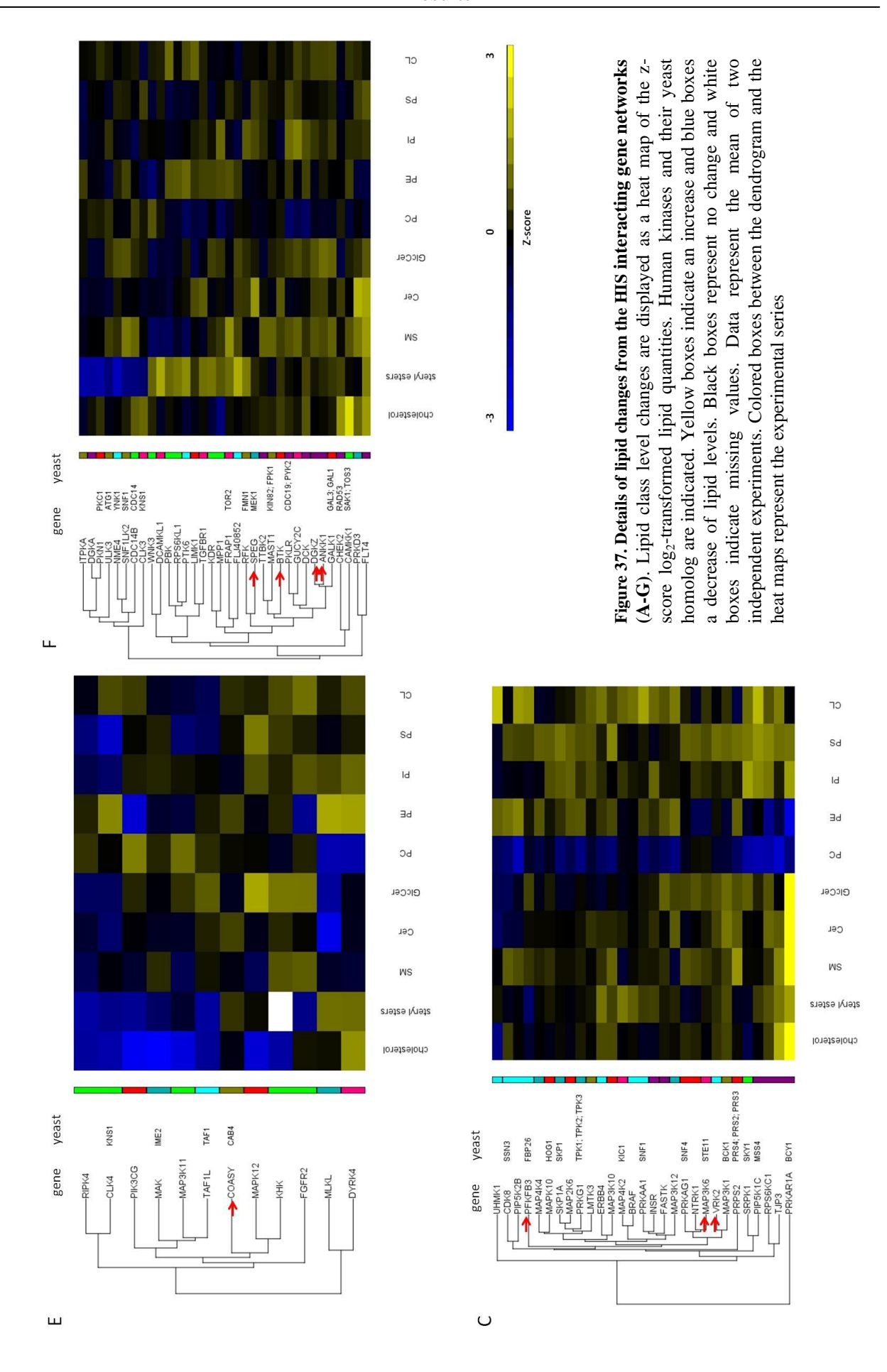


Figure 36. Graph visualization of the resulting HIS network for the 1,000 strongest interactions as inferred on the kinome dataset. Visualization is as on <a href="http://www.his2graph.net/">http://www.his2graph.net/</a>. Edge colors represent specific patterns of lipid changes; edge thickness, the strength of the interaction and arrows, the directionality of the interaction. On following pages selected interacting gene networks (A-G) are represented with their corresponding phenotypes displayed as heat maps representing the z-score of each gene for each lipid class.





Out of the 368 input genes, the HIS retrieved 150 candidate genes with significant phenotype in one or several classes of lipids. The subnetworks of genes were selected by eye according to the colors of the HIS network. Some genes found in one subnetwork could be part of another one, actually. Overall, it is noteworthy that all genes cluster in subnetworks showing similar patterns of lipid changes with a dominant phenotype for some lipids. The subnetworks A and G, for instance present opposite phenotypes with opposite changes for PC and PE. Subnetwork B rather shows specific changes in anionic phospholipids. C is specific of changes in CL level; D presents a decrease in sphingolipids. Finally, subnetworks E and F show more specific changes in sterols.

If we look closer at the phenotype of each subnetwork, we can see that it can even be more subtle. Indeed, changes in the level of major lipid class can be associated with different changes in their composition in fatty acyl chains.

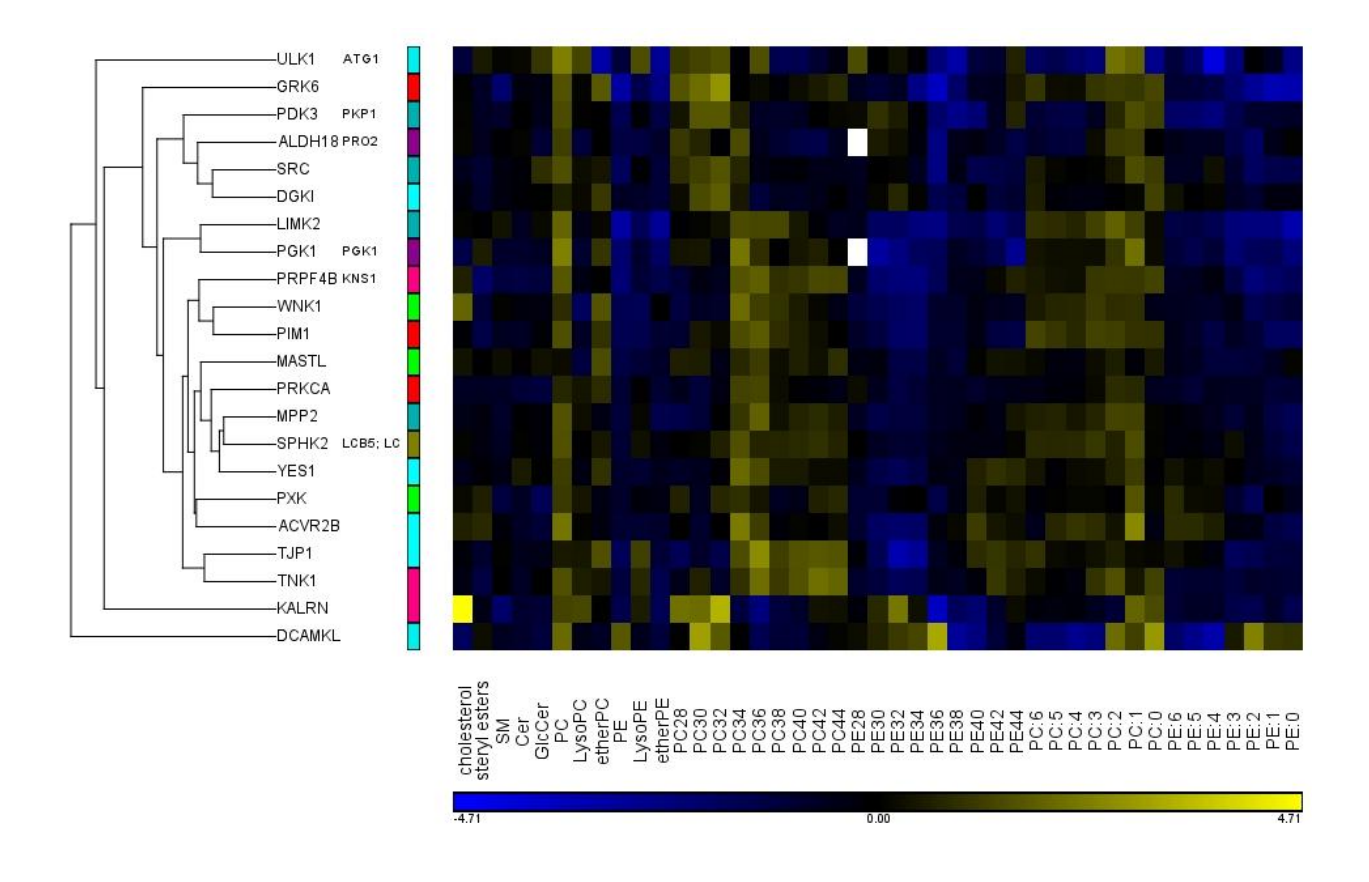
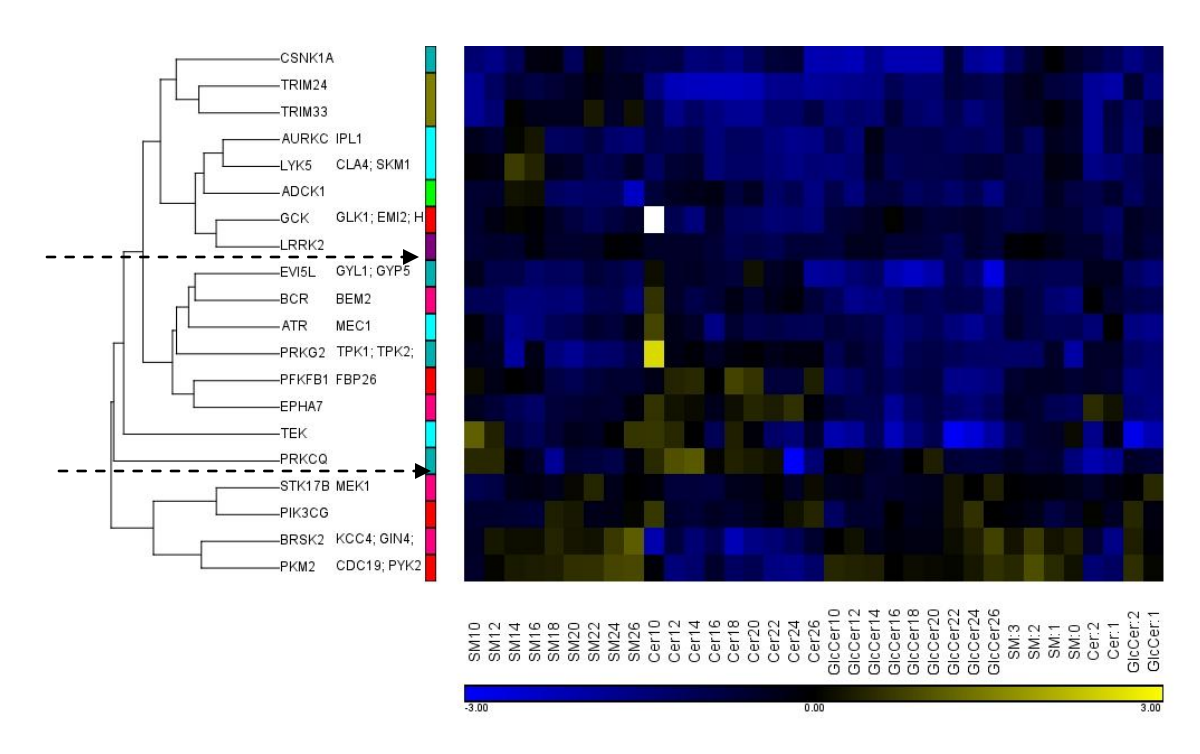


Figure 38. Details of phospholipid changes from the HIS interacting gene subnetworks A Changes in the level of lipid classes are displayed as a heat map of the z-score log<sub>2</sub>-transformed lipid quantities. Human kinases and their yeast homolog are indicated. Yellow boxes indicate an increase and blue boxes a decrease of lipid levels. Black boxes represent no change and white boxes indicate missing values. Data represent the mean of two independent experiments. Colored boxes between the dendrogram and the heat maps represent the experimental series

For instance, we can see that in the subnetwork A (**Fig. 38**), where PC are increased and PE decreased, these changes are chain length specific. ULK1, GRK6, PDK3, ALDH18A1, SRC, DGKI, KALRN and DCAMKL rather increase in short chain PC whereas the other hits increase PC with long chain FA. Moreover, the heatmap also shows that for YES1, PXK, ACVR2B, TJP1 and TNK1, the decrease in PE doesn't concern PE with long chain FA (PE>40) that increase as long chain PC. Finally, it is noteworthy that LysoPC don't necessarily follow the modifications in PC contrary to most of genes showing a decrease in PE, except TJP1, TNK1 and KALRN.

Details of subnetworks B, C, E and F are even more complex and show several sub clusters with specific combinations of FA changes in PLs (data not shown). In subnetwork D that present a decrease in sphingolipids, we can see that some changes are FA specific such as for GlcCer with genes STK17B, PIK3CG and PKM2 and we can distinguish three subclusters in Figure 39: the upper one that decreases Cer and GlcCer with a FA chain specific decrease of SM; a second subcluster in the middle where complex SLs are particularly decreased and a last group of genes below with the opposite phenotype.



**Figure 39. Details of sphingolipid changes from the HIS interacting gene subnetworks D.** Changes in the level of lipid classes are displayed as a heat map of the z-score  $\log_2$ -transformed lipid quantities. Human kinases and their yeast homolog are indicated. Yellow boxes indicate an increase and blue boxes a decrease of lipid levels. Black boxes represent no change and white boxes indicate missing values. Data represent the mean of two independent experiments. Colored boxes between the dendrogram and the heat maps represent the experimental series

Finally, in the subnetwork G where everything seems to increase except PC that decreases, the phenotypes are also more subtle (**Fig. 40A**). PC decrease is mostly coupled to an increase of LysoPC, certainly resulting from the action of phospholipase A1 and phospholipids (**Fig. 40B**) as well as ceramide changes are often FA chain length-specific for SRPK1, PFKFB3, PRKAG1 and NTRK1 (**Fig. 40C**).

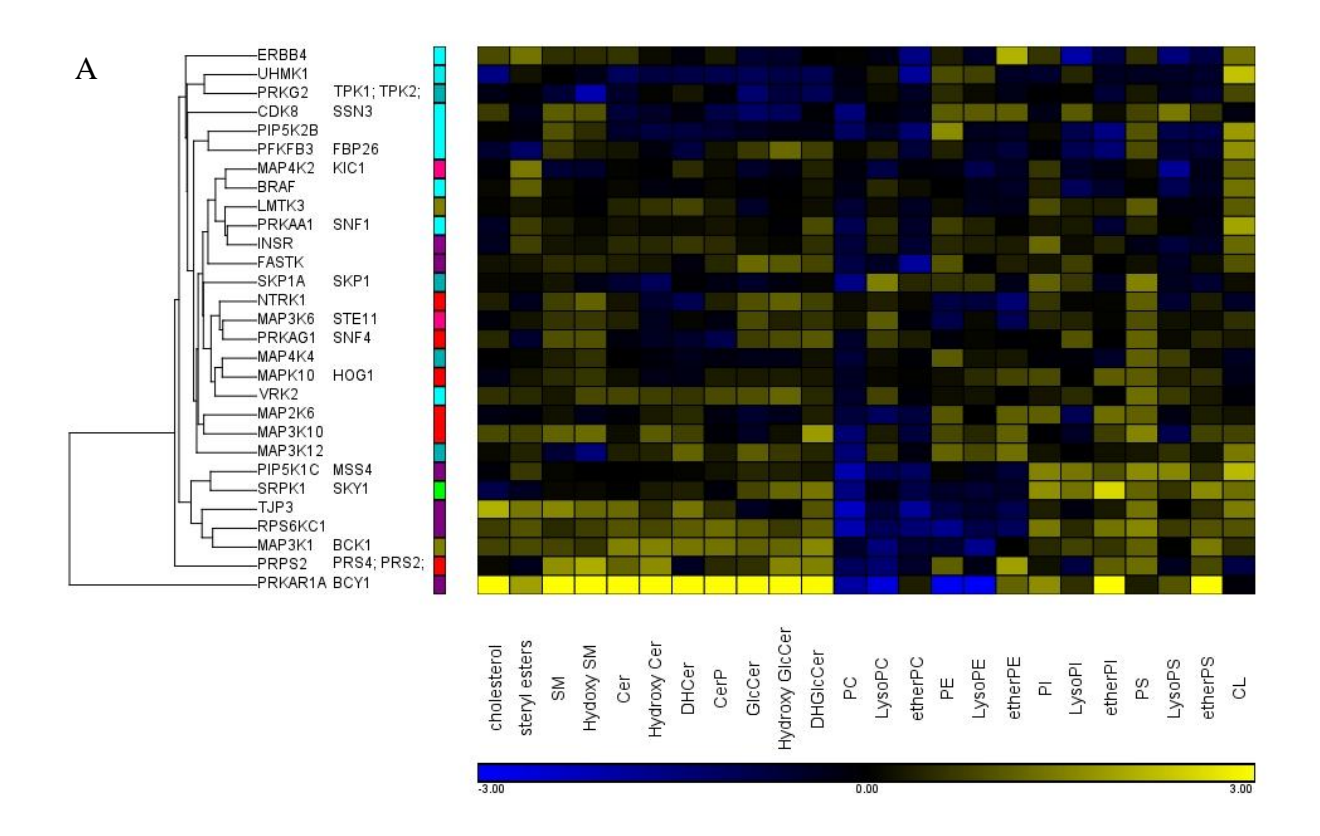
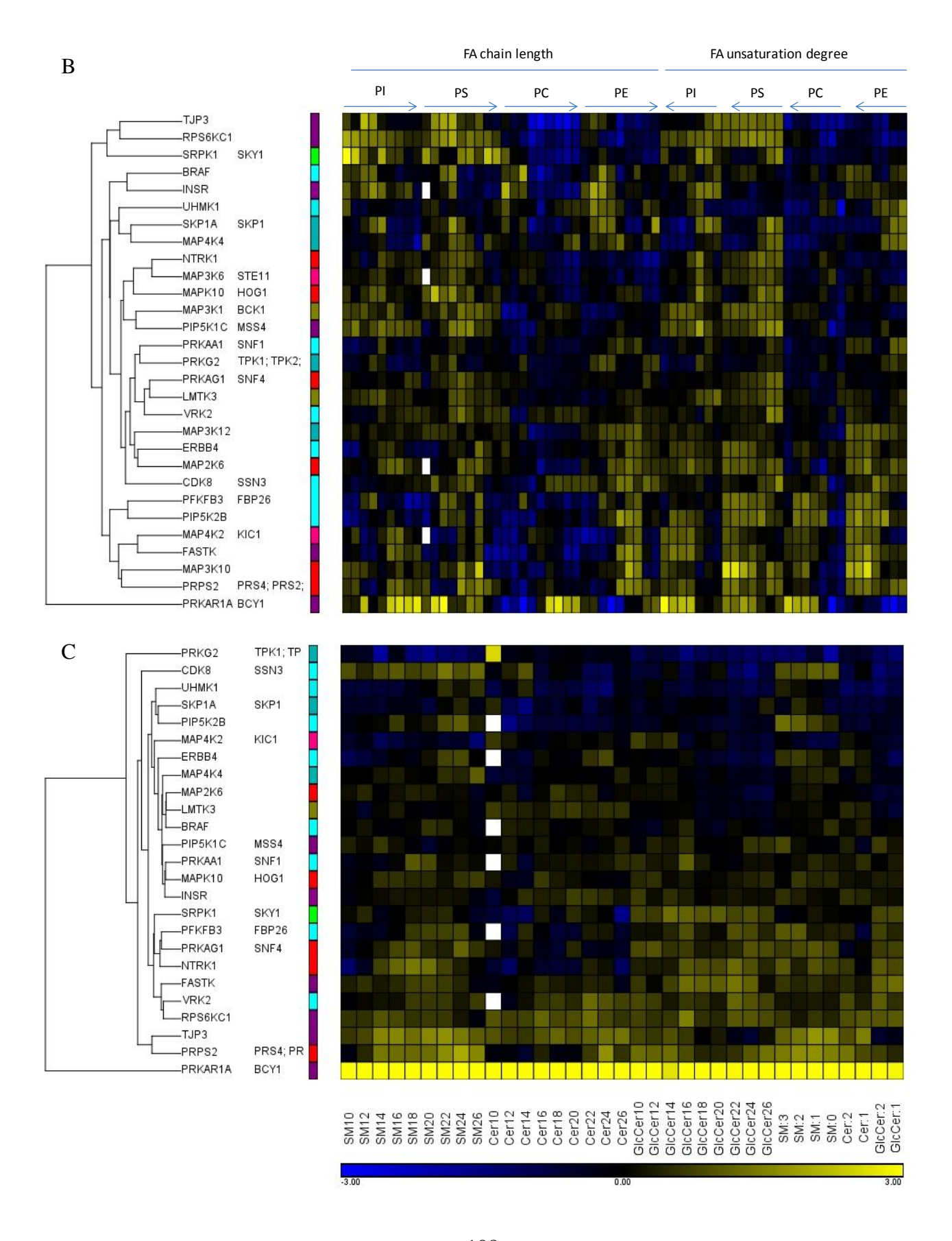


**Figure 40. Details of lipid changes from the HIS interacting gene subnetworks G (both pages). A.** lipid classes, **B.** phospholipids, **C.** sphingolipids. Lipid class level changes are displayed as a heat map of the z-score log<sub>2</sub>-transformed lipid quantities. Human kinases and their yeast homolog are indicated. Yellow boxes indicate an increase and blue boxes a decrease of lipid levels. Black boxes represent no change and white boxes indicate missing values. Data represent the mean of two independent experiments. Colored boxes between the dendrogram and the heat maps represent the experimental series. The arrows indicate increasing FA chain length and unsaturation degree.



## 2.2.6 Validation of candidate genes based on literature

In order to assess if the candidate genes with top-ranking interactions from the HIS analysis were directly linked to the regulation of lipid metabolism and validate some of the hits according to literature, I looked at their function, both individually, based on literature and through a gene annotation enrichment analysis for each subnetwork of genes with similar lipid profile changes using internet databases. The automatic annotation of the genes was performed using the internet software GeneALaCart (http://www.genecards.org/) and a gene annotation enrichment analysis was performed using the WebGestalt, standing for "WEB-based GEne SeT AnaLysis Toolkit" (Wang et al, 2013). Both GeneALaCart and WebGestalt integrate information from different public resources. Selected kinases were tested for their enrichment in pathways using KEGG and Pathway Commons and diseases. The enrichment analysis of genes in GO terms was not pertinent for further analysis and data are not shown. An analysis of gene interactions for each subnetwork was also performed using the STRING database and interesting interactions could be found but the lists of interacting genes were similar to those of pathway enrichment. Therefore, STRING data are not shown. The gene annotation enrichment was performed for each individual sub network of genes with different patterns of lipid changes using the Human genome as reference set and can be found in appendix (p127). Finally, in order to know if candidate genes were already candidate genes in the regulation of lipid metabolism, they were compared to hits from other siRNA screens through the website Genome RNAi (Schmidt et al, 2013). All annotations of the hits are listed in appendix (p127).

The results from the gene annotation enrichment analysis show that several genes strongly disturbing the lipidome are already known as component of growth factors signaling pathways and regulators of energy metabolism. For instance, subnetworks A, C and D are particularly enriched in genes from signal transduction and metabolism pathways: LKB1 (18 genes), PI3K-mTOR signaling pathways (8 genes), Ephrin A and B pathway (3 genes), ErbB receptor signaling (21 genes), etc. Furthermore, subnetwork G, which presents the strongest phenotype for steryl esters is particularly enriched in mitogen-activated protein kinases (MAPKs). However, this analysis did not make appear all the genes acting in the same biological processes. This link was possible only through the manual analysis of gene annotations performed automatically using GeneALaCart and through the complement of literature. Finally, out of 151 genes, one third (50

genes) is directly linked to the regulation of energy metabolism, and more particularly to the regulation of growth factor receptors, mTOR complexes, AMPK and glycolysis (**Fig. 41**). Among them, some are also known to directly regulate lipid metabolism and lipogenesis. The lipid profiles resulting from their silencing contribute to the validation of the screen. Out of the 151 candidate kinases, 52 were also previously described as important regulators of endocytosis (Liberali et al, 2008; Pelkmans et al, 2005) and Golgi integrity (Chia et al, 2012) in siRNA screens performed in HeLa cells. The list of all hits, their annotation and their comparison with other screens is available in appendixthe appendix (p127).

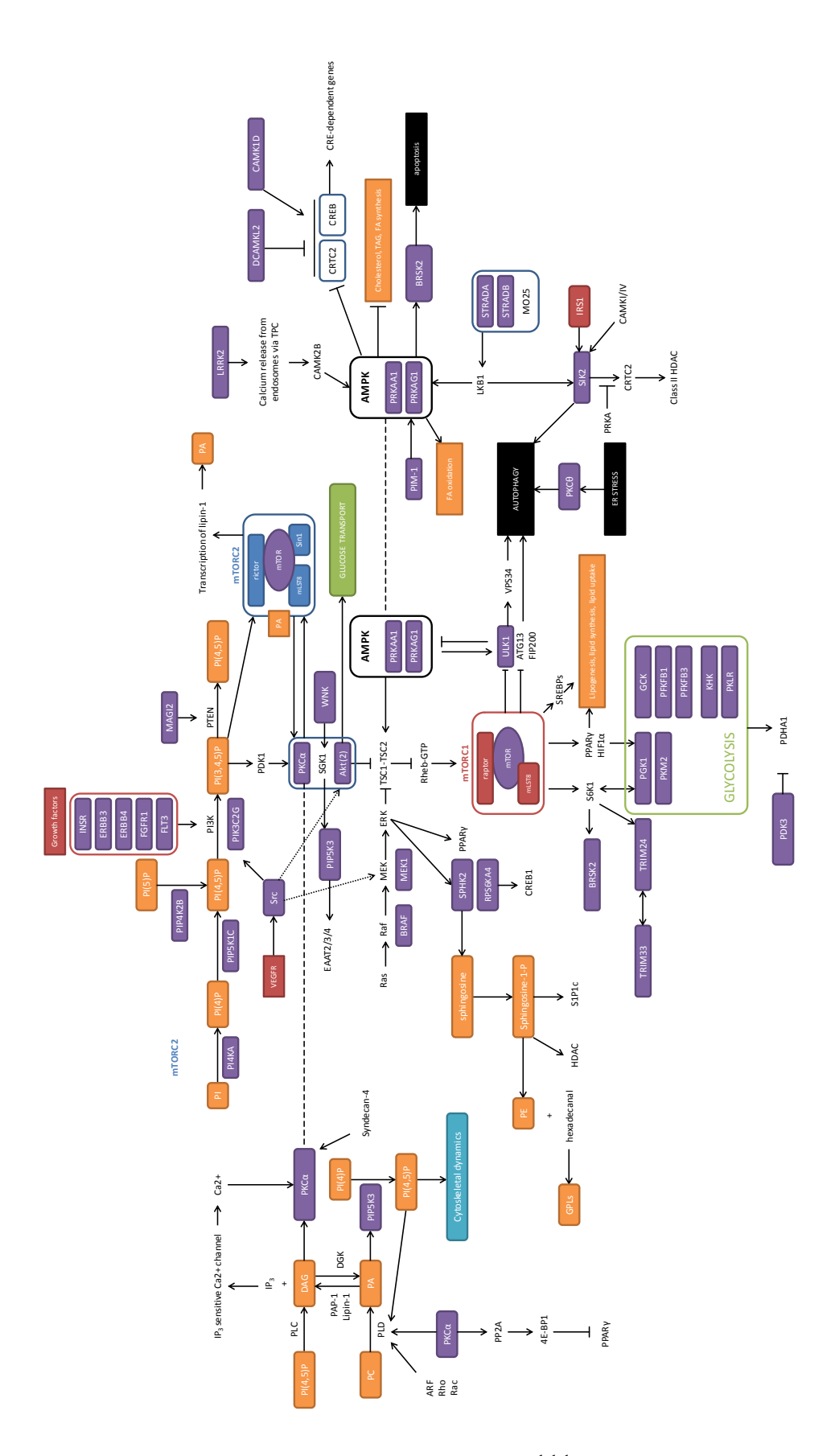
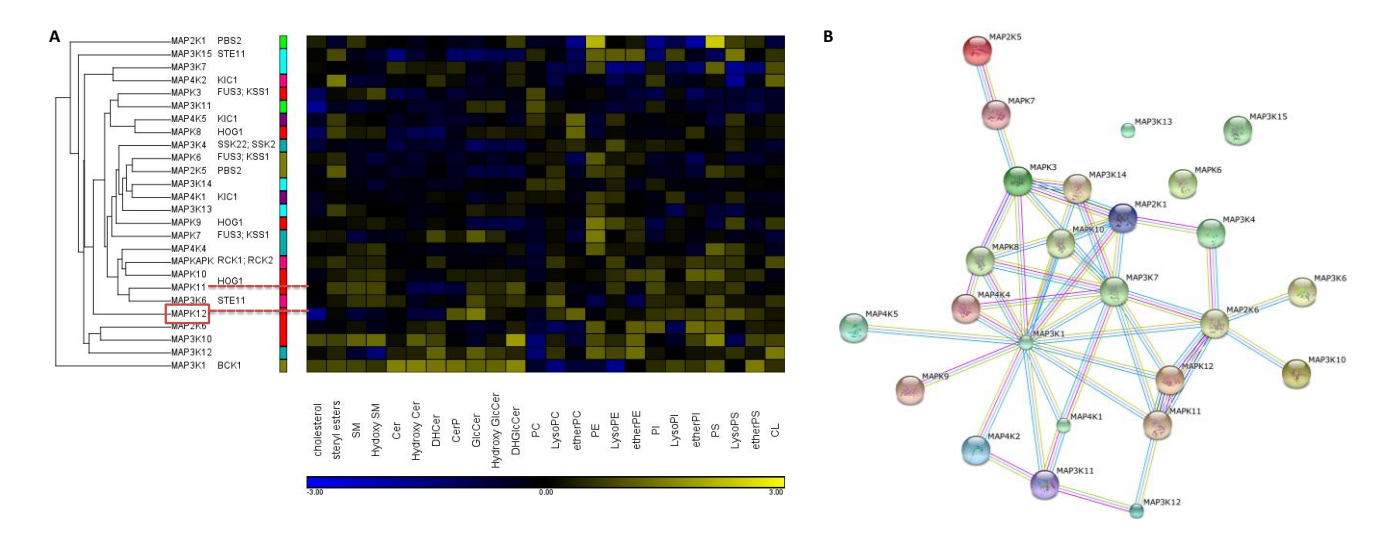


Figure 41. Non-exhaustive functional map of candidate kinase involved in the regulation of energy metabolism. All sources can be found in the appendix.

# 2.2.7 Hypothesis-driven analysis of lipid profiles

The analysis of the screen can be either completely exploratory, based on statistical methods to select candidate genes with potentially interesting phenotypes, or hypothesis-driven. Among the large number of hypotheses to test, one can already look at kinase families to see if their knockdown leads to similar lipid profiles. In this way, I compared the lipid profiles of homolog kinases from the final dataset (368 genes) by hierarchical clustering. As an example, I chose the large family of mitogen-activated protein kinases (MAPKs), the phosphoinositide kinases and the members of the tripartite motif (TRIM) family because some of them appear in the list of candidate genes retrieved from the HIS analysis.

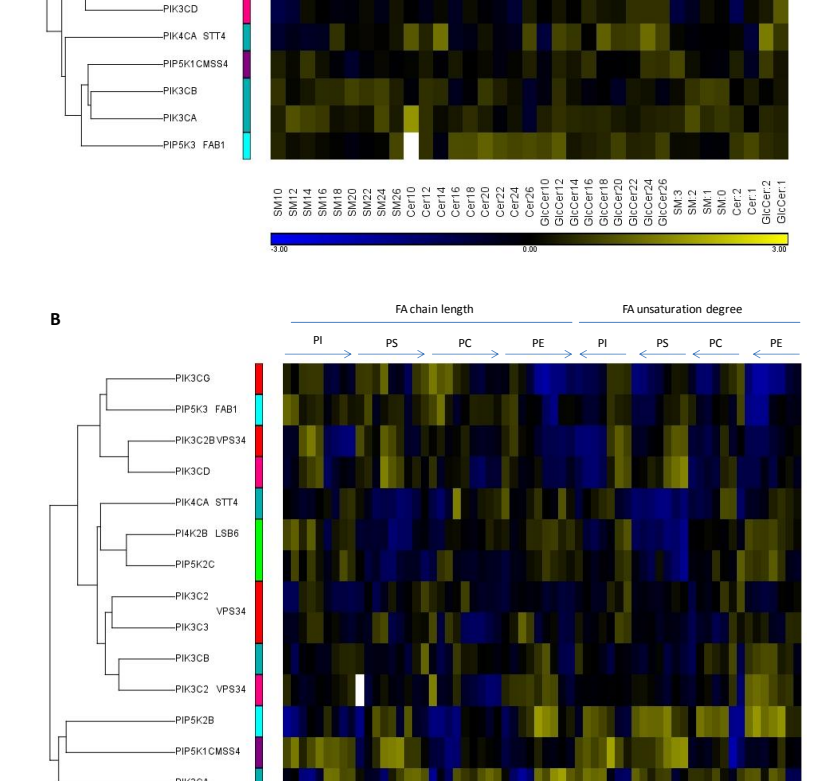
MAPKs represent a large class of signaling molecules involved in several biological processes but they often interact in the same pathways (**Fig. 42**) and some of them such as the four p38-MAPKs comprising MAPK11-14, can be particularly implicated in specific cell responses like apoptosis, cell proliferation and autophagy. When analyzing the dataset, it appears that the silencing of the different MAPKs leads to different profiles (**Fig. 42**) but also that some MAPKs cluster together and lead to similar phenotypes like the two p38-MAPKs: MAPK11 and MAPK12 that induce a decrease of ceramide levels in concomitance with the increase of PI, PS and GlcCer.



**Figure 42. Lipid changes in MAPK. A.** Lipid class level changes are displayed as a heat map of the z-score log<sub>2</sub>-transformed lipid quantities. Human kinases and their yeast homolog are indicated. Yellow boxes indicate an increase and blue boxes a decrease of lipid levels. Black boxes represent no change and white boxes indicate missing values. Data represent the mean of two independent experiments. Colored boxes between the dendrogram and the

heat maps represent the experimental series. **B.** Map of predicted interactions between MAP kinases identified from a STRING analysis. Connecting lines are color coded by the type of evidence used to build the cluster.

Phosphoinositide kinases are a family of lipid kinases able to phosphorylate the inositol ring of PI (PIK) and phosphoinositides (PIPK). They play a role in signal transduction, lipid metabolism, energy homeostasis as well as in the integrity of organelles and some can physically interact (**Fig. 43**)(Balla, 2013). Several kinases can phosphorylate the same phosphoinositide and their silencing could induce similar lipid profiles but not necessarily because they can be organelle-specific and not necessarily regulate the same pool of lipids and. The hierarchical clustering of their lipid profile shows that certain share the same lipid profiles (**Fig. 43**). However, these clusters can differ between sphingolipids (**Fig. 43A**) and phospholipids (**Fig. 43B**).



PIK3CG

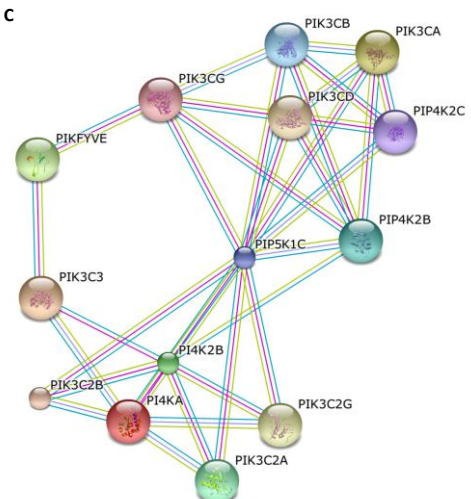


**Figure** Lipid changes phosphoinositide kinases. A. Changes in the level of lipid class are displayed as a heat map of the z-score log<sub>2</sub>-transformed lipid quantities. Yellow boxes indicate an increase and blue boxes a decrease of lipid levels. Black boxes represent no change and white boxes indicate missing values. Data represent the mean of two independent experiments. Colored boxes between the dendrogram and the heat maps represent the experimental series. The arrows indicate increasing FA chain length and unsaturation degree B. Map predicted interactions between phosphoinositides kinases.

Finally, concerning genes from the TRIM family, the HIS analysis had already highlighted the similarity of TRIM24 and TRIM33 lipid profiles. TRIM kinases are transcriptional cofactors that interact with distinct transcription factors but that associate in complexes: TRIM24-TRIM33 in majority or TRIM24-TRIM28-TRIM33, in interaction with chromatin (Herquel et al, 2011b). When comparing the lipid profiles of HeLa MZ silenced for these three cofactors, it appears that they all lead to similar lipid profiles but that the phenotype of TRIM28 is weaker and induces opposite changes in PE (**Fig.43**).

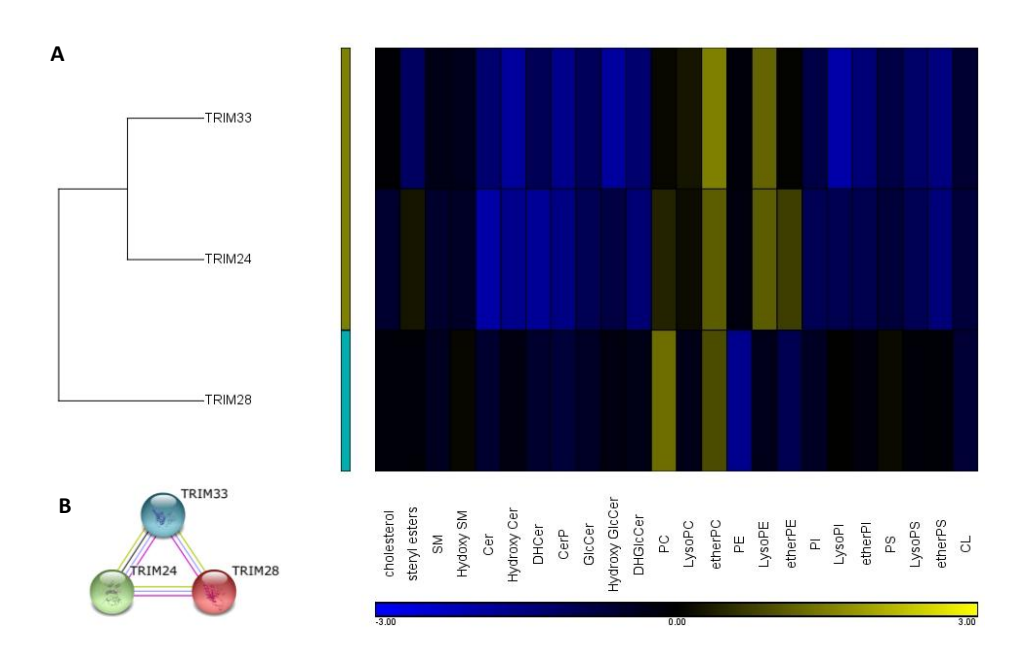


**Figure 44. Lipid changes in different families of kinases. A.** MAPK and **B.** TRIM family. Lipid class level changes are displayed as a heat map of the z-score log<sub>2</sub>-transformed lipid quantities. Human kinases and their yeast homolog are indicated. Yellow boxes indicate an increase and blue boxes a decrease of lipid levels. Black boxes represent no change and white boxes indicate missing values. Data represent the mean of two independent experiments. Colored boxes between the dendrogram and the heat maps represent the experimental series. The arrows indicate increasing FA chain length and unsaturation degree

# 2.2.8 Ongoing research

The analysis of the kinome-wide siRNA screen dataset is still ongoing. If the primary screen is done and candidate genes are identified in different lipid classes, the confirmation of potentially interesting hits by control of gene silencing and repetition with individual siRNAs is ongoing and their role remains to be defined through a validation process. The comparison of lipidomic results between the kinome-wide siRNA screen in Human cells and data obtained from a library of mutant yeast for kinases and phosphatases performed in parallel in our lab by Dr. Aline Xavier Da Silveira Dos Santos makes already appear some common candidate genes whose function in lipid homeostasis could be conserved in eukaryotes. Moreover, lipidomic data are currently analyzed in comparison with endocytosis results obtained from a kinome-wide siRNA screen performed in similar conditions (same siRNA library, same cell line) by D. Prisca Liberali (ETH, Zurich) in order to determine which genes affecting cell trafficking affect lipid homeostasis. Finally, some parts of the dataset are currently part of ongoing collaboration projects with other research groups.

In parallel to this explorative siRNA screen, two hypothesis-driven projects in lipidomics were performed in collaboration with Dr. Mathieu Frechin and Dr. Prisca Liberali from the group of Lucas Pelkmans (ETH, Zurich) but data cannot be described here since they are not published, yet.

## 3. Screening of Dynamic Amphiphiles as siRNA Delivery System in Mammalian Cells

In 2010, in parallel of the project of kinome-wide RNAi screen, I tested a potential transfection reagent synthesized in the group of Pr. Stefan Matile (University of Geneva) that could be an alternative to the expensive Lipofectamine<sup>TM</sup> RNAiMax. From a simple test, this small project that underlined new concepts about the cell entry of lipoplexes became a real screen.

## 3.1. Summary of the research

While targeted knockdown of gene-causing disease in Humans by RNA interference is promising, delivery of small RNAs in vivo is still difficult. Most transfection reagents are liposome-based and cross plasma membrane through active mechanisms such as endocytosis. Because of problems in uptake and toxicity, efficient delivery by such nanocarriers often depends on the cell type and most molecules working in vitro, fail in vivo (Davis et al, 2010; Lv et al, 2006; Peer & Lieberman, 2011). Solutions to this limitation could come from a novel class of dynamic amphiphiles developed in the team of Stefan Matile at the University of Geneva (NCCR Chemical Biology). Easy to prepare, these molecules can carry nucleic acids inside artificial vesicles, suggesting an ability to passively diffuse across phospholipid bilayers in conjugation with DNA (Montenegro et al, 2011). In order to test if they can also carry nucleic acids in living cells, I performed a robotically assisted siRNA transfection assay in HeLa cells stably expressing GPI-eGFP (Biomolecular Screening Facility, EPFL). This assay was comparable to the one described in (Akinc et al, 2008). Instead of luciferase, the siRNA target was eGFP. The knockdown efficacy was monitored with a plate reader. Manual experiments had already demonstrated that siRNA transfected with some of these dynamic amphiphiles show an eGFP knockdown at least equivalent to transfection with commercial transfection reagent, which is based on the liposome technology ( $Lipofectamine^{TM}RNAiMax\ from\ Life\ Technology$ ).

Assistance of the robot allowed screening six different concentrations of siRNA/amphiphiles complexes from a chemical library comprising more than 200 compounds. These amphiphiles, synthesized in Matile lab, resulted from the dynamic and covalent assembly of hydrophobic tails

(aldehyde/ketones, thiols) with positively charged heads (hydrazones, oximes or disulfides bridges) (Montenegro et al, 2012). The screen revealed a dozen of active compounds able to carry siRNA into HeLa cells with a knockdown efficiency greater than 50% and few or no toxicity. After confirmation, siRNA transfection with active amphiphiles was optimized in HeLa cells expressing GPI-eGFP in order to reach a knockdown efficiency as good as Lipofectamine TM RNAiMax. A time-course assay revealed that GFP knockdown was faster with dynamic amphiphiles than Lipofectamine TM, suggesting a different manner of crossing cell membranes for siRNA/amphiphiles complexes. siRNA Transfection capacity of active amphiphiles was also performed in challenging cell types, such as Human Primary Skin Fibroblasts (courtesy from Dr Charna Dibner, HUG), with siRNA targeting GAPDH mRNA. The transfection was more efficient with the most active dynamic amphiphiles than with Lipofectamine RNAiMax. Then, the characterization of siRNA/amphiphiles particles was monitored using Density Light Scattering (DLS). The last step, in collaboration with Pr. Shiroh Futaki (Japan) consisted in determining which cellular mechanisms, such as endocytosis, were involved in the delivery of siRNA by the best amphiphile candidate into HeLa cells.

#### 3.2. Articles

These two articles summarize the project. The first paper is an introduction to the concepts and chemical studies that led to the screen. The second article is the publication that resulted from the screen of the library of dynamic amphiphiles used as siRNA transfection reagents in mammalian cells.

- Montenegro J, Gehin C, Bang EK, Fin A, Doval DA, Riezman H, Sakai N, Matile S.
   (2012) Conceptually new entries into cells. Chimia (Aarau). 65(11):853-8. doi: 10.2533/chimia.2011.853.
- Gehin C, Montenegro J, Bang EK, Cajaraville A, Takayama S, Hirose H, Futaki S, Matile S, Riezman H. (2013) Dynamic amphiphile libraries to screen for the "fragrant" delivery of siRNA into HeLa cells and human primary fibroblasts. J Am Chem Soc. 135(25):9295-8. doi: 10.1021/ja404153m

#### **DISCUSSION**

# 1. Analysis of candidate genes from the siRNA kinome-wide screen

During this thesis, I developed a genetic perturbation screen in Human cells in combination with techniques of targeted lipidomics using MS in order to find candidate genes that control membrane lipid homeostasis. For the first time, it was possible to observe simultaneously and precisely the function of many genes on a large range of membrane lipid species. Most of research projects focus only on the lipid classes that could be potentially affected by specific signaling pathways/genes. This is particularly true for research in Cancer or in metabolic syndromes that focus on markers of tumorigenesis such as sphingolipids or on lipogenesis, respectively, without taking in account the rest of the lipidome whereas it could help to understand the whole phenomena. However, recent studies showed that metabolic and signaling pathways involved in the regulation of lipid metabolism are relatively coordinated. For instance in 2013, Chen P.W. and colleagues described the dynamics and coordination of metabolic pathways during heat stress response in yeast by measuring gene expression, enzyme activity and the amount of metabolites involved in the regulation of sphingolipid synthesis (Chen et al, 2013). In the field of Parasitology, the team of Michael Barrett in Glasgow demonstrated the importance of metabolomics (the large-scale study of metabolites, including lipids from an organism) to understand the dynamics of metabolic pathways implicated during the infection of human by parasites and how this allows optimizing the drug treatment depending on the phase of infection (Creek et al, 2012). Finally in 2014, Yu Y and colleagues observed for the first time how hypoxia modifies the lipidome of HeLa cells using MS and showed that in their conditions, hypoxia induces a decrease of PI coupled to rise of LysoPC and LysoPE (Yu et al, 2014) but they didn't analyzed changes in sphingolipids.

After validation of the experimental method through a pilot screen and quality controls, filtering of samples with non-analyzable lipid profiles or non-correlated duplicates, the lipid profiles of 368 genes were statistically analyzed according to different methods. Out of the 368 kinases, my results show that 151 candidate genes can induce significant changes in the level of one or several lipid classes. Candidate genes from the primary screen could be clustered into seven groups sharing similar patterns of lipid changes. Among them, some candidates are

certainly false-positive hits resulting from the sum of factors accumulated during the experiment, such as: off-target effects (Jackson & Linsley, 2010), cellular stress, risks of lipid hydrolysis by lipase when harvesting cells or fatty acid oxidation during the extraction, extraction efficiency, mass spectrometer accuracy, normalization, etc. However, the analysis of quality controls dispersed all along the screening experiment suggests that these are specific lipid changes. Moreover, no series/plate effect was observed after normalization. Indeed, as indicated by the color code on Figure 32, genes clustering together are not particularly enriched in specific series of experiments. Finally, the large number of putative candidates is not really surprising. First, because the number of phenotypic readouts is quite important (10 when analyzing changes per lipid class, more than 700 when analyzing changes in individual lipid species). Therefore, several combinations of phenotypes are possible. Second, as reported in previous publications, results from siRNA screens in HeLa cell lines showed that many kinases are necessary to ensure clathrin- and caveolae-dependent endocytosis (208 out of 590 kinases) (Pelkmans et al, 2005) or the integrity of the Golgi (around 20% of 948 kinases and phosphatases) (Chia et al, 2012). Knowing that endocytosis is essential to nutrient intake and signaling and that the integrity of the Golgi is required for the synthesis and trafficking of many membrane lipids, it is not surprising that many genes influence lipid homeostasis, too.

In my results, I rarely observe significant modifications in only one lipid class. Yet, metabolic pathways are highly connected together and many compensation pathways exist. This certainly explains why most of lipid changes are not significant. For instance, ceramides can be either de novo synthesized or result from the salvage pathway though sphingomyelin hydrolysis (ref salvage pathway), de novo PC or ceramide synthesis involves different isoforms per enzyme such as choline kinase or ceramide synthases, respectively (Gibellini & Smith, 2010), PI results either from de novo pathway or from the dephosphorylation of phosphoinositides (Balla, 2013), fatty acid can come from diet or being de novo synthesized (Cook, 2008), sterols can be provided by lipoproteins contained in the serum-containing medium, etc. Moreover, as observed in the pilot screen, silencing genes directly involved in lipid synthesis, such as choline kinase, ethanolamine kinases or HMGCR, doesn't necessarily induce specific changes in PC, PE or sterols. Instead, many candidate genes from the kinome-wide screen play important role in the regulation of metabolism and in the proper functioning of organelles. Indeed, as indicated in figure 41, out of 151 candidate kinases, around one third is involved in glycolysis, PI3K/Akt/mTOR signaling

pathway and in the regulation of AMPK. Interestingly, it was recently shown that the transcriptome of an adherent HeLa cell line (Kyoto) is reduced compared to the Illumina Human Bodymap 2.0, particularly in genes coding for proteins involved in lipid catabolic processes and its transcriptome is also enriched in transcripts preferentially linked to cell proliferation, transcription and DNA repair (Landry et al, 2013). Therefore, it is not surprising that the silencing of genes linked to these processes leads to strong disturbances in cells, including in lipid metabolism. Moreover, cancer cells are known to present a specific lipid metabolism: they increase nutrient uptake, channeling of the glycolytic product pyruvate into Acetyl CoA, increase biosynthetic genes for fatty acids, cholesterol and other phospholipids, including phosphatidylcholine (Arsenault et al, 2013), through the control PI3K/Akt/mTOR signaling (Santos & Schulze, 2012; Ward & Thompson, 2012). They also express PKM2, a specific isoform of pyruvate kinase with lower activity that induces the accumulation of glycolytic products that can be transformed into glycerol and serine and provide building blocks for lipid de novo synthesis. Several kinases involved in the control of these metabolic alterations, including PKM2 were represented among genes that disturbed the most the lipidome (Fig. 41), showing that the screen identified the expected genes. Moreover, out of the 151 candidate kinases, 52 were also previously described as regulators of different steps of endocytosis (Liberali et al, 2008; Pelkmans et al, 2005) and of Golgi integrity (Chia et al, 2012) (cf appendix). The proper functioning of endocytosis is necessary for the activation of mTORC1 (Flinn et al, 2010). Endocytosis is also required to regulate cholesterol homeostasis (Goldstein & Brown, 2009). On the other hand the integrity of the Golgi is indispensable to the synthesis of complex sphingolipids as well as several signaling pathways involved in the regulation of lipid homeostasis (Lev, 2006). Therefore, finding several kinases involved both in lipid homeostasis, in membrane compartmentalization and/or in PI3K/Akt/mTOR signaling pathway seems logical, too.

If the representation of many kinases in the control of lipid homeostasis can be explained by their function in the regulation of energy metabolism or of membrane compartments, the function of several candidate genes in lipid homeostasis is still unknown. Among them, kinases from the tripartite motif (TRIM) family, namely TRIM24 and TRIM33, for instance, present a particularly strong phenotype with a decrease in the ceramides and GlcCer, coupled to an increase of etherPC and LysoPE (**Fig.44**). TRIM24 (TIF1 $\alpha$ ) and TRIM33 (TIF1 $\gamma$ ) are cofactors of transcription. They

are part of a subgroup of the TRIM family that also comprises TRIM28 (TIFβ). TRIM24. TRIM33 and TRIM28 interact with different transcription factors but interact also together and form multiprotein complexes together (TRIM24-TRIM33 and TRIM24-28-33) with other chromatin components that modulate signaling pathways and tumor progression (Herquel et al, 2011a; Herquel et al., 2011b). However, their precise role in cancer is controversial, especially for TRIM24 that can be tumor suppressor or enhancer depending on conditions (Herquel et al, 2011a). TRIM24 can be activated through the PI3K/Akt/mTOR/S6K1 signaling pathway to activate the transcription of rRNA in response to nutrient availability (Mayer et al, 2004) and activate itself the PI3K/Akt/mTOR pathway by activating the transcription of PIK3CA (Zhang et al, 2014). On the other side, depletion of TRIM33 is lethal for mice suggesting that its role in development is not redundant (Kim & Kaartinen, 2008). It also regulates cell proliferation and TGF-beta signaling but the list of its partners is still unknown (Herquel et al, 2011a). Since the complex TRIM24-TRIM33 seems to have synergistic effects in the regulation of B-myc, for instance, (Herquel et al, 2011b) and since their individual knockdown in HeLa cells induces exactly the same lipid modifications, I think that this complex plays a role in the regulation of lipid homeostasis.

Other potentially interesting candidate kinases could be associated with different functions that previously described in literature. For example, LYK5 (STRADA) and ALS2CR2 (STRADB), two genes that activate LKB1, an activator of AMPK, disturb the lipidome of HeLa cells (Hawley et al, 2003). Yet, in HeLa cells, the expression of LKB1 is extremely low and instead, AMPK is activated by CAMKKβ in a calcium-dependent manner (Fogarty et al, 2010). In my results, LKB1 doesn't induce significant lipid changes, which is consistent with its absence of expression. Both LYK5 and ALS2CR2 induce a decrease of SLs coupled to the increase of PC, suggesting that, even dissociated from the regulation of LKB1, these kinases still function together in processes with an impact on lipid metabolism.

Several genes seem to play interesting roles in lipid homeostasis and this screen clusters together genes that have not previously been associated with similar functions. In order to understand the pertinence of these associations, the validation and mechanism of changes they induce in lipid needs to be investigated.

## 2. How to interpret observed modifications of lipid profiles?

The HIS analysis identified 7 major patterns of lipid changes. However, one can wonder what could induce such combinations of changes. Here, I draw some hypotheses about the major ones.

## • Simultaneous changes in the blocks PC-PE, PI-PS-CL or SM-Cer-GlcCer

During the screen, I analyzed the quantity of lipids using different methods of mass spectrometry. For instance, PC and PE were quantified together in positive mode, SM-Cer-GlcCer in positive mode too but with another method adapted to SL and PI-PS were analyzed in negative mode. Despite tight controls, a frequent update and high maintenance of the machines as well as discarding of bad MS cycles after the run, it is not impossible that similar changes in all lipids from one of these three blocks come from machine vagaries. One way to discriminate technical problems from biological observations is to analyze in details the lipid profile and not only the total amount of lipid class. If observed lipid changes vary with fatty acyl composition (monoacylated, hydroxylation, chain length, unsaturation), it is reasonable to think that it doesn't come from the machine.

#### Ratio PC/PE

One of the strongest observed phenotypes is the increase of PC/PE ratio in subnetwork A. PC and PE are the major phospholipids in mammalian cells and they mostly result from de novo synthesis via the Kennedy pathway in the ER. However, these pathways are connected and PC can also result from the sequential methylation of PE by phosphatidylethanolamine N-methyltransferase (PEMT) in the MAM (Gibellini & Smith, 2010). The ratio between PC and PE levels is tightly regulated in cells because the quantity of conic-shaped PE tends to deform membrane structures (Dowhan, 2008). Increased PC/PE ratio can be associated with an upregulation of PEMT in the liver of obese mice and leads to ER stress (Watanabe et al, 2014). In HeLa cells, an increase of PC/PE ratio could be linked to the deficiency of the PC synthesis via the Kennedy pathway, which is compensated by PEMT in order to prevent a raise of PE leading

to membrane deformation as well as to supply ceramides with phosphocholine to make SM. The transcription of PEMT is negatively regulated by the transcription factor Sp1, which is at the same time a positive regulator of the cytidylyltransferase, the rate limiting enzyme of de novo PC synthesis by the Kennedy pathway (Vance, 2013). Moreover, Sp1 transcriptional activity is modulated by phosphorylation through many kinases whose some are directly linked to the regulation of glucose and insulin via PI3K signaling (Chu, 2012). One of them, PRKCA enhances Sp1 DNA binding and is also a candidate gene from subnetwork A (Fig. 37). Silencing PRKCA induces an increase of both PC and etherPC, more particularly PC32-36 with 0 or one unsaturation. This increase is coupled to the decrease of PE and etherPE with rather short FAs, too (Fig. 38). This observation suggests that PRKCA could be a positive regulator of the Kennedy pathway through the control of CCT and PEMT transcription by Sp1. In order to validate this hypothesis, it would be interesting to know if the PRKCA-dependent DNA binding of Sp1 is directly linked to the transcription of CCT and PEMT, through a chromatin immunoprecipitation (CHIP) experiment, for instance.

As suggested by analyzing the phenotype of PRKCA silencing, the simultaneous observation of LysoPL, etherPL and their FA composition can give precious indications about the precise pathways involved in the observed lipid changes. In the case of PC, for instance, its regulation can also come from its hydrolysis by different phospholipase that induce different signaling pathways. For instance, a decrease of PC coupled to the increase of LysoPC is certainly linked to the action of phospholipase A1 (PLA1) that plays important roles in many signaling pathways by releasing LysoPC and FA, as in subnetwork G. On the other side, PC hydrolysis by phospholipase D (PLD) will produce PA and choline (Hermansson et al, 2011). PLD1 is also activated by phosphorylation via PRKCA (Kim et al, 1999). Therefore, the silencing of PRKCA should also prevent the hydrolysis of PC in this manner and block the consecutive regulation of cytoskeleton resulting from the activation of PIKVE by PA.

## • Anionic phospholipids

In subnetwork B and C, we observe specific changes in phospholipids PI, PS and CL, sometimes coupled to the increase of PC. As described in the chapter Introduction (p11), the synthesis pathway of PS differs completely from PI and CL. Moreover, in order to maintain a

negative charge of membrane constant, mammalian cells seem to adapt the quantity of negatively-charged phospholipids according to still unknown mechanisms (Hermansson et al, 2011). This is apparently what happens for ULK1 in subnetwork A, SRPK2, EPHA3, MATK, FLT3, ADRBK1 and MAP2K1 in subnetwork B (**Fig. 37**), for which the strongest phenotypes include opposite regulations of PI and PS, suggesting a defect in the regulation of one of these lipids resulting in the automatic compensation by the unknown homeostatic mechanism. However, several other candidate genes present the same phenotype for both anionic lipids and might be involved in the regulation of negatively-charged phospholipid homeostasis.

#### Sphingolipids

The regulation of sphingolipid homeostasis and its crosstalk with other metabolic pathways has been reviewed in the paper "sphingolipids homeostasis in the web of metabolic routes" that we published in 2013 together with Dr. Maria-Auxiliadora Aguilera Romero. With the kinomewide siRNA screen in mammalian cells, it is now possible to confront theory to reality by analyzing how changes in the amount of sphingolipids can be coupled to other lipids. Except for subnetwork D and F that group candidate genes presenting a specific decrease or increase of SLs, respectively (Fig. 37, 39), changes in SLs are often coupled to other lipid changes and phenotypes are still under analysis. On the other hand, subnetwork D present candidate genes that seem specifically involved in the regulation of SL homeostasis. Three phenotypes can be highlighted: 1) decrease of Cer and GlcCer, 2) decrease of SM and GlcCer coupled to the increase of Cer and 3) the increase of complex SLs coupled to the decrease of Cer. Opposite phenotypes between Cer and complex SLs can result from defects in the transport of ceramides to the Golgi for phenotype 2 or from the accumulation of complex SLs as described for the third phenotype. The specific accumulation of complex SLs could be due to lysosomal/endosomal accumulation as in Niemann-Pick type C disease. However, this accumulation was not coupled to an increase of cholesterol.

Among candidate genes, TRIM24 and TRIM33 associate with the first phenotype, a strong decrease of Cer and GlcCer coupled to the increase of PC. Knowing that all target genes of this complex are not known, it could be involved in the regulation of sphingolipids. Among

candidates, there are also some genes involved in energy metabolism such as PKM2 and PFKFB1 that present an opposite phenotype. I still don't have any good hypothesis to explain these results.

#### • Modulation of sterol quantities

The subnetworks E and F presented both strong phenotypes in sterols. In subnetwork E, both cholesterol and cholesteryl esters present the same phenotype indicating that de novo cholesterol synthesis was affected whereas in subnetwork F, only the amount of cholesterol esters is deregulated. The regulation of intracellular levels of cholesterol esters is very important for the comprehension of atherosclerosis. Indeed, during this disease, cholesterol esters accumulate in macrophages and induce their transformation in foam cells. This accumulation is due to the inhibition of autophagy by p38-MAPK in macrophages (Mei et al, 2012). Indeed, inhibition of autophagy regulates intracellular lipid stores (Singh et al, 2009). Therefore, it is possible that modulation of cholesterol esters in the screen results from the modulation of autophagy and lysosomal fusion. However, results from the screen are contrasted. Some candidates such as PIK3CG or the p38 MAPK12, which are involved in the inhibition of autophagy, show a decrease of sterols when silenced. On the contrary, the knockdown of PRKAA1 induces the accumulation steryl esters. On the other hand, incoherently, the silencing of FRAP1 (MTOR) that inhibits autophagy induces a specific accumulation of steryl esters whereas its downregulation should induce autophagy. However, this screen was not performed in starvation conditions and maybe MTOR deficiency has other effects when cells have enough nutrients. In this sense, an siRNA screen for kinases that suppress macroautophagy in optimal growth conditions showed that some kinases regulate the formation of autophagosomes in MTOR-independent way. Finally, sterol regulation can also result from the modulation of cholesterol efflux by ATP-binding cassette transporters (Li et al, 2013).

## 3. Lessons from the screening "experience" and perspectives

Primary results from the kinome-wide siRNA screen in HeLa cells could be discussed for hours. In this thesis manuscript, I presented the main results per lipid classes but a more detailed analysis of fatty acyl composition of lipids represents an even richer dataset with the possibility to elaborate more precise hypotheses about the interconnection between the different lipid classes and better establish the biological processes involved. However, the exploratory analysis of such a dataset is an ant's work because, if statistical methods allow selecting hits for some phenotypic readout, correlating similar phenotypes with specific FA distribution across several lipid classes is much more challenging. Thus, it is easier to start with a precise question but to come back to the whole lipid profile in order to understand the answer.

My screen results also show a predominant role of the control of central carbon metabolism in the regulation of membrane lipid homeostasis, more than other biological processes, linking directly nutrient sensing to energy storage and the plasticity of membrane structure. If this link seems logical, its coordination is still not understood. Lipidomics can help to understand this coordination through the explanation of combined lipid changes that can give an idea about pathways directly involved in these changes. However, given the difficulty I had to make the link between several genes from the screen that were involved in the regulation of common processes I think that one challenge in future is to improve protein interactions and pathway databases and to -omics data to these pathways in order to better visualize functional gene interactions and elaborate more precise hypothesis about the coordination of biological processes in response to genetic perturbations.

#### **APPENDIX**

Content description of the excel file "Appendix" (please contact howard.riezman@unige.ch)

#### 1. siRNAs

Sheet 1. List of siRNAs sequences used in the pilot screen (Qiagen)

Sheet 2. MISSION siRNA Kinome library (Sigma-Aldrich)

## 2. Oligonucleotide sequences of primers

Sheet 3. List of DNA sequences used for confirmation of gene knockdown by qRT-PCR

#### 3. Discarded conditions

Sheet 4. CellProfiler analysis

Sheet 5. List of discarded conditions based on cytotoxicity, technical issues and pairwise correlation between biological replicates.

## 4. Multiple reaction monitoring assay

Sheet 6. List of lipid ions masses and charges used for multiple reaction monitoring.

#### 5. Data

Sheet 7. Pilot screen results: lipid quantities corrected to phosphate and z-scores

Sheet 8. Primary screen results per lipid category.

Sheet 9. Gene annotation enrichment of subnetworks from the HIS analysis

# **ABBREVIATIONS**

AMPK: AMP-activated protein kinase

**CE:** cholesteryl esters

**Cer**: ceramides **Cho**: choline

CHO: Chinese hamster ovary

CL: cardiolipin

CV: coefficient of variation

**DAG**: diacylglycerol

**DLS:** density light scattering **DsRNA:** double-stranded RNA

**EE:** early endosome

ER: endoplasmic reticulum

**EthN**: ethanolamine

**FA:** fatty acid

GC-MS: gas chromatography mass spectrometer

**GFP:** green fluorescent protein **GalCer**: galactosylceramide **GlcCer**: glucosylceramide

**GPI:** glycosylphosphatidylinositol

**GPL**: glycerophospholipid **GSL**: glycosphingolipid

HIS: hierarchical interaction score

IMM: inner membrane of mitochondria

LBPA: lysobisphosphatidic acid

LCB: long chain base
LE: late endosome

LTP: lipid-transfer protein
LysoPL: lysophospholipid

**KO**: knockout

MAM: mitochondria-associated membrane

MRM: multiple reaction monitoring

**MS**: mass spectrometry

**MUFA:** monounsaturated fatty acid

MVBs: multivesicular bodies

**mTOR:** mammalian target of rapamycin **OMM:** outer membrane of mitochondria

PA: phosphatidic acidPC: phosphatidylcholinePC#: principal component

**PCA:** Principal Component Analysis

**PCho**: phosphocholine

PCR: polymerase chain reaction
PE: phosphatidylethanolamine
PC: phosphatidylethanolamine

PG: phosphatidylglycerol PI: phosphatidylinositol PIP: phosphoinositide

PL: phospholipid

**PM:** plasma membrane **PS**: phosphatidylserine

PUFA: polyunsaturated fatty acid

RNAi: RNA interference

qRT-PCR: quantitative real time PCR

**S1P**: sphingosine-1-phosphate **SiRNA**: small-interfering RNA

SD: standard deviationSL: sphingolipidSM: sphingomyelin

**SiRNA:** small interfering RNA **SPT:** serine palmitoyl transferase

**SREBP:** Sterol regulatory element-binding protein

**SsRNA**: single-stranded RNA

**TAG**: triacylglycerol

**TLC**: thin layer chromatography **TSQ**: triple stage quadrupole

# **BIBLIOGRAPHY**

- Adams M (2010) Discovering the lipid bilayer. Nature education 3: 20
- Aguilera-Romero A, Gehin C, Riezman H (2013) Sphingolipid homeostasis in the web of metabolic routes. *Biochimica et biophysica acta*
- Akinc A, Zumbuehl A, Goldberg M, Leshchiner ES, Busini V, Hossain N, Bacallado SA, Nguyen DN, Fuller J, Alvarez R, Borodovsky A, Borland T, Constien R, de Fougerolles A, Dorkin JR, Narayanannair Jayaprakash K, Jayaraman M, John M, Koteliansky V, Manoharan M, Nechev L, Qin J, Racie T, Raitcheva D, Rajeev KG, Sah DW, Soutschek J, Toudjarska I, Vornlocher HP, Zimmermann TS, Langer R, Anderson DG (2008) A combinatorial library of lipid-like materials for delivery of RNAi therapeutics. *Nature biotechnology* **26:** 561-569
- Alderson NL, Rembiesa BM, Walla MD, Bielawska A, Bielawski J, Hama H (2004) The human FA2H gene encodes a fatty acid 2-hydroxylase. *The Journal of biological chemistry* **279:** 48562-48568
- Arsenault DJ, Yoo BH, Rosen KV, Ridgway ND (2013) ras-Induced up-regulation of CTP:phosphocholine cytidylyltransferase alpha contributes to malignant transformation of intestinal epithelial cells. *The Journal of biological chemistry* **288:** 633-643
- Balla T (2013) Phosphoinositides: tiny lipids with giant impact on cell regulation. Physiological reviews 93: 1019-1137
- Banerji S, Ngo M, Lane CF, Robinson CA, Minogue S, Ridgway ND (2010) Oxysterol binding protein-dependent activation of sphingomyelin synthesis in the golgi apparatus requires phosphatidylinositol 4-kinase IIalpha. *Molecular biology of the cell* **21:** 4141-4150
- Bektas M, Allende ML, Lee BG, Chen W, Amar MJ, Remaley AT, Saba JD, Proia RL (2010) Sphingosine 1-phosphate lyase deficiency disrupts lipid homeostasis in liver. *The Journal of biological chemistry* **285**: 10880-10889
- Bennett SA, Valenzuela N, Xu H, Franko B, Fai S, Figeys D (2013) Using neurolipidomics to identify phospholipid mediators of synaptic (dys)function in Alzheimer's Disease. *Frontiers in physiology* **4:** 168
- Betz C, Hall MN (2013) Where is mTOR and what is it doing there? The Journal of cell biology 203: 563-574
- Birmingham A, Selfors LM, Forster T, Wrobel D, Kennedy CJ, Shanks E, Santoyo-Lopez J, Dunican DJ, Long A, Kelleher D, Smith Q, Beijersbergen RL, Ghazal P, Shamu CE (2009) Statistical methods for analysis of high-throughput RNA interference screens. *Nature methods* **6:** 569-575
- Bjorkhem I, Lovgren-Sandblom A, Leoni V, Meaney S, Brodin L, Salveson L, Winge K, Palhagen S, Svenningsson P (2013) Oxysterols and Parkinson's disease: evidence that levels of 24S-hydroxycholesterol in cerebrospinal fluid correlates with the duration of the disease. *Neuroscience letters* **555**: 102-105
- Brites P, Waterham HR, Wanders RJ (2004) Functions and biosynthesis of plasmalogens in health and disease. *Biochimica et biophysica acta* **1636:** 219-231

- Brown MS, Goldstein JL, Krieger M, Ho YK, Anderson RG (1979) Reversible accumulation of cholesteryl esters in macrophages incubated with acetylated lipoproteins. *The Journal of cell biology* **82:** 597-613
- Cansell M, Gouygou JP, Jozefonvicz J, Letourneur D (1997) Lipid composition of cultured endothelial cells in relation to their growth. *Lipids* **32:** 39-44
- Carman GM, Han GS (2006) Roles of phosphatidate phosphatase enzymes in lipid metabolism. *Trends in biochemical sciences* **31:** 694-699
- Carobbio S, Rodriguez-Cuenca S, Vidal-Puig A (2011) Origins of metabolic complications in obesity: ectopic fat accumulation. The importance of the qualitative aspect of lipotoxicity. *Current opinion in clinical nutrition and metabolic care* **14:** 520-526
- Carpenter AE, Jones TR, Lamprecht MR, Clarke C, Kang IH, Friman O, Guertin DA, Chang JH, Lindquist RA, Moffat J, Golland P, Sabatini DM (2006) CellProfiler: image analysis software for identifying and quantifying cell phenotypes. *Genome biology* 7: R100
- Chan RB, Oliveira TG, Cortes EP, Honig LS, Duff KE, Small SA, Wenk MR, Shui G, Di Paolo G (2012) Comparative lipidomic analysis of mouse and human brain with Alzheimer disease. *The Journal of biological chemistry* **287**: 2678-2688
- Chandran S, Machamer CE (2012) Inactivation of ceramide transfer protein during pro-apoptotic stress by Golgi disassembly and caspase cleavage. *The Biochemical journal* **442:** 391-401
- Chen PW, Fonseca LL, Hannun YA, Voit EO (2013) Coordination of rapid sphingolipid responses to heat stress in yeast. *PLoS computational biology* **9:** e1003078
- Cheng D, Jenner AM, Shui G, Cheong WF, Mitchell TW, Nealon JR, Kim WS, McCann H, Wenk MR, Halliday GM, Garner B (2011) Lipid pathway alterations in Parkinson's disease primary visual cortex. *PloS one* **6:** e17299
- Cheng H, Wang M, Li JL, Cairns NJ, Han X (2013) Specific changes of sulfatide levels in individuals with pre-clinical Alzheimer's disease: an early event in disease pathogenesis. *Journal of neurochemistry* **127:** 733-738
- Chia J, Goh G, Racine V, Ng S, Kumar P, Bard F (2012) RNAi screening reveals a large signaling network controlling the Golgi apparatus in human cells. *Molecular systems biology* **8:** 629
- Chu S (2012) Transcriptional regulation by post-transcriptional modification--role of phosphorylation in Sp1 transcriptional activity. *Gene* **508:** 1-8
- Clarke NG, Dawson RM (1981) Alkaline O leads to N-transacylation. A new method for the quantitative deacylation of phospholipids. *The Biochemical journal* **195:** 301-306
- Cook HWaM, C.R. (2008) Fatty acid desaturation and chain elongation in eukaryotes Vol. 1, fifth edition edn.: Elsevier Science B.V.

- Creek DJ, Anderson J, McConville MJ, Barrett MP (2012) Metabolomic analysis of trypanosomatid protozoa. *Molecular and biochemical parasitology* **181:** 73-84
- Crimi M, Esposti MD (2011) Apoptosis-induced changes in mitochondrial lipids. *Biochimica et biophysica acta* **1813**: 551-557
- D'Angelo G, Vicinanza M, De Matteis MA (2008) Lipid-transfer proteins in biosynthetic pathways. *Current opinion in cell biology* **20:** 360-370
- Dahiya R, Brasitus TA (1986) Glycosphingolipid patterns of fetal and adult small intestinal mucosa in the sheep. *Biochimica et biophysica acta* **875**: 220-226
- Dan P, Edvardson S, Bielawski J, Hama H, Saada A (2011) 2-Hydroxylated sphingomyelin profiles in cells from patients with mutated fatty acid 2-hydroxylase. *Lipids in health and disease* **10:** 84
- Danai LV, Guilherme A, Guntur KV, Straubhaar J, Nicoloro SM, Czech MP (2013) Map4k4 suppresses Srebp-1 and adipocyte lipogenesis independent of JNK signaling. *Journal of lipid research* **54:** 2697-2707
- Davis ME, Zuckerman JE, Choi CH, Seligson D, Tolcher A, Alabi CA, Yen Y, Heidel JD, Ribas A (2010) Evidence of RNAi in humans from systemically administered siRNA via targeted nanoparticles. *Nature* **464:** 1067-1070
- Deeley JM, Hankin JA, Friedrich MG, Murphy RC, Truscott RJ, Mitchell TW, Blanksby SJ (2010) Sphingolipid distribution changes with age in the human lens. *Journal of lipid research* **51:** 2753-2760
- Dowhan WaB, M. (2008) Functional roles of lipids in membranes. In *Biochemistry of lipids, lipoproteins and membranes*, Vance DEaV, J. E. (ed), 1. Elsevier Science B. V.
- Drin G (2014) Topological Regulation of Lipid Balance in Cells. Annual review of biochemistry
- Eaton JM, Mullins GR, Brindley DN, Harris TE (2013) Phosphorylation of lipin 1 and charge on the phosphatidic acid head group control its phosphatidic acid phosphatase activity and membrane association. *The Journal of biological chemistry* **288:** 9933-9945
- Elbashir SM, Harborth J, Lendeckel W, Yalcin A, Weber K, Tuschl T (2001) Duplexes of 21-nucleotide RNAs mediate RNA interference in cultured mammalian cells. *Nature* **411:** 494-498
- Epstein S, Kirkpatrick CL, Castillon GA, Muniz M, Riezman I, David FP, Wollheim CB, Riezman H (2012) Activation of the unfolded protein response pathway causes ceramide accumulation in yeast and INS-1E insulinoma cells. *Journal of lipid research* **53:** 412-420
- Fabrias G, Munoz-Olaya J, Cingolani F, Signorelli P, Casas J, Gagliostro V, Ghidoni R (2012) Dihydroceramide desaturase and dihydrosphingolipids: debutant players in the sphingolipid arena. *Progress in lipid research* **51:** 82-94

- Fadok VA, Voelker DR, Campbell PA, Cohen JJ, Bratton DL, Henson PM (1992) Exposure of phosphatidylserine on the surface of apoptotic lymphocytes triggers specific recognition and removal by macrophages. *Journal of immunology* **148:** 2207-2216
- Fahy E, Subramaniam S, Murphy RC, Nishijima M, Raetz CR, Shimizu T, Spener F, van Meer G, Wakelam MJ, Dennis EA (2009) Update of the LIPID MAPS comprehensive classification system for lipids. *Journal of lipid research* **50 Suppl:** S9-14
- Faubert B, Boily G, Izreig S, Griss T, Samborska B, Dong Z, Dupuy F, Chambers C, Fuerth BJ, Viollet B, Mamer OA, Avizonis D, DeBerardinis RJ, Siegel PM, Jones RG (2013) AMPK is a negative regulator of the Warburg effect and suppresses tumor growth in vivo. *Cell metabolism* 17: 113-124
- Fire A, Xu S, Montgomery MK, Kostas SA, Driver SE, Mello CC (1998) Potent and specific genetic interference by double-stranded RNA in Caenorhabditis elegans. *Nature* **391**: 806-811
- Flinn RJ, Yan Y, Goswami S, Parker PJ, Backer JM (2010) The late endosome is essential for mTORC1 signaling. *Molecular biology of the cell* **21:** 833-841
- Fogarty S, Hawley SA, Green KA, Saner N, Mustard KJ, Hardie DG (2010) Calmodulin-dependent protein kinase kinase-beta activates AMPK without forming a stable complex: synergistic effects of Ca2+ and AMP. *The Biochemical journal* **426**: 109-118
- Ford JH (2010) Saturated fatty acid metabolism is key link between cell division, cancer, and senescence in cellular and whole organism aging. *Age* **32:** 231-237
- Foster DA (2013) Phosphatidic acid and lipid-sensing by mTOR. Trends in endocrinology and metabolism: TEM 24: 272-278
- Fugmann T, Hausser A, Schoffler P, Schmid S, Pfizenmaier K, Olayioye MA (2007) Regulation of secretory transport by protein kinase D-mediated phosphorylation of the ceramide transfer protein. *The Journal of cell biology* **178:** 15-22
- Gallala HD, Sandhoff K (2011) Biological function of the cellular lipid BMP-BMP as a key activator for cholesterol sorting and membrane digestion. *Neurochemical research* **36:** 1594-1600
- Ganley IG, Pfeffer SR (2006) Cholesterol accumulation sequesters Rab9 and disrupts late endosome function in NPC1-deficient cells. *The Journal of biological chemistry* **281:** 17890-17899
- Gey C, Seeger K (2013) Metabolic changes during cellular senescence investigated by proton NMR-spectroscopy. *Mechanisms of ageing and development* **134:** 130-138
- Gibellini F, Smith TK (2010) The Kennedy pathway--De novo synthesis of phosphatidylethanolamine and phosphatidylcholine. *IUBMB life* **62:** 414-428

- Giussani P, Colleoni T, Brioschi L, Bassi R, Hanada K, Tettamanti G, Riboni L, Viani P (2008) Ceramide traffic in C6 glioma cells: evidence for CERT-dependent and independent transport from ER to the Golgi apparatus. *Biochimica et biophysica acta* **1781**: 40-51
- Glunde K, Raman V, Mori N, Bhujwalla ZM (2005) RNA interference-mediated choline kinase suppression in breast cancer cells induces differentiation and reduces proliferation. *Cancer research* **65:** 11034-11043
- Goldstein JL, Brown MS (1987) Regulation of low-density lipoprotein receptors: implications for pathogenesis and therapy of hypercholesterolemia and atherosclerosis. *Circulation* **76:** 504-507
- Goldstein JL, Brown MS (2009) The LDL receptor. Arteriosclerosis, thrombosis, and vascular biology 29: 431-438
- Goursot A, Mineva T, Bissig C, Gruenberg J, Salahub DR (2010) Structure, dynamics, and energetics of lysobisphosphatidic acid (LBPA) isomers. *The journal of physical chemistry B* **114:** 15712-15720
- Grimard V, Massier J, Richter D, Schwudke D, Kalaidzidis Y, Fava E, Hermetter A, Thiele C (2008) siRNA screening reveals JNK2 as an evolutionary conserved regulator of triglyceride homeostasis. *Journal of lipid research* **49:** 2427-2440
- Grzelczyk A, Gendaszewska-Darmach E (2013) Novel bioactive glycerol-based lysophospholipids: new data -- new insight into their function. *Biochimie* **95:** 667-679
- Guan XL, Riezman I, Wenk MR, Riezman H (2010) Yeast lipid analysis and quantification by mass spectrometry. *Methods in enzymology* **470:** 369-391
- Guan XL, Souza CM, Pichler H, Dewhurst G, Schaad O, Kajiwara K, Wakabayashi H, Ivanova T, Castillon GA, Piccolis M, Abe F, Loewith R, Funato K, Wenk MR, Riezman H (2009) Functional interactions between sphingolipids and sterols in biological membranes regulating cell physiology. *Molecular biology of the cell* **20:** 2083-2095
- Guo L, Zhou D, Pryse KM, Okunade AL, Su X (2010) Fatty acid 2-hydroxylase mediates diffusional mobility of Raft-associated lipids, GLUT4 level, and lipogenesis in 3T3-L1 adipocytes. *The Journal of biological chemistry* **285**: 25438-25447
- Gupta V, Patwardhan GA, Zhang QJ, Cabot MC, Jazwinski SM, Liu YY (2010) Direct quantitative determination of ceramide glycosylation in vivo: a new approach to evaluate cellular enzyme activity of glucosylceramide synthase. *Journal of lipid research* **51:** 866-874
- Hammond SM, Boettcher S, Caudy AA, Kobayashi R, Hannon GJ (2001) Argonaute2, a link between genetic and biochemical analyses of RNAi. *Science* **293**: 1146-1150
- Han X, Rozen S, Boyle SH, Hellegers C, Cheng H, Burke JR, Welsh-Bohmer KA, Doraiswamy PM, Kaddurah-Daouk R (2011) Metabolomics in early Alzheimer's disease: identification of altered plasma sphingolipidome using shotgun lipidomics. *PloS one* **6:** e21643

- Hanada K, Kumagai K, Tomishige N, Kawano M (2007) CERT and intracellular trafficking of ceramide. *Biochimica et biophysica acta* **1771:** 644-653
- Hanada K, Kumagai K, Tomishige N, Yamaji T (2009) CERT-mediated trafficking of ceramide. *Biochimica et biophysica acta* **1791**: 684-691
- Hanada K, Kumagai K, Yasuda S, Miura Y, Kawano M, Fukasawa M, Nishijima M (2003) Molecular machinery for non-vesicular trafficking of ceramide. *Nature* **426:** 803-809
- Hannich JT, Umebayashi K, Riezman H (2011) Distribution and functions of sterols and sphingolipids. *Cold Spring Harbor perspectives in biology* **3**
- Hannun YA, Obeid LM (2008) Principles of bioactive lipid signalling: lessons from sphingolipids. *Nature reviews Molecular cell biology* **9:** 139-150
- Hardie DG, Ross FA, Hawley SA (2012) AMPK: a nutrient and energy sensor that maintains energy homeostasis. *Nature reviews Molecular cell biology* **13:** 251-262
- Hawley SA, Boudeau J, Reid JL, Mustard KJ, Udd L, Makela TP, Alessi DR, Hardie DG (2003) Complexes between the LKB1 tumor suppressor, STRAD alpha/beta and MO25 alpha/beta are upstream kinases in the AMP-activated protein kinase cascade. *Journal of biology* 2: 28
- Hermansson M, Hokynar K, Somerharju P (2011) Mechanisms of glycerophospholipid homeostasis in mammalian cells. *Progress in lipid research* **50:** 240-257
- Herquel B, Ouararhni K, Davidson I (2011a) The TIF1alpha-related TRIM cofactors couple chromatin modifications to transcriptional regulation, signaling and tumor suppression. *Transcription* 2: 231-236
- Herquel B, Ouararhni K, Khetchoumian K, Ignat M, Teletin M, Mark M, Bechade G, Van Dorsselaer A, Sanglier-Cianferani S, Hamiche A, Cammas F, Davidson I, Losson R (2011b) Transcription cofactors TRIM24, TRIM28, and TRIM33 associate to form regulatory complexes that suppress murine hepatocellular carcinoma. *Proceedings of the National Academy of Sciences of the United States of America* **108**: 8212-8217
- Herrero-Martin G, Hoyer-Hansen M, Garcia-Garcia C, Fumarola C, Farkas T, Lopez-Rivas A, Jaattela M (2009) TAK1 activates AMPK-dependent cytoprotective autophagy in TRAIL-treated epithelial cells. *The EMBO journal* **28:** 677-685
- Hibbitt O, Agkatsev S, Owen C, Cioroch M, Seymour L, Channon K, Wade-Martins R (2012) RNAi-mediated knockdown of HMG CoA reductase enhances gene expression from physiologically regulated low-density lipoprotein receptor therapeutic vectors in vivo. *Gene therapy* **19:** 463-467
- Houtkooper RH, Vaz FM (2008) Cardiolipin, the heart of mitochondrial metabolism. *Cellular and molecular life sciences: CMLS* **65:** 2493-2506

- Hruz T, Wyss M, Docquier M, Pfaffl MW, Masanetz S, Borghi L, Verbrugghe P, Kalaydjieva L, Bleuler S, Laule O, Descombes P, Gruissem W, Zimmermann P (2011) RefGenes: identification of reliable and condition specific reference genes for RT-qPCR data normalization. *BMC genomics* **12:** 156
- Huang da W, Sherman BT, Lempicki RA (2009) Systematic and integrative analysis of large gene lists using DAVID bioinformatics resources. *Nature protocols* **4:** 44-57
- Inoki K, Kim J, Guan KL (2012) AMPK and mTOR in cellular energy homeostasis and drug targets. *Annual review of pharmacology and toxicology* **52:** 381-400
- Jackson AL, Linsley PS (2010) Recognizing and avoiding siRNA off-target effects for target identification and therapeutic application. *Nature reviews Drug discovery* **9:** 57-67
- Jensen-Urstad AP, Song H, Lodhi IJ, Funai K, Yin L, Coleman T, Semenkovich CF (2013) Nutrient-dependent phosphorylation channels lipid synthesis to regulate PPARalpha. *Journal of lipid research* **54:** 1848-1859
- Jensen LJ, Kuhn M, Stark M, Chaffron S, Creevey C, Muller J, Doerks T, Julien P, Roth A, Simonovic M, Bork P, von Mering C (2009) STRING 8--a global view on proteins and their functional interactions in 630 organisms. *Nucleic acids research* 37: D412-416
- Kanehisa M, Goto S, Sato Y, Kawashima M, Furumichi M, Tanabe M (2014) Data, information, knowledge and principle: back to metabolism in KEGG. *Nucleic acids research* **42:** D199-205
- Kim J, Kaartinen V (2008) Generation of mice with a conditional allele for Trim33. Genesis 46: 329-333
- Kim Y, Han JM, Park JB, Lee SD, Oh YS, Chung C, Lee TG, Kim JH, Park SK, Yoo JS, Suh PG, Ryu SH (1999) Phosphorylation and activation of phospholipase D1 by protein kinase C in vivo: determination of multiple phosphorylation sites. *Biochemistry* **38:** 10344-10351
- Kim YJ, Guzman-Hernandez ML, Balla T (2011) A highly dynamic ER-derived phosphatidylinositol-synthesizing organelle supplies phosphoinositides to cellular membranes. *Developmental cell* **21:** 813-824
- Kinoshita T, Fujita M, Maeda Y (2008) Biosynthesis, remodelling and functions of mammalian GPI-anchored proteins: recent progress. *Journal of biochemistry* **144:** 287-294
- Kitatani K, Idkowiak-Baldys J, Hannun YA (2008) The sphingolipid salvage pathway in ceramide metabolism and signaling. *Cellular signalling* **20:** 1010-1018
- Kok JW, Nikolova-Karakashian M, Klappe K, Alexander C, Merrill AH, Jr. (1997) Dihydroceramide biology. Structure-specific metabolism and intracellular localization. *The Journal of biological chemistry* **272:** 21128-21136
- Kumagai K, Kawano-Kawada M, Hanada K (2014) Phosphoregulation of the Ceramide Transport Protein CERT at Serine 315 in the Interaction with VAMP-associated Protein (VAP) for Inter-organelle Trafficking of Ceramide in Mammalian Cells. *The Journal of biological chemistry*

- Landry JJ, Pyl PT, Rausch T, Zichner T, Tekkedil MM, Stutz AM, Jauch A, Aiyar RS, Pau G, Delhomme N, Gagneur J, Korbel JO, Huber W, Steinmetz LM (2013) The genomic and transcriptomic landscape of a HeLa cell line. *G3* 3: 1213-1224
- Laplante M, Sabatini DM (2009) An emerging role of mTOR in lipid biosynthesis. *Current biology: CB* 19: R1046-1052
- Laplante M, Sabatini DM (2013) Regulation of mTORC1 and its impact on gene expression at a glance. *Journal of cell science* **126:** 1713-1719
- Lev S (2006) Lipid homoeostasis and Golgi secretory function. Biochemical Society transactions 34: 363-366
- Lev S (2010) Non-vesicular lipid transport by lipid-transfer proteins and beyond. *Nature reviews Molecular cell biology* **11:** 739-750
- Lewis CA, Griffiths B, Santos CR, Pende M, Schulze A (2011) Genetic ablation of S6-kinase does not prevent processing of SREBP1. *Advances in enzyme regulation* **51:** 280-290
- Li G, Gu HM, Zhang DW (2013) ATP-binding cassette transporters and cholesterol translocation. IUBMB life
- Liberali P, Ramo P, Pelkmans L (2008) Protein kinases: starting a molecular systems view of endocytosis. *Annual review of cell and developmental biology* **24:** 501-523
- Lingwood D, Simons K (2010) Lipid rafts as a membrane-organizing principle. Science 327: 46-50
- Liu X, Erikson RL (2003) Polo-like kinase (Plk)1 depletion induces apoptosis in cancer cells. *Proceedings of the National Academy of Sciences of the United States of America* **100:** 5789-5794
- Lloyd-Evans E, Morgan AJ, He X, Smith DA, Elliot-Smith E, Sillence DJ, Churchill GC, Schuchman EH, Galione A, Platt FM (2008) Niemann-Pick disease type C1 is a sphingosine storage disease that causes deregulation of lysosomal calcium. *Nature medicine* **14:** 1247-1255
- Lloyd-Evans E, Platt FM (2010) Lipids on trial: the search for the offending metabolite in Niemann-Pick type C disease. *Traffic* **11:** 419-428
- Loizides-Mangold U (2013) On the future of mass-spectrometry-based lipidomics. The FEBS journal 280: 2817-2829
- Loizides-Mangold U, David FP, Nesatyy VJ, Kinoshita T, Riezman H (2012) Glycosylphosphatidylinositol anchors regulate glycosphingolipid levels. *Journal of lipid research* **53:** 1522-1534
- Lombard J, Lopez-Garcia P, Moreira D (2012) The early evolution of lipid membranes and the three domains of life. *Nature reviews Microbiology* **10:** 507-515

- Lv H, Zhang S, Wang B, Cui S, Yan J (2006) Toxicity of cationic lipids and cationic polymers in gene delivery. *Journal of controlled release:* official journal of the Controlled Release Society **114:** 100-109
- Lykidis A, Wang J, Karim MA, Jackowski S (2001) Overexpression of a mammalian ethanolamine-specific kinase accelerates the CDP-ethanolamine pathway. *The Journal of biological chemistry* **276:** 2174-2179
- Maceyka M, Sankala H, Hait NC, Le Stunff H, Liu H, Toman R, Collier C, Zhang M, Satin LS, Merrill AH, Jr., Milstien S, Spiegel S (2005) SphK1 and SphK2, sphingosine kinase isoenzymes with opposing functions in sphingolipid metabolism. *The Journal of biological chemistry* **280**: 37118-37129
- Manning G, Whyte DB, Martinez R, Hunter T, Sudarsanam S (2002) The protein kinase complement of the human genome. *Science* **298**: 1912-1934
- Mao C, Xu R, Bielawska A, Obeid LM (2000) Cloning of an alkaline ceramidase from Saccharomyces cerevisiae. An enzyme with reverse (CoA-independent) ceramide synthase activity. *The Journal of biological chemistry* **275:** 6876-6884
- Martel C, Esposti DD, Bouchet A, Brenner C, Lemoine A (2012) Non-alcoholic steatohepatitis: new insights from OMICS studies. *Current pharmaceutical biotechnology* **13:** 726-735
- Matsuo H, Chevallier J, Mayran N, Le Blanc I, Ferguson C, Faure J, Blanc NS, Matile S, Dubochet J, Sadoul R, Parton RG, Vilbois F, Gruenberg J (2004) Role of LBPA and Alix in multivesicular liposome formation and endosome organization. *Science* **303**: 531-534
- Matyash V, Liebisch G, Kurzchalia TV, Shevchenko A, Schwudke D (2008) Lipid extraction by methyl-tert-butyl ether for high-throughput lipidomics. *Journal of lipid research* **49:** 1137-1146
- Mayer C, Zhao J, Yuan X, Grummt I (2004) mTOR-dependent activation of the transcription factor TIF-IA links rRNA synthesis to nutrient availability. *Genes & development* **18:** 423-434
- McMillin JB, Dowhan W (2002) Cardiolipin and apoptosis. Biochimica et biophysica acta 1585: 97-107
- McNamara JR, Warnick GR, Cooper GR (2006) A brief history of lipid and lipoprotein measurements and their contribution to clinical chemistry. *Clinica chimica acta; international journal of clinical chemistry* **369:** 158-167
- Mei S, Gu H, Ward A, Yang X, Guo H, He K, Liu Z, Cao W (2012) p38 mitogen-activated protein kinase (MAPK) promotes cholesterol ester accumulation in macrophages through inhibition of macroautophagy. *The Journal of biological chemistry* **287:** 11761-11768
- Meikle PJ, Christopher MJ (2011) Lipidomics is providing new insight into the metabolic syndrome and its sequelae. *Current opinion in lipidology* **22:** 210-215
- Mizutani Y, Kihara A, Chiba H, Tojo H, Igarashi Y (2008) 2-Hydroxy-ceramide synthesis by ceramide synthase family: enzymatic basis for the preference of FA chain length. *Journal of lipid research* **49:** 2356-2364

- Monserrate JP, York JD (2010) Inositol phosphate synthesis and the nuclear processes they affect. *Current opinion in cell biology* **22:** 365-373
- Montenegro J, Bang EK, Sakai N, Matile S (2012) Synthesis of an enlarged library of dynamic DNA activators with oxime, disulfide and hydrazone bridges. *Chemistry* **18:** 10436-10443
- Montenegro J, Fin A, Matile S (2011) Comprehensive screening of octopus amphiphiles as DNA activators in lipid bilayers: implications on transport, sensing and cellular uptake. *Organic & biomolecular chemistry* **9:** 2641-2647
- Mullen TD, Hannun YA, Obeid LM (2012) Ceramide synthases at the centre of sphingolipid metabolism and biology. *The Biochemical journal* **441:** 789-802
- Mullen TD, Spassieva S, Jenkins RW, Kitatani K, Bielawski J, Hannun YA, Obeid LM (2011) Selective knockdown of ceramide synthases reveals complex interregulation of sphingolipid metabolism. *Journal of lipid research* **52:** 68-77
- Natter K, Kohlwein SD (2013) Yeast and cancer cells common principles in lipid metabolism. *Biochimica et biophysica acta* **1831:** 314-326
- Nhek S, Ngo M, Yang X, Ng MM, Field SJ, Asara JM, Ridgway ND, Toker A (2010) Regulation of oxysterol-binding protein Golgi localization through protein kinase D-mediated phosphorylation. *Molecular biology of the cell* **21:** 2327-2337
- Okino N, He X, Gatt S, Sandhoff K, Ito M, Schuchman EH (2003) The reverse activity of human acid ceramidase. *The Journal of biological chemistry* **278:** 29948-29953
- Owen JL, Zhang Y, Bae SH, Farooqi MS, Liang G, Hammer RE, Goldstein JL, Brown MS (2012) Insulin stimulation of SREBP-1c processing in transgenic rat hepatocytes requires p70 S6-kinase. *Proceedings of the National Academy of Sciences of the United States of America* **109:** 16184-16189
- Pata MO, Hannun YA, Ng CK (2010) Plant sphingolipids: decoding the enigma of the Sphinx. *The New phytologist* **185**: 611-630
- Peer D, Lieberman J (2011) Special delivery: targeted therapy with small RNAs. Gene therapy 18: 1127-1133
- Pelkmans L, Fava E, Grabner H, Hannus M, Habermann B, Krausz E, Zerial M (2005) Genome-wide analysis of human kinases in clathrin- and caveolae/raft-mediated endocytosis. *Nature* **436:** 78-86
- Perry RJ, Ridgway ND (2006) Oxysterol-binding protein and vesicle-associated membrane protein-associated protein are required for sterol-dependent activation of the ceramide transport protein. *Molecular biology of the cell* **17:** 2604-2616
- Potter KA, Kern MJ, Fullbright G, Bielawski J, Scherer SS, Yum SW, Li JJ, Cheng H, Han X, Venkata JK, Khan PA, Rohrer B, Hama H (2011) Central nervous system dysfunction in a mouse model of FA2H deficiency. *Glia* **59:** 1009-1021

- Prashek J, Truong T, Yao X (2013) Crystal structure of the pleckstrin homology domain from the ceramide transfer protein: implications for conformational change upon ligand binding. *PloS one* **8:** e79590
- Rouser G, Fkeischer S, Yamamoto A (1970) Two dimensional then layer chromatographic separation of polar lipids and determination of phospholipids by phosphorus analysis of spots. *Lipids* **5**: 494-496
- Ruangsiriluk W, Grosskurth SE, Ziemek D, Kuhn M, des Etages SG, Francone OL (2012) Silencing of enzymes involved in ceramide biosynthesis causes distinct global alterations of lipid homeostasis and gene expression. *Journal of lipid research* **53:** 1459-1471
- Rysman E, Brusselmans K, Scheys K, Timmermans L, Derua R, Munck S, Van Veldhoven PP, Waltregny D, Daniels VW, Machiels J, Vanderhoydonc F, Smans K, Waelkens E, Verhoeven G, Swinnen JV (2010) De novo lipogenesis protects cancer cells from free radicals and chemotherapeutics by promoting membrane lipid saturation. *Cancer research* **70:** 8117-8126
- Salaun C, Greaves J, Chamberlain LH (2010) The intracellular dynamic of protein palmitoylation. *The Journal of cell biology* **191:** 1229-1238
- Santos CR, Schulze A (2012) Lipid metabolism in cancer. The FEBS journal 279: 2610-2623
- Schekman R (2013) Discovery of the cellular and molecular basis of cholesterol control. *Proceedings of the National Academy of Sciences of the United States of America* **110:** 14833-14836
- Scherer WF, Syverton JT, Gey GO (1953) Studies on the propagation in vitro of poliomyelitis viruses. IV. Viral multiplication in a stable strain of human malignant epithelial cells (strain HeLa) derived from an epidermoid carcinoma of the cervix. *The Journal of experimental medicine* **97:** 695-710
- Schmidt EE, Pelz O, Buhlmann S, Kerr G, Horn T, Boutros M (2013) GenomeRNAi: a database for cell-based and in vivo RNAi phenotypes, 2013 update. *Nucleic acids research* **41:** D1021-1026
- Shah ZH, Jones DR, Sommer L, Foulger R, Bultsma Y, D'Santos C, Divecha N (2013) Nuclear phosphoinositides and their impact on nuclear functions. *The FEBS journal* **280:** 6295-6310
- Shalem O, Sanjana NE, Hartenian E, Shi X, Scott DA, Mikkelsen TS, Heckl D, Ebert BL, Root DE, Doench JG, Zhang F (2014) Genome-scale CRISPR-Cas9 knockout screening in human cells. *Science* **343**: 84-87
- Shannon P, Markiel A, Ozier O, Baliga NS, Wang JT, Ramage D, Amin N, Schwikowski B, Ideker T (2003) Cytoscape: a software environment for integrated models of biomolecular interaction networks. *Genome research* **13:** 2498-2504
- Siddique MM, Li Y, Wang L, Ching J, Mal M, Ilkayeva O, Wu YJ, Bay BH, Summers SA (2013) Ablation of dihydroceramide desaturase 1, a therapeutic target for the treatment of metabolic diseases, simultaneously stimulates anabolic and catabolic signaling. *Molecular and cellular biology* **33:** 2353-2369

- Simons K, Sampaio JL (2011) Membrane organization and lipid rafts. Cold Spring Harbor perspectives in biology 3: a004697
- Singh R, Kaushik S, Wang Y, Xiang Y, Novak I, Komatsu M, Tanaka K, Cuervo AM, Czaja MJ (2009) Autophagy regulates lipid metabolism. *Nature* **458:** 1131-1135
- Skelhorne-Gross G, Reid AL, Apostoli AJ, Di Lena MA, Rubino RE, Peterson NT, Schneider M, SenGupta SK, Gonzalez FJ, Nicol CJ (2012) Stromal adipocyte PPARgamma protects against breast tumorigenesis. *Carcinogenesis* 33: 1412-1420
- Snijder B, Liberali P, Frechin M, Stoeger T, Pelkmans L (2013) Predicting functional gene interactions with the hierarchical interaction score. *Nature methods* **10:** 1089-1092
- Snijder B, Sacher R, Ramo P, Liberali P, Mench K, Wolfrum N, Burleigh L, Scott CC, Verheije MH, Mercer J, Moese S, Heger T, Theusner K, Jurgeit A, Lamparter D, Balistreri G, Schelhaas M, De Haan CA, Marjomaki V, Hyypia T, Rottier PJ, Sodeik B, Marsh M, Gruenberg J, Amara A, Greber U, Helenius A, Pelkmans L (2012) Single-cell analysis of population context advances RNAi screening at multiple levels. *Molecular systems biology* 8: 579
- Steenbergen R, Nanowski TS, Beigneux A, Kulinski A, Young SG, Vance JE (2005) Disruption of the phosphatidylserine decarboxylase gene in mice causes embryonic lethality and mitochondrial defects. *The Journal of biological chemistry* **280**: 40032-40040
- Stryer L. BJM, Tymoczko J.L. (2012) Biochemistry, seventh edn.: W. H. Freeman & company.
- Sud M, Fahy E, Cotter D, Brown A, Dennis EA, Glass CK, Merrill AH, Jr., Murphy RC, Raetz CR, Russell DW, Subramaniam S (2007) LMSD: LIPID MAPS structure database. *Nucleic acids research* **35:** D527-532
- Sugiki T, Takeuchi K, Yamaji T, Takano T, Tokunaga Y, Kumagai K, Hanada K, Takahashi H, Shimada I (2012) Structural basis for the Golgi association by the pleckstrin homology domain of the ceramide trafficking protein (CERT). *The Journal of biological chemistry* **287:** 33706-33718
- Swanton C, Marani M, Pardo O, Warne PH, Kelly G, Sahai E, Elustondo F, Chang J, Temple J, Ahmed AA, Brenton JD, Downward J, Nicke B (2007) Regulators of mitotic arrest and ceramide metabolism are determinants of sensitivity to paclitaxel and other chemotherapeutic drugs. *Cancer cell* 11: 498-512
- Tafesse FG, Vacaru AM, Bosma EF, Hermansson M, Jain A, Hilderink A, Somerharju P, Holthuis JC (2014) Sphingomyelin synthase-related protein SMSr is a suppressor of ceramide-induced mitochondrial apoptosis. *Journal of cell science* **127**: 445-454
- Taha TA, Kitatani K, El-Alwani M, Bielawski J, Hannun YA, Obeid LM (2006) Loss of sphingosine kinase-1 activates the intrinsic pathway of programmed cell death: modulation of sphingolipid levels and the induction of apoptosis. *FASEB journal: official publication of the Federation of American Societies for Experimental Biology* **20:** 482-484
- Taniguchi M, Kitatani K, Kondo T, Hashimoto-Nishimura M, Asano S, Hayashi A, Mitsutake S, Igarashi Y, Umehara H, Takeya H, Kigawa J, Okazaki T (2012) Regulation of autophagy and its associated cell death by "sphingolipid

- rheostat": reciprocal role of ceramide and sphingosine 1-phosphate in the mammalian target of rapamycin pathway. *The Journal of biological chemistry* **287:** 39898-39910
- Tettamanti G, Bassi R, Viani P, Riboni L (2003) Salvage pathways in glycosphingolipid metabolism. *Biochimie* **85:** 423-437
- Tomishige N, Kumagai K, Kusuda J, Nishijima M, Hanada K (2009) Casein kinase I{gamma}2 down-regulates trafficking of ceramide in the synthesis of sphingomyelin. *Molecular biology of the cell* **20**: 348-357
- Toschi A, Lee E, Xu L, Garcia A, Gadir N, Foster DA (2009) Regulation of mTORC1 and mTORC2 complex assembly by phosphatidic acid: competition with rapamycin. *Molecular and cellular biology* **29:** 1411-1420
- Uchida Y, Hama H, Alderson NL, Douangpanya S, Wang Y, Crumrine DA, Elias PM, Holleran WM (2007) Fatty acid 2-hydroxylase, encoded by FA2H, accounts for differentiation-associated increase in 2-OH ceramides during keratinocyte differentiation. *The Journal of biological chemistry* **282:** 13211-13219
- Valenza M, Rigamonti D, Goffredo D, Zuccato C, Fenu S, Jamot L, Strand A, Tarditi A, Woodman B, Racchi M, Mariotti C, Di Donato S, Corsini A, Bates G, Pruss R, Olson JM, Sipione S, Tartari M, Cattaneo E (2005) Dysfunction of the cholesterol biosynthetic pathway in Huntington's disease. The Journal of neuroscience: the official journal of the Society for Neuroscience 25: 9932-9939
- van Meer G (2005) Cellular lipidomics. The EMBO journal 24: 3159-3165
- van Meer G, de Kroon AI (2011) Lipid map of the mammalian cell. Journal of cell science 124: 5-8
- Vance DE (2013) Phospholipid methylation in mammals: from biochemistry to physiological function. *Biochimica et biophysica acta*
- Wallner S, Schmitz G (2011) Plasmalogens the neglected regulatory and scavenging lipid species. *Chemistry and physics of lipids* **164:** 573-589
- Wang J, Duncan D, Shi Z, Zhang B (2013) WEB-based GEne SeT AnaLysis Toolkit (WebGestalt): update 2013. *Nucleic acids research* **41:** W77-83
- Wang J, Hudson R, Sintim HO (2012) Inhibitors of fatty acid synthesis in prokaryotes and eukaryotes as anti-infective, anticancer and anti-obesity drugs. *Future medicinal chemistry* **4:** 1113-1151
- Wang X, Rao RP, Kosakowska-Cholody T, Masood MA, Southon E, Zhang H, Berthet C, Nagashim K, Veenstra TK, Tessarollo L, Acharya U, Acharya JK (2009) Mitochondrial degeneration and not apoptosis is the primary cause of embryonic lethality in ceramide transfer protein mutant mice. *The Journal of cell biology* **184:** 143-158
- Ward PS, Thompson CB (2012) Metabolic reprogramming: a cancer hallmark even warburg did not anticipate. *Cancer cell* 21: 297-308

- Watanabe M, Nakatsuka A, Murakami K, Inoue K, Terami T, Higuchi C, Katayama A, Teshigawara S, Eguchi J, Ogawa D, Watanabe E, Wada J, Makino H (2014) Pemt deficiency ameliorates endoplasmic reticulum stress in diabetic nephropathy. *PloS one* **9:** e92647
- Wenk MR (2005) The emerging field of lipidomics. Nature reviews Drug discovery 4: 594-610
- WHO. (2013) Cardiovascular diseases (CVDs). p. Fact sheet N°317.
- Wixon J, Kell D (2000) The Kyoto encyclopedia of genes and genomes--KEGG. Yeast 17: 48-55
- Wu G, Aoyama C, Young SG, Vance DE (2008) Early embryonic lethality caused by disruption of the gene for choline kinase alpha, the first enzyme in phosphatidylcholine biosynthesis. *The Journal of biological chemistry* **283:** 1456-1462
- Wu G, Lu ZH, Kulkarni N, Ledeen RW (2012) Deficiency of ganglioside GM1 correlates with Parkinson's disease in mice and humans. *Journal of neuroscience research* **90:** 1997-2008
- Wu G, Vance DE (2010) Choline kinase and its function. Biochemistry and cell biology = Biochimie et biologie cellulaire 88: 559-564
- Yalcin A, Clem B, Makoni S, Clem A, Nelson K, Thornburg J, Siow D, Lane AN, Brock SE, Goswami U, Eaton JW, Telang S, Chesney J (2010) Selective inhibition of choline kinase simultaneously attenuates MAPK and PI3K/AKT signaling. *Oncogene* **29:** 139-149
- Ye J, Coulouris G, Zaretskaya I, Cutcutache I, Rozen S, Madden TL (2012a) Primer-BLAST: a tool to design target-specific primers for polymerase chain reaction. *BMC bioinformatics* **13:** 134
- Ye J, Mancuso A, Tong X, Ward PS, Fan J, Rabinowitz JD, Thompson CB (2012b) Pyruvate kinase M2 promotes de novo serine synthesis to sustain mTORC1 activity and cell proliferation. *Proceedings of the National Academy of Sciences of the United States of America* **109**: 6904-6909
- You JS, Lincoln HC, Kim CR, Frey JW, Goodman CA, Zhong XP, Hornberger TA (2014) The role of diacylglycerol kinase zeta and phosphatidic acid in the mechanical activation of mammalian target of rapamycin (mTOR) signaling and skeletal muscle hypertrophy. *The Journal of biological chemistry* **289:** 1551-1563
- Young MM, Kester M, Wang HG (2013) Sphingolipids: regulators of crosstalk between apoptosis and autophagy. Journal of lipid research **54:** 5-19
- Yu Y, Vidalino L, Anesi A, Macchi P, Guella G (2014) A lipidomics investigation of the induced hypoxia stress on HeLa cells by using MS and NMR techniques. *Molecular bioSystems* **10**: 878-890
- Zhang LH, Yin AA, Cheng JX, Huang HY, Li XM, Zhang YQ, Han N, Zhang X (2014) TRIM24 promotes glioma progression and enhances chemoresistance through activation of the PI3K/Akt signaling pathway. *Oncogene*

- Zhang XD (2011a) Illustration of SSMD, z score, SSMD\*, z\* score, and t statistic for hit selection in RNAi high-throughput screens. *Journal of biomolecular screening* **16:** 775-785
- Zhang XD (2011b) Optimal high-throughput screening: practical experimental design and data analysis for genome-scale RNAi research, Cambridge: Cambridge University Press.
- Zitomer NC, Mitchell T, Voss KA, Bondy GS, Pruett ST, Garnier-Amblard EC, Liebeskind LS, Park H, Wang E, Sullards MC, Merrill AH, Jr., Riley RT (2009) Ceramide synthase inhibition by fumonisin B1 causes accumulation of 1-deoxysphinganine: a novel category of bioactive 1-deoxysphingoid bases and 1-deoxydihydroceramides biosynthesized by mammalian cell lines and animals. *The Journal of biological chemistry* **284:** 4786-4795